Université de Lorraine
Collegium Sciences et Technologies
École Doctorale « Ressources Procédés Produits Environnement »

Unité Mixte de Recherche 1136 INRA / UL
Interactions Arbres / Microorganismes
Centre INRA de Nancy

Thèse présentée pour l'obtention du titre de

Docteur de l'Université de Lorraine
en Biologie Végétale et Forestière

par **Vincent HERVÉ**

Bacterial-fungal interactions in wood decay: from wood physicochemical properties to taxonomic and functional diversity of *Phanerochaete chrysosporium*-associated bacterial communities

Les interactions bactéries-champignons dans le bois en décomposition : des propriétés physico-chimiques du bois à la diversité taxonomique et fonctionnelle des communautés bactériennes associées à Phanerochaete chrysosporium

Soutenance publique prévue le 28 mai 2014

Membres du jury

Rapporteurs
Joy E.M. Watts, Senior Lecturer, University of Portsmouth, United Kingdom
Pilar Junier, Assistant Professor, University of Neuchâtel, Switzerland

Examinateurs
Alain Sarniguet, Directeur de Recherche, INRA de Rennes
Philippe Gérardin, Professeur, Université de Lorraine
Pascale Frey-Klett, Directrice de Recherche, INRA de Nancy, Directrice de thèse
Éric Gelhaye, Directeur de Recherche, INRA de Nancy, Co-directeur de thèse

“I have always looked upon decay as being just as wonderful and rich an expression of life as growth.”

Reflections on writing

Henry Miller

Acknowledgements

First I would like to thank Dr Joy Watts, Dr Pilar Junier, Dr Philippe Gérardin and Dr Alain Sarniguet for reviewing this PhD thesis.

A la fin de cette quarantaine (de mois) nancéienne, je tiens également à remercier quelques personnes. Tout d'abord merci à Pascale Frey-Klett et Eric Gelhaye pour avoir encadré cette thèse. Pascale, merci pour le temps et l'énergie investis dans ce projet, merci pour votre disponibilité, pour toutes nos discussions, pour vos conseils fructueux et pour la liberté de travail que vous m'avez accordée durant ce projet.

J'aimerais ensuite remercier deux personnes indirectement responsable de ce travail, Thomas W. Dunlop et Pascal-Jean Lopez. Thanks Tom for supervising my first lab experience. Merci Pascal pour ces premiers mois dans le monde la microbiologie environnementale, et surtout pour m'avoir initié très tôt aux approches pluridisciplinaires.

Un grand merci à Frédéric Mothe. Merci Fred d'avoir toujours pris le temps de répondre à mes questions, de m'avoir suivi dans ce projet un peu exploratoire avec le scanner et également de m'avoir permis d'en savoir un peu plus sur le monde du bois. J'ai beaucoup appris.

Je tiens également à remercier très chaleureusement Alain Mercanti. Merci pour l'accueil des plus sympathiques à l'atelier et merci pour le sacré coup de pouce que tu as donné à la préparation de toutes mes manip'.

Merci à également à Maryline Harroué, pour m'avoir formé aux méthodes de préparation d'échantillons de bois pour les analyses microscopiques.

Je veux également remercier Élodie Ketter pour les quelques mois qu'elle a passé à l'INRA. Merci pour tout ce que tu as généré dans ce projet. Du bon boulot Mlle Ketter.

Je voudrais également remercier Xavier Le Roux pour toutes nos discussions, enrichissantes et fertiles.

Merci à Jean-Claude Pierrat pour son aide et ses conseils forts utiles en statistique.

Christophe Rose, dit LU. Un merci gigantesque pour toutes ces manip' de dernière année et pour tout ce qui en résulte. Merci pour cette formation accélérée en microanalyse, pour toutes nos discussions improvisées et puis pour le reste. Merci également à Bertrand Van de Moortèle pour les superbes images au FEG.

Merci à Carine Cochet, Christophe Calvaruso et Patrick Riveron pour leurs aide et conseils pour les analyses chimiques. Tous vos conseils ont été précieux et extrêmement utiles. Merci également à Marie-Pierre Turpault pour son temps et ses conseils.

Un très grand merci à Jean-Paul Maurice et Gérard Trichies. Merci pour ces discussions mycologiques et le partage de vos connaissances. Merci Gérard pour tous ces échanges. J'ai encore beaucoup à apprendre.

J'aimerais également remercier chaleureusement Marc Buée. Merci Marc pour toutes ces plaisantes discussions et pour tous les conseils et tuyaux que tu as pu me prodiguer.

I also would like Sanjay Antony Babu. Thanks mate for all our conversations and your sound advice.

Je remercie également Jean-Louis Churin, notamment pour cette semaine dense de manip' en tandem, plein d'histoires invraisemblables et de franche rigolade.

Merci également à Fabien Halkett pour nos récentes et riches discussions.

Enfin, tout cela n'aurait pas eu la même saveur sans un certain nombre de rencontres dans les environs. J'en profite donc pour saluer également les personnes avec qui j'ai eu le plaisir de discuter, du boulot et puis surtout d'autres choses autour d'un verre de moût fermenté. Alice, Adeline, Emmanuelle, Béatrice, Cyrille, Patrice, Laura, Panos, Pete, Josh, Mauricio, Ari, Sebastian, Emilie, Benjamin, Stéphane, Yann, Cendrella, Mathilde, Aurore, PJ, Fabrice, Nicolas (Bottinelli), JB, Balazs, Alisha, Sapna, Zoltan, Jianping, Antoine, Michaël, Félix, Thibaut, Emeline, Julien, Nicolas (Métral), Herminia, Laure, Maïra, Nina et Leticia.
Mention spéciale pour Nicolas (Cichocki) et Jaime.

Table of Contents

- Chapter 1 -

Introduction

Résumé

Dans les écosystèmes terrestres, la majorité du carbone fixé est contenu dans la lignocellulose, le constituant principal des plantes vasculaires. Les arbres concentrent cette lignocellulose dans leur xylème secondaire, plus communément dénommé bois. Du point de vue des cycles biogéochimiques, la décomposition du bois est donc processus important dans le fonctionnement des écosystèmes forestiers, notamment pour ce qui concerne le recyclage du carbone. En effet, le bois mort en forêt représente environ 10 à 20 % de la biomasse végétale, constituant ainsi une réserve importante de carbone. Cette décomposition du bois est un processus long, s'étalant sur plusieurs décennies et résultant de l'action facteurs biotiques et abiotiques.

Le bois est principalement composé de trois polymères représentant plus de 90 % de sa masse sèche : la cellulose, les hémicelluloses et la lignine. La cellulose et les hémicelluloses sont des polysaccharides alors que la lignine, plus difficilement dégradable est un polymère d'alcools aromatiques. Le bois est un matériau hétérogène dont la composition chimique et la structure cellulaire dépendent de l'espèce végétale et des conditions environnementales de croissance de l'arbre. Par exemple, le bois des conifères (gymnospermes) contient globalement plus de lignine mais moins d'azote et de phosphore que le bois des feuillus (angiospermes). Au sein du même arbre, cette hétérogénéité est également présente avec une composition chimique différente entre l'aubier et le duramen. Enfin, au sein d'un anneau de croissance ou cerne du bois, on peut distinguer le bois de printemps et le bois d'été, plus dense mais contenant moins de lignine que le précédent.

De part sa composition chimique et sa nature hétérogène, le bois est un matériau dont la dégradation est complexe. Dans les forêts tempérées, les microorganismes, en particulier les champignons basidiomycètes saprotrophes, sont les principaux agents de la décomposition du bois. Parmi les champignons décomposeurs, on distingue généralement trois grandes catégories : les pourritures blanches, les pourritures brunes et les pourritures dites molles. Les pourritures blanches dégradent tous les constituants du bois (cellulose, hémicelluloses et lignine) alors que les pourritures brunes, également appelées pourritures cubiques, ne dégradent principalement que la cellulose et les hémicelluloses. Les pourritures molles dégradent la cellulose et les hémicelluloses. Certaines espèces peuvent également dégrader la lignine. D'autres champignons, des moisissures et des levures, peuvent également coloniser le bois mort. Bien que moins étudiées dans ce contexte, les bactéries sont également impliquées

dans la décomposition du bois et sont capables de dégrader la cellulose et les hémicelluloses. De plus, certaines souches impliquées dans la dégradation de la lignine ont été identifiées. En milieu forestier, ces communautés bactériennes présentent une grande diversité. On les retrouve également dans le bois en décomposition en milieu aquatique.

La décomposition du bois par ces microorganismes résulte principalement de l'action d'une pléthore d'activités enzymatiques extracellulaires. La cellulose et les hémicelluloses sont dégradées par des enzymes hydrolytiques, respectivement les cellulases et hémicellulases. La cellulose peut également être dégradée par des processus oxydatifs, via la réaction de Fenton notamment. Les molécules de lignine sont quant à elles dégradées par des enzymes oxydatives et non spécifiques, telles que les péroxydases et les laccases. Au delà du rôle des microorganismes dans le processus de décomposition du bois, il a également été montré que les radiations ultra-violettes ou encore les pluies acides sont capables d'altérer la structure chimique du bois. L'ensemble de ce processus de décomposition du bois est influencé par de nombreux facteurs, comme la température annuelle moyenne, l'humidité, la densité initiale du bois ou encore le diamètre du tronc.

Le bois mort est également un habitat particulier en forêt, abritant une grande diversité d'organismes décomposeurs de bois ou non, des bactéries aux petits mammifères en passant par les champignons, les plantes et les invertébrés. Cet habitat est dynamique, avec une structure et un substrat évoluant au cours du processus de dégradation. Il en résulte des successions de communautés fongiques en fonction de l'état de décomposition du bois. Ces successions ont également été observées chez certains insectes xylophages, chez les lichens et les bryophytes. Cet habitat apparaît donc comme complexe. De nombreux organismes y interagissent au sein d'un véritable réseau trophique. Nombre de ces interactions ont été évoquées dans la littérature mais peu étudiées. C'est le cas notamment des interactions microbiennes entre les bactéries et les champignons.

Bactéries et champignons cohabitent et interagissent dans de nombreux et divers environnements. Les interactions bactéries-champignons ont été étudiées par exemple lors du processus de vinification ou de maturation du fromage, dans les poumons de patients atteints de fibrose cystique ou encore dans les sols forestiers. Ces interactions sont rarement neutres et peuvent influencer la structure des communautés microbiennes ainsi que le fonctionnement d'une niche écologique. La mycosphère se définit comme l'environnement proche des hyphes d'un champignon. Différentes études ont révélé que la présence d'un champignon pouvait modifier la diversité et la structure des communautés bactériennes associées à ce champignon

dans un environnement donné, traduisant ainsi un effet mycosphère. A l'inverse, la présence d'une communauté bactérienne peut également influencer la biologie du champignon.

Dans le bois en décomposition, bactéries et champignons interagissent. Pourtant, on ne sait que peu de choses sur le fonctionnement de ces communautés microbiennes mixtes. Aussi, le travail présenté dans cette thèse a pour ambition d'explorer, à différentes échelles, ces interactions bactéries-champignons lors du processus de décomposition du bois. Notre première hypothèse de travail était qu'il existe un effet mycosphère des champignons lignivores sur les communautés bactériennes associées au bois en décomposition. Nous avons donc cherché à savoir si un champignon de pourriture blanche pouvait influencer les diversités taxonomiques et fonctionnelles des communautés bactériennes dans un environnement lignocellulosique. Notre seconde hypothèse de travail était que ces interactions bactéries-champignons qui se développent dans le bois influencent le processus de dégradation du bois . Nous avons donc voulu savoir si la présence d'une communauté bactérienne dans la mycosphère d'un champignon décomposeur pouvait moduler la capacité lignocellulolytique de ce champignon. Enfin nous avons tenté d'évaluer la contribution respective des différents acteurs de cette interaction dans le processus de décomposition du bois.

Face à la complexité de ce processus et pour pouvoir tester ces deux hypothèses de travail, nous avons décidé de travailler avec un système biologique simplifié ne contenant que trois composantes : un champignon décomposeur, une communauté bactérienne et le bois. De même, au regard de la diversité des essences de bois et des organismes impliqués dans la décomposition de ces derniers, nous nous sommes focalisés sur deux modèles biologiques. Le hêtre *Fagus sylvatica*, un angiosperme relativement abondant dans les forêts tempérées européennes, a été choisi comme bois modèle dans tout ce travail. Concernant le partenaire fongique, notre choix s'est porté sur le champignon modèle de pourriture blanche *Phanerochaete chysosporium*, un basidiomycète dont la biologie (génome, transcriptome, protéome extracellulaire) a été très étudiée et que l'on retrouve dans les écosystèmes forestiers européens, colonisant principalement le bois des angiospermes.

L'ensemble des expériences menées pour tester nos deux hypothèses de travail a été réalisé à l'échelle du microcosme, afin de pouvoir travailler dans des conditions contrôlées et aussi de pouvoir répliquer les expériences. Afin d'évaluer le processus de décomposition, une méthode de suivi des variations de densité du bois lors de sa décomposition a été développée (Chapitre 2). Pour tester notre première hypothèse, nous avons combiné une approche non-

cultivable (Chapitre 3) et cultivable (Chapitre 4) sur les communautés bactériennes associées au bois en décomposition, en présence ou en absence de *P. chrysosporium*. La seconde hypothèse a été testée avec une approche polyphasique incluant la mesure d'activités enzymatiques extracellulaires microbiennes et l'analyse physicochimique du bois en décomposition (Chapitre 5).

1 Introduction

1.1 Preamble

Most of the carbon fixed by the terrestrial ecosystems is contained in the lignocellulose complex, which is the main structural component of vascular plants and of humic substances derived from them. Trees concentrate this lignocellulose in wood. Thus, in forest ecosystems, wood degradation is an important process in biogeochemical cycles, particularly for nutrient cycling (Kauffman *et al.* 1995) and carbon cycle (Barford *et al.* 2001). Indeed, dead wood in forests represents around 10 to 20 % of the plant biomass, constituting an important store of carbon (Cornwell *et al.* 2009). From a recently dead standing tree to a completely decomposed tree, wood degradation is a long process being spread over several decades and which results from biotic and abiotic processes. Dead wood is a particular habitat in forest ecosystems, providing different ecological niches (Hodge & Peterken 1998).

First trees appeared on Earth around 310 million years ago (Ma) during the Devonian period. Gymnosperms, a group containing conifers (*Pinophyta* division), cycads (*Cycadidae* subclass), Gnetophyte (*Gnetidae* subclass) and Ginkgo (*Ginkgoidae* subclass), appeared first (Figure 1.1). Conifers represent an ecologically important group of woody plants since they are the dominant plants of large areas such as boreal forests. Wood of conifers is called softwood. Later, around 165 Ma during the Jurassic period, angiosperms appeared. Angiosperms are very diverse and include broad-leaved trees which are dominant in tropical and subtropical forests. Wood of non-monocot angiosperm is called hardwood. Thus, gymnosperms and angiosperms represent two distinct plant groups, which differ in many ways including in term of wood composition. These differences of wood composition will result in different wood degradation processes.

The colonisation of land by fungi was estimated around 1000 Ma by Heckman et al. (2001). However, the fungi able to decompose lignocellulose have appeared later. A recent study estimated that *Agaricomycetes*, a class of fungi containing *inter alia* ligninolytic fungi, appeared around 290 Ma and that the first ligninolytic enzyme arose at approximately 295 Ma (Floudas *et al.* 2012). The emergence of these fungi coincided with the strong decrease of organic carbon burial around the end of the Carboniferous period, *i.e.*, around 300 Ma (Robinson 1990). Indeed, before this period, lignin was not decomposed and organic carbon from dead trees accumulated as coal deposit. Thus, the appearance of organisms able to

entirely decompose wood profoundly changed the carbon cycle (Floudas *et al.* 2012).

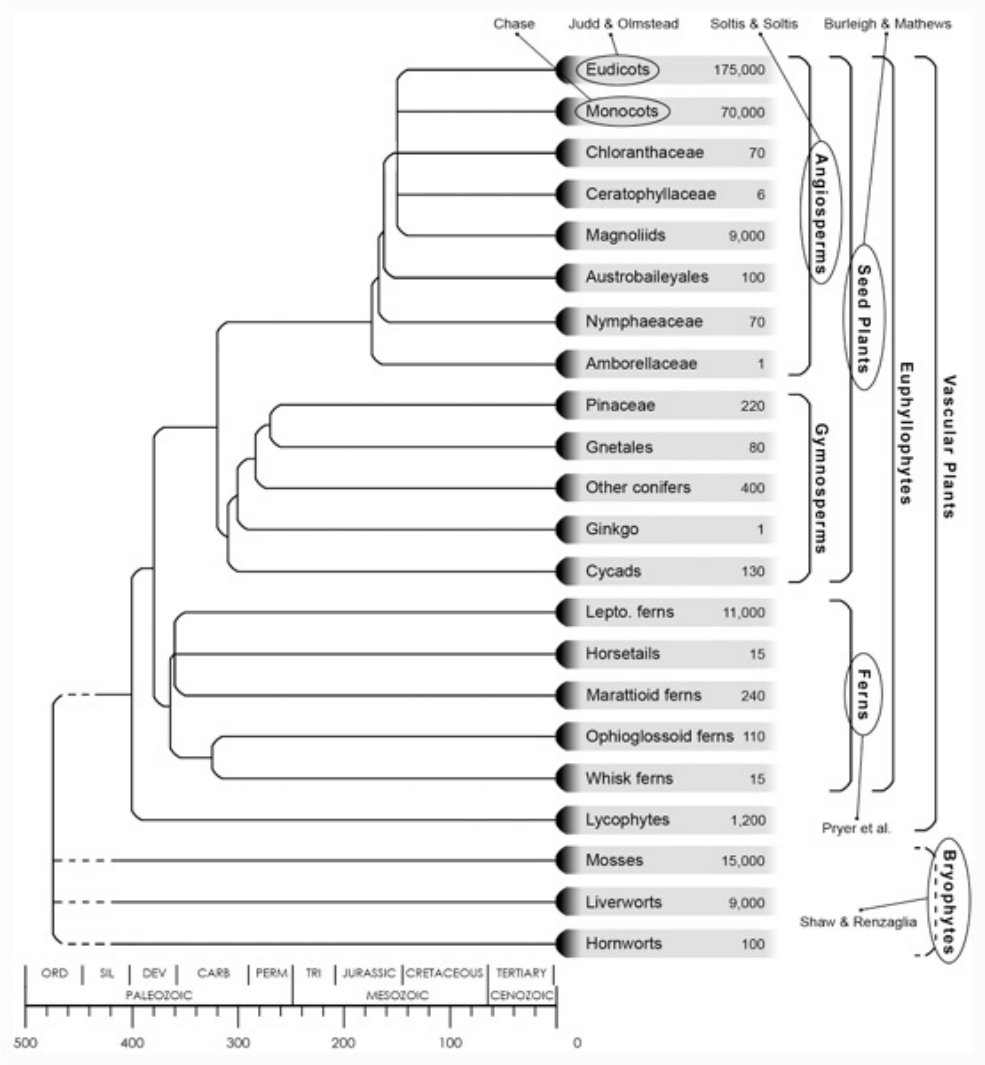

Figure 1.1 *Chronogram showing estimates of phylogenetic relationships and divergence times among the major groups of extant land plants (from Palmer et al., 2004).*

1.2 Wood composition

1.2.1 Chemical composition

Wood is a heterogenous organic material. It is a fibrous structural tissue found in trees and corresponding to the secondary xylem. It is mainly composed of three polymers, cellulose, hemicellulose and lignin, representing more than 90% of the dry wood weight (Pu *et al.* 2011). Pectin, an heteropolysaccharide, can represent from 1 to 4% of the wood cell wall. Low molecular weight compounds called extractives, such as terpenes, tannins, lignans and flavonoids are also present in wood. These extractives are part of the tree defence systems against fungi and arthropods. Finally, wood also contains low quantities (<2%) of mineral elements, called ash. Composition and concentration of ashes vary with tree species and with the environmental conditions of the tree growth.

1.2.1.1 Cellulose

Cellulose is the most abundant organic polymer on Earth. It is the major constituent of wood, accounting for 40-50% of the dry wood weight of both gymnosperm and angiosperm trees (Stockland, Siitonen & Jonsson 2012). Cellulose is a polymeric carbohydrate composed of β-1,4 linked D-glucopyranose molecules joined together in long linear chains. The disaccharide formed by these two glucoses is called cellobiose. This cellobiose unit contains two anhydroglucose units, with the molecular formula $(C_6H_{10}O_5)_n$ (Figure 1.2). In wood, the degree of polymerisation *n* is about 10 000.

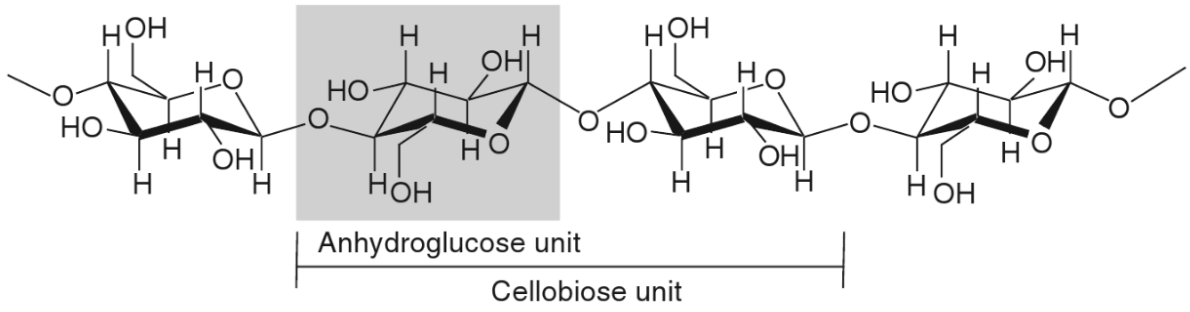

Figure 1.2. *Structure of cellulose molecule showing the anhydroglucose monomeric unit, the glycosidic 1-4 inter-monomeric bond and the cellobiose unit (from Pereira et al., 2003).*

Cellulose molecules are symmetrical. Because of the presence of hydroxyl groups in

cellulose chains, intramolecular and intermolecular H bonds in cellulose are created (Figure 1.3). Such lateral associations of cellulose molecules create highly ordered supramolecular structures called crystalline microfibrils. These microfibrils, in turn, associate into larger cellulose fibres or are bound together with hemicelluloses and lignin, creating a mechanically strong material.

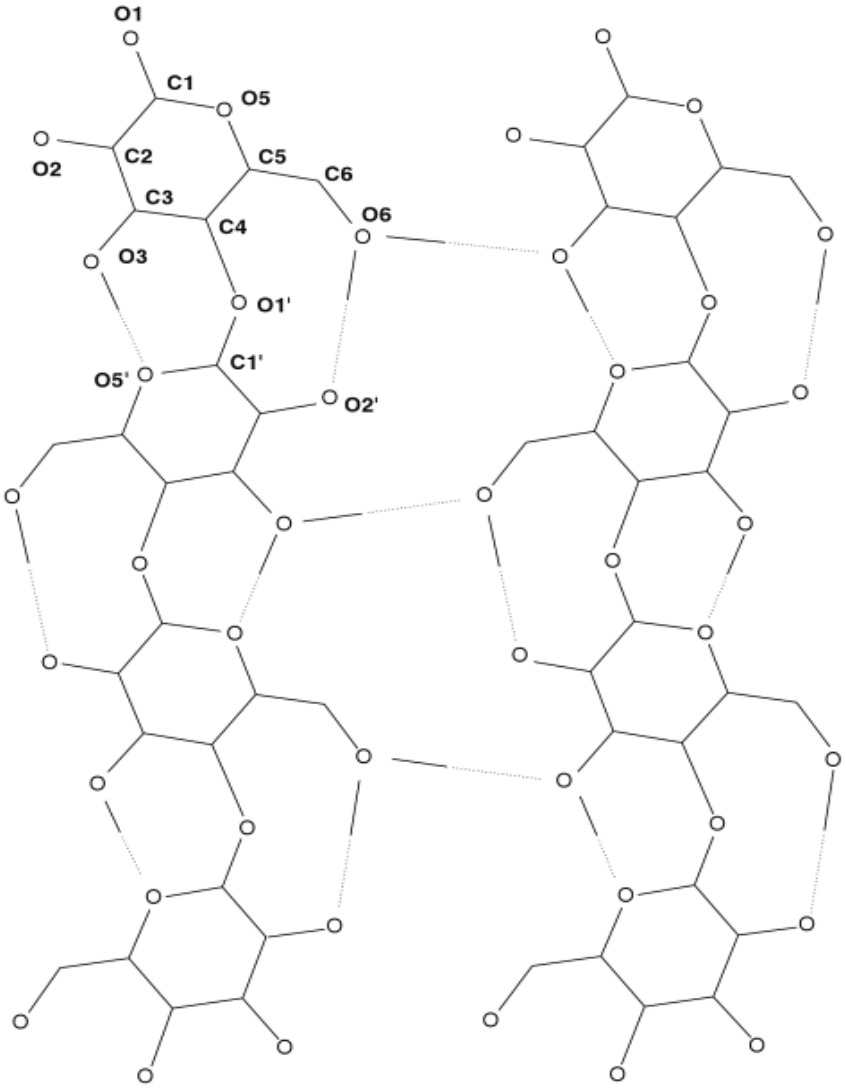

Figure 1.3. *Intramolecular and intermolecular H bonding in cellulose (from Pereira et al., 2003).*

1.2.1.2 Hemicelluloses

Hemicelluloses are also polysaccharides, but containing many different carbohydrate monomers (heteropolysaccharides). Contrary to cellulose, hemicellulose has a branched

structure and hemicellulose molecules do not aggregate together. However they can co-crystallize with cellulose microfibrils and also combine with lignin to form a non-crystalline structure in which the cellulose microfibrils are embedded (Stockland *et al.* 2012) (Figure 1.4).

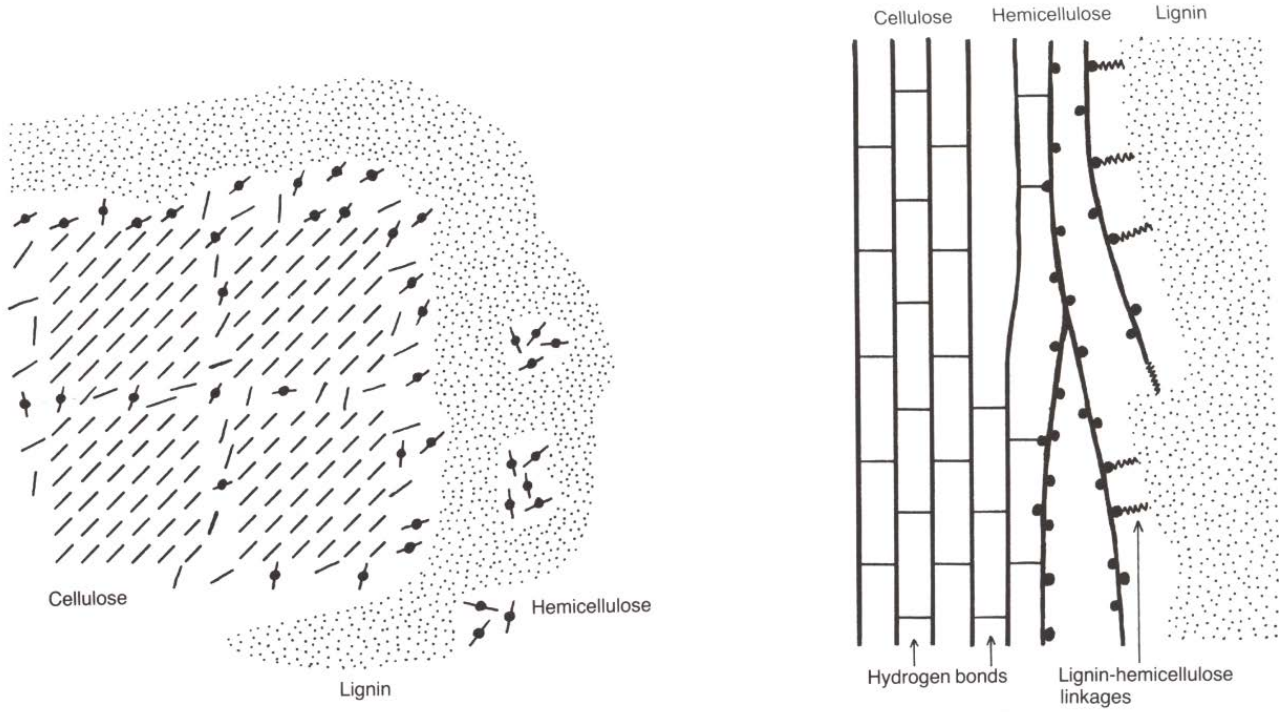

Figure 1.4. *Microdistribution of the wood macromolecules (from http://www.mtu.edu/forest/)*

Different types of hemicellulose exist in which the backbone can be a homopolysaccharide such as xyloglucan or heteropolyssacharide such as glucomannan. Hemicelluloses also differ in term of side chain composition which can contain from one to three monosaccharides (Gírio *et al.* 2010). Different types and different proportions of hemicelluloses occur in softwoods (wood of conifers) and hardwoods (wood of non-monocot angiosperm). Indeed, in softwood, the predominant hemicelluloses are mannans (galactoglucomannan and glucomannan) while in hardwood the predominant hemicelluloses are xylans (xyloglucan and glucuronoxylan) (Table 1.1). Concerning the proportion of hemicelluloses in total dry wood weight, it tends to be higher in hardwood (25-40%) than in sofwood (25-30 %) (Stockland *et al.* 2012).

Polysaccharide type	Biological origen	Abbreviation	Amount[a]	Units			DP[b]	Schematic representation
				Backbone	Side chains	Linkage		
Arabinogalactan	Softwoods	AG	1–3;35[c]	β-D-Galp	β-D-Galp α-L-Araf β-L-Arap	β-(1 → 6) α-(1 → 3) β-(1 → 3)	100–600	
Xyloglucan	Hardwoods, grasses	XG	2–25	β-D-Glcp β-D-Xylp	β-D-Xylp β-D-Galp α-L-Araf α-L-Fucp Acetyl	β-(1 → 4) α-(1 → 3) β- (1 → 2) α-(1 → 2) α-(1 → 2)		
Galactoglucomannan	Softwoods	GGM	10–25	β-D-Manp β-D-Glcp	β-D-Galp Acetyl	α-(1 → 6)	40–100	
Glucomannan	Softwoods and hardwoods	GM	2–5	β-D-Manp β-D-Glcp			40–70	
Glucuronoxylan	Hardwoods	GX	15–30	β-D-Xylp	4-O-Me-α-D-GlcpA Acetyl	α-(1 → 2)	100–200	
Arabinoglucuronoxylan	Grasses and cereals, softwoods	AGX	5–10	β-D-Xylp	4-O-Me-α-D-GlcpAβ-L-Araf	α-(1 → 2) α-(1 → 3)	50–185	
Arabinoxylans	Cereals	AX	0.15–30	β-D-Xylp	α-L-Araf/Feruloy	α-(1 → 2) α-(1 → 3)		
Glucuronoarabinoxylans	Grasses and cereals	GAX	15–30	β-D-Xylp	α-L-Araf 4-O-Me-α-D-GlcpA Acetyl	α-(1 → 2) α-(1 → 3)		
Homoxylans	Algae	X		β-D-Xylp[c]				

[a] %, dry biomass.
[b] Degree of polymerization.
[c] May also present β-(1 → 3) linkages on the backbone; * (up to) in the heartwood of larches ⬡, β-D-Galp; ●, β-D-Glcp; ○, β-D-Manp; ●, β-D-Xylp; ⬭, β-L-Araf; ○, β-L-Arap; ◇, α-L-Fucp; ●, 4-O-Me-α-D-GlcpA; ▼, Acetyl; ◆, Feruloyl.

Table 1.1 *Main types of polysaccharides present in hemicelluloses (from Gírio et al., 2010).*

1.2.1.3 Lignin

Lignin is the second most abundant organic polymer on Earth, accounting for approximately 30% of the organic carbon in the biosphere (Boerjan, Ralph & Baucher 2003). It has a complex molecular structure made up of aromatic subunits. Indeed, lignin is produced by the oxidative coupling of three monolignols, differently methoxylated: p-coumaryl alcohol, coniferyl alcohol, and sinapyl alcohol. These monolignols are incorporated into lignin in the form of the phenylpropanoids p-hydroxyphenyl (H), guaiacyl (G), and syringal (S) units, respectively (Figure 1.5).

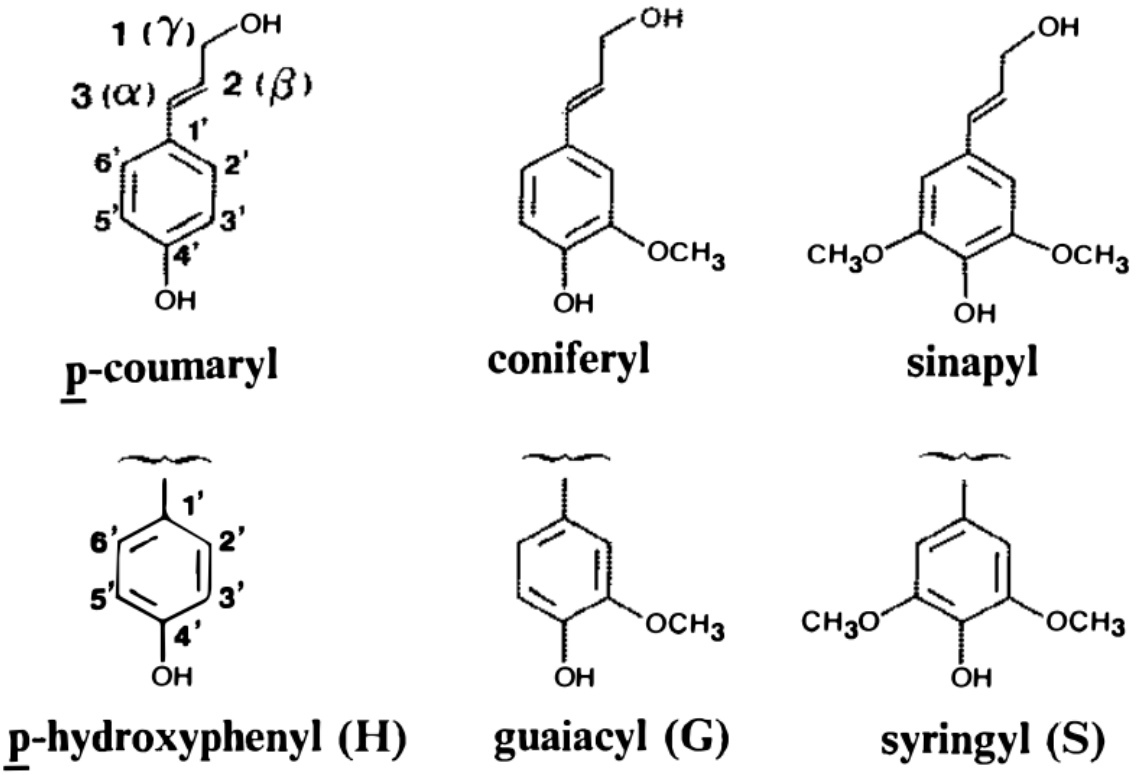

Figure 1.5. *The three monolignols and their corresponding structural units in lignin (from Lewis and Yamamoto, 1990).*

Thus, lignin forms a heterogeneous three-dimensional structure in which phenylpropanoid units are linked with covalent C-C and C-O-C bonds (Figure 1.6). Such structure is highly resistant to enzymatic degradation. Lignin composition and proportion in wood vary between angiosperms and gymnosperms. Indeed, lignin of gymnosperms consists almost entirely of G with small quantities of H whereas lignin of non-monocot angiosperms

consists of a mixture of a mixture of G and S, with very small quantities of H. Finally, lignin is present in larger amount in gymnosperms (25-32%) than in angiosperms (15-25%) (Weedon *et al.* 2009).

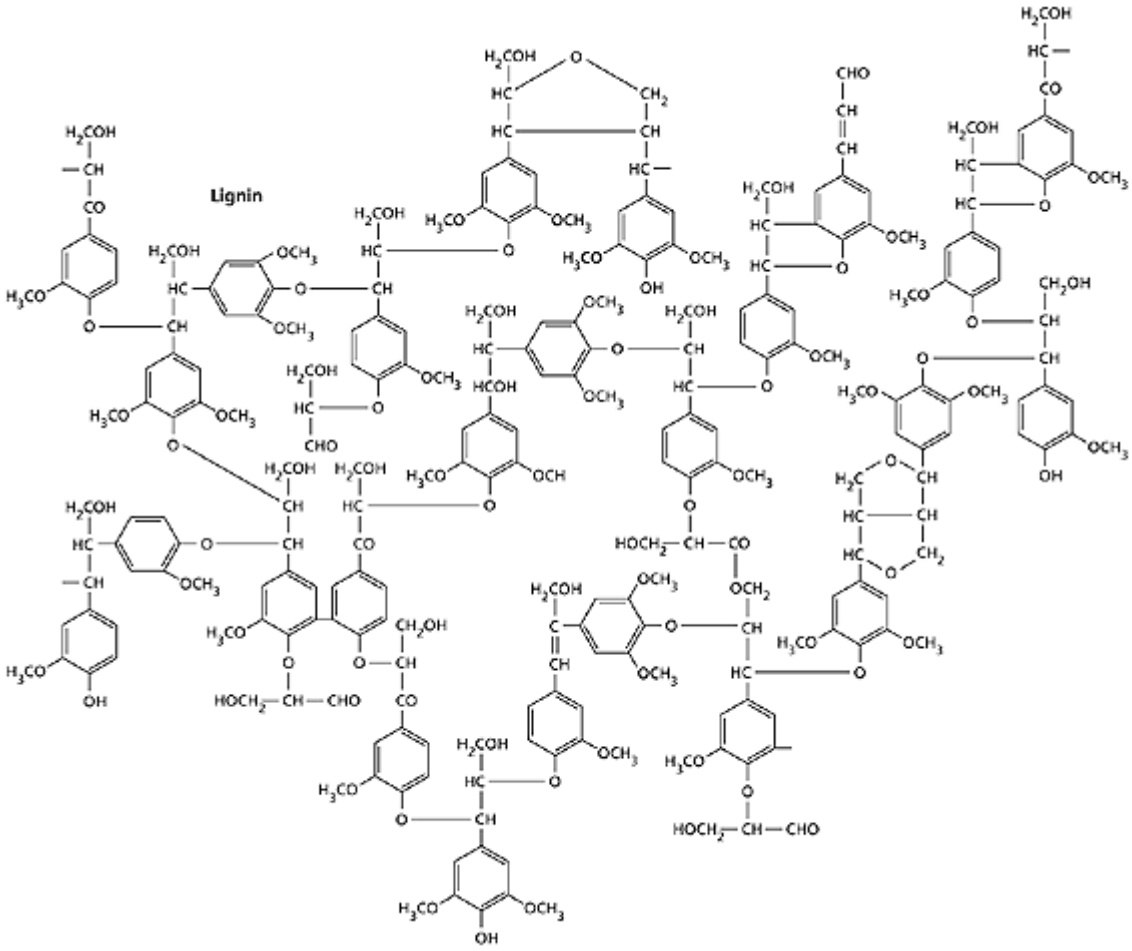

Figure 1.6. *Partial structure of a hypothetical lignin molecule from European beech (Fagus sylvatica). The phenylpropanoid units that make up lignin are not linked in a simple, repeating way. The lignin of beech contains G-, S- and H-units derived from coniferyl alcohol, sinapyl alcohol, and para-coumaryl alcohol respectively, in the approximate ratio 100:70:7 (from Plant Physiology online, 5th edition*).

1.2.2 Wood cell structure

The wood cell wall is organised in layers of different thicknesses (Figure 1.7) where the distribution pattern of wood macromolecules is not homogenous (Figure 1.8). When the cells grow, they first make a primary wall, mainly composed of cellulose, hemicellulose and

pectin. When the cells have reached their full size, they form a secondary cell wall inside the primary wall. The secondary wall consists of three layers: the outer (S1), the middle (S2) and the inner secondary wall layer (S3), containing different ratios of cellulose, hemicellulose and lignin. The space between neighbouring cells corresponds to the middle lamella. It is filled with lignin, calcium and pectin substances. It acts as a cement between the cells.

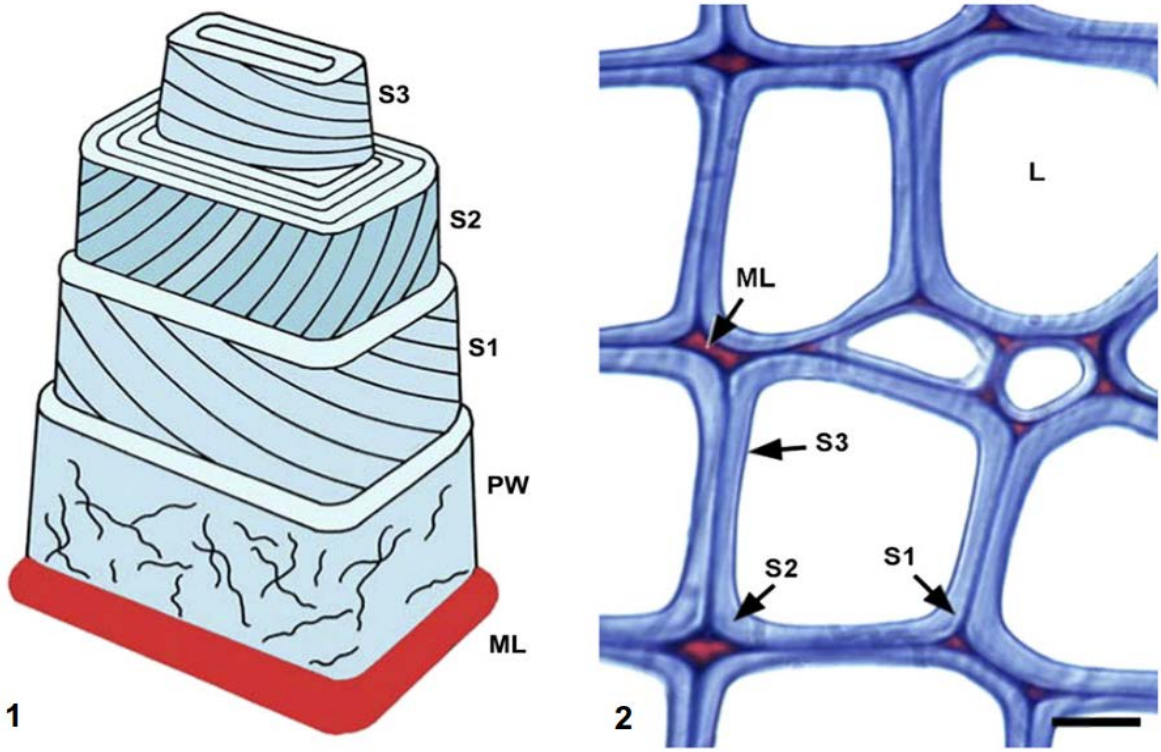

Figure 1.7. 1. *Wood cell wall model with the five cell-wall layers: the middle lamella (ML), the primary wall (PW), and the three-layer secondary wall (S): outer (S1), middle (S2) and inner secondary wall layer (S3).* ***2.*** *Traverse section of earlywood tracheids. L, lumen. Bar, 10 µm (from Schwarze, 2007).*

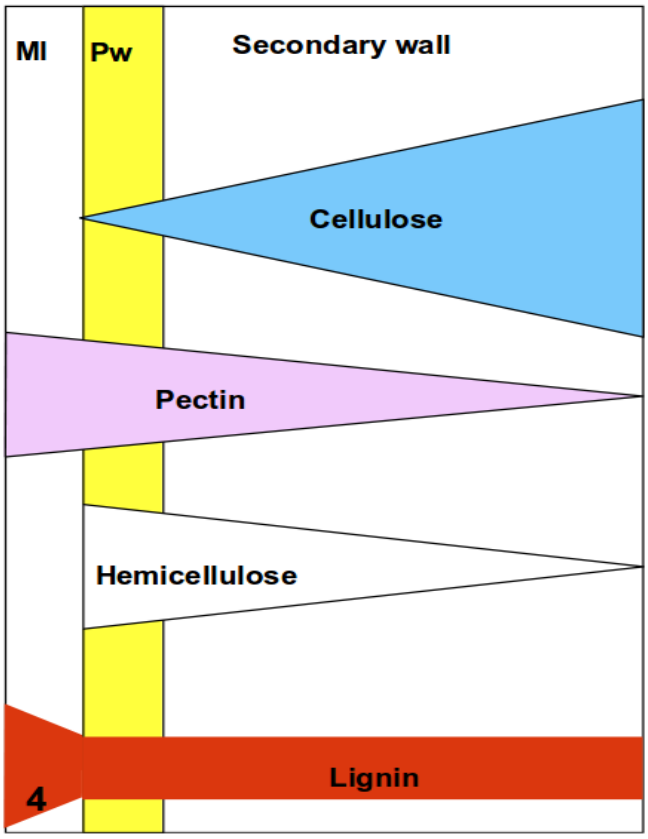

Figure 1.8 *Diagrammatic representation of the relative distribution of the main cell wall constituents within the different layers of the cell wall (from Schwarze, 2007).*

1.2.3 Heterogeneity of wood

The common point of the previous sections is the wood variability, notably between gymnosperms (softwoods) and angiosperms (hardwoods). As mentioned above, lignin composition and concentration as well as hemicelluloses composition and concentration differ between gymnosperms and angiosperms. Others wood trait values are also different between gymnosperm and angiosperm species. Indeed, wood density, phosphorus (P) concentration, nitrogen (N) concentration and conduit area (vessels compared to tracheids) are significantly higher in angiosperms compared to gymnosperms (Weedon *et al.* 2009).

The previous comparisons only concern differences between tree species. However, variations within a single tree also exist (Figure 1.9). First, wood can be distinguished from bark. The bark corresponds to different tissues outside the vascular cambium and consists of the outer bark and the inner bark (Franceschi *et al.* 2005). The outer bark is produced by the

cork cambium (phellogen) and is mostly composed of dead cells with high levels of suberin while the inner bark is produced by the vascular cambium and is composed of living tissues with high concentration of nutrients. Inside the xylem, it is also possible to distinguish heartwood from sapwood. The sapwood contains the only living cells in the xylem and produces extractives compounds. However it also contains non-living cells. It has a conductive function and also provides strength to the tree stem. The heartwood is composed of dead cells. It has a higher concentration of extractives and a lower water content compared to sapwood. Variations in mineral nutrient concentrations have also been described. Indeed, concentrations of P, N and K (potassium) are lower in heartwood compared to sapwood (Meerts 2002). Variations in density at fresh state can also be detected between heartwood and sapwood (Longuetaud, Mothe & Leban 2007). The formation of heartwood often (but not always) results in a colouring of the wood. The heartwood provides strength and mechanical support to the tree stem.

At the cellular level, the heterogeneity of the wood can also be observed. For trees grown in temperate climates, growth rings are visible in a tree cross section. Growth rings are the result of the annual growth of the vascular cambium (Figure 1.9). Growth rings consist of two distinct segments: the earlywood (also known as spring wood) in the inner portion of the growth ring and the latewood (also knows as summer wood) in the outer portion. Cells of the earlywood have a large radial diameter while latewood cells have smaller radial diameter and thicker cell walls (Figure 1.10). The latewood has a higher density than the earlywood (Bouriaud *et al.* 2004), but carbon (C) content and lignin content are higher in earlywood compared to latewood (Lamlom & Savidge 2003).

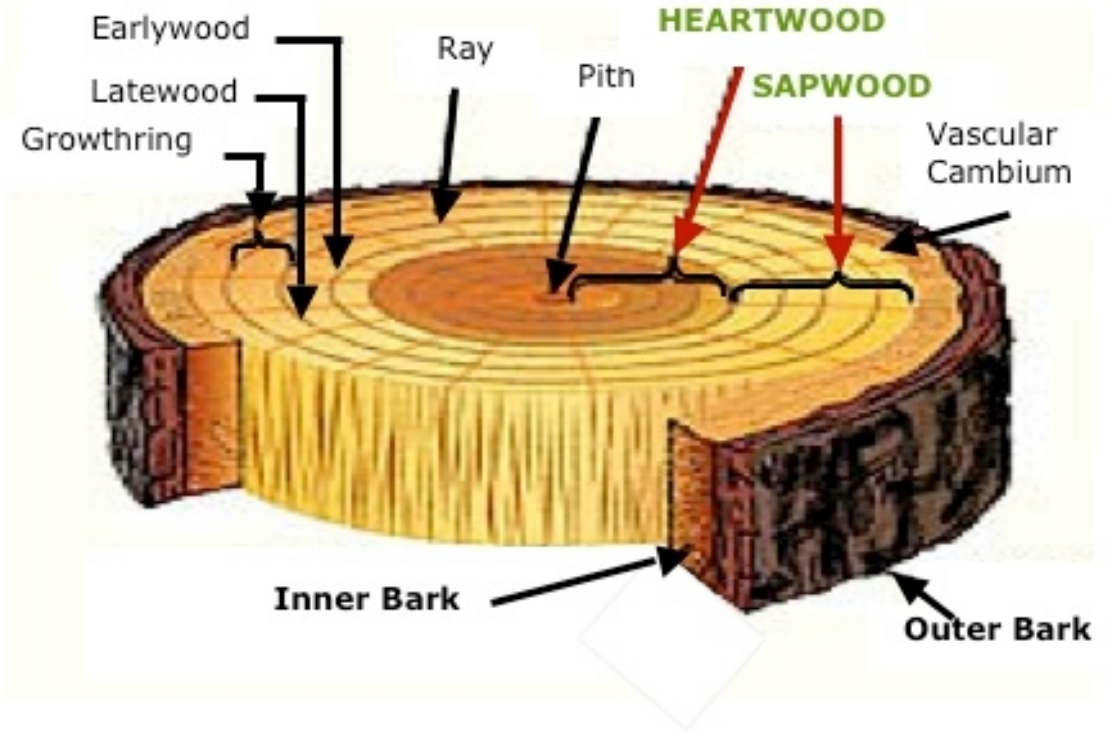

Figure 1.9. *Cross section of a tree trunk with wood anatomy description (adapted from © Merriam-Webster Inc.).*

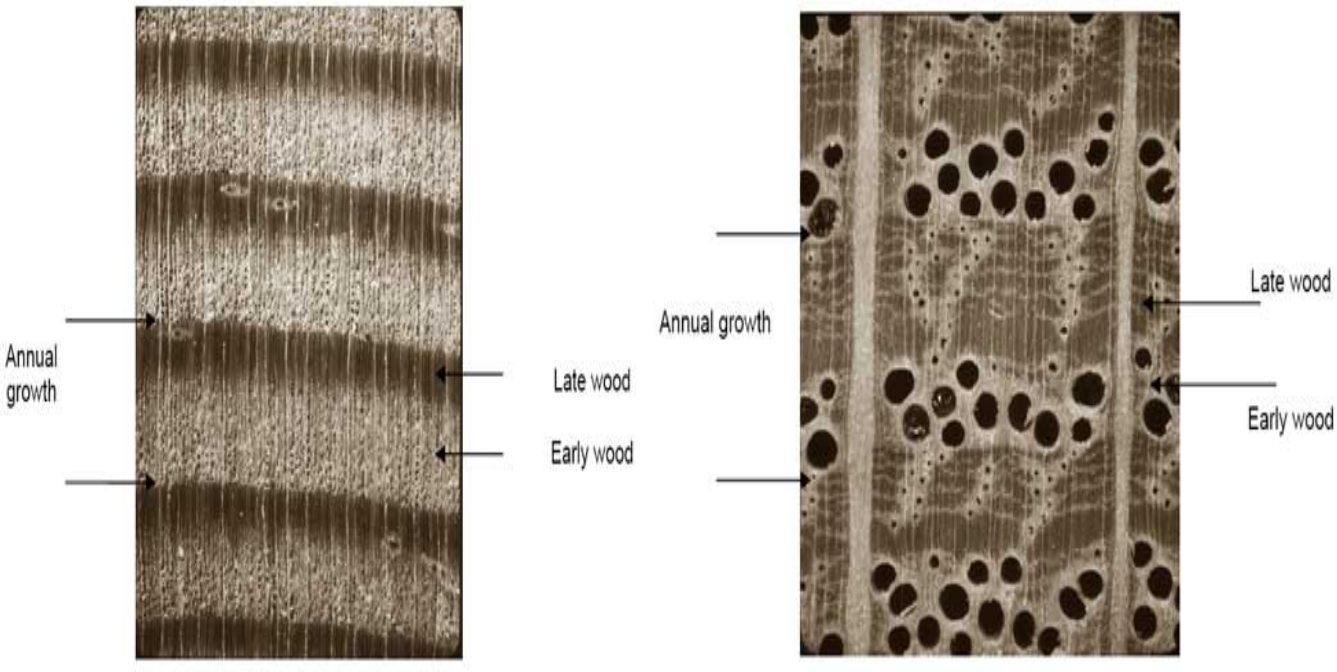

Figure 1.10. (Left) *Transversal sections of softwood (Pseudotsuga menziesii) and* ***(Right)*** *hardwood (Quercus rubra) highlighting differences between earlywood and latewood (images from www.fao.org).*

1.3 The process of wood degradation

Because wood is a complex and heterogenous substrate with recalcitrant compounds, its natural degradation is the result of a long process depending on both biotic and abiotic factors, as well as on the wood traits of the tree species (Cornwell *et al.* 2009).

1.3.1 The microbial degradation of wood

Microorganisms, notably saprotrophic basidiomycete fungi, are the major agents of the wood decomposition in temperate climate forests. The microbial degradation of wood is mainly the result of an enzymatic degradation. Indeed, wood-decaying microorganisms possess a large array of enzymes, allowing them to decompose one or several wood components.

1.3.1.1 Fungi

Wood-decaying fungi are rich in species numbers and functionally diverse. Traditionally, these fungi are divided into three major categories: white rot, brown rot and soft rot, which are distinguishable from their overall effects on wood coloration and consistency. The table 1.2 summarises some features of the different types of rots. Others members of the fungal kingdom are also involved in wood degradation, such as moulds, blue-stain fungi and yeasts.

	White rot simultaneous rot	White rot selective delignification	Brown rot	Soft rot
Properties of decayed wood	Bleached appearance, lighter in colour than sound wood, moist, soft, spongy, strength loss after advanced decay; brittle fracture	Bleached appearance, lighter in colour than sound wood, moist, soft, spongy, strength loss after advanced decay; fibrous appearance	Brown, dry, crumbly, powdery, brittle consistency, breaks up into cubes, drastic loss of strength at initial stage of decay; very uniform ontogeny of wood decay	Soft consistency in wet environments; brown and crumbly in dry environments; generally uniform ontogeny of wood decay
Host and wood type	Hardwood, rarely softwood	Hardwood and softwood	Softwoods; seldom hardwoods; forest ecosystems and timber	Generally hardwoods (softwoods very slightly degraded); forest ecosystems, waterlogged woods
Cell wall constituents degraded	Cellulose, lignin and hemicellulose	Initial attack selective for hemicelluloses and lignin, later also cellulose	Cellulose and hemicelluloses; lignin slightly modified; in some cases, extended decomposition of hardwood (including middle lamella)	Cellulose and hemicelluloses; lignin slightly altered
Anatomical features	Cell wall attacked progressively from lumen; erosion furrows associated with hyphae	Lignin decomposition in middle lamella and secondary wall; middle lamella dissolved by diffusible agents (not in contact with hyphae), radial cavities in cell wall	Decomposition at a great distance from hyphae (diffusion mechanism); entire cell wall attacked rapidly with cracks and clefts	Cell wall attack in the proximity of hyphae starts from cell lumen; longitudinal cylindrical cavities in secondary wall or secondary wall erosion from cell lumen
Examples of causal agent	Basidiomycetes (e.g. *Trametes versicolor, Irpex lacteus, Phanerochaete chrysosporium, Fomes fomentarius*)	Basidiomycetes (e.g. *Ganoderma australe, Phlebia tremellosa, Ceriporiopsis subvermispora, Pleurotus* spp., *Phellinus pini*)	Basidiomycetes exclusively (e.g. *Gloeophyllum* spp., *Laetiporus sulphureus, Piptoporus betulinus, Postia placenta, Serpula lacrymans, Coniophora puteana*)	Mainly ascomycetes; some white-rot (*Inonotus hispidus*) and brown-rot (*Rigidoporus crocatus*) basidiomycetes cause facultative soft-rot decay

On the previous page:

Table 1.2 *Comparison of structural and chemical features caused by saprotrophic fungi during different types of wood decay (adapted from Baldrian, 2008).*

1.3.1.1.1 White-rot fungi

White-rot fungi can completely degrade all the structural wood components, which are cellulose, hemicelluloses and lignin, using a large set of enzymes. They all belong to the Basidiomycota phylum. Two forms of white rot have been described: the simultaneous rot and the selective delignification (Otjen & Blanchette 1986) (Table 1.2). Concerning the simultaneous rot, the mycelium grows through the wood within the lumen. Under the action of lignocellulolytic enzymes, cell walls are progressively degraded from the inside (Figure 1.11. A.). *Trametes versicolor, Irpex lacteus, Phanerochaete chrysosporium, Fomes fomentarius, Ganoderma applanatum and Phellinus robustus* are species that display this kind of white-rot (Blanchette 1984; Martínez *et al.* 2005).

Concerning the selective delignification, the white-rot fungi first attack the lignin and hemicelluloses, from the secondary cell wall to the middle lamella, by diffusion of low molecular weight compounds from the hyphae growing in the lumen. Then, the cellulose is degraded (Figure 1.11. B.). *Ganoderma australe*, *Phlebia tremellosa*, *Ceriporiopsis subvermispora, Pleurotus* spp., *Phellinus pini* and *Xylobolus frustulatus* are species that display this form of white-rot (Blanchette 1984; Martínez *et al.* 2005). It should be mentioned that some fungi can exhibit both forms of white rot. White-rot fungi are the dominant decomposers of hardwoods and thus, are responsible for most of the wood decomposition in temperate and tropical forests (Tuor, Winterhalter & Fiechter 1995). However, several white-rot fungi decompose softwoods.

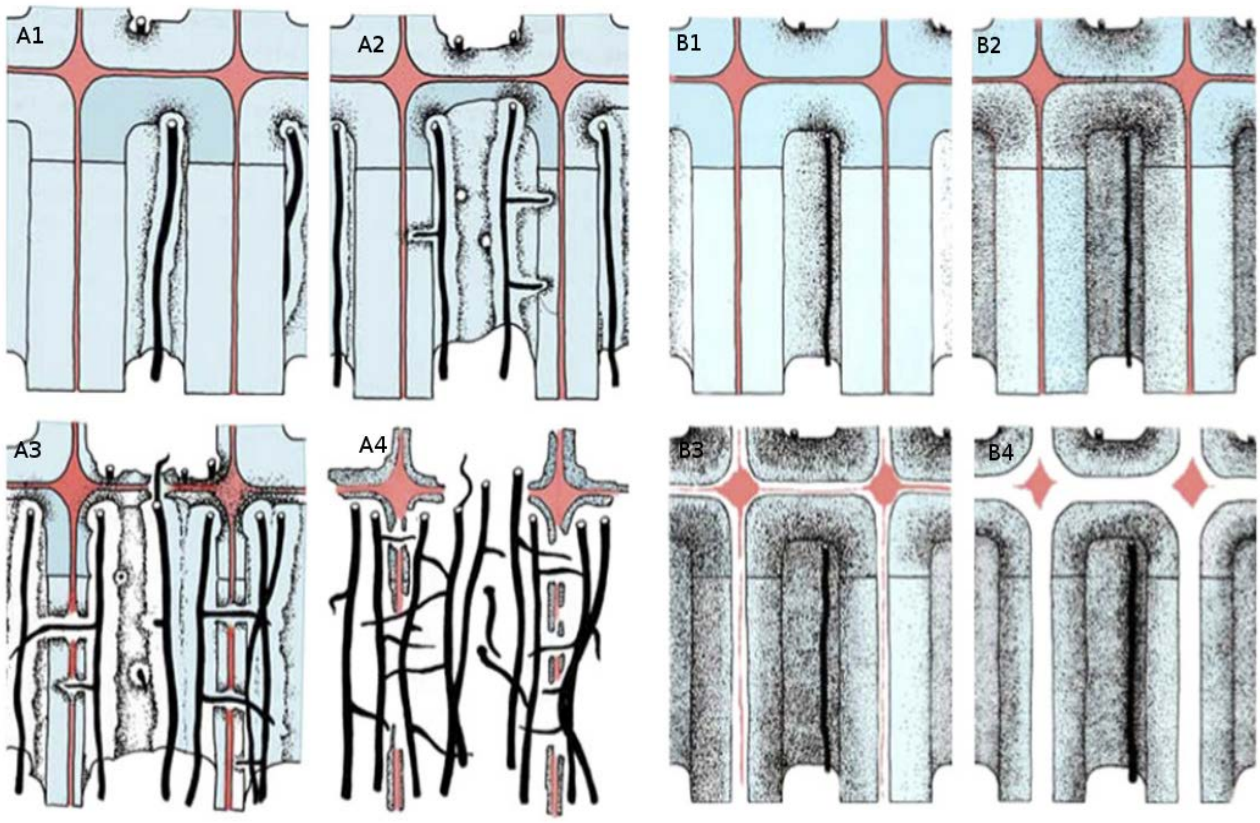

A B

Figure 1.11 *Schematic drawings showing micro-morphological features of the two different forms of white-rot* ***A.*** *Simultaneous rot* ***B.*** *Selective delignification (from Schwarze, 2007).*

1.3.1.1.2 Brown-rot fungi

Brown-rot fungi have the ability to decompose cellulose and hemicelluloses. They can also slightly alter the lignin (Yelle *et al.* 2008), but can not decompose it. They all belong to the Basidiomycota phylum. Similarly to white-rot fungi, brown-rot fungi colonise wood cells from the empty lumen (Figure 1.12). At the early stage of the decay, the degradation is non-enzymatic (Green & Highley 1997). Small extracellular reactive oxygen species (ROS) and oxalic acid are secreted by the hyphae and diffuse into the cell wall. These ROS participate to the cellulose and hemicellulose depolymerisation, via the Fenton reaction which produces hydroxyl radicals (Hammel *et al.* 2002). ROS and oxalic acid also acidify the local environment of the hyphae, which facilitates the carbohydrate hydrolysis (Shimada *et al.* 1994). At more advanced stage of decay, enzymatic processes (cellulases) are involved in the degradation to complete the breakdown of hemicelluloses and cellulose. It results in a characteristic appearance of the wood, with a brown colour due to the lignin and numerous

cracks across the direction of the fibres, which justifies why brown rot is also called “cubic rot”. *Gloeophyllum* spp., *Laetiporus sulphureus*, *Piptoporus betulinus*, *Postia placenta*, *Serpula lacrymans* and *Coniophora puteana* are brown-rot fungi. The brown-rot fungi mainly occur in coniferous trees and thus, are the principal wood decayers in boreal forests (Gilbertson 1981; Renvall 1995). However, some brown-rot fungi are equally commonly found on both hardwoods and softwoods (e.g. *Fomitopsis pinicola*) and others predominantly decompose hardwoods (e.g. *Laetiporus sulphureus*) (Stockland *et al.* 2012).

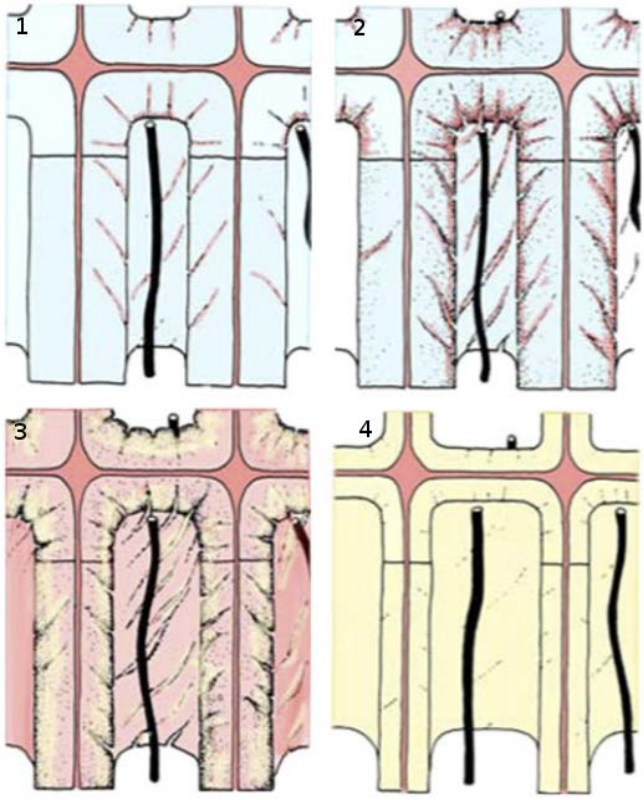

Figure 1.12. *Schematic drawings showing micro-morphological features of the brown rot, with the degradation of cellulose and hemicelluloses (from Schwarze 2007).*

1.3.1.1.3 Soft-rot fungi

Soft-rot fungi are primarily ascomycetes. They degrade the cellulose and hemicelluloses in the central layer (S2) of the secondary cell wall (Savory 1954) and some species (e.g. *Xylaria hypoxylon*) also decompose the lignin (Liers *et al.* 2006). Hyphal growth inside the wood differs from white and brown rot. Indeed, soft-rot fungi grow inside the cell wall, forming biconical and cylindrical cavities along the cellulose microfibrils (Blanchette *et*

al. 2004) (Figure 1.13). Soft-rot fungi are the main decay agents of wood with high water content (Stockland *et al.* 2012), such as waterlogged wood (Björdal, Nilsson & Daniel 1999) and archaeological wood (Filley *et al.* 2001).

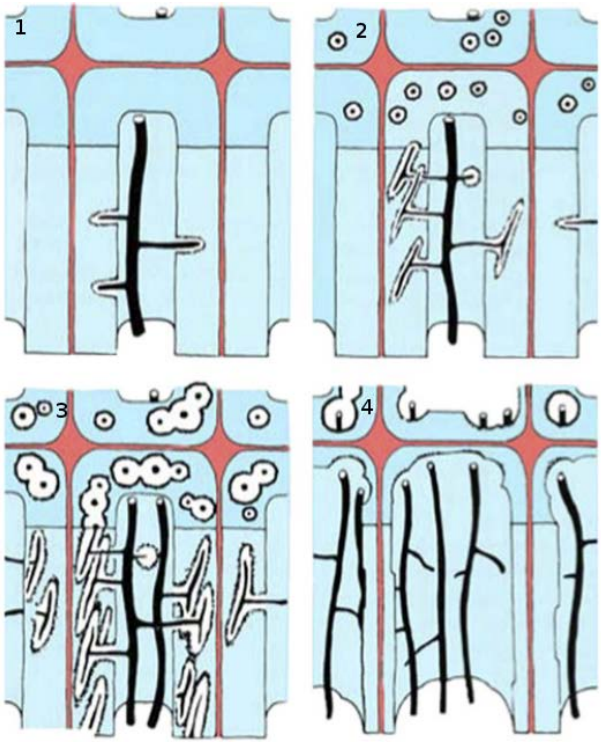

Figure 1.13. *Schematic drawings showing micro-morphological features of the soft rot, with the formation of cavities in the S2 layer (from Schwarze 2007).*

1.3.1.1.4 Other fungi involved in wood degradation

Others members of the fungal kingdom are also involved in wood degradation. Moulds (*Ascomycota* and *Zygomycota*) and blue-stain fungi (*Ascomycota*) grow on wood surface and cause discoloration of the woody material (Hukka & Viitanen 1999). They mainly use simple carbohydrates as source of energy. Examples of mould fungi found on wood are: *Aspergillus* spp., *Penicillium* spp., *Trichoderma* spp., *Mortierella parvispora* and *Mucor hiemalis* (Fukasawa, Osono & Takeda 2009). Moreover, *Trichoderma harzianum* has been shown to be able to decompose holocellulose in decayed wood (Fukasawa, Osono & Takeda 2011). The saprotrophic filamentous ascomycete *Podospora anserina* has also been shown to able to grow on lignin, cellulose and xylan based media (Espagne *et al.* 2008) as well as on wood shavings (Bourdais *et al.* 2012). Yeasts are also found in decaying wood and are able to mineralise polymeric compounds of wood (Botha 2011). For example, members of the genera

Candida, *Pichia* and *Spencermartinsiella* have been isolated from decaying wood and were reported to be able to assimilate products of wood degradation such as xylose and cellobiose (Péter *et al.* 2003, 2011; Guo, Zhu & Bai 2012; Dlauchy, Lee & Péter 2012).

1.3.1.2 Bacteria

Although the mechanism of bacterial wood decomposition has been less studied, they are an active component in both terrestrial and aquatic environments (Greaves 1971). Indeed, bacteria are able to decompose the wood carbohydrates such as cellulose and hemicelluloses (Lynd *et al.* 2002). Bacteria have also been reported to be able to degrade lignin (Crawford *et al.* 1973; Li, Yuan & Yang 2008; Bugg *et al.* 2011). Different patterns of bacterial wood attack have been identified: pit border decay (three types), pit margo and torus decay, tracheid and fibre decay, ray and vessel decay (Greaves 1969). In 1971, H. Greaves classified wood bacterial inhabitants in four categories: (i) the bacteria which affect the permeability of the wood to liquids, but do not significantly alter wood strength; (ii) the bacteria, which may affect the strength properties of the wood and which are able to attack the cell walls; (iii) the bacteria, which functioning as an integral part of the total wood microflora, contribute to the ultimate breakdown of the wood; and (iv) finally those more passive colonisers which do not contribute to the wood breakdown, but which may be able to influence the organisms which do by the production of inhibitory or promoting compounds (Greaves 1971). Later, three different patterns of bacterial degradation of wood cell wall were clearly defined: tunnelling, erosion and cavitation (Singh & Butcher 1991). Tunnelling bacteria can degrade wood carbohydrates and lignified elements (tracheids, fibres, vessels). They penetrate the cell wall from the lumen face and then degrade it by tunnelling from the S3 layer to the middle lamella (Figures 1.14 and 1.15). Erosion bacteria also attach the cell wall from the lumen towards the middle lamella, but produce erosion troughs in the exposed faces of the cell wall (Figures 1.14 and 1.15) (Singh 2007). Cavitation bacteria form irregular cavities within the secondary cell wall that are oriented perpendicular to the long direction of the fibres. They mainly decompose carbohydrates of the secondary wall and leave residual wall material in the cavities (Blanchette 2000).

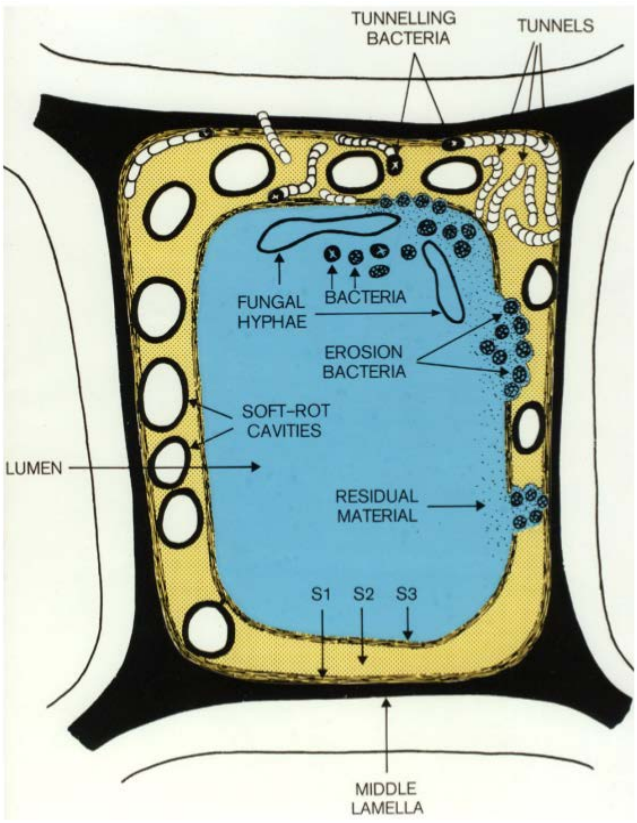

Figure 1.14. *A diagram illustrating decay patterns produced during cell wall degradation by soft rot fungi and tunnelling and erosion bacteria (from Singh 2007).*

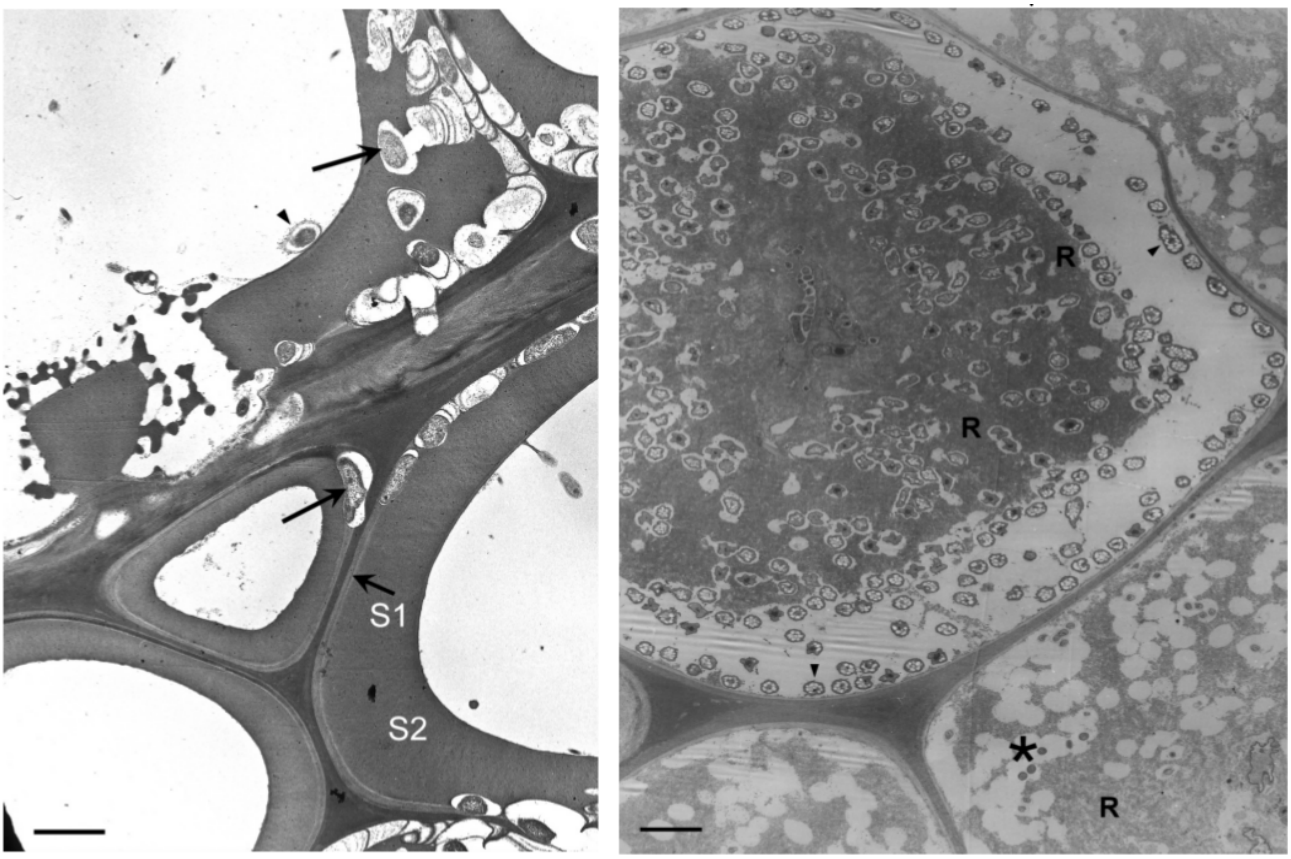

Figure 1.15. *Transmission electron microscopy image of wood degraded by bacteria. Bar=2 µm.* ***(Left)*** *Fibre-tracheid walls in Alstonia scholaris wood attacked by tunnelling bacteria (arrows). Bacteria are present within S1 and S2 layers. The arrowhead points to a bacterium in close contact with the lumen face of the cell wall.* ***(Right)*** *Tracheid cell walls in Pinus sylvestris wood attacked by erosion bacteria (arrowheads), which are abundantly present along the cell wall and within cell wall residues (R) in one tracheid. Erosion bacteria are absent from other tracheids, which contain abundant cell wall residues and some scavenging bacteria (*) (from Singh 2007).*

1.3.1.3 Enzymatic degradation of wood

As mentioned above, the microbial degradation of wood involves numerous and diverse enzymes. The biochemistry of this process is complex and here, only an overview of the enzymatic degradation of wood in aerobic conditions is proposed.

1.3.1.3.1 Degradation of cellulose

To decompose cellulose, aerobic fungi and bacteria use extracellular cellulase

enzymes. Occasionally, for bacteria, the enzyme are present in complexes at the cell surface (Lynd *et al.* 2002). Cellulases are hydrolytic enzymes that break the β-1,4-glycosidic linkages of cellulose. Three types of cellulases are involved in the cellulolysis. Endoglucanases (endo-1,4-β-glucanases, EGs) hydrolyse internal bonds and release new terminal ends. Cellobiohydralases (exo-1,4-β-glucanases, CBHs) hydrolyse the existing or the endoglucanase-generated chain ends. Both EGs and CBHs release cellobiose molecules. β-glucosidases cleave the cellobiose and finally release two molecules of glucose (Pérez *et al.* 2002) (Figure 1.16).

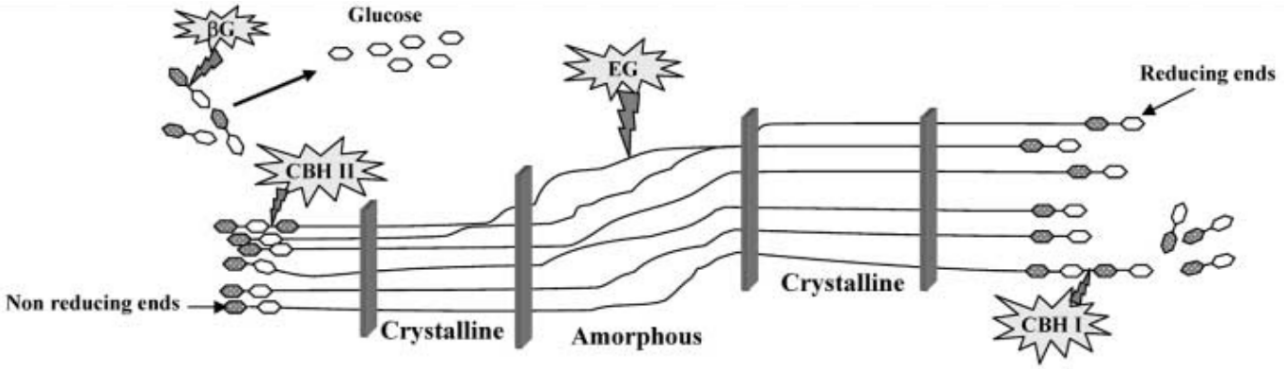

Figure 1.16. *Enzymatic degradation of cellulose to glucose. CBHI Cellobiohydrolase I acts on the reducing ends; CBHII cellobiohydrolase II acts on the non-reducing ends; EG endoglucanases hydrolyze internal bonds. β-G β-Glucosidase cleaves the cellobiose disaccharide to glucose. (from Pérez et al. 2002).*

In addition to enzymatic systems, oxidative processes can also be involved in cellulose degradation by wood-rotting basidiomycetes (Baldrian & Valášková 2008). Indeed, hydrogen peroxide (H_2O_2) can be produced by some rotting fungi and then be transformed into hydroxyl radicals (OH•), via the Fenton reaction:

$$H_2O_2 + Fe^{2+} + H^+ \rightarrow H_2O + Fe^{3+} + OH\bullet$$

These hydroxyl radicals are able to cleave cellulose.

1.3.1.3.2 Degradation of hemicelluloses

Hemicelluloses are degraded to monosaccharides and acetic acid, by different hydrolytic enzymes, called hemicellulases, acting in cooperation. According to the hemicellulose composition, *i.e.* primarily xylan in hemicellulose of hardwood and mannan in

hemicellulose of softwood (see 1.2.1.2 section), the enzymes involved in the degradation differ. There are five steps involved in hemicellulose degradation (Pérez *et al.* 2002) (Figure 1.17). First, an enzyme, endoxylanase or endomannase, attacks internal points of the main chain of hemicellulose to produce smaller molecule fragments. Then, these small fragments are hydrolysed by β-xylosidase or β-glucosidase to produce monosaccharides: xylose or glucose and mannose, respectively. Finally, three different enzymes break specific bonds between the side chains and the main chain.

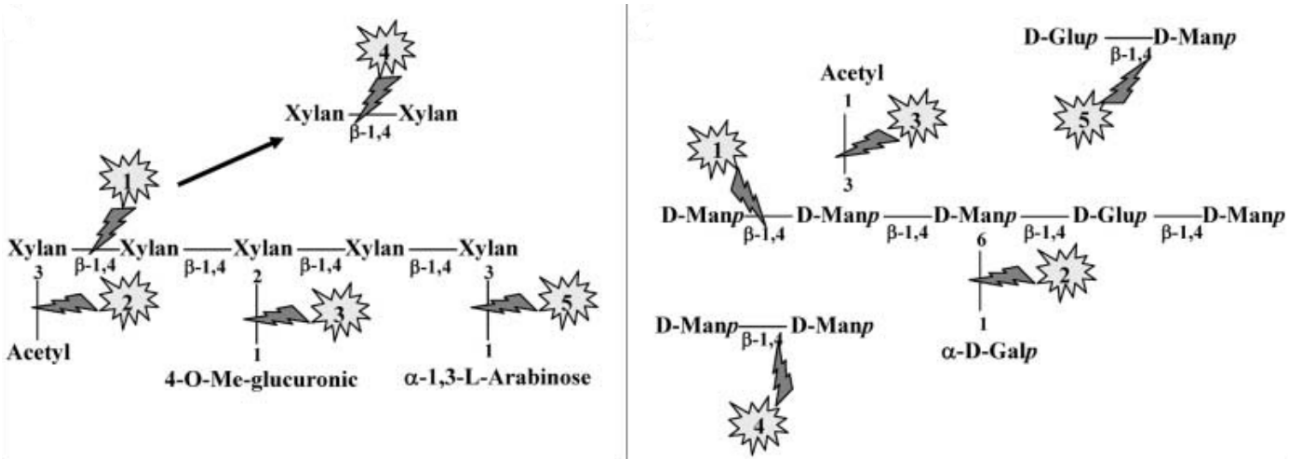

Figure 1.17. (Left) *Enzymatic degradation of glucuronoxylans, found in hardwoods. 1 Endoxylanase, 2 acetylxylan-esterase, 3 α-glucuronidase, 4 β-xylosidase, 5 α-arabinase.* ***(Right)*** *Enzymatic hydrolysis of glucomannan found in softwoods. 1 Endomannase, 2 α-galactosidase, 3 acetylglucomannan-esterase, 4 β-mannosidase, 5 β-glucosidase (from Pérez et al. 2002).*

In 2012, 1495 bacterial genomes from different phyla were analysed (Mba Medie *et al.* 2012) using the Carbohydrate Active Enzyme (CAZy) database (Cantarel *et al.* 2009; Levasseur *et al.* 2013) to search for genes encoding for cellulases, hemicellulases and pectinases. This analysis revealed that 38% of the genomes analysed encoded at least one cellulase gene. Half of these genomes (19.2% of the total amount of genomes) belongs to bacteria with saprophytic lifestyle and possesses at least one cellulase gene and three or more hemicellulase and pectinase genes, suggesting that many bacteria can decompose wood carbohydrates.

1.3.1.3.3 Degradation of lignin

Because of its structure and properties (see section 1.2.1.3), lignin is highly resistant to biodegradation. The degradation of lignin differs from the degradation of wood carbohydrates. Indeed, microbial ligninolysis involves non-specific, non-hydrolytic and extracellular degrading systems, which has been described as “enzymatic combustion” (Kirk & Farrell 1987). Thus, ligninolytic enzymes are non-specific, oxidative and extracellular. As mentioned above, wood-rotting fungi, especially white-rot fungi, are the main agents of lignin degradation in forest ecosystems. These fungi possess ligninolytic systems which consist of oxidases, peroxidases and hydrogen peroxide producing enzymes (Baldrian 2008). Laccases are oxidases that oxidise their substrates using molecular oxygen (Baldrian 2006). They are produced by numerous wood-rotting fungi and involved in lignin decomposition (Leonowicz *et al.* 2001).

Peroxidases are oxidases that require the presence of extracellular hydrogen peroxide to oxidise their substrates. The hydrogen peroxide is usually formed by the oxidation of different extracellular metabolites. There are three types of fungal ligninolytic peroxidases: lignin peroxidases (LiP), manganese peroxidases (MnP) and versatile peroxidases (VP). LiP preferentially catalyses the cleavage of the C_{α}-C_{β} bond of the propyl side chain of lignin (Kirk & Farrell 1987). LiP is also capable of oxidising various phenolic and non-phenolic substrates (ten Have & Teunissen 2001). Veratryl alcohol, an aromatic compound and secondary metabolite produced by some white-rot fungi, is necessary for LiP catalysis. LiP is produced by fewer white-rot fungi than MnP and laccase. MnP oxidises Mn^{2+} to Mn^{3+} which is then stabilised by chelation. The chelated Mn^{3+} is diffusible and can oxidise phenols, non-phenolic aromatic compounds and carboxylic acids (Hofrichter 2002). VP combines the catalytic properties of LiP, MnP and plant / microbial peroxidases oxidising phenolic compounds (Ruiz-Dueñas *et al.* 2001).

Other extracellular enzymes are also involved in lignin degradation, in particular oxidases generating hydrogen peroxide. Indeed, peroxidases require hydrogen peroxide. These oxidases include aryl-alcohol oxidase (AAO), glyoxal oxidase (GLOX) (Kersten 1990). Finally, some mycelium-associated dehydrogenases that reduce lignin-derived compounds are also involved in lignin decomposition, *e.g.* aryl-alcohol dehydrogenases (AAD) (Gutierrez *et al.* 1994) and quinone reductases (QR) (Guillén *et al.* 1997). Thus, microbial lignin degradation is the result of the cooperation of several enzymes (Figure 1.18).

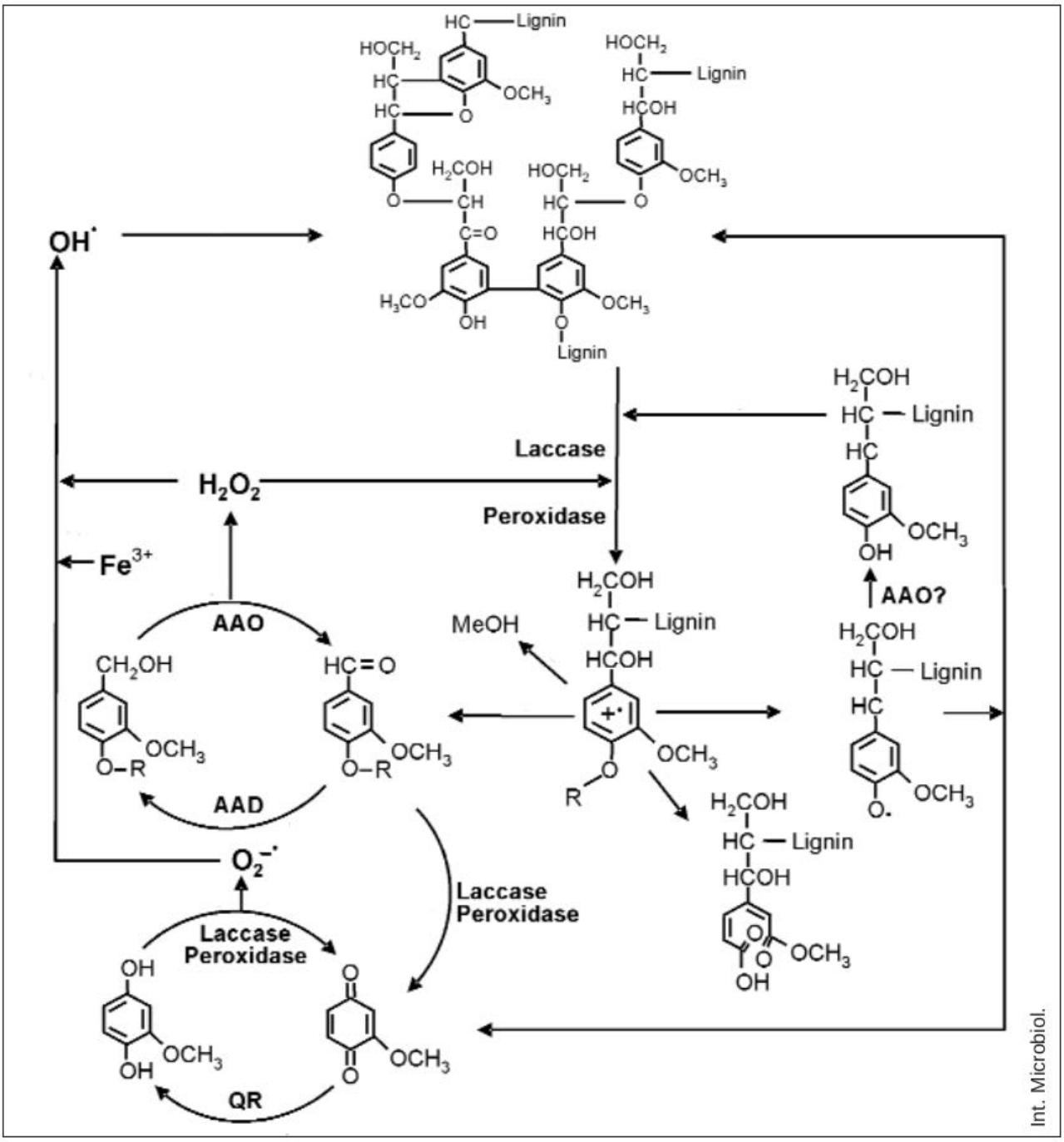

Figure 1.18. *Schematic representation of lignin biodegradation including enzymatic reactions and oxygen activation. AAO, aryl-alcohol oxidase ; AAD, aryl-alcohol dehydrogenase ; QR, quinone reductase (from Martínez et al. 2005).*

Concerning the lignin degradation by bacteria, peroxidases have also been identified (Ramachandra, Crawford & Hertel 1988; Ahmad *et al.* 2011; Brown & Chang 2014). Laccases are also found in bacteria (Ausec *et al.* 2011) and thus are potentially involved in lignin degradation (Ahmad *et al.* 2010).

1.3.2 The animal degradation of wood

In terrestrial ecosystems, many invertebrates feed on wood and thus are important agents of wood decomposition (Ausmus 1977). Among them, termites (*Isoptera*) and wood-boring beetles (*Coleoptera*) are thought to have a significant impact on wood decay, at global scale (Cornwell *et al.* 2009). These insects degrade wood with both physical and enzymatic actions. Indeed, they grind wood with their mandibles to reduce the particle size and decrease the crystallinity of the cellulose. The ability to then digest lignocellulose is primarily due to a nutritional symbiosis between the insects and their intestinal microbiota (Breznak 1982). Indeed, cellulases produced by gut-associated bacteria have been detected in the gut of termites (Tokuda & Watanabe 2007) as well as cellulose-degrading bacterium and fungi in the gut of *Saperda vestita*, a wood-boring longhorned beetle (Delalibera, Handelsman & Raffa 2005). Some termites also possess, in their hindgut, symbiotic protists with cellulase genes (Ohkuma 2003).

Enzymatic degradation actions can also occur on wood, outside the gut of insects, thanks to other insect-associated microorganisms. Indeed, among termites and beetles, some species are fungus-farming insects: fungus-growing termites and ambrosia beetles, respectively (Figure 1.19) (Mueller & Gerardo 2002). These relationships have been described as symbiotic, more precisely an ectosymbiosis, where the insect farmers cultivate fungi for food. Interestingly, bacteria are also present in theses symbiotic environments (Visser *et al.* 2012; Hulcr *et al.* 2012). Regarding the termite – fungal association, Actinobacteria (Visser *et al.* 2012) and *Bacillus* sp. (Um *et al.* 2013) have been isolated from fungus-growing termites colonies and have been reported to produce selective molecules against host antagonists, and so to act as defensive symbionts. Similarly, in the beetle-fungal association, a *Streptomyces* sp. producing an antifungal molecule called mycangimycin was identified and the mycangimycin has been shown to inhibit beetle's fungal antagonist (Scott *et al.* 2008; Oh *et al.* 2009). Ambrosia fungi can be saprotrophic, providing nitrogen from the phloem to the larvae (Ayres *et al.* 2000), or tree pathogens (Hulcr & Dunn 2011). Concerning the termite – fungal association, only the termites members of the subfamily *Macrotermitinae* have developed an ectosymbiosis with fungi of the genus *Termitomyces* (Aanen *et al.* 2002). The *Termitomyces* fungi are saprotrophic and can degrade lignin, cellulose and hemicelluloses from plant-derived material (Hyodo *et al.* 2003; Ohkuma 2003). The fungus-growing termites cultivate the fungus in their nest, on a particular medium, made of termite faecal pellets with partially digested plant debris and called the fungus comb (Figure 1.19).

Figure 1.19. (Left) *The ambrosia beetle Xylosandrus crassiusculus with eggs inside a garden of its symbiont fungus, Ambrosiella xylebori (gray-coloured surface) (from Hulcr & Dunn 2011).* ***(Right)*** *Macrotermes bellicosus fungus-growing termites on a fungal comb colonised by Termitomyces sp. (from Mueller & Gerardo 2002).*

At global scale, termite contribution to wood decay and thus to global carbon cycle is not negligeable (Ulyshen & Wagner 2013). They also affect locally the wood turnover, by their presence. However, it is worth to highlight that termites are not evenly distributed around the globe. They are largely absent from cold-temperate, boreal and polar regions, but present their highest diversities and abundances in tropical rain forests and tropical savannas (Figure 1.20) (Cornwell *et al.* 2009).

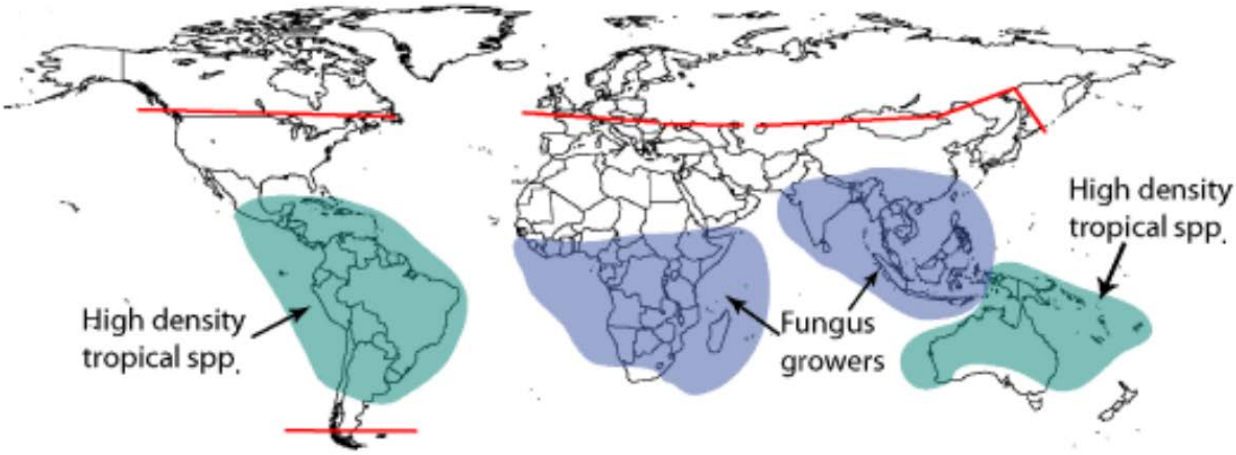

Figure 1.20. *Global distribution map of termites. Red lines represent the cutoff points beyond which no termites are found; areas with fungus-growing termites are in blue and areas with non-fungus growing termites are in green (from Cornwell et al. 2009).*

1.3.3 The abiotic degradation of wood

In terrestrial ecosystems, wood degradation can also result from abiotic factors. Solar ultraviolet B (UV-B) radiations can degrade lignocellulosic material by a process called photodegradation. For wood, it corresponds to a photochemical mineralisation of carbon and in particular, of lignin molecules which are effective light-absorbing compounds over a wide range of wavelengths (Austin & Ballaré 2010). In contrast, cellulose is not photodegraded. Photodegradation is mainly important in dry environments with high irradiance, such as semi-arid (Austin & Vivanco 2006) and arid ecosystems (Day, Zhang & Ruhland 2007; Gallo *et al.* 2009).

Acid rains can also have degradative effect on wood (Hon 1994), as well as leaching, a process corresponding to the removal of soluble material by water such as dissolved organic carbon and polyphenols of wood (Spears & Lajtha 2004). All these abiotic factors involved in wood degradation can facilitate the biotic degradation, by increasing the accessibility of the woody substrate.

1.3.4 Factors affecting the wood degradation process

The process of wood degradation is non-uniform across the globe. The heterogeneity of wood and the diversity of agents and mechanisms involve in wood degradation participate

to the variability of this process. Additionally, climate, site environment and physicochemical parameters affect this process (Weedon *et al.* 2009).

In forest, mean annual temperature, initial density of wood and diameter of logs are the main determinants of wood decay rates (Mackensen, Bauhus & Webber 2003). For smaller woody fragments (wood blocks and sawdust), it has been shown that the initial decay of wood in soil is influenced by the size of the fragment, the soil origin and the nitrogen availability (van der Wal *et al.* 2007). The wood degradation process depends also on some wood functional traits. For instance, in the case of angiosperms, wood density and decay rate are significantly correlated (Chave *et al.* 2009) ; nitrogen content, phosphorus content and C:N ratio also influence significantly the wood decomposition rate (Weedon *et al.* 2009).

The microbial degradation of wood, mainly driven by saprotrophic basidiomycetes, is affected by environmental variables. Extracellular enzyme activities and wood decomposition rates have been shown to increase with moisture content (A'Bear *et al.* 2014). An increase in temperature also results in an increase of wood decomposition rate (Boddy 1983). Variations in fungal species richness also influence wood decomposition by fungi, with the decomposition rate decreasing with fungal richness, under a constant temperature (Fukami *et al.* 2010). However, under a fluctuating temperature regime, co-existence of few species increases wood decomposition rate (Toljander *et al.* 2006). Diverse types of interactions exist between wood-decaying basidiomycetes, but competitive interactions have been shown to be the most common and such interactions might influence the fungal community functioning (Boddy 2000). Bacteria are also involved in wood degradation and are known to interact with fungi during this process (de Boer *et al.* 2005; Frey-Klett *et al.* 2011). For instance, the presence of white-rot fungi colonising wood blocks has been shown to reduce the number of wood-inhabiting bacteria and to alter the bacterial community composition (Folman *et al.* 2008). The bacterial strains isolated from decaying-wood colonised by *Hypholoma fasciculare* have been described as acid-tolerant strains able to grow at pH 4 (Valásková *et al.* 2009). However, compared to fungi, little is known about the factors affecting wood degradation by bacteria. Finally, interactions between saprotrophic fungi and invertebrate grazers also influence the rate of wood decay (Crowther, Boddy & Hefin Jones 2012).

1.4 Biodiversity of organisms associated with decaying wood

In terrestrial ecosystems, dead wood accommodates a very high species diversity of saproxylic organisms. Stockland, Siitonen and Jonsson (2012) defined the term saproxylic as “any species that depends, during some part of its life, upon wounded or decaying woody material from living, weakened or dead trees”. Among saproxylic microorganisms, fungi have been studied for decades and their communities present high diversity and richness in decaying trees (Kubartová *et al.* 2012). Saproxylic fungi include wood-decaying fungi, but also mycorrhizal fungi and mycoparasites (Zugmaier, Bauer & Oberwinkler 1994).

Fungal successions are well-known phenomena (Frankland 1998) and the temporal dimension of the process of wood degradation is very important. Indeed, during this process, wood substrate quality constantly evolves with time. Fungal community succession on decaying Norway spruce has been described with decreasing wood density and C : N ratio, and increasing moisture and lignin content (Rajala *et al.* 2012). According to the decay stage of Norway spruce, the proportion of fungal life strategy groups is also evolving. Soft-rot fungi are present only in the early stage of decay while brown- and white-rot are present in all stages, but in varying proportions (Figure 1.21). Richness of active fungi has also been shown to increase with decomposition stage (Rajala *et al.* 2011). Myxomycetes (*Amoebozoa*) are also known to colonise coarse woody debris in forests (Ko *et al.* 2009) and to present community succession according to the stage of decay (Takahashi & Hada 2009).

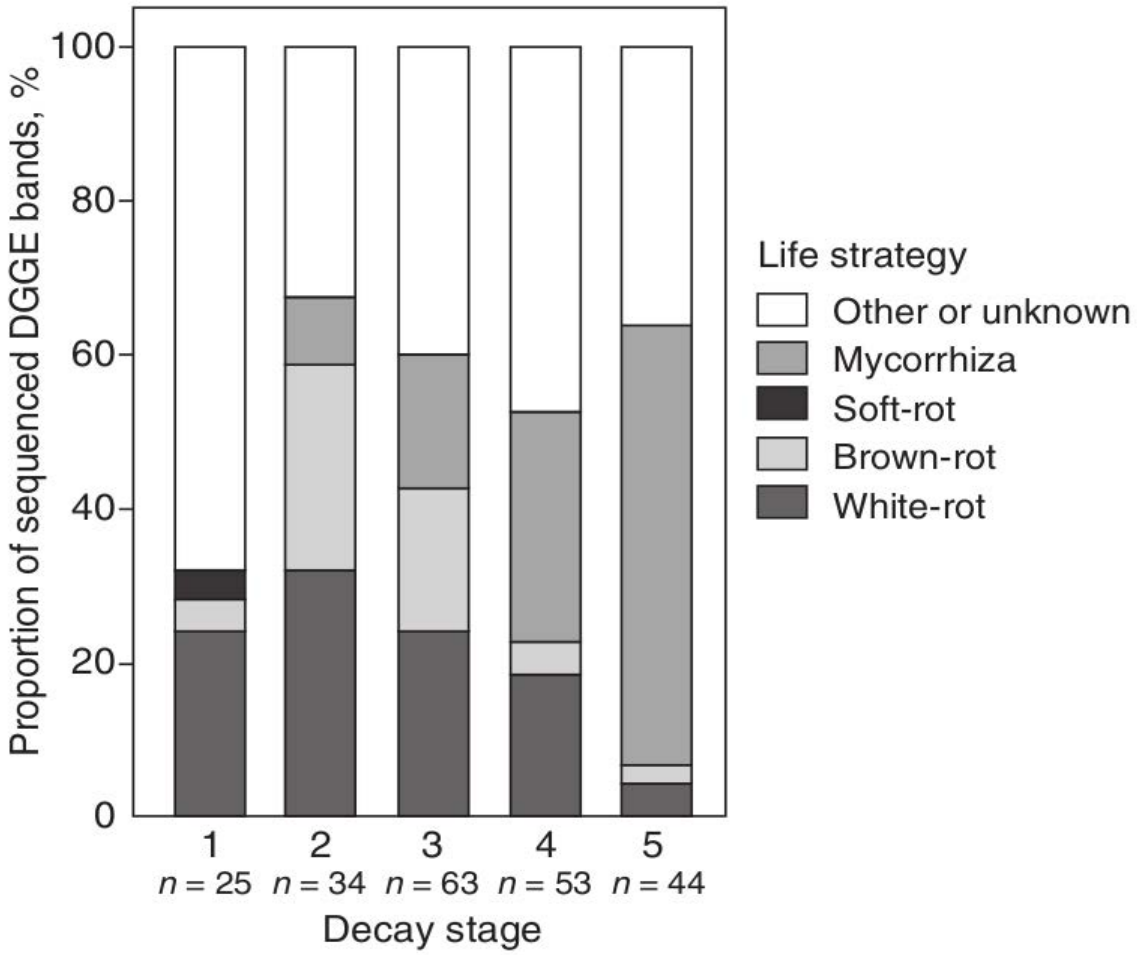

Figure 1.21. *Succession of fungal life strategy groups during the decomposition of Norway spruce logs. Decay stage of the logs was classified from 1 to 5 (1 being a recently dead tree and 5 being an almost decomposed tree). Fungal identification was based on the comparison of DNA sequences of excised ITS-DGGE bands with reference sequences in public databases (from Rajala et al. 2012).*

While the role of bacteria in wood decay has been less studied, they are also present and highly diverse on decaying wood (Zhang et al. 2008a). *Proteobacteria* has been reported to be the major phylum among bacterial communities associated with decaying-wood (Zhang *et al.* 2008a; Valásková *et al.* 2009; Sun *et al.* 2014). The structure of these bacterial communities is influenced by the types of forest soils where the wood is decomposing and the composition of these bacterial communities has been shown to be stable over months during the early stages of wood colonisation (Sun *et al.* 2014).

Saproxylic organisms growing on the surface of dead wood, called epixylic, include mosses (*Bryophyta*), liverworts (*Marchantiophyta*) and lichens. It has been shown that macrolichen and bryophyte species composition varies with the stage of wood decay (Botting & DeLong 2009).

Animal kingdom also possesses saproxylic species. Saproxylic insects are a diverse, species-rich (several hundreds) and dominant functional group on dead wood (Grove 2002). These insects have different trophic habits and interaction types (predator, commensal) (Quinto *et al.* 2012). Indeed, insects can be xylophagous, saprophagous or xylomycetophagous (inhabiting wood and consuming fungi growing in wood or cultivating them for feeding). Vertebrates are also associated with dead wood. Cavity-nesting birds, especially woodpeckers (*Picidae*), are known to use tree cavities as nest sites (Harmon *et al.* 1986; Martin & Eadie 1999). Finally, small mammals (e.g. mouse, shrew, squirrel) also use tree cavities and logs for shelter and nesting (Harmon *et al.* 1986; McCay 2000).

Such diversity and richness of species in the same habitat lead to a network of interactions between whole the saproxylic species. Trophic interactions are known and a saproxylic food web has been described (Figure 1.22) (Stockland *et al.* 2012).

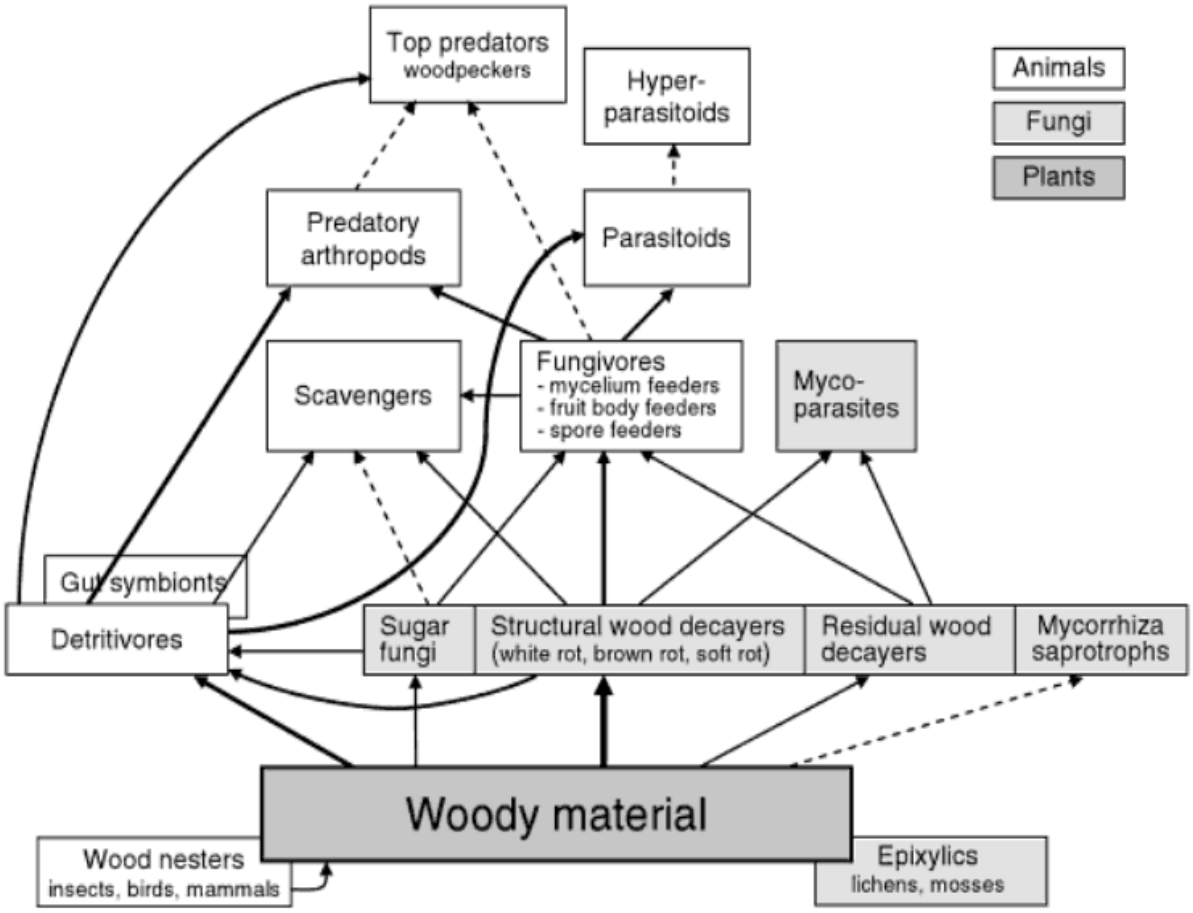

Figure 1.22. *A saproxylic food web, with organisms sorted by their functional roles at different trophic levels. Arrows indicate the main nutrition and energy flows and the thickness of the arrows indicates the magnitude of that pathway (from Stockland et al. 2012). Epixylics include both fungi and plants. Gut symbionts include bacteria, fungi and protists.*

Decaying wood is a habitat where various saproxylic species interact. A part of these species is directly involved in the process of wood degradation and this process is the result of complex interactions between the members of this biotic community. Thus, it raises the question of the taxonomic and functional diversities of the organisms involved in wood degradation, especially among the microorganisms. Indeed, as mentioned several times in the previous sections, saprotrophic basidiomycetes are the main agents of wood decomposition in forest ecosystems, but bacteria are also involved in this process even if they have been much less studied.

1.5 Working hypotheses and objectives

Bacteria and fungi are known to cohabit and interact in numerous environments (Frey-Klett *et al.* 2011). For instance, bacterial-fungal interactions have been studied during the wine-making process (Alexandre *et al.* 2004), during the maturation of cheese (Addis *et al.* 2001), on ancient manuscripts (Michaelsen, Piñar & Pinzari 2010), in the lungs of cystic fibrosis patients (Mowat *et al.* 2010), in nectar of plants (Vannette, Gauthier & Fukami 2013), forest soils (Frey-Klett *et al.* 2005) and contaminated soils (Andersson *et al.* 2000).

The mycosphere corresponds to the microhabitat surrounding fungal hyphae (Frey-Klett, Garbaye & Tarkka 2007). It is known that some soil fungi (Warmink, Nazir & van Elsas 2009), pathogenic fungi (Dewey, Wong & Seery 1999) or symbiotic fungi (Nuccio *et al.* 2013) can influence the bacterial community structure and composition in their mycosphere. On the contrary, bacteria can affect fungal development. For example, bacteria have been shown to induce spore germination in bark beetle fungal symbionts (Adams *et al.* 2009) and to promote the growth of a white-rot fungus (Kamei *et al.* 2012). Thus, these bacterial-fungal interactions significantly affect the functioning of ecological niches such as the rumen of lambs (Chaucheyras-Durand *et al.* 2010), the rhizosphere (Frey-Klett *et al.* 2007), soils (Ushio, Miki & Balser 2013) or ant nests (Currie 2001).

Decaying wood is also a habitat where bacteria and fungi interact (de Boer *et al.* 2005). However, little is know about the functioning of the complex microbial communities associated with decaying-wood. Therefore, the present work intends to explore bacterial-fungal interactions during the process of wood degradation, at different levels.

Our first working hypothesis was that a mycosphere effect also exists on the bacterial communities surrounding wood-decaying fungi during the process of wood decomposition. We thus questioned whether the presence of a white-rot fungus affects both the taxonomic and functional structures of bacterial communities in a woody environment.

Our second hypothesis was that bacterial-fungal interactions taking place on wood influence the wood degradation process. Theoretically, these interactions can be synergistic, antagonistic or neutral. We questioned whether the presence of bacteria can modulate the lignocellulolytic system of a white-rot fungus, and we intented to evaluate the respective contribution of the different actors of this interaction to the process of wood degradation.

To test these hypotheses, we decided to use a simplified biological system containing

three members, *i.e.* wood, fungi and bacteria. Concerning the wood and the fungus, biological models were selected: the hardwood *Fagus sylvatica* and the white-rot fungus *Phanerochaete chrysosporium*.

1.6 Biological models

Faced with the diversity of organisms associated with dead wood and with the heterogeneity of the wood substrate, we decided to use biological models for the present work.

1.6.1 ***Fagus sylvatica***

Fagus sylvatica L., the European beech is an angiosperm belonging to the *Fagaceae* family (Figure 1.23). Its distribution extends from southern England and southern Sweden to the Apennins of southern Italy. It is a dominant or co-dominant tree in a wide range of habitats, making it one of the most important forest trees in Europe (Giesecke *et al.* 2006). This is the main reason why we decided to use beech wood in all the present work. Beech wood is diffuse porous to semi-ring porous (Figure 1.24) and its average density is 0.72 $g.cm^{-3}$ (Schwarze 2007). Heartwood and sapwood can be distinguished. The beech wood used in our work originates from Haye forest (Meurthe et Moselle, France) and was kindly provided by the INRA UMR1092 LERFOB.

Figure 1.23. *Beech forest in Europe.*

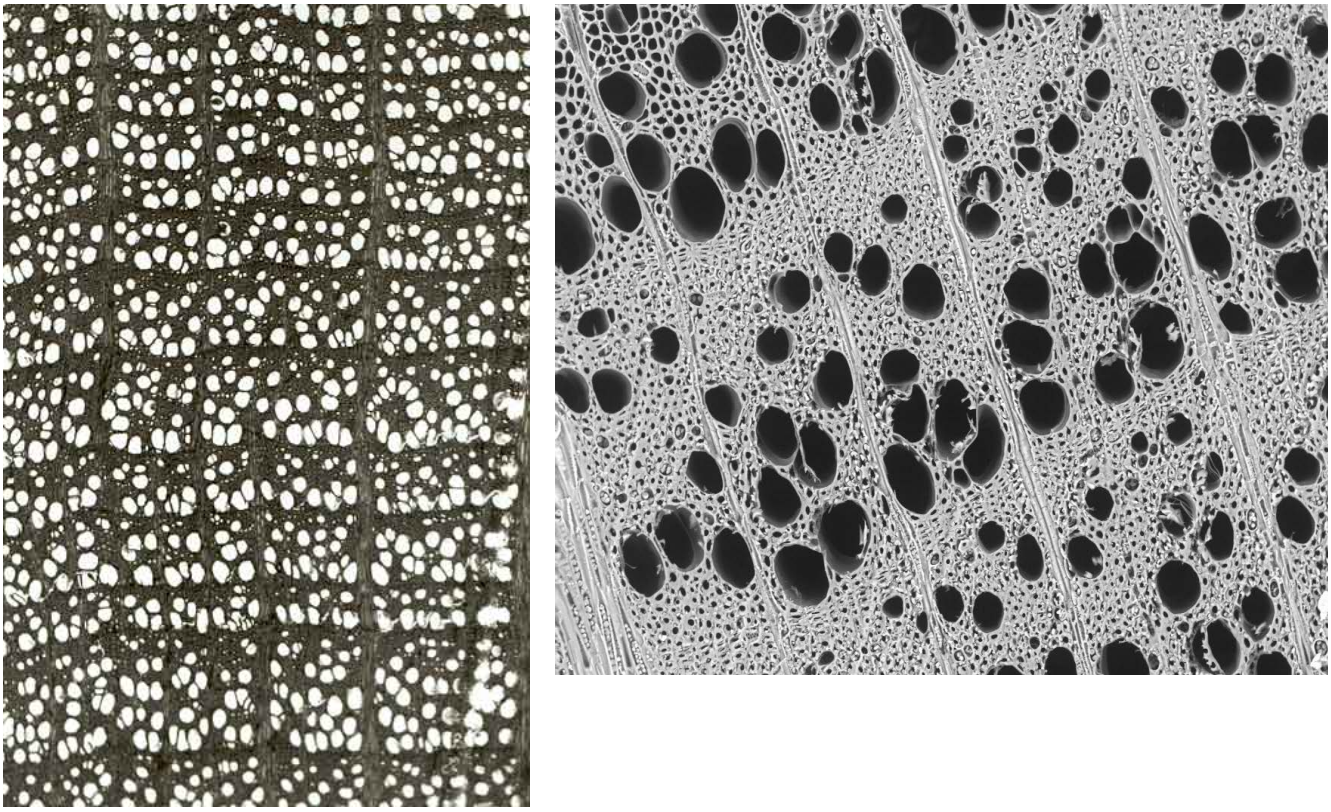

Figure 1.24. (Left) *Transversal section (from http://www.woodanatomy.ch/)* ***(Right)*** *and scanning electron microscope image (from Christophe Rose, INRA Nancy) of Fagus sylvatica.*

1.6.2 ***Phanerochaete chrysosporium***

Phanerochaete is a genus of wood-inhabiting *Basidiomycota*, belonging to the *Phanerochaetaceae* family (Larsson 2007), and to the *Polyporales* order of the *Agaricomycetes* class (Wu *et al.* 2010). It is a polyphyletic genus (De Koker *et al.* 2003; Wu *et al.* 2010). All members of the *Phanerochaete* genus are white-rot fungi. Their basidiocarps are resupinate and *Phanerochaete* species belong to corticioid fungi. According to the *Cortbase* database version 2 (Parmasto, Nilsson & Larsson 2004), 136 species of *Phanerochaete* have been described, which represents a large genus among the corticioid fungi. *Phanerochaete* is also a geographically widespread genus, isolated in Europe and Russia (Dresler-Nurmi *et al.* 1999), in Asia (Wu 1998), in South Africa (De Koker *et al.* 1998), in North America (Burdsall & Eslyn 1974) and in South America (Martinez & Nakasone 2005), on both angiosperms and gymnosperms.

The *Phanerochaete chrysosporium* species was first described by Burdsall and Eslyn in 1974. A strain was isolated in the Sonoran Desert, Arizona, in 1971, on dead wood of *Platanus wrightii* or Arizona sycamore. The anamorphic state of *P. chrysosporium* is also know as *Sporotrichum pulverulentum*. Later, *P. chrysosporium* was extensively studied, in particular for its lignin-degrading enzymes (Tien & Kirk 1983), such as lignin peroxidases (LiP) (Johjima *et al.* 1999) and manganese peroxidases (MnP) (Bonnarme & Jeffries 1990). It has also been used for bioremediation studies, to degrade pentachlorophenol (PCP) (Shim & Kawamoto 2002) or reactive dyes (Gao *et al.* 2008). In natural ecosystems, *P. chrysosporium* has been found in Russia and Kazakhstan (Dresler-Nurmi *et al.* 1999), as well as on beech wood chips in Austria (Fackler *et al.* 2007). Interestingly, this species has also been described in France (Gérard Trichies, personal communication) in Murol (Puy de Dôme) on *Fagus sylvatica*, in Ludelange-Tressange (Moselle) on *Alnus glutinosa*, in Bistroff (Moselle) on *Salix sp.* (Figure 1.25) and in Senon (Meuse) on *Populus nigra* (Figure 1.26). According to the literature, *P. chrysosporium* mainly colonises hardwoods.

The genome of the strain *Phanerochaete chrysosporium* RP-78 we used in the present work was sequenced in 2004 (Martinez *et al.* 2004), being the first sequenced genome of *Basidiomycota* as well as the first white-rot fungus sequenced. This strain RP-78 is homokaryotic (Stewart, Gaskell & Cullen 2000). Analysis of its 29.9 Mb genome revealed a large array of genes encoding lignocellulolytic enzymes (Larrondo, Vicuna & Cullen 2005). Concerning its extracellular oxidative systems involved in lignin degradation, ten lignin peroxidase (LiP) genes, six manganese peroxidase (MnP) genes, seven copper radical oxidase

genes, one cellobiose dehydrogenase (CDH) gene, five multicopper oxidase (MCO) genes were identified in the genome (Floudas *et al.* 2012). Interestingly, contrary to other white-rot fungi, no sequence encoding conventional laccases was found in *P. chrysosporium* genome. Concerning the extracellular carbohydrate active enzymes involved in the degradation of cellulose, hemicellulose and pectin, more than 240 sequences in *P. chrysosporium* RP78 genome encode putative carbohydrate active enzymes, including a minimum of 50 cellulases. Concerning the intracellular enzymes related to lignocellulose degradation, 149 cytochrome P450 genes (Floudas *et al.* 2012) and 25 glutathione S transferase (GST) genes (Morel *et al.* 2013) were identified. Interestingly, the genome of another *Phanerochaete* species, *P. carnosa* which has been almost exclusively isolated from softwoods, was recently compared to *P. chrysosporium* genome (Suzuki *et al.* 2012). Comparative genomics revealed that these fungi have a distinct genetic basis, adapted to the type of wood they colonise, *i.e.*, hardwood for *P. chrysosporium* and softwood for *P. carnosa*.

Because this white-rot fungus has been extensively studied, because it is present in European forests, preferentially colonising hardwoods such as *Fagus sylvatica*, the tree specis we selected as wood model, and because the genome, transcriptome and secretome of the strain RP7 are particularly well known (Martinez *et al.* 2004; Vanden Wymelenberg *et al.* 2009; Kim *et al.* 2010), we selected *P. chrysosporium* RP78 as our fungal model in all our work.

Figure 1.25 *Anamorph stage of P. chrysosporium on a Salix sp. trunk in Bistroff (Moselle), France in June 2004 (with the authorisation of the author, Gérard Trichies).*

Figure 1.26 *Teleomorph stage of P. chrysosporium on a Populus nigra trunk in Senon (Meuse), France in July 2009 (with the authorisation of the author, Gérard Trichies).*

1.7 Approaches and methods of analysis

The present work aims to test two main hypotheses. Firstly, that a mycosphere effect also exists on the bacterial communities surrounding wood-decaying fungi during the process of wood decomposition and that the presence of a white-rot fungus can shape both the taxonomic and functional structures of bacterial communities in a woody environment. Secondly, we hypothesised that the bacterial-fungal interactions taking place on wood influence the wood degradation process and that the presence of bacteria can modulate the lignocellulolytic system of a white-rot fungus.

All the experiments presented in this work were performed in microcosms. In natural environments, wood degradation depends on numerous biotic and abiotic variables as well as on interactions between these variables. Working under controlled conditions is an alternative to reduce this high number of variables and to be able to answer specific questions. Microcosm experiments offer the opportunity to work under controlled conditions and also to have replicated experiments (Prosser 2010). Microcosm experiments are also powerful tools to study large-scale ecological questions (Benton *et al.* 2007). Concerning the woody material, two forms were used: sawdust and wood blocks. For each experiment, the wood substrate which was used, originates from planks of a single tree of *Fagus sylvatica*. This was done in order to reduce the heterogeneity of the substrate, even if chemical variability inside a tree exists. All the woody material was sterilised prior to utilisation to be able to strictly control the inoculated microorganisms.

To test the first hypothesis, we used controlled conditions in which the white-rot fungus *P. chrysosporium* was able to decompose wood as well as to create a niche to potentially influence wood-associated bacterial communities. Since the time required to detect a mycosphere effect in decaying-wood was unknown, we used an enrichment procedure combined with a microcosm scale experiment to increase the probability to detect a mycosphere effect and to characterise the bacterial communities of the white-rot mycosphere. To achieve these objectives, different methods were used. To study the taxonomy of wood-associated bacteria and of bacterial communities from the white-rot mycosphere, a dual approach was used in the same kinetic study. A culture-independent method, namely 16S rRNA gene-based pyrosequencing, and a culture-dependent, based on a bacterial collection, were used to analysed the bacterial communities of the same samples (Chapters 3 and 4, respectively). The functional characterisation of these communities was performed using

selective media. Since a bacterial collection was made from these samples, a part of the strains was also characterised with selective media, Biolog microplates and bacterial-fungal confrontation tests (Chapter 4).

To test the second hypothesis, we used kinetic studies, lasting several months and with several sampling dates, in order to qualitatively evaluate the process of wood degradation, especially in the early stages of the degradation. First, mass and density of wood blocks colonised by *P. chrysosporium* were measured during five months. Density measurements of decaying-wood were performed using X-ray computed tomography (CT) coupled with an in-house plugin (Chapter 2). Then, to evaluate the respective contribution of *P. chrysosporium* and selected bacterial strains to the process of wood degradation over time, we used a polyphasic approach (Chapter 5). We monitored the activities of a set of enzymes involved in wood degradation, during six months. To understand the ecoenzymatic stoichiometry of decaying wood, carbon content, nitrogen content and pH of the sawdust were also measured. To evaluate the wood degradation, the surface of wood blocks colonised by different microorganisms was analysed by scanning electron microscopy (SEM) coupled with energy dispersive X-ray spectroscopy (EDS) and wavelength dispersive X-ray spectroscopy (WDS). The elemental composition of these wood blocks was also analysed by inductively coupled plasma atomic emission spectroscopy (ICP-AES), in order to understand the dynamics of some elements during the wood decomposition. In parallel, mass and density were also measured.

- Chapter 2 -

X-ray computed tomography, a method to monitor the process of wood degradation by a white-rot fungus

Résumé

La biodégradation du bois est un processus de grande importance, tant pour le stockage du carbone dans les forêts et son implication dans les cycles biogéochimiques globaux que pour des domaines appliqués de la science comme la préservation et la protection du matériau bois ou encore la transformation des produits dérivés du bois.

De nombreuses méthodes existent pour suivre la biodégradation du bois à différentes échelles. Il peut s'agir d'une simple estimation visuelle prenant en compte l'aspect du bois ou d'un suivi de la perte de masse du matériau, permettant d'obtenir une appréciation générale et approximative du processus. Des méthodes basées sur la mesure de caractéristiques mécaniques ou chimiques du bois ont également été développées, apportant des informations plus spécifiques sur l'altération du matériau. D'un point de vue mécanique, les modules d'élasticité et de rupture du bois peuvent être mesurés. Des analyses chimiques peuvent également être mises en œuvre pour estimer les concentrations en macromolécules du bois (cellulose, lignine) ou analyser la composition élémentaire du bois (carbone, azote, phosphore). Ce type de mesures apporte des données quantitatives précises mais implique la destruction de l'échantillon analysé et requiert certaines étapes de préparation de l'échantillon. Des approches microscopiques ont également été employées, permettant d'étudier et de quantifier, à l'échelle cellulaire, le processus de biodégradation. Ici encore, la préparation des échantillons peut devenir chronophage et présenter un obstacle à la réalisation d'études quantitatives sérieuses sur un nombre d'échantillons représentatifs. Enfin, ces méthodes diffèrent également par leur sensibilité, c'est à dire ici la capacité à détecter des stades précoces de dégradation du bois. Aussi, malgré l'éventail relativement large des méthodes existantes, il existe toujours un besoin de nouvelles méthodes quantitatives, rapides, sensibles et non destructrices permettant d'étudier le processus de décomposition du bois afin d'en comprendre la complexité en tenant notamment compte de l'hétérogénéité du matériau bois.

Dans ce chapitre, nous rendons compte d'une autre méthode permettant de suivre le processus de dégradation du bois de manière quantitative, rapide et non destructive. Il s'agit du scanner tomographique à rayons X. Cette méthode permet de mesurer précisément la densité d'un matériau, y compris celle du bois. Or, la densité est considérée comme un trait fonctionnel important des arbres et du matériau bois qui en dérive. La mesure de cette densité est donc une variable pertinente à analyser dans le cadre d'un suivi du processus de décomposition du bois. L'objectif du travail présenté dans ce chapitre est de valider

l'utilisation du scanner tomographique à rayons X comme méthode d'analyse du processus de dégradation du bois. Pour ce faire, nous avons réalisé un suivi cinétique de la dégradation du hêtre *Fagus sylvatica* par le champignon modèle de pourriture blanche *Phanerochaete chrysosporium* pendant cinq mois, en analysant les variations de masse et de densité des échantillons de hêtre. Les densités ont été mesurées avec un scanner tomographique à rayons X puis analysées à l'aide d'un module d'extension spécifique. Cette méthode, rapide, précise et non destructive, a permis de réaliser des cartes de densité des échantillons de bois, avec une précision de l'ordre du millimètre. Les variations de masse et de densité se sont révélées significativement corrélées. Au sein d'un échantillon, il nous a été possible de distinguer les cernes de croissance du bois. Il a également été possible de montrer que la dégradation du hêtre par *P. chrysosporium* est un processus hétérogène. En effet, les mesures de perte de densité ont révélé que les zones les moins denses des échantillons de bois étaient préférentiellement dégradées par le champignon, suggérant que le bois de printemps, moins dense que le bois d'été, est dégradé plus rapidement ou dégradé en premier.

Pour conclure, nos résultats démontrent que la tomographie à rayons X est une méthode adaptée pour l'étude du processus de dégradation du bois au cours du temps. Cette méthode peut potentiellement s'ouvrir avec un large champ d'applications, depuis l'analyse des éprouvettes de bois utilisées pour les tests normatifs relatifs à la protection du bois jusqu'à l'analyse de troncs d'arbre en forêt, à différents stades de décomposition. Cette méthode sera de nouveau utilisée dans le Chapitre 5 afin de comparer l'effet de différents inocula microbiens (*P. chrysosporium*, une communauté bactérienne et *P. chrysosporium* associé à cette communauté bactérienne) sur le processus de dégradation du hêtre *Fagus sylvatica*.

L'ensemble des travaux présentés dans ce chapitre ont été publiés dans un article intitulé *Density mapping of decaying wood using X-ray computed tomography*, paru dans le journal *International Biodeterioration & Biodegradation* (2014, volume 86, pages 358-363).

2 X-ray computed tomography, a method to monitor the process of wood degradation by a white-rot fungus

The present chapter corresponds to an article entitled “Density mapping of decaying wood using X-ray computed tomography” published in *International Biodeterioration & Biodegradation* journal in 2014, volume 86, pages 358-363.

http://dx.doi.org/10.1016/j.ibiod.2013.10.009

Authors and affiliations:

Vincent Hervé[1,2*], Frédéric Mothe[3,4], Charline Freyburger[3,4], Eric Gelhaye[1,2], Pascale Frey-Klett[1,2]

[1] *INRA, Interactions Arbres – Microorganismes, UMR1136, F-54280 Champenoux, France.*

[2] *Université de Lorraine, Interactions Arbres – Microorganismes, UMR1136, F-54500 Vandoeuvre-lès-Nancy, France.*

[3] *INRA, UMR 1092 LERFOB, F-54280 Champenoux, France*

[4] *AgroParisTech, UMR 1092 LERFOB, F-54000 Nancy, France*

*Corresponding author: E-mail: vincent.herve8@gmail.com or viherve@nancy.inra.fr; Phone: +33 (0)3 83 39 41 49; Address: Centre INRA Nancy, UMR1136 IAM, Route d'Amance, 54280 Champenoux, France.

Keywords: X-ray computed tomography; density; wood degradation; *Phanerochaete chrysosporium; Fagus sylvatica*.

2.1 Abstract

Wood biodegradation is a central process at the crossroads of several disciplines. It is not only important for carbon storage in forests, but it is also important for wood conservation, wood protection and wood transformation products. Many methods already exist for studying wood biodegradation; however, they present several drawbacks, being time-consuming or destructive. Moreover, they provide little information regarding the complexity of the degradation process and the heterogeneity of the wood substrate. Based on a kinetic study of the biodegradation of *Fagus sylvatica* by the white-rot fungus *Phanerochaete chrysosporium*, we developed an X-ray computed tomography method coupled with an in-house plugin for fast, non-destructive and accurate measurement of the density variations of decaying wood. This method allowed us to examine the spatial heterogeneity of woody decayed material at the millimetre scale, providing information about the fungal pattern of degradation. Thus, X-ray computed tomography is an efficient tool that can be used for measuring the degradation of a variety of wood substrates ranging from small normalised wood blocks to fallen logs in the forest.

2.2 Introduction

Understanding the wood biodegradation process is important at the theoretical level to better understand wood biogeochemistry (Boddy & Watkinson 1995), as well as at the applied level (Råberg, Terziev & Daniel 2013). Numerous fungal species live in association with wood. However, saprotrophic basidiomycetes have been described as the most important decomposers in environments ranging from forest ecosystems (Kubartová *et al.* 2012) to indoor buildings (Schmidt 2007). These fungi use a large set of extracellular enzymes to mineralise the wood lignin and carbohydrates such as cellulose and hemicelluloses (Baldrian 2008). Decomposition of wood by these fungi causes economic losses (Schwarze, Engels & Mattheck 2004) and problems for the conservation of historic woods (Blanchette 2000). However, ligninolytic fungi also have biotechnological applications in the food and textile industries, as well as for soil bioremediation (Rodríguez Couto & Toca Herrera 2006). In particular, these fungi are important in the field of wood science, where they are used for biopulping and biobleaching (Blanchette *et al.* 1988; Singh *et al.* 2010).

Various methods have been developed to evaluate wood degradation at different scales. Visual estimation and mass loss have been traditionally used to estimate the stage of alteration on a global scale. For example, the European standard EN113 (EN113, 1996),

which is the reference method for evaluating the efficacy of wood preservatives, is based on the mass loss of standardised wood blocks incubated with wood-decaying fungi. This method is fast but not very informative with regard to the biodegradation process. The evaluation of wood alteration can also rely on the physical, mechanical and chemical properties of the wood. Based on mechanical tests, the strength loss of the wood can be used to measure degradation (Winandy & Morrell 1993). Meanwhile, chemical analyses (Freschet *et al.* 2012) can reveal variations in macromolecule concentration (lignin and cellulose) in the wood or can provide elemental compositions (carbon and nitrogen) following biodegradation. The delignification process has also been followed by near- and mid-infrared spectroscopy (Schwanninger *et al.* 2004). Unfortunately, while offering a wealth of information, these methods destroy the sample. At the cellular scale, wood degradation can also be monitored and quantified using microscopy (Schwarze 2007). While extremely accurate, microscopic approaches require time for sample preparation and are not well adapted for quantitative studies. Thus, there is a need to develop new methods for monitoring wood biodegradation that can quickly detect and quantify the early signs of degradation so that preventative measures can be taken.

Both X-ray microdensitometry and electric resistivity tomography have been reported to be good techniques for studying wood decay, and these techniques are based on density loss analysis (Bucur *et al.* 1997; Macchioni, Palanti & Rozenberg 2007) and variations in electric resistivity (Bieker *et al.* 2010) of the decaying wood, respectively. X-ray computed tomography (CT) is an imaging procedure that computes 3D maps of objects based on X-ray attenuation for estimation of their density (Freyburger *et al.* 2009). Interestingly, wood density has been described as an important wood functional trait and as an integrator of wood properties (Chave *et al.* 2009). X-ray CT is faster than X-ray microdensitometry and provides higher resolution than electric resistivity tomography. It is non-destructive and accurate to the millimetre scale or higher. X-ray CT data acquisition is fast, taking only a few seconds for a slice without the need for sample preparation. Finally, it provides fast 3D analysis of relatively important volumes (0.1 m^3 or more) with good enough precision for quantitative studies. Initially, the X-ray CT technique was developed for medical imaging, but it has recently been used for the analysis of various materials. According to recent literature reviews (Wei, Leblon & La Rocque 2011; Longuetaud *et al.* 2012), CT scanning has mainly been used in wood science for detecting internal log features such as pith, growth rings, heartwood/sapwood, knots and decay.

Here, we applied the X-ray CT technique for imaging density of wood during fungal biodegradation. We performed a kinetic study of beech wood (*Fagus sylvatica* L.) degradation by the model white-rot fungus *Phanerochaete chrysosporium* RP78 (Martinez *et al.* 2004) under controlled conditions. The biodegradation process was monitored both by traditional mass loss analysis and by density loss analysis using the X-ray CT technique.

2.3 Materials and methods

2.3.1 Fungal strain

P. chrysosporium (strain RP78) (Martinez *et al.* 2004), a well-known white-rot fungus (Burdsall & Eslyn 1974), was obtained from the Center for Forest Mycology Research, Forest Products Laboratory (Madison, Wisconsin, USA). This strain was maintained at 25˚C on 3% malt agar slants.

2.3.2 Experimental design

The kinetics of wood decay was evaluated using beech (*Fagus* sylvatica) wood blocks (50×24×6 mm) incubated in the presence or absence of *P. chrysosporium* in 90-mm Petri dishes containing malt (30 $g.l^{-1}$) agar (20 $g.l^{-1}$) medium. Wood blocks were all sampled from the same heartwood plank (24 mm thick). The blocks were free of knots and other visual defects (Figure 2.1). Samples (n=108) were cut with a circular saw in the radial (50 mm) and axial directions (6 mm). In the axial direction, two samples in a row were considered as biological replicates because of their proximity.

The wood blocks were autoclaved (20 min, 120˚C, dry cycle) twice with 2 days in between each autoclave cycle. Half of the wood samples were inoculated with a 5 mm-diameter fungal plug of *P. chrysosporium* RP78, which was placed 3 cm from the periphery of the block. For each of these wood samples, the corresponding biological replicate received a wet sterile piece of cotton only as a control. The sterile wet cotton was used to maintain constant moisture inside the Petri dish and to detect any microbial contamination growing in the dishes. No microbial growth was detected during the 150 days of incubation. Plates were sealed with adhesive tape and incubated at 25˚C in the dark for 0, 15, 30, 60 or 150 days. The experimental design consisted of 2 treatments (wood blocks inoculated with or without the white-rot fungus *P. chrysosporium*), 5 incubation times (0, 15, 30, 60 and 150 days) and 12 replicates for each condition (for both time and type of inoculation). For incubation time t=0

(*i.e.*, just after autoclaving), there was just one condition (*i.e.*, no fungal inoculation). Thus, there were only 12 samples. Altogether, this led to 1×12+2×12×4 = 108 wood blocks analysed for nine conditions (Figure 2.1).

2.3.3 Data acquisition and analysis

The mass, volume and density were measured for each sample for both the wet (*i.e.*, directly after sampling) and dry states (*i.e.*, after 24 h at 103˚C) after removing the surface fungal mycelium. Masses were measured using an AG204 analytical balance (Mettler Toldeo) (nearest 0.1 mg). Volumes were estimated from the width, length and thickness of each wood block measured using a digital caliper (nearest 0.01 mm). Wood density data were acquired with a Brightspeed Exel 4 (General Electric Healthcare) CT scanner using 80 kV voltage and 50 mA intensity (Freyburger et al., 2009) (https://www2.nancy.inra.fr/unites/lerfob/plateforme/equipements/scanner.html). The 3D reconstruction process was performed using the "DETAIL" filter, providing 512×512 slices with a transverse resolution of 0.1875 mm/pixel and a distance between slices of 0.625 mm. Images were analysed using ImageJ v1.43 (Schneider, Rasband & Eliceiri 2012) and an in-house plugin written in Java (available on request from the authors). This method allowed extraction and subdivision of the data according to a grid pattern. For each condition (*i.e.*, time and type of inoculation), scanned images of the 12 replicates were obtained in the initial state and after incubation (0, 15, 30, 60 or 150 days) for both the wet and dry states. The 50×24 mm^2 surface of each CT slice was analysed using 40×20 subdivisions, with one subdivision representing 42 pixels. For each 6 mm-thick side of each wood block, 7 slices were used. This procedure led to the 3D mapping of 40×20×7 = 5600 elements per scanned wood sample. Pixels with densities less than 0.2 $g.cm^{-3}$ were removed. It was assumed that these pixels corresponded to entirely biodegraded areas. Pixels with a density greater than 0.2 $g.cm^{-3}$ were counted and averaged to compute the area and mean density of each element. Loss of density 3D maps were obtained for each sample at a given time *t* by subtracting the mean density of each element in the dry state at times 0 and *t*. The global density loss for each sample was estimated using the means of these values weighted by the area. Global volumes, obtained by summing the elemental volumes and masses as the quotient of volume and density, were also computed for each sample.

The Wilcoxon signed rank test and sign test were used to compare sample distributions. Relationships between two variables were estimated using either linear or non-linear regression based on the lowest values of the root-mean-square error (RMSE) and the

Akaike Information Criterion (AIC). Indices of dispersion corresponded to the variance to mean ratio. Statistical analyses and graphics were computed using R software version 2.14 (R Development Core Team 2013).

2.4 Results and discussion

F. sylvatica degradation by *P. chrysosporium* led to a mass loss of 13.74 ± 0.61 % (mean ± SEM) after 150 days of incubation (Figure 2.2A). The kinetic study of biodegradation revealed a linear relationship between time and mass loss with a very good correlation (R^2=0.95, p< 0.001), which is consistent with a previous study reported by Bucur et al. (1997) (R^2=0.98) who monitored beech blocks incubated with *Trametes versicolor*. After 150 days of incubation, the global density loss of the wood samples was 13.07± 0.59 % (Figure 2.2B). The density losses did not significantly differ from the mass losses (sign test, p=0.39). The density and mass losses were correlated (R^2=0.78, p< 0.001). This result is consistent with a previous report by Macchioni et al. (2007) (r=0.97 for 6 beech wood samples incubated in the presence of *Coniophora puteana*). Compared to the mass loss data, the density loss data showed higher variance. The relationship between the density loss and time was non-linear and was best fitted by a power model, which provided the lowest RMSE and AIC (RMSE=2.04, AIC=272.85). The difference between the mass loss and the density loss can be explained by volume variations in the wood blocks because volume is equal to the ratio of mass to density. We calculated the densities from the manually measured volumes and masses and compared them to the mean densities obtained from X-ray CT. A linear relationship (R^2=0.91, p< 0.001, data not shown) was obtained between the two estimations of wood density, demonstrating the accuracy of the X-ray CT wood decay density measurement. We hypothesised that the variability in the density of the wood blocks at t=0 (Figure 2.2) was due to autoclave treatment and the drying step before the mass and density measurements because wood exposure to high temperatures for short periods can lead to degradation and changes in hemicellulose (Hillis 1984). Initial mass and density measurements were performed for all of the samples before the wood blocks were sterilised. However, at t=0, the samples were autoclaved, leading to a slight mass loss of 0.13 ± 0.01 % (Figure 2.2A) and a higher mean density loss of 0.99 ± 0.52 % (Figure 2.2B). Despite both sources of variability, at t=15 days of incubation with the white-rot fungus, enough significant differences were detected (Wilcoxon test, p <0.005) for both mass and density losses compared to samples from t=0.

Wood is known to be a heterogeneous material. Furthermore, wood degradation is not evenly distributed (Fackler *et al.* 2010). The spatial distribution of extracellular enzymes secreted by saprotrophic basidiomycetes is also non-uniform on natural substrates (Šnajdr *et al.* 2011). Thus, to monitor and understand the spatial variability of wood biodegradation, a very fine scale analysis is required. While mass measurement gives only one value per sample, X-ray CT data can give access to a high number of values corresponding to the density extracted from a defined grid pattern (here 40×20 subdivisions) for each sample. This approach enables analysis of the spatial heterogeneity of wood density. In the present study, we first compared the data from decayed samples with control samples (*i.e.*, not inoculated with white-rot fungus). A linear relationship between the control and decayed samples was observed (R^2=0.65, p< 0.001, data not shown). Indices of dispersion were calculated to estimate the variability for each sample. The index of dispersion (D) was significantly lower (Wilcoxon test, p <0.001, data not shown) for control samples (D= 1.805 ± 0.006) compared to decayed samples (D= 2.018 ± 0.007). This finding showed that the density of the wood samples colonised by white-rot fungus was more variable than the density in the absence of the fungus after only 15 days of incubation, which revealed that under controlled conditions, wood degradation by white-rot fungus was a non-homogeneous process at the level of wood density. This result not only confirmed previous microscopic studies (Blanchette 1984), but above all, it provided quantitative data with respect to wood heterogeneity.

Due to the high resolution of the heatmap visualisation (each subdivision corresponded to the median of 294 values, *i.e.*, to 10.5 mm^3), we were able to examine the spatial heterogeneity of wood density for each block. This observation allowed us to distinguish the growth rings (Figure 3.3A, t=0). The latewood was denser than the earlywood, as described previously by Bouriaud et al. (Bouriaud *et al.* 2004). Interestingly, mapping the wood density along with the kinetics of degradation led to a better understanding of the process of fungal wood decay. From the heatmaps, we observed that the edges, especially those from the radial axes, were preferentially biodegraded (*i.e.*, they showed lower density). This finding may be explained by the fact that the wood blocks were cut along these edges, increasing the substrate accessibility to the fungal hyphae. It should be noted that these density data were acquired from dried samples. The same analyses were performed on data acquired in the fresh state (*i.e.*, directly after sampling) to indirectly detect decayed zones with local changes in moisture content, as suggested by several studies cited by Wei et al. (2011). Unfortunately, it was not possible to clearly detect such zones during the kinetic study (data

not shown), possibly due to the relatively short duration of the decay experiment (150 days).

In addition to the results of this qualitative analysis, a quantitative analysis revealed other characteristics of the fungal attack on the beechwood blocks. According to the relationship between the relative density loss and the initial density for each wood block during the kinetic experiments, we observed a decreasing trend for the slopes of regression lines (Figure 3.3B). At t=0, the slope of the regression line was slightly positive (slope=0.037). The slope then decreased at each step and became negative from t=30 days (slope=-0.040) to t=150 days (slope=-0.141). A comparison of the distribution of the slopes for the 12 samples showed that the slopes at t=150 days were significantly lower (Wilcoxon test, $p<0.001$) than the slopes at t=0. The coefficients of determination for the linear regression were very low (R^2 values between 0.0018 and 0.041), indicating poor correlations between the relative density loss and the initial density, although the correlations were significant ($p<0.001$). A negative slope indicates that areas with lower density are preferentially degraded by the fungus. We observed such a trend over time, indicating that the beechwood zones with lower density, corresponding potentially to earlywood, were either preferentially degraded or degraded faster by *P. chrysosporium*. In contrast, Macchioni et al. (2007) previously showed that the latewood of beechwood incubated with the brown-rot fungus *Coniophora puteana* was attacked more severely than the earlywood, indicating that there may be underlying differences between brown and white-rot fungal attack patterns. Such differences in degradation patterns between earlywood and latewood have already been described with respect to the wood decay type and the type of wood (Schwarze 2007), as well as among white-rot decay types (Blanchette 1984). From a practical point of view, as the differences between earlywood and latewood are more evident in softwood than in hardwood, revealing differences in density variations during softwood decay should be more easily achieved than for hardwood decay.

Collectively, our results show that X-ray CT coupled with CT image processing is relevant for measuring the density variations between and within samples during fungal biodegradation. Because X-ray CT gives access to the spatial variability in wood density at the millimetre scale, it is valuable for investigating the variability of wood degradation patterns. Indeed, wood decomposition is a complex and non-uniform process that is influenced by the compositional and structural differences between softwood and hardwood (Weedon *et al.* 2009) and among the wood substrate (heartwood/sapwood (Schowalter, Zhang & Sabin 1998), earlywood/latewood (Blanchette 1984)). Different wood decay types (soft,

brown or white-rot (Schwarze 2007)) and abiotic drivers of the wood degradation (moisture, temperature, etc.) (Donnelly *et al.* 1990) also influence this process. Monitoring the variability in wood degradation remains a real challenge for the wood industry and for the conservation of archaeological wood (Blanchette 2000). X-ray CT could be a complementary instrument for monitoring mass losses or chemical composition variations, providing new data about density variations at the millimetre scale. In the case of field experiments, it could be used to estimate wood density more precisely than traditional methods (e.g., measuring the ratio of wood oven-dry mass to volume) (Freschet *et al.* 2012). For long-term studies, such as the LOGLIFE experiment (Cornelissen *et al.* 2012) that follows the decomposition of different trees on two different sites over fifteen years analysing several wood functional traits (including density), as well as the diversity of wood-associated microbial and invertebrate communities, X-ray CT can accurately monitor the kinetics of wood volume and wood density for different logs. Finally, if included in normative test procedures, such as EN113 (EN113, 1996), X-ray CT could provide a large database of wood densities corresponding to different wood species degraded by different types of organisms (bacteria, fungi, microbial consortia and wood-feeding invertebrates), allowing predictive modelling of wood degradation.

2.5 Conclusion

The use of X-ray computed tomography coupled with image analysis provided a fast, non-destructive and accurate new method for studying wood degradation using density mapping. In particular, it allowed us to monitor the spatial heterogeneity in wood density during the biodegradation process at the millimetre scale. This method could have many applications ranging from normative tests for wood protection to ecological studies on coarse woody debris.

2.6 Acknowledgments

This work was supported by a grant from Lorraine Region, an ANR project (ANR-09-BLAN-0012) and IFR110 / EFABA. The ImageJ plugin used for analysing the density losses through CT images was developed thanks to the ANR EMERGE project (ANR-08-BIOE-003). The UMR1136 INRA Université de Lorraine ‘Interactions Arbres Microorganismes’ and the UMR1092 INRA AgroParisTech 'LERFoB' are supported by the French National Research Agency through the Laboratory of Excellence ARBRE (ANR-12- LABXARBRE-

01). The English language was reviewed by American Journal Experts. We thank A. Mercanti for the help with wood sampling. We also thank Julien Sainte-Marie, Meriem Fournier, Jean Michel Leban and Philippe Gérardin for helpful discussions.

2.7 Figures

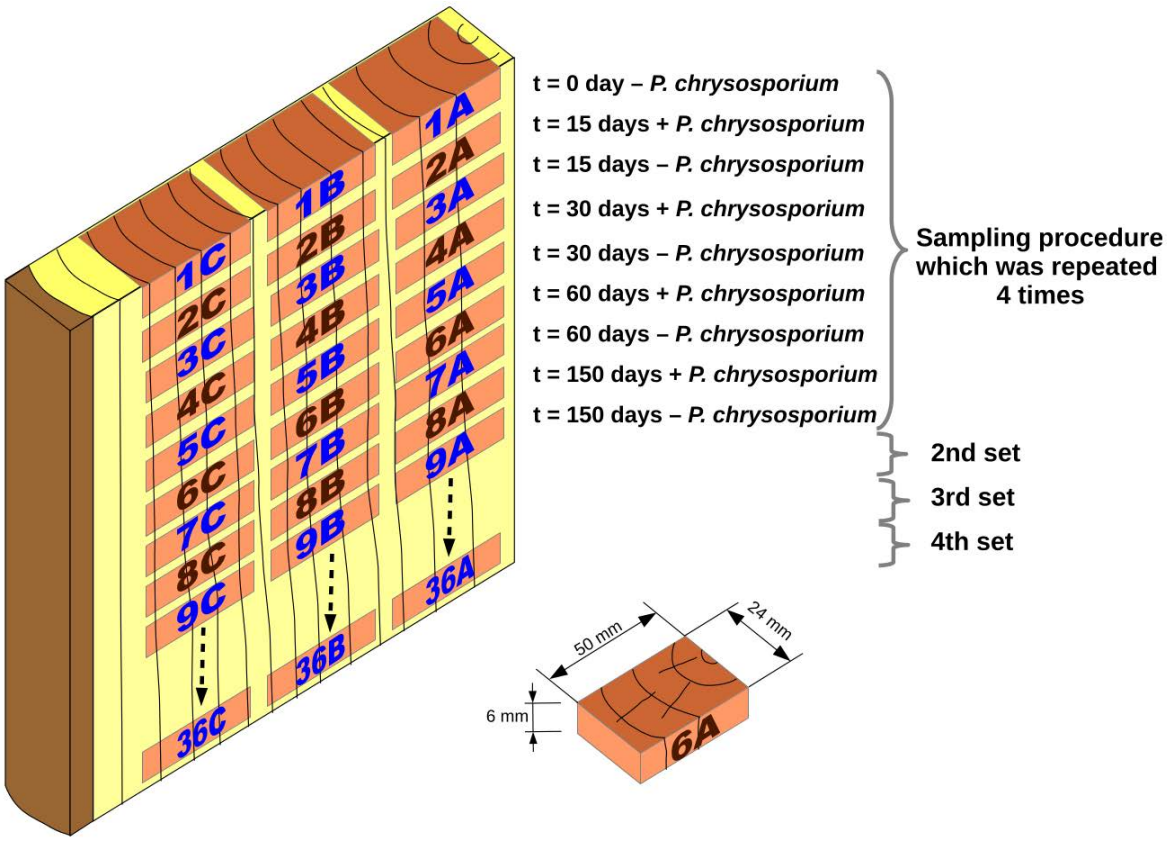

Figure 2.1. Diagram of the experimental design. In total, 108 samples of 50 mm x 24 mm x 6 mm in size (radial, tangential and longitudinal directions, respectively) were cut within a plank and divided into 4 sets of 36 samples (numbered 1A to 9C, 10A to 18C, 19A to 27C and 28A to 36C). There were 9 conditions for time (0, 15, 30, 60 and 150 days) and type of inoculation (with or without the white-rot fungus *P. chrysosporium*), with *n*=12 replicates for each condition (from the 3 rows (called A, B and C) and the 4 sets). In the axial direction, two consecutive samples from a row were considered as biological replicates because of their proximity. These replicates were incubated with or without *P. chrysosporium* (*e.g.*, samples 4A and 5A).

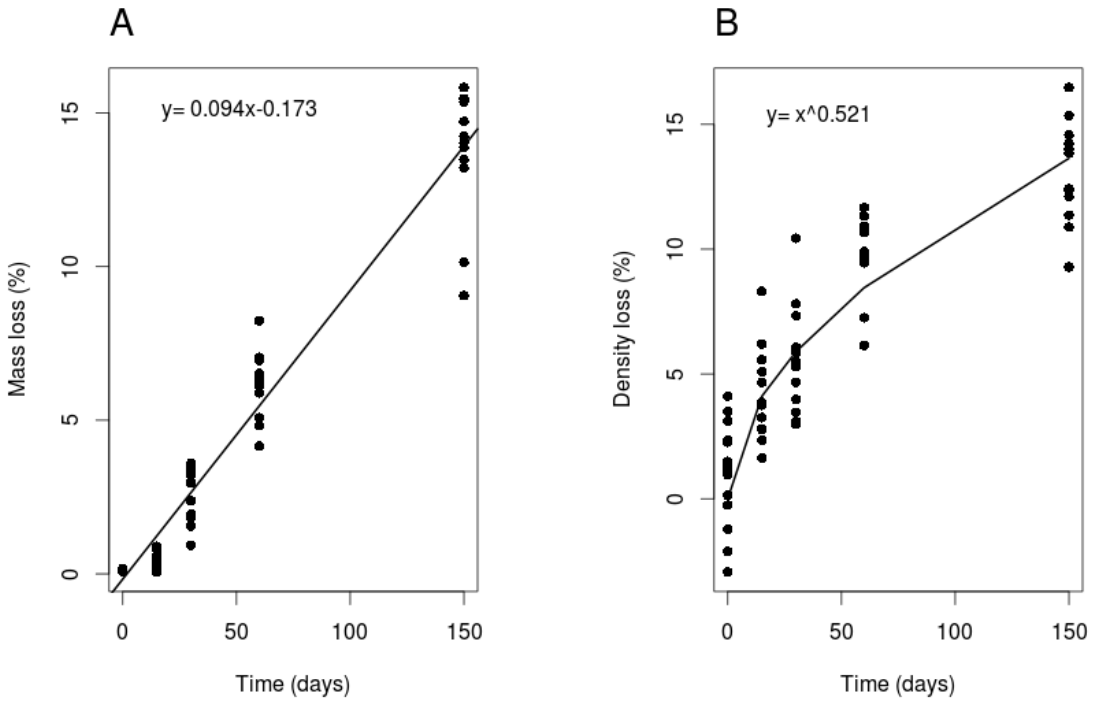

Figure 2.2. (A) Relative mass loss (%) and (**B)** relative density loss (%) of beechwood blocks incubated with *P. chrysosporium* over time (*n*= 12).

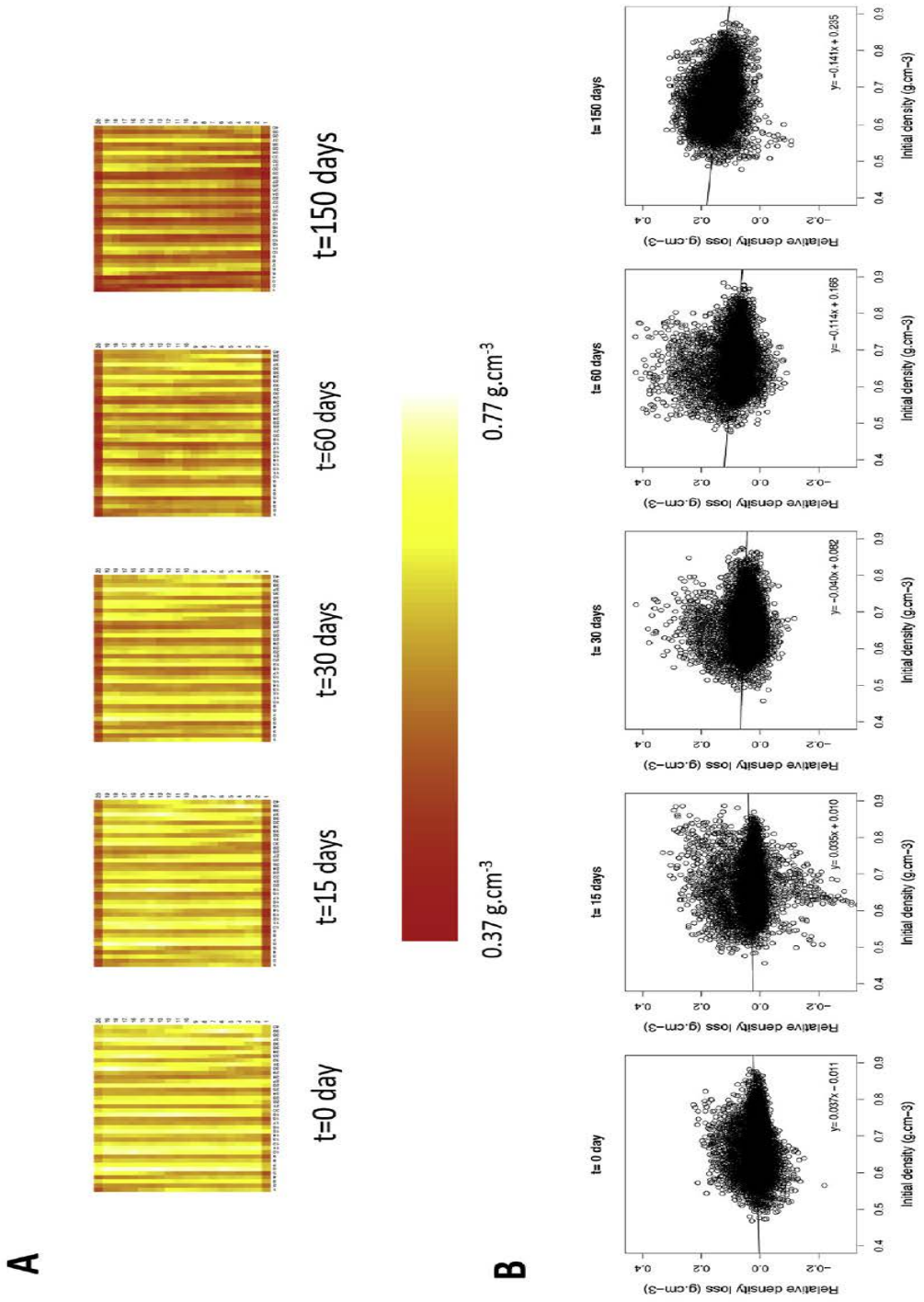

Figure 2.3. (A) Density mapping of beechwood blocks incubated with *P. chrysosporium* for 0, 15, 30, 60 and 150 days using heatmap visualisation based on a 40×20 grid pattern. Each heatmap corresponds to one wood block (n=1). Each subdivision corresponds to the median of 294 values. (**B)** Temporal evolution of the relationship between the relative density loss ($g.cm^{-3}$) and the initial density ($g.cm^{-3}$) of the samples incubated with *P. chrysosporium* (n=12) for 0, 15, 30, 60 and 150 days. Linear regressions are shown (R^2<0.041, p<0.001).

- Chapter 3 -

Influence of wood substrate and of the white-rot fungus *Phanerochaete chrysosporium* on the composition of bacterial communities associated with decaying wood

Résumé

Au sein des écosystèmes forestiers, la dégradation du bois est l'un des processus majeurs impliqués dans les cycles biogéochimiques. Dans les forêts tempérées et boréales, ce processus est principalement dû à des champignons basidiomycètes saprotrophes, dont font partie les champignons de pourriture blanche. Ces champignons ont la capacité de dégrader les constituants majeurs du bois que sont la cellulose, les hémicelluloses et la lignine. Les communautés fongiques associées au bois ont été particulièrement bien décrites dans la littérature scientifique, tant au niveau de leur composition que de leur dynamique spatio-temporelle. Par ailleurs, des communautés bactériennes ont également été décrites comme étant partie intégrante de cette niche écologique particulière qu'est le bois en décomposition. Pourtant, jusqu'à présent dans ce contexte de fragmentation du complexe lignocellulosique en forêt, les interactions entre ces deux communautés de microorganismes phylogénétiquement éloignés, n'ont été que très peu étudiées. Dans d'autres niches écologiques en revanche telles que la mycorhizosphère, le fromage lors de son processus de maturation ou encore dans certaines termitières et certaines fourmilières, l'effet d'un champignon sur la diversité taxonomique des communautés bactériennes résidentes a été clairement démontré (Frey-Klett *et al.* 2011).

Nous nous sommes donc posés la question de l'influence d'un champignon filamenteux décomposeur du bois sur les communautés bactériennes présentes dans son environnement proche, autrement dit la question d'un éventuel effet mycosphère sur ces communautés bactériennes lors du processus de dégradation du bois. Pour répondre à cette question, une approche en microcosme a été mise en place. Dans un premier temps, nous avons extrait une suspension microbienne à partir d'un sol forestier (alocrisol). Ensuite, cette suspension a été inoculée dans des microcosmes contenant uniquement de la sciure de hêtre (*Fagus sylvatica*) stérile, en présence ou en absence du champignon de pourriture blanche *Phanerochaete chrysosporium*. Après douze semaines d'incubation, les microcosmes ont été échantillonnés et une partie de ces échantillons a été inoculée dans de nouveaux microcosmes afin d'induire par enrichissement la sélection de communautés bactériennes préférentiellement associées à la présence du champignon et/ou au bois de hêtre. Trois semaines plus tard, l'opération a été répétée et un dernier échantillonnage a eu lieu après un total de dix-huit semaines. Nous avons analysé la diversité et la structure de ces communautés bactériennes en fonction des étapes d'enrichissement et de la présence du champignon par pyroséquençage d'un fragment de

l'ARN ribosomal 16S.

A partir des séquences obtenues, des courbes de raréfaction ont été générées pour chaque échantillon. De manière intéressante, les courbes relatives aux échantillons de sciure étaient asymptotiques, indiquant que toute la diversité de ces échantillons avait été explorée. Ce n'était pas le cas pour l'inoculum microbien initial isolé du sol forestier. Notre analyse de la diversité de ces communautés a révélé que les communautés associées au bois dans les microcosmes présentaient une richesse beaucoup plus faible que celle de l'inoculum initial. La matrice bois apparaît donc ici comme un filtre environnemental pour les communautés bactériennes. La présence de la plupart des unités taxonomiques opérationnelles (OTUs) étaient variables au cours du temps et entre les réplicats, indépendamment du traitement, suggérant l'implication de processus stochastiques dans la structuration des communautés bactériennes. Cependant, deux OTUs, l'un appartenant à la famille des *Xanthomonadaceae* et l'autre au genre *Rhizobium*, représentant ensemble environ 50 % de l'abondance relative bactérienne, ont pu être détectés dans tous les microcosmes contenant de la sciure, indépendamment de la présence de *P. chrysosporium.* Ce résultat suggère un lien entre l'environnement bois et ces deux OTUs. Concernant l'effet mycosphère, il a été démontré que, sur la base des abondances relatives, la composition des communautés bactériennes était significativement influencée par la présence de *P. chrysosporium* après douze semaines d'incubation. De plus, il a été observé que des membres du genre *Burkholderia* étaient toujours présents dans les microcosmes contenant *P. chrysosporium*. Ces derniers représentent donc des bioindicateurs taxonomiques potentiels de la mycosphère des champignons de pourriture blanche.

La mise en évidence d'un effet mycosphère de *P. chrysosporium* sur la diversité taxonomique des communautés bactériennes associées au bois en décomposition soulève la question de l'impact de la présence d'un champignon de pourriture blanche sur la diversité fonctionnelle de ces communautés bactériennes. De manière plus globale, cet effet mycosphère pose la question du rôle de ces communautés bactériennes associées au champignon dans le processus de dégradation du bois.

L'ensemble des travaux présentés dans ce chapitre ont été acceptés pour publication dans le journal *Environmental Microbiology*. Ils font l'objet d'une publication intitulée *Diversity and structure of bacterial communities associated with Phanerochaete chrysosporium during wood decay*.

3 Influence of wood substrate and of the white-rot fungus *Phanerochaete chrysosporium* on the composition of bacterial communities associated with decaying wood

The present chapter corresponds to an article entitled “Diversity and structure of bacterial communities associated with *Phanerochaete chrysosporium* during wood decay” and accepted for publication in *Environmental Microbiology* journal in November 23rd, 2013.

DOI: 10.1111/1462-2920.12347

Vincent Hervé[1,2*], Xavier Le Roux[3], Stéphane Uroz[1,2], Eric Gelhaye[1,2] and Pascale Frey-Klett[1,2]

[1] *INRA, Interactions Arbres – Microorganismes, UMR1136, F-54280 Champenoux, France.*

[2] *Université de Lorraine, Interactions Arbres – Microorganismes, UMR1136, F-54500 Vandoeuvre-lès-Nancy, France.*

[3] *INRA, Université de Lyon, Université Lyon 1, CNRS, UMR 5557 & USC1364, Ecologie Microbienne, Villeurbanne, France.*

*For correspondence. E-mail: vincent.herve8@gmail.com or viherve@nancy.inra.fr; Phone: +33 (0)3 83 39 41 49; Fax: +33 (0)3 83 39 40 69; Address: Centre INRA Nancy, UMR1136 IAM, Route d'Amance, 54280 Champenoux, France.

Running title: Bacteria of the white-rot mycosphere

Keywords: bacterial-fungal interactions, bacterial diversity, *P. chrysosporium*, mycosphere, wood decay, *Burkholderia*

3.1 Abstract

Wood recycling is key to forest biogeochemical cycles, largely driven by microorganisms such as white-rot fungi which naturally coexist with bacteria in the environment. We have tested whether and to what extent the diversity of the bacterial community associated with wood decay is determined by wood and/or by white-rot fungus *Phanerochaete chrysosporium.* We combined a microcosm approach with an enrichment procedure, using beech sawdust inoculated with or without *P. chrysosporium*. During eighteen weeks, we used 16S rRNA gene-based pyrosequencing to monitor the forest bacterial community inoculated into these microcosms. We found bacterial communities associated with wood to be substantially less diverse than the initial forest soil inoculum. The presence of most bacterial OTUs varied over time and between replicates, regardless of their treatment, suggestive of the stochastic processes. However, we observed two OTUs belonging to *Xanthomonadaceae* and *Rhizobium*, together representing 50% of the relative bacterial abundance, as consistently associated with the wood substrate, regardless of fungal presence. Moreover, after twelve weeks, the bacterial community composition based on relative abundance was significantly modified by the presence of the white-rot fungus. Effectively, members of the *Burkholderia* genus were always associated with *P. chrysoporium*, representing potential taxonomic bioindicators of the white-rot mycosphere.

3.2 Introduction

Trees play a key role in biogeochemical cycles and in particular in carbon sequestration (Dewar & Cannell 1992). In forests, wood recycling is mainly driven by microorganisms which use a large set of enzymes to decompose the different wood components such as cellulose (Lynd *et al.* 2002) and lignin (Kirk & Farrell 1987). Among these microorganisms, saprotrophic basidiomycetes have been described as the most important decomposers, particularly white-rot fungi which are capable of mineralising both lignin and wood carbohydrates such as cellulose and hemicelluloses (Baldrian 2008). Bacteria are also closely associated with wood decay (Greaves 1971; Clausen 1996). It has been clearly shown that bacterial communities associated with decaying wood in forests present a high diversity (Zhang *et al.* 2008a). Even if their relative efficiency is lower than that of saprotrophic basidiomycetes, bacteria like those belonging to *Actinobacteria* also have the ability to degrade cellulose (Schellenberger, Kolb & Drake 2010), found in forest ecosystems

(Stursová *et al.* 2012). Moreover, model bacteria such as the strain *Sphingobium* sp. SYK-6 (Masai, Katayama & Fukuda 2007) have been found to be involved in lignin degradation (Li *et al.* 2008; Bugg *et al.* 2011; DeAngelis *et al.* 2011).

To date studies on microbial wood decay have mainly focused on fungal communities (Kubartová *et al.* 2012) and have largely ignored the possible role of bacterial communities interacting with saprotrophic fungi (Folman *et al.* 2008). These two phylogenetically distant groups of microorganisms have been found to coexist in numerous natural environments (Frey-Klett *et al.* 2011), including those of decaying wood in forests (Valásková *et al.* 2009). Bacterial-fungal interactions can be positive, negative or neutral for one or both contributors. For example, the white-rot fungus *Hypholoma fasciculare* has been shown to be capable of reducing the total number of bacteria colonising wood (Folman *et al.* 2008; De Boer *et al.* 2010). Bacterial mycophagy has also been described in different environments (Leveau & Preston 2008). Under controlled conditions, some bacterial strains have been proven capable of promoting (Kamei *et al.* 2012; Bontemps *et al.* 2013) or inhibiting (Radtke, Cook & Anderson 1994) the growth of white-rot fungi. More specifically, from a functional point of view, it has been suggested that bacterial-fungal interactions during the wood decay process might be beneficial for both partners through a series of enzymatic reactions. The fungus begins by hydrolysing recalcitrant lignocellulose, releasing breakdown products assimilable by the fungal-associated bacteria, the latter contributing to cellulose degradation and helping the fungus gain access to lignin (de Boer *et al.* 2005). Furthermore, because nitrogen concentration in wood is known to be low, it is possible that nitrogen-fixing bacteria promote fungal growth (Clausen 1996).

The mycosphere defines the microhabitat surrounding fungal hyphae. It has been proven that many soil fungi (Warmink & van Elsas 2009), symbiotic (Nuccio *et al.* 2013) as well as pathogenic (Dewey *et al.* 1999) structure the diversity of the bacterial community in their mycosphere, a phenomenon that has been called the mycosphere effect (Frey-Klett *et al.* 2007). The mycospheric bacteria can have positive or negative impact in the plant-fungus relationship. Despite these potentially important interactions, the mycosphere effect has not been extensively studied in the case of wood decaying fungi (Folman *et al.* 2008; Valásková *et al.* 2009). Therefore a need exists to characterise the bacterial communities specifically associated with white-rot fungi during wood decay in order to further understand their potential contribution to wood decomposition.

The aim of our study was to determine whether and to what extent the model white-rot

fungus *Phanerochaete chrysosporium* influences the bacterial community structure during the wood decay process and to assess how the bacterial community composition evolves over time. *P. chrysosporium* is an extensively studied white-rot fungus, well described at the genomic level (Larrondo *et al.* 2005). Its use in biotechnology has also been well documented (Gao *et al.* 2008). We decided to use a microcosm experiment to determine the extent to which the bacterial community composition was shaped by the presence of wood substrate and to what extent by white-rot fungus during the wood decay process. Beech (*Fagus sylvatica* L.) sawdust was selected to be used as homogenised wood substrate and a microbial community extracted from soil from a beech forest was used as initial inoculum. The microbial suspension was selectively inoculated with or without *P. chrysosporium* in microcosms, followed by enrichment which was repeated three times (Fig. 3.1). While enrichment and microcosm approaches do not mimic field experiments, they are suitable for testing ecological hypotheses (Benton *et al.* 2007; Bradford, Watts & Davies 2010; Martin *et al.* 2012). We selected 16S rRNA amplicon pyrosequencing to monitor the variations in the taxonomic composition (richness and relative abundance) of the bacterial communities associated, or not associated, with the white-rot fungus during the lignocellulose degradation process. Our aim was to create an environment conducive to the coexistence of *P. chrysosporium* together with bacteria on wood substrate to test the hypothesis that the fungus has a selective effect on the bacterial communities.

3.3 Materials and methods

3.3.1 Inoculum sampling

The sampling site is located in Montiers sur Saulx, France (48°32' North, 05°18' East). Soil (cambisol) cores were collected in a forest dominated by beech using sterilised core borer (20 cm depth), after removing the overlying litter. After homogenising soil samples, 260g of soil were mixed with 2 litres of sterile water and a slurry was made using a Waring Blender (Waring, Torrington, CT, USA). Microorganisms were then extracted using Nycodenz (Axis Shield, Oslo, Norway) density gradient (1.3 $g.ml^{-1}$) centrifugation, according to Lindahl & Bakken (1995). Briefly, 50 ml sterile Nalgene tubes (Thermo Scientific,Waltham, MA, USA) were filled with 20 ml of soil suspension and 11.6 ml of Nycodenz and then centrifuged at 10 000 x *g* during 90 min. Finally, the aqueous top layers of the gradient gently recovered after centrifugation were washed twice and resuspended into sterile water. The microbial

suspension highly enriched in bacteria obtained during this step, called E0, was used as an initial microbial inoculum for the microcosm assay described below. Bacterial concentration was estimated at 8.10^3 CFU.ml^{-1} by plate counting on 10% tryptic soy (3 g.l^{-1}, Becton, Dickinson and Company) agar (15 g.l^{-1}) (TSA) medium containing or not cycloheximide (100 mg.l^{-1}, Sigma Aldrich, Saint Louis, MO, USA). The inoculum was thoroughly mixed throughout the inoculation process.

3.3.2 Experimental design

The microcosm experiment consisted of three successive enrichment steps in microcosms (140 mm Petri dishes sealed with adhesive tape) filled with 75 cm^3 of beech (*Fagus sylvatica* L.) sawdust sieved (2 mm mesh) and autoclaved (20 min, 120 °C) twice, with 2 days in between (Fig. 3.1). This led to a 0.5 cm layer of sawdust in the microcosm. The initial sterility of the sawdust was checked by plating sawdust suspensions at different dilutions on 10% TSA medium and by incubating them for 7 days at 25°C. No microbial growth was detected. Fungal inocula were prepared on beech wood blocks (50×30×10 mm). First, wood blocks were sterilised (autoclaved twice, 20 min, 120 °C, with 2 days in between). The initial sterility of the wood blocks was checked by plating woodblock suspensions at different dilutions on 10% TSA medium and by incubating them for 7 days at 25°C. No microbial growth was detected. The wood blocks were then incubated with *P. chrysosporium* in Petri dishes, containing malt (30 g.l^{-1}) agar (20 g.l^{-1}) medium for 19 weeks, at 25°C, in dark conditions (Hervé *et al.* 2014a).

The microcosms were inoculated in three different microbial conditions, corresponding to three different treatments. In one treatment – called BF (for bacteria + fungus *i.e. P. chrysosporium*) – the microbial suspension E0 (16 ml) was spread carefully over all of the sterile sawdust after having placed a beech block inoculated with the white-rot fungus *Phanerochaete chrysosporium* RP78 in the center of the microcosm. In a second treatment – called B (for bacteria, *i.e* without *P. chrysosporium*) – the microbial suspension E0 (16 ml) was spread carefully over all of the sterile sawdust and a sterile beech wood block was placed over the mixture in the center of the microcosm. A control treatment – called F (for fungus only *i.e P. chysosporium* without the microbial suspension) – consisted in sterile sawdust, humidified with 16 ml of sterile water, over which was placed a beech block inoculated the white-rot fungus *P. chrysosporium* RP78. For the first step (E1), microcosms were incubated during 12 weeks to allow the establishment of fungal colony and / or bacterial

communities. At the end of this period (E1), we used a 2 cm diameter round punch to sample 1.54 cm^3 of the sawdust with associated bacteria and/or fungal hyphae. We conducted sampling at four equally distant sites within each microcosm and pooled and homogenised together these 4×1.54 cm^3 of sawdust. Half was used to inoculate sterile sawdust in the center of a new microcosm (Figure 3.1) and the other half was used for molecular analyses. Two further enrichment steps were performed every three weeks (E2 and E3 samples; Figure 3.1), using the same procedure for the three treatments. For B and BF treatments, ten replicates were made at each steps. For the F treatment (control), five replicates were made. All manipulations were done under sterile conditions, using a biosafety cabinet. All microcosms were incubated at 25°C in the dark.

To monitor the variations in bacterial diversity, a subset of 22 microcosms was selected (Figure 3.1): three for the B treatment for each step (E1, E2 and E3) and four for the BF treatment for each step. The bacterial diversity from the E0 inoculum was also analysed. The presence of *P. chrysosporium* was checked for each BF microcosm (see below). The presence of other fungi, originally belonging to the E0 inoculum, was evaluated by light transmission microscopy and by observing spores in the Nycodenz extract as well as by plating several dilutions of the microbial suspensions obtained from the 22 samples on malt (30 $g.l^{-1}$) agar (20 $g.l^{-1}$) medium with five replicates per sample for the B and BF treatments at each interval. The plates were then incubated for five days at 25°C. Fungal colonies were found present in all samples, with a concentration increasing from E0 to E3 and with visibly different phenotypes, which were distributed at random regardless of the treatment and the sampling time.

3.3.3 DNA extraction, PCR amplification and sequencing of bacterial pyrotags

Total DNA was extracted from 0.2 g of each sawdust sample using the FastDNA SPIN Kit for soil (MP Biomedicals, Solon, OH, USA) following the manufacturer's instructions. The variable region V5-V6 of the bacterial 16S rRNA gene was amplified using the primers 787r (5'-MxxxATTAGATACCYTGTAGTCC-3') and 1073f (5'-NxxxACGAGCTGACGACARCCATG-3'), where M and N represent the linkers CCATCTCATCCCTGCGTGTCTCCGACTCAG and CCTATCCCCTGTGTGCCTTGGCAGTCTCAG respectively and xxx represents the sample identification bar coding key (tag) and the multiplex identifier (MID) (Sundquist *et al.* 2007).

PCR reactions were performed in a 50 µl final volume containing 20 µl Master Mix (5 PRIME, Hamburg, Germany), 24 µl water Mol Bio grade (5 PRIME, Hamburg, Germany), 2.5 µl of each primer (10 µM) and 1 µl DNA. The PCR conditions used were 94°C for 4 min, 30 cycles of 30 s at 94°C (denaturation), 48°C for 1 min (annealing) and 72°C for 90 s (extension), followed by 10 min at 72°C. Each sample was amplified in seven replicates and subsequently pooled before being purified using QIAquick PCR purification kit (QIAGEN, Hilden, Germany) and quantified using both NanoDrop 1000 spectrophotometer (Thermo Scientific, Hertfordshire, UK) and Low DNA Mass Ladder (Invitrogen, Carlsbad, CA, USA). Amplicons were sequenced using the 454-pyrosequencing GS-FLX Titanium technology (Roche 454 Life Sciences, Branford, CT, USA) at Beckman Coulter Genomics (Danvers, MA, USA).

3.3.4 Sequence processing

Sequence processing was performed using the Mothur software version 1.29.1 (Schloss *et al.* 2009) and by largely following the Schloss standard operating procedure (Schloss, Gevers & Westcott 2011). Briefly, sequencing errors were reduced by implementation of the AmpliconNoise algorithm and low-quality sequences were removed (minimum length 200 bp, allowing 1 mismatch to the barcode, 2 mismatches to the primer, and homopolymers no longer than 8 bp). Sequences were then trimmed to keep only high quality reads ($Q \geq 35$). Chimera were removed using the chimera.uchime mothur command. Singletons were included in the analysis. Sequences were aligned and classified against the SILVA bacterial SSU reference database v 102 (Pruesse *et al.* 2007). Finally, sequences were assigned to genus-level phylotypes using the naïve Bayesian classifier implemented in Mothur and the operational taxonomic unit (OTU) was defined at the 97% similarity level. These sequence data have been submitted to the GenBank database under accession numbers SRR900229 to SRR900250 (study SRP023174).

3.3.5 Detection of *P. chrysosporium* in the microcosms

To ensure that *P. chrysosporium* RP78 remained present in the different BF microcosms selected for analysis of diversity in the bacterial communities, nested PCR were performed for its detection. In the first phase, ITS1 and ITS4 regions were amplified by PCR (95°C for 3 min, 30 cycles of 30 s at 95°C, 52°C for 30 s and 72°C for 60 s, followed by 10 min at 72°C). These PCR products were then amplified using specific PCR amplification

for *P. chrysosporium* according to Lim et al. (2007), using Pchr-F (5'-GAGCATCCTCTGATGCTTT-3') and ITS4 primers. Both PCR reactions were performed in a 25 µl final volume containing 10 µl Master Mix (5 PRIME, Germany), 10 µl water Mol Bio grade (5 PRIME, Germany), 1.25 µl of each primer (10 µM) and 2.5 µl DNA. PCR products were purified using MultiScreen HTS filter plates (Millipore, Ireland) and then sequenced using Sanger method at Eurofins MWG (Ebersberg, Germany). *P. chrysosporium* was detected in all studied microcosms in the E1, E2 and E3 steps.

3.3.6 Estimation of the wood decomposition

Because wood decay is a long process, to gauge the rate of wood decay, two further enrichment steps (E4 and E5) were performed using the same procedure, with the three treatments (B, BF, F) and all of the replicates. The E5 step was incubated for 190 days at 25°C. Size and color of the E5 sawdusts were observed and compared to the control sawdust *i.e.* sterilised sawdust. A subset of each sample was dried at 55°C and then ground in a 10 ml zirconium oxide mill (Retsch, Haan, Germany). Carbon and nitrogen concentrations of each subsample were measured using a CHN analyser NC2500 (ThermoQuest, CE Instruments) (Palviainen *et al.* 2008).

3.3.7 Data analysis

Statistical tests were computed using the R software version 2.14 (R Development Core Team 2013). Rarefaction curves, diversity indices (both calculated from 10^6 iterations) and relative abundances of OTUs were estimated using Mothur (Schloss *et al.* 2009). Analysis of similarity (ANOSIM) and similarity percentage (SIMPER) (999 permutations) were performed using PRIMER 6 (PRIMER-E Ltd, Plymouth, UK) based on a Bray-Curtis dissimilarity matrix from relative abundance of the OTUs (Clarke 1993). A phylogenetic distance matrix was generated using the UniFrac method (Lozupone & Knight 2005) with a tree generated in Mothur, using NAST-based aligner (DeSantis *et al.* 2006a; Schloss 2009) and SILVA sequence set (Pruesse *et al.* 2007) for alignment and Clearcut (Sheneman, Evans & Foster 2006) to generate a neighbor joining tree.

Based on the results, several core microbiomes (Shade & Handelsman 2012) were defined (Table 3.2) and analysed based either on their relative abundance or presence/absence. B-BF core microbiome was defined as OTUs present in all B plus BF samples, while BF and B core microbiomes consisted in OTUs present in all BF or B samples, respectively (*i.e.* all

replicates and all steps for the given treatment). In addition to these three core microbiomes, we also defined time-specific core microbiomes, *i.e.* OTUs present in all replicates of a given treatment, or both treatments, at one or two sampling date(s) only (E1, E2 or E3). Finally, a category containing all the others OTUs was also considered, representing OTUs without consistent occurrence according to treatment or date.

3.4 Results

3.4.1 Wood biodegradation

To ensure that the inoculated microorganisms were involved in the lignocellulolytic process, sawdust from microcosms was analysed after 190 days of incubation. Carbon and nitrogen concentrations were measured. The C/N ratio (Figure 3.4.A) was found to be significantly higher in sterile saw dust (control) compared to B, BF and F treatments (Wilcoxon test, $p < 0.01$), indicating that the wood had being altered by the presence of microorganisms during the incubation period (Palviainen *et al.* 2008). We observed that the C/N ratio was lower (Wilcoxon test, $p < 0.02$) in the presence of *P. chrysosporium* alone (F treatment) than when *P. chrysosporium* was not present (B treatment), confirming that *P. chrysosporium* is a more efficient wood decomposer. Colour is also considered a qualitative indicator of wood decay (Schwarze 2007). When compared to sterile sawdust (Figure 3.4.B), sawdust inoculated only with the white-rot fungus was lighter in colour and appeared bleached (Figure 3.4.E), indicating loss of lignin. When bacteria were introduced (treatments B and BF), the sawdust appeared brown and darker in colour (Figures 3.4.C, 3.4.D), indicating cellulose degradation. Finally, with regards to wood particle size, we observed incubation with microorganisms led to a significant decrease in beech particles (compare Figure 3.4.B with Figures 3.4.C, 3.4.D and 3.4.E). Considered together, these results confirmed that the process of wood decay took place during the course of the microcosm experiment.

3.4.2 Pyrotag sequencing results

In total, 22 samples were analysed with ¼ 454 run to obtain a total of 215 742 raw pyrotag reads. After quality filtering and chimera removal, 88 652 sequences remained to be analysed, showing an average length of 248 bp and a number of sequences per sample varying

from 1599 to 6110. These variations were independent of the treatment (ANOVA, $p>0.07$). Sequence clustering yielded a total of 3553 bacterial OTUs with a 97% sequence similarity threshold. To normalise the data based on the sample containing the lowest number of sequences, 1599 sequences were subsampled in each sample. For this subsampling, the average Good's coverage estimator (Good 1953) was observed as 0.986 ± 0.004 (mean ± standard error of the mean), meaning that sequence sampling was 98.6% complete. With the exception of the E0 inoculum, rarefaction curves (Figure 3.2.A) almost reached an asymptote for 1599 OTUs. Good's coverage and rarefaction curves showed that communities were sufficiently sampled to permit us to estimate the actual community richness.

3.4.3 Diversity analysis

$Chao_1$ estimation (Figure 3.2.B) revealed a significant difference between the richness in the bacterial community extracted from the forest soil (E0) that served as inoculum in the experiment, and the bacterial communities that evolved in the gnotobiotic environment of our microcosms. Indeed, estimation of the number of OTUs was close to seven times lower in sawdust (mean values between 50 and 84 taxa) than in soil (535 taxa), indicating that the sawdust had acted as an environmental filter. Richness was found to be similar for microcosms within and between treatments, with one exception being that E1B showed a richness level significantly higher than E2B (Figure 3.2.B; one-sided Wilcoxon test, $p < 0.04$). The presence of the white-rot fungus showed no significant effect on the richness level of the bacterial community. The Shannon index-based measure of evenness J (Figure 3.5.A) and Shannon diversity index H (Figure 3.5.B) supported the same results; bacterial communities in the microcosms characterised by similar levels of evenness and diversity. The only noteworthy difference observed appeared to be between E1BF and E2BF (one-sided Wilcoxon test, $p < 0.015$) for both J and H, which were higher for E1BF.

3.4.4 Analysis of similarity of community composition between treatments

To test whether treatment or time had any effect on the bacterial community, we performed one-way ANOSIM (Table 3.1). During the first step of the enrichment (E1), the bacterial community associated with *P. chrysosporium* (E1BF) was found to be significantly different from the one without (E1B) ($R=0.796$, $p<0.03$). This difference appeared to become less pronounced over time and non-statistically significant ($R=0.13$, $p=0.2$ at E2; $R=0.037$, $p=0.429$ at E3), indicating that the effect of *P. chrysosporium* on the overall structure of the bacterial community was observed exclusively during the initial step of bacterial colonization

of the sawdust. The overall bacterial community structure also significantly changed with time with noted consistency, but only in the presence of *P. chrysosporium* between the first and second steps (E1BF versus E2BF, R=0.729, p<0.03), demonstrating a time-dependent effect of the white-rot fungus on the structure of the wood-associated bacterial communities.

When considering the phylogenetic distance (unweighted UniFrac metric) between bacterial communities (Figure 3.6), E0 appeared to be separated from the microcosm samples. All samples from E1 were clustered, within which the E1B and E1BF replicates were clustered into two distinct groups. This confirmed the selective effect of *P. chrysosporium* on the composition of the bacterial communities during the first step of enrichment.

3.4.5 Temporal changes in the overall structure of the bacterial communities

To better characterise how the structures of the bacterial communities changed over time, we surveyed the dissimilarity of community structures between replicates in the B treatment (without *P. chrysosporium*), between replicates in the BF treatment (with *P. chrysosporium*), and between those from both B and BF treatments (Figure 3.7). For a given treatment, the average dissimilarity between replicates increased (from 37.6 and 29.4 to 72.8 and 65.7% for B and BF treatments, respectively). This highlighted a divergence in bacterial communities structure within replicates over time, for both B and BF treatments. However the degree of divergence was higher with the absence of *P. chrysosporium*, confirming a selective structural effect of the white-rot fungus on the associated bacterial community. The average dissimilarity between treatments B and BF revealed a similar trend, with a less pronounced increase over time (from 49.0 to 69.1%). The dissimilarity of community structure between replicates of the BF treatment was lower than that observed between B and BF treatments, accentuating the effect the white-rot had on bacterial community structures.

3.4.6 Analysis of core microbiomes

One B-BF core microbiome containing the OTUs present in all of the B plus BF samples was successfully identified, along with one core microbiome for B or BF treatment, defined as OTUs present in all B or BF samples during the three respective sampling times. Time-specific core microbiomes were also identified, *i.e.* OTUs present in all replicates of one or both treatments, on only one or two sampling dates. The pattern of these core microbiomes strongly differed when considering the relative abundance (Figures 3.3.A and 3.3.C) or the number of OTUs (Figures 3.3.B and 3.3.D). Indeed, the B-BF core microbiome, constant over

time, corresponded to only two OTUs (just over 0.5 % of the average total number of OTUs), but represented half of the total bacterial abundance (the mean at 50.0 %) (Table 3.2). Both OTUs represented only 0.14% of the relative abundance in the initial inoculum E0. This underlined the high degree of selection of these two OTUs in the microcosms, with or without the fungus and consistent over time, when compared to the E0 community (Figures 3.3.A and 3.3.C).

The BF core microbiome corresponded to only one OTU (on average 0.4 % of the total number of OTUs observed in BF samples) and represented 0.4% of the total bacterial abundance (Table 3.2, Figures 3.3.A and 3.3.B). In addition, time-specific BF core microbiomes were identified, *i.e.* 8, 1 and 2 OTUs at date E1, E2 and E3 respectively, which corresponded to 0.7 to 22.8 % of relative bacterial abundance observed in the BF samples. Similarly, the B core microbiome corresponded to one OTU and represented 2.1 % of the total bacterial abundance while time-specific B core microbiomes corresponded to 9, 1 and 4 OTUs at dates E1, E2 and E3 respectively, which corresponded to 0.5 to 11.3 % of relative bacterial abundance in the B samples (Table 3.2, Figures 3.3.C and 3.3.D). Conversely, the OTUs not belonging to any core categories, *i.e.,* those not specific to any groups (treatment x date), were largely dominant in term of OTUs number (95.5 % on average) but much less important in term of relative abundance (25.7 % on average). Thus, most of temporal variations in community composition within and between treatments originated from low abundant OTUs, whereas core microbiomes included notably more abundant OTUs.

3.4.7 Taxonomic assignment of the discriminating OTUs and major phyla

The most abundant OTU present in all microcosms (Table 3.2) belonged to the *Xanthomonadaceae* family (with a mean relative abundance of 45.7%), regardless of the treatment, suggesting a strong affinity between *Xanthomonadaceae* and wood substrate. Interestingly, *Burkholderia* was the only genus found for BF core OTUs, suggesting that there might be particular links between *P. chrysosporium* and populations belonging to this bacterial genus. Two OTUs related to *Burkholderia* (OTU 954) and *Burkholderiaceae* (OTU 925) were also found in time-specific B core microbiome in E1 (Table 2), with relative abundance close to those found in the initial inoculum E0 (0.98% and 0.10% for OTU 925 and OTU 954 respectively), suggesting a forest soil origin of these OTUs. Considering the different OTUs related to *Burkholderia* or *Burkholderiaceae* in the microcosms, it was not possible to detect all of them in the initial inoculum because not all the diversity was covered in E0 (unsaturated rarefaction curve, see Figure 3.2.A). On the date E1, where the influence of

P. chrysosporium was considered the highest, time-specific BF core taxa contained eight OTUs, belonging to *Actinobacteria* (two OTUs) and *Proteobacteria* (six OTUs) phyla. Among these OTUs, the most abundant was the OTU 1034, assigned to *Sphingomonas* genus (mean relative abundance 12.35 %).

Concerning the OTUs that did not belong to any core categories, *Proteobacteria* was the major phylum in terms of both OTUs number and relative abundance, with an increasing trend from E1 to E3: from 57.4 to 68.8% for OTUs number, and from 6.0 to 24.4% for mean relative abundance. More generally, *Proteobacteria* was by far the major phylum in microcosms, representing from 84.7 to 96.8% of the relative abundance of wood-associated bacterial diversity but only 34.4% in the initial inoculum E0 (Figure 3.8). Among other major phyla, *Actinobacteria* decreased their abundance along the enrichment steps (from 4.65 to 0.06 %) while *Bacteroidetes* increased in abundance (from 0.02 to 4.75%) (Table 2). Additionally, both *Firmicutes* (10.4% of OTUs number and 2.1% of relative abundance) and *Acidobacteria* (6.7% of OTUs number and 2.5% of relative abundance) contributed to the wood-associated bacterial diversity (Figure 3.8).

3.5 Discussion

We hypothesised that the bacterial communities associated with *P. chrysosporium* developing on wood sawdust were different from those observed colonising wood sawdust with no fungus, both different again from the bacterial community of original forest soil. To decipher the selective effects of wood substrate and of white-rot fungus on bacterial communities and to characterise the mycosphere bacterial communities during the wood decay process, we combined a microcosm experiment with a high-throughput sequencing approach.

In our study, significant reduction of bacterial diversity was observed during the enrichment steps in the woody environment compared to the original soil environment, further supported by saturation of the rarefaction curves (Figure 3.2.A), highlighting the existence of an enrichment pressure exerted by the wood, on the microbial community. Notably, in addition to this wood effect, both the Bray-Curtis and the UniFrac distance matrix analyses highlighted the fact that the structures of the bacterial communities associated with or without *P. chrysosporium*, were different, demonstrating that after twelve weeks of incubation (E1) the white-rot fungus significantly shaped the wood-associated bacterial

communities. Such results strengthen the relevance of our strategy of monitoring the relative impact of both a wood environment and a white-rot fungus on the soil bacterial communities by combining a microcosm approach with high-throughput sequencing. These results also confirm that high-throughput sequencing and microcosm scale approaches together are appropriate tools to monitor bacterial communities associated with global scale processes like wood biodegradation (Benton *et al.* 2007).

In order to precisely understand the changes of the structure of the different bacterial communities, a core microbiome analysis was performed based on identified OTUs (Shade & Handelsman 2012). We defined several core microbiomes and determined that the OTUs not belonging to any core were to be considered the stochastic component of the system. Core microbiome analysis revealed that in the microcosms an important part of the bacterial diversity could not exclusively be ascribed to the presence of *P. chrysosporium* and / or to the woody environment, specifically in terms of the number of existing OTUs (Figures 3.3.B and 3.3.D). A noteworthy factor was the presence of other fungi found in our microcosms, initially belonging to the E0 inoculum. These fungi, which developed on the woody matrix, could have impacted the bacterial community structure. No correlation was found between fungal phenotypes and time or treatments suggesting that changes observed in the diversity of other fungi cannot explain treatment or time effects. However, because the concentration of these other fungi increased over time, their abundance likely had an effect on the temporal variations of the bacterial community structure, as suggested by the progressive dissimilarity observed between community structures within and between treatments (Figure 3.7). In addition, our results showed the importance of the stochastic processes in bacterial community assemblage (Caruso *et al.* 2011), in a woody environment. Indeed, in our microcosm experiment performed under controlled conditions and by using homogenised beech sawdust, the dissimilarity within replicates of the B or BF treatment increased with each of the enrichment steps (Figure 3.7) suggesting stochastic variations of the bacterial communities. Such evolution may be due to a subsampling effect in the initial soil microbial community used to inoculate the different microcosms (E1). It can also be due to the serial subsampling performed to inoculate the microcosms at the different steps of the enrichment. Likewise, the importance of the stochastic force in our experiment could be viewed in the light of the neutral theory (Hubbell 2001; Chave 2004) which proposes that the community assemblage rules are governed by stochastic processes. This theory could explain the high number of OTUs which could not be described as belonging to any core in our experiment,

representing the stochastic component of the microcosms.

The stochastic component of our system was less important when considering the relative abundance (Figures 3.3.A and 3.3.C) rather than the number of OTUs (Figures 3.3.B and 3.3.D). More precisely, the stochastic component in terms of relative abundance always represented a minor fraction, *i.e.* 9%, 34% and 27% for enrichment steps E1, E2 and E3, respectively. This suggests that the relative abundance of major OTUs was strongly influenced by deterministic factors: the woody environment, represented here as sawdust, acting as an environmental factor (compare the constant B-BF core microbiomes between E0 and E1) and the white-rot fungus *P. chrysosporium* (compare the time specific BF core microbiomes between E0 and E1) acting as a biotic determinant. Both characterise the mycosphere effect of a white-rot fungus during the lignocellulolytic process. Mycosphere effect of white-rot fungi has already been described by Folman and colleagues (2008), who showed, using soil microcosms, that the presence of *Hypholoma fasciculare* and *Resinicium bicolor* on wood blocks reduced the total number of bacteria and altered the composition of the bacterial community, according to the analysis of denaturing gradient gel electrophoresis patterns of directly amplified 16S rRNA gene fragments. Our study is complementary to the one of Folman and colleagues (2008). Indeed, we tested the hypothesis of a mycosphere effect on the bacterial communities during the wood decay process which is why we used only a woody substrate as the growth matrix in the microcosms. We also monitored the mycosphere effect over time, using an enrichment method to follow the time-evolution of bacterial communities. Finally, the use of 16S rRNA amplicon based pyrosequencing allowed us to describe extensively and exhaustively the taxonomic bacterial diversity associated with *P. chrysosporium* and / or with the sawdust, at the genus as well as at the OTU level.

Once the woody environment and the white-rot fungus were described as being deterministic factors and because our diversity analysis was based on saturated rarefaction curves, it was only possible to clearly distinguish between treatments a few discriminating OTUs. With regards to the wood effect, the major OTU (OTU 1042), present in all microcosms with very high relative abundance (mean 45.7%), belonged to the *Xanthomonadaceae* family which has been previously described as being dominant among bacterial isolates from beech wood (Folman *et al.* 2008). Using various databases and classifiers, more information was obtained for this OTU. While the Ribosomal Database Project classifier (Wang *et al.* 2007) provided similar result to the SILVA database assigning this OTU to the *Xanthomonadaceae* taxon, Greengenes (DeSantis *et al.* 2006b) proposed

taxonomic assignment as being at the genus level with significant alignments (> 99% similarity) with *Luteibacter* and *Rhodanobacter* spp. EzTaxon-e (Kim *et al.* 2012) and BLASTN against the 16S ribosomal RNA database (NCBI) provided similar results to Greengenes, adding a third genus, *Dyella*. The *Luteibacter* genus had previously been found in freshly cut pine wood (Noll *et al.* 2010) and described as potentially involved in lignin catabolism (Bugg *et al.* 2011). The *Dyella* genus had previously found to be isolated in the white-rot mycosphere from *H. fasciulare*, in both microcosm (Folman *et al.* 2008) and field (Valásková *et al.* 2009) experiments. Additionally, *Dyella* were found to be highly active bacteria in the gut flora of a wood-feeding beetle larvae (Reid *et al.* 2011). This suggests a potential role in the process of wood degradation, supported by the fact that *Dyella koreensis* sp. nov. has been reported to be able to use cellulose as its sole source of energy (An *et al.* 2005). Lastly, the *Rhodanobacter* genus was found present in forest litter (Stursová *et al.* 2012) and forest soil (Hartmann *et al.* 2012). Considered together, these results reveal that the taxon and genera, to which OTU 1042 can be assigned, are linked to wood-related environments. The fact that OTU 1042 had been selected from the original soil bacterial community and identified as being the major OTU present in all microcosms filled with beech sawdust, strongly suggests that OTU 1042 is a taxonomic indicator of lignocellulosic environment. The second important OTU (OTU 1025), showing a mean relative abundance of 4.3 % throughout all microcosms (B-BF core), belonged to the *Rhizobium* genus. It has been found in archaeological waterlogged wood (Landy *et al.* 2008), in the gastrointestinal tract of wood-eating catfish (McDonald, Schreier & Watts 2012) and in decaying wood in forest (Zhang *et al.* 2008a; Tian *et al.* 2009), confirming its association with the decayed wood niche. Because nitrogen is a limiting factor for the biology of wood decaying fungi, it has been suggested that nitrogen-fixing bacteria, like *Rhizobia* (Dreyfus, Elmerich & Dommergues 1983), could possibly counterbalance the wood nitrogen deficiency (Clausen 1996). Here the fact that an OTU assigned to the *Rhizobium* genus was selected in all microcosms supports Clausen's hypothesis.

Interestingly, we found the *Actinobacteria* phylum, described as containing lignocellulolytic bacteria (Kirby 2005), to be less and less abundant along the enrichment steps (from 4.65 to 0.06 %) for both B and BF treatments. Among this phylum, OTU 814 assigned as *Mycobacterium* was abundant in the first step of the enrichment (3.36 %), considerably less in the second (0.3 %) and completely absent in the third. However, the *Mycobacterium* genus had previously been detected in decaying wood (Zhang *et al.* 2008a).

These results might be explained by existing competitive behaviors between bacteria colonising the same niche. Indeed, *Bacteroidetes* appeared to become increasingly abundant along the enrichment steps (from 0.02 to 4.75 %), suggesting adaptation to the decayed wood environment (Table 3.2). This phylum was also detected in decaying wood (Valásková *et al.* 2009) as well as in the gut flora of xylophagous cerambycid larvae (Reid *et al.* 2011), suggesting the existence of a potential link between some members of *Bacteroidetes* phylum and the lignocellulosic substrate.

Concerning the mycosphere effect, *Burkholderia* was the only genus found in all BF cores. One OTU (OTU 954), belonging to the *Burkholderia* genus and with low relative abundance (0.167%), was also found in the time-specific B core microbiome in E1. However, five OTUs (OTUs 1036, 1043, 932, 1037 and 970) with higher relative abundance (0.297%, 2.189%, 0.407%, 0.172% and 0.657%, respectively) were found specifically in the BF core microbiomes, throughout the enrichment, showing preferential recruitment of *Burkholderia* by *P. chrysosporium* during the process of wood decay. While *Burkholderia* species have previously been described as existing in various environments (Coenye & Vandamme 2003), many of them are known to interact with fungi with different ecological traits. For example, this genus has been shown to be abundant in the mycosphere of the ectomycorrhizal fungi *Scleroderma citrinum* and *Xerocomus pruinatus* (Uroz *et al.* 2012). It has also been found to be associated with lichens (Grube *et al.* 2009) and some members of this genus have been found to be able to comigrate with hyphae of the saprotrophic fungus *Lyophyllum* sp. (Warmink & van Elsas 2009). Several *Burkholderia* strains have even been isolated from cultures of *P. chrysosporium* (Seigle-Murandi *et al.* 1996) and *Phanerochaete sordida* (Lim *et al.* 2003). In our study, however, we revealed for the first time the coexistence of the *Burkholderia* genus with the white-rot fungus *P. chrysosporium* during the wood degradation process. Interestingly, an additional level of interaction has also been described between *Burkholderia* and fungi, with *Burkholderia* being bacterial endosymbionts of arbuscular mycorrhizal fungi (Bianciotto & Bonfante 2002; Levy *et al.* 2003) and plant pathogenic fungus (Partida-Martinez *et al.* 2007). Such results raise the question of the ecological origin of the *Burkholderia* found in all of the BF cores of our microcosm experiment. Further studies will be required to determine whether they have a soil or a fungal origin. In E1 when the influence of white-rot fungus was the most prominent, OTU 1034, belonging to the *Sphingomonas* genus, was the most abundant OTU (12.35 %) in the BF time-specific core. Interestingly, this genus is also known to be associated with fungi (Boersma *et al.* 2009;

Lecomte, St-Arnaud & Hijri 2011) and was proved to be able to degrade polycyclic aromatic hydrocarbons (Shi, Fredrickson & Balkwill 2001). Such examples beg the question of functional complementation between mycospheric bacteria and the white-rot fungi during the wood decay process (de Boer *et al.* 2005), where both partners are able to decompose lignocellulosic substrates.

3.6 Conclusion

For the first time, bacterial communities coexisting in the white-rot mycosphere have been extensively and exhaustively described using 16S rRNA amplicon based pyrosequencing. We showed that *P. chrysosporium* shapes the composition of the wood bacterial community, with regards to the relative abundance of taxa, during the lignocellulolytic process. The significant selection observed demonstrates that the white-rot mycosphere is a true ecological niche accommodating specific bacterial communities. The mycosphere niche has been described for mycorrhizal (Warmink *et al.* 2009; Nuccio *et al.* 2013), pathogenic (Dewey *et al.* 1999) and saprotrophic (Valásková *et al.* 2009) fungi. Here, we highlight that *P. chrysosporium* is a new example of fungus closely interacting with bacterial communities in its natural environment, *i.e.* wood. We were able to identify eight specific OTUs selected by the fungus after twelve weeks of incubation, belonging to *Actinobacteria* and *Proteobacteria* phyla and representative of a significant relative abundance of the total community. These specific OTUs should be considered to be potential taxonomic bioindicators of white-rot mycosphere. Future research should focus on isolation and functional characterisation of these white-rot associated bacteria to better understand bacterial-fungal interactions and to assess the role of this complex microbial consortia in lignocellulose recycling.

3.7 Acknowledgments

This work was supported by a grant from Lorraine Region, an ANR project (ANR-09-BLAN-0012) and IFR110 / EFABA. The UMR IaM is supported by a grant overseen by the French National Research Agency (ANR) as part of the "Investissements d'Avenir" program (ANR-11-LABX-0002-01, Lab of Excellence ARBRE). X. Le Roux was supported by grants from INRA-EFPA. We thank A. Mercanti, C. Calvaruso and M.P. Turpault for the help with sampling and P. Riveron for the help with chemical analysis. We also thank S. Antony-Babu

and M. Buée for very helpful discussions, P.D. Schloss for help and advice on bioinformatic analysis and A. Orsini for review of the English language.

3.8 Figures and tables

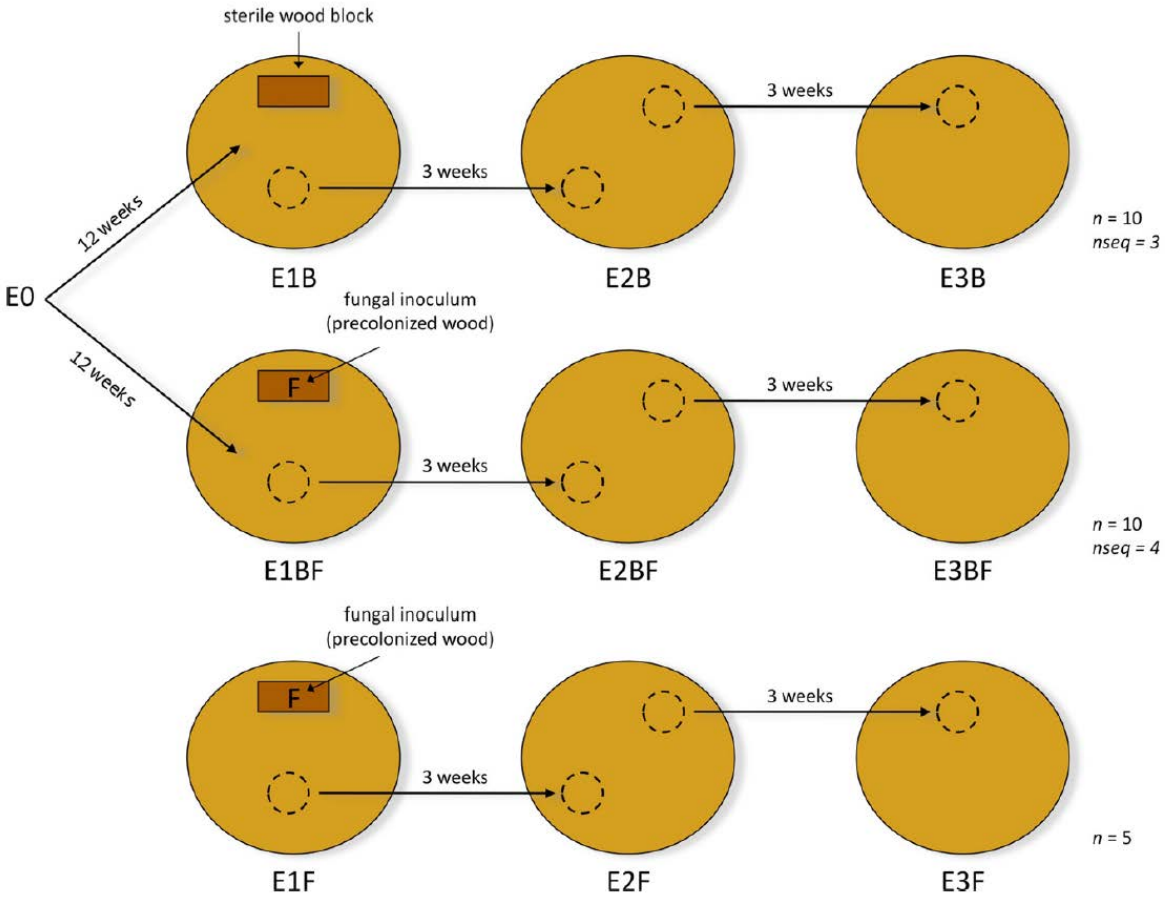

Figure 3.1. Diagram illustrating the experimental design within the microcosm. E0, a microbial suspension extracted from forest soil, was used as the initial inoculum. E0 was mixed with sterile sawdust as growth matrix, in two conditions: including (BF) or excluding (B) white-rot fungus *P. chrysosporium* previously inoculated on a beech wood block (F). After twelve weeks of incubation (E1), an enrichment was performed every three weeks (from E1 to E3) using a fraction taken from on microcosm to inoculate a new sterile microcosm. A treatment inoculated exclusively with *P. chrysosporium* (called F) was performed as a control.

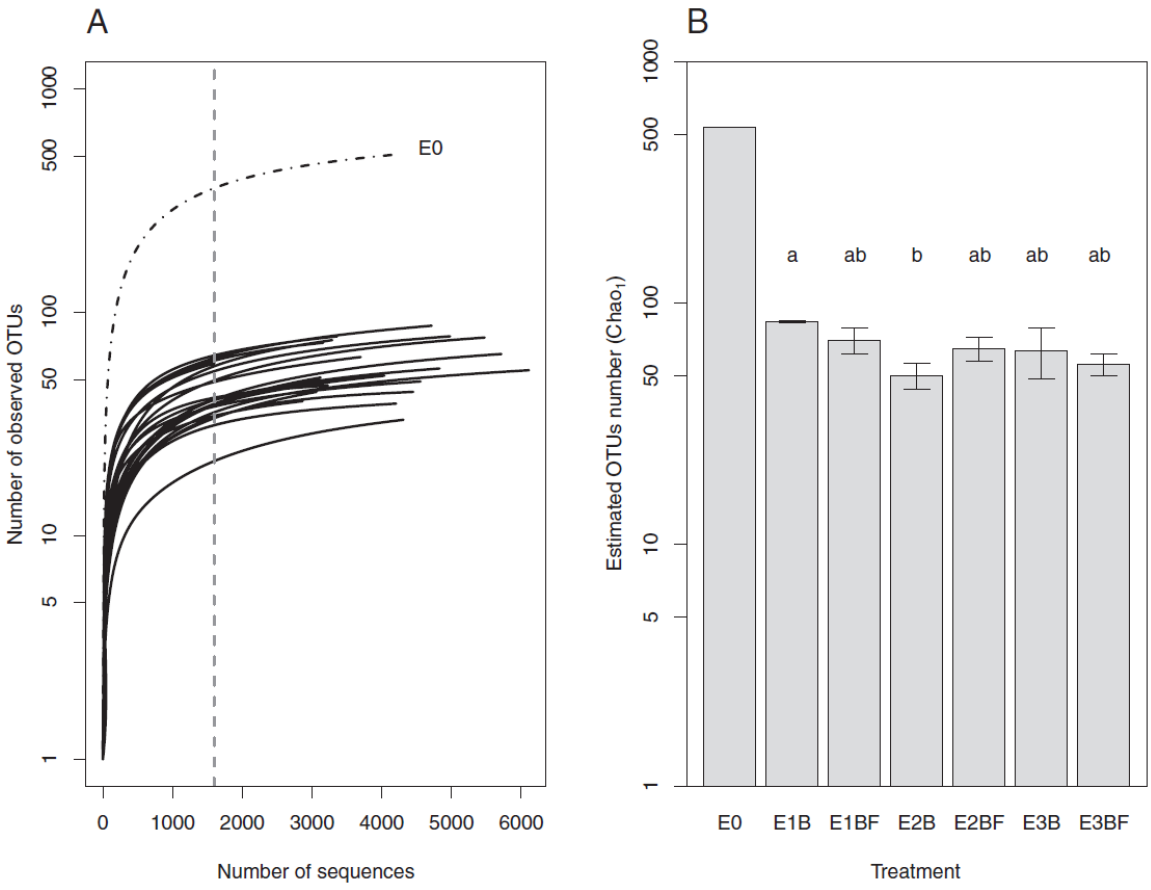

Figure 3.2. Analysis of diversity. **(A)** Rarefaction curves for the number of observed OTUs (logarithmic scale), defined by no more than 3% difference between 16S rRNA gene sequences. To compare the number of observed OTUs, each sample was normalized at 1599 sequences (vertical dotted line), corresponding to the smallest sample. **(B)** Comparison of $Chao_1$ richness estimator (logarithmic scale) between treatments. Error bars indicate standard error of the mean and small letters above (a, b) indicate significantly different distributions (Wilcoxon test, $p<0.05$). For B treatment (without *P. chrysosporium*), $n=3$; for BF treatment (with *P. chrysosporium*), $n=4$. E0 (inoculum, $n=1$) was not included in statistical tests.

	R	***p* value**
E1B, E1BF	**0.796**	**0.029**
E2B, E2BF	0.13	0.2
E3B, E3BF	0.037	0.429
E1BF, E2BF	**0.729**	**0.029**
E1BF, E3BF	**0.469**	**0.029**
E2BF, E3BF	0.281	0.086
E1B, E2B	0.259	0.2
E1B, E3B	0.259	0.1
E2B, E3B	-0.111	0.7
E1B, E2BF	**0.593**	**0.029**
E1B, E3BF	0.5	0.057
E1BF, E2B	**0.63**	**0.029**
E1BF, E3B	**0.574**	**0.029**
E2B, E3BF	0.333	0.114
E2BF, E3B	0.389	0.057

Table 3.1. Analysis of similarity between treatments. One-way ANOSIM based on Bray-Curtis matrix. Significant differences ($p<0.05$) are presented in bold.

Core	*OTUs*	*Taxonomic assignment*	*Mean Relative Abundance (%)*
B-BF core (constant across time)	Otu 1042	*Xanthomonadaceae*	45.69
	Otu 1025	*Rhizobium*	4.33
BF core (constant across time)	Otu 1036	*Burkholderia*	0.39
B core (constant across time)	Otu 1018	*Edaphobacter*	2.11
B-BF core in E1	Otu 889	*Hyphomicrobium*	6.68
	Otu 970	*Burkholderia*	4.48
	Otu 984	*Bradyrhizobiaceae*	3.25
	Otu 1032	*Burkholderia*	2.98
	Otu 733	*Bradyrhizobium*	1.75
	Otu 951	*Rhodospirillales*	1.31
	Otu 1022	*Burkholderiaceae*	1.16
	Otu 991	*Phenylobacterium*	0.48
BF core in E1	Otu 1034	*Sphingomonas*	12.35
	Otu 814	*Mycobacterium*	3.36
	Otu 1043	*Burkholderia*	2.19
	Otu 657	*Rhodospirillales*	1.33
	Otu 932	*Burkholderia*	0.41
	Otu 832	*Conexibacter*	0.38
	Otu 672	*Methylocella*	0.27
	Otu 1037	*Burkholderia*	0.17
B core in E1	Otu 1016	*Paenibacillus*	2.88
	Otu 586	*Paenibacillus*	2.71
	Otu 1030	*Hoeflea*	1.75
	Otu 945	*Teichococcus*	1.15
	Otu 1045	*Sediminibacterium*	1.15
	Otu 925	*Burkholderiaceae*	0.50
	Otu 1035	*Cohnella*	0.44
	Otu 954	*Burkholderia*	0.17
	Otu 558	*Acinetobacter*	0.15
B-BF core in E2	Otu 984	*Bradyrhizobiaceae*	0.17
BF core in E2	Otu 970	*Burkholderia*	0.66
B core in E2	Otu 889	*Hyphomicrobium*	0.46
B-BF core in E3	Otu 1032	*Burkholderia*	22.26
	Otu 1037	*Burkholderia*	0.57
BF core in E3	Otu 1034	*Sphingomonas*	4.67
	Otu 1043	*Burkholderia*	4.47

B core in E3	Otu 1030	*Hoeflea*	6.38
	Otu 1035	*Cohnella*	2.38
	Otu 945	*Teichococcus*	1.92
	Otu 979	*Paenibacillaceae*	0.15
Others OTUs in E1		*Proteobacteria* (57.44 %)	6.03
		Actinobacteria (9.74 %)	0.91
		Acidobacteria (5.64 %)	0.83
		Firmicutes (9.74 %)	0.78
		Verrucomicrobia (0.5 %)	0.38
		Chlamydiae (1.03 %)	0.09
		Bacteroidetes (1.03 %)	0.02
Others OTUs in E2		*Proteobacteria* (68.05 %)	22.09
		Bacteroidetes (4.14 %)	3.56
		Firmicutes (7.69 %)	0.42
		Actinobacteria (4.73 %)	0.38
		Acidobacteria (7.10 %)	0.19
		Chlamydiae (1.78 %)	0.04
		Verrucomicrobia (1.78 %)	0.03
		Cyanobacteria (0.59 %)	0.01
Others OTUs in E3		*Proteobacteria* (68.82 %)	24.44
		Bacteroidetes (2.35 %)	4.75
		Firmicutes (14.12 %)	1.40
		Acidobacteria (5.29%)	0.30
		Actinobacteria (1.74 %)	0.06
		Chlamydiae (0.59 %)	0.01

Table 3.2. Taxonomic assignment and mean relative abundance of the OTUs present in the different core microbiomes.

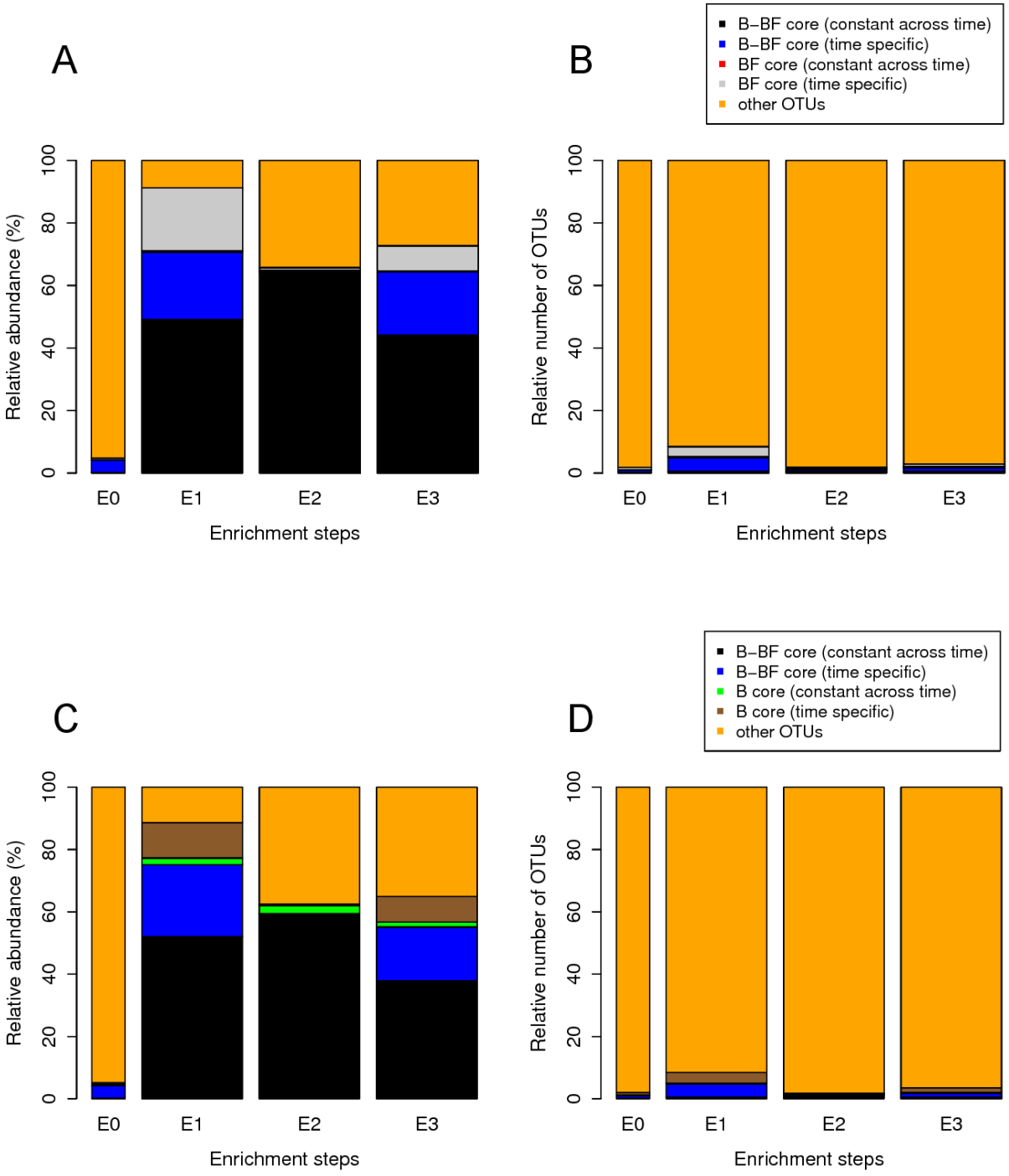

Figure 3.3. Temporal variations of the different core microbiomes during the enrichment, based on **(A, C)** relative abundance and **(B, D)** relative number of OTUs, and focusing on **(A, B)** BF treatment (containing *P. chrysosporium)* and **(C, D)** B treatment (without *P. chrysosporium).*

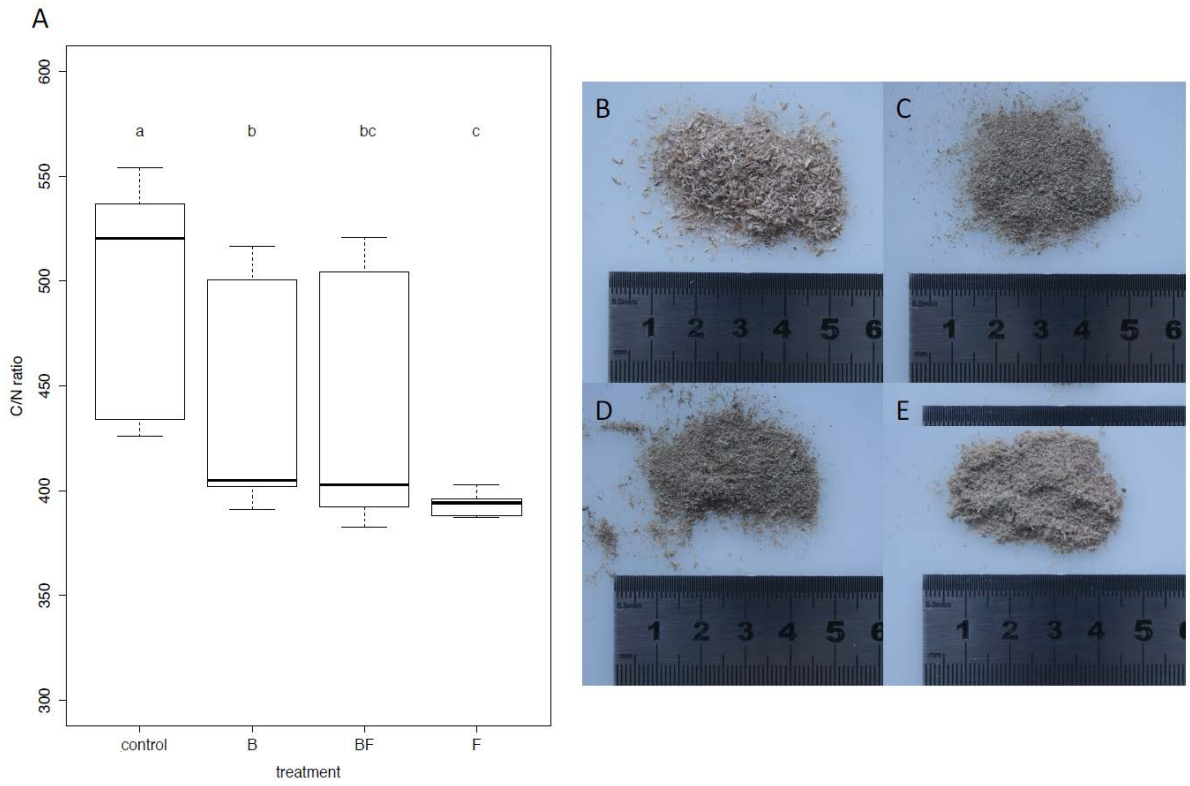

Figure 3.4. Wood decay characterisation after 190 days of incubation. **(A)** C/N ratio. Small letters (a, b, c) above the boxplots indicate significantly different distributions (Wilcoxon test, $p<0.05$), $n=10$ except for F, $n=5$. Images of the dried sawdust. **(B)** Control sample (sterile sawdust). (**C)** B treatment. **(D)** BF treatment. **(E)** F treatment.

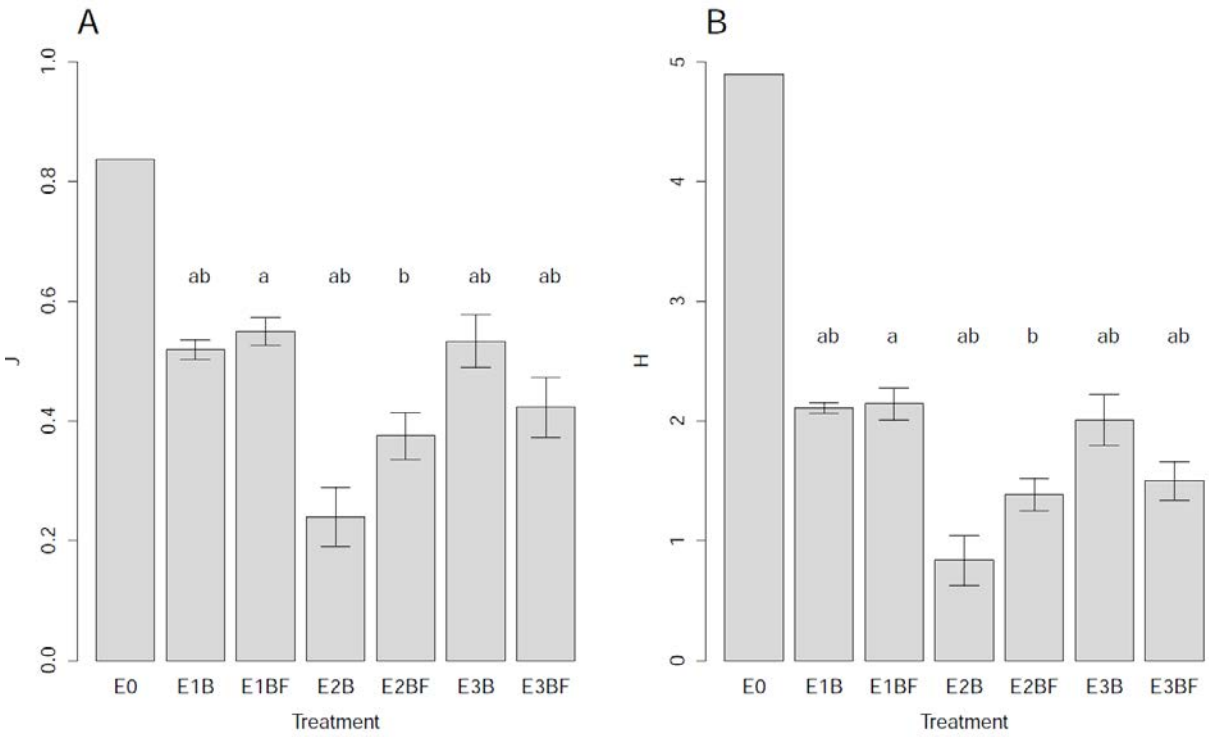

Figure 3.5. Comparison of **(A)** Shannon index-based measure of evenness J and **(B)** Shannon diversity index H between treatments. Error bars indicate standard error of the mean, different letters above indicate significantly different distributions (Wilcoxon test, $p<0.05$). For B treatment, $n=3$; for BF treatment $n=4$. E0 ($n=1$) was not included in statistical tests.

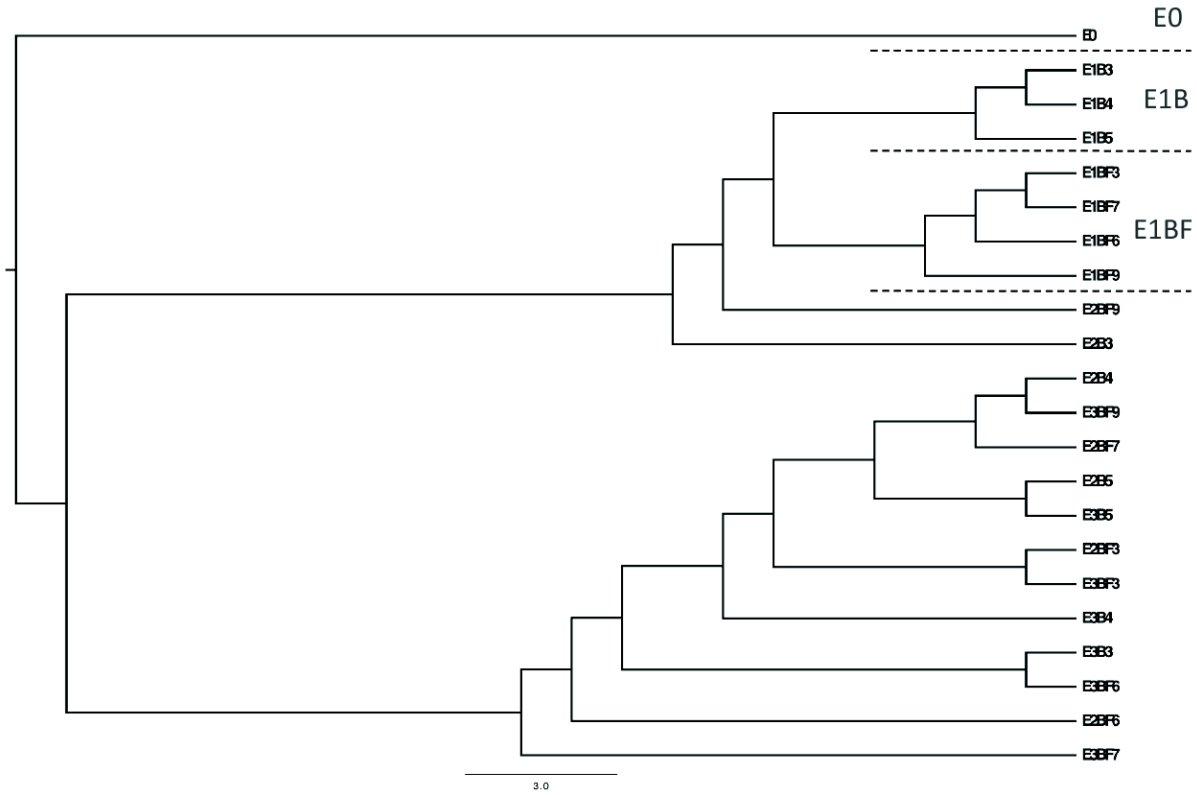

Figure 3.6. UPGMA clustering based on unweighted UniFrac distance. Branches are proportional to this distance.

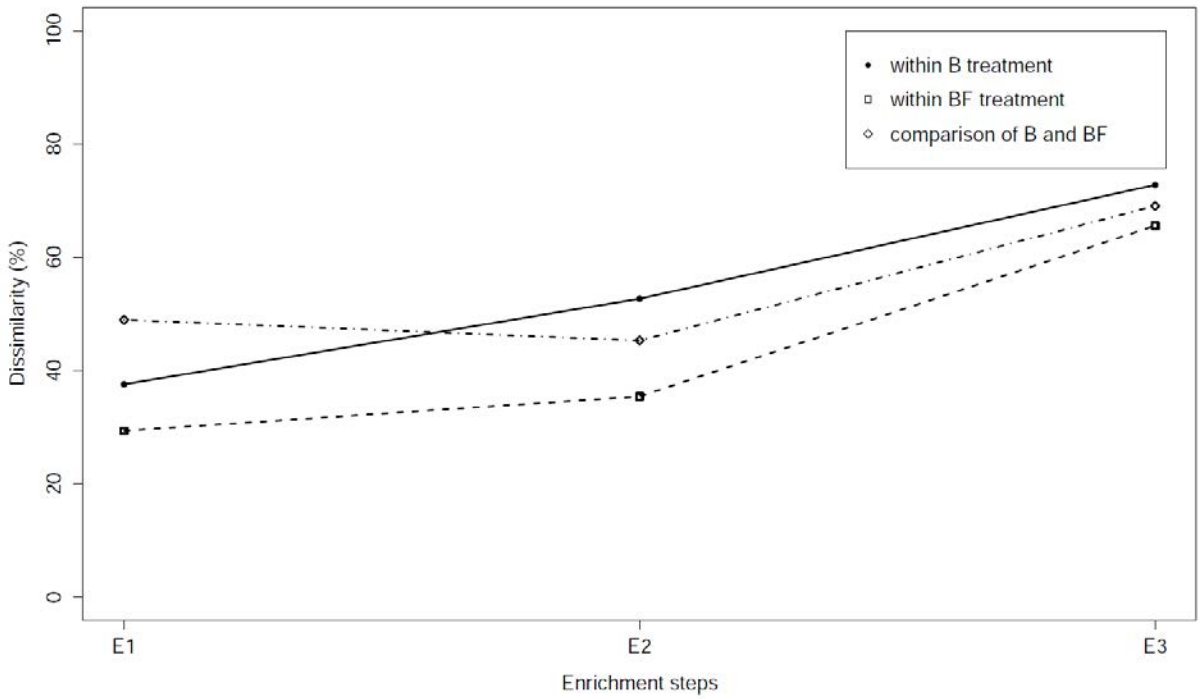

Figure 3.7. Evolution of dissimilarity percentage within replicates and between treatments during the enrichment steps, based on SIMPER analysis.

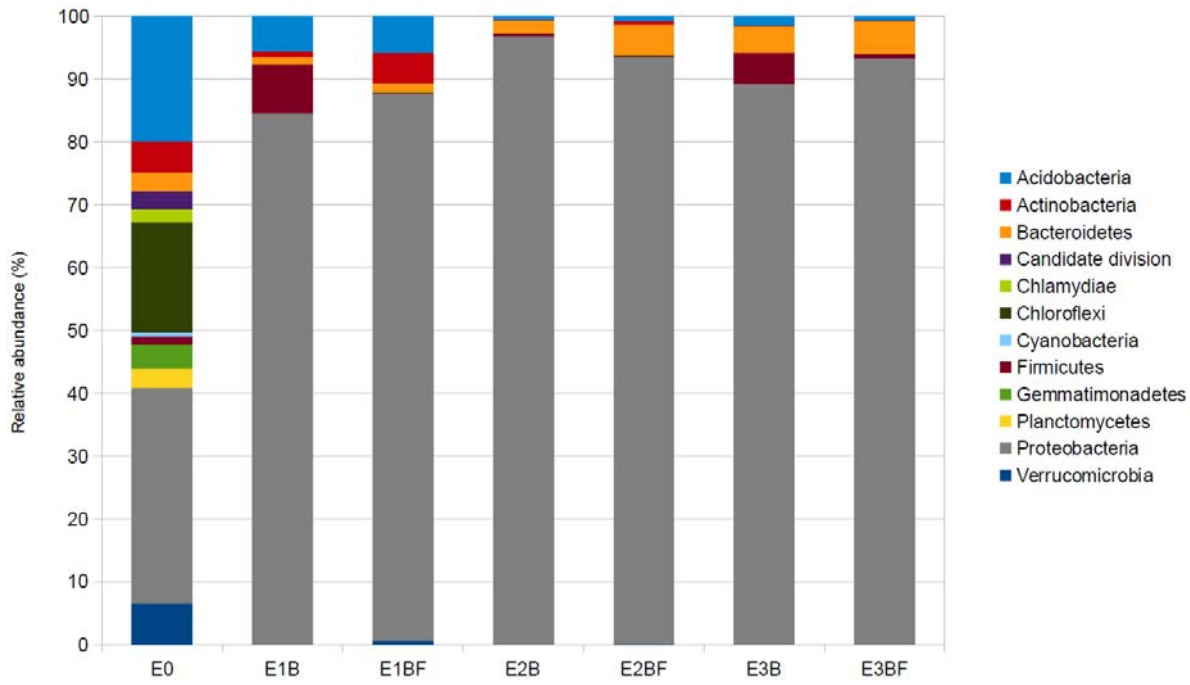

Figure 3.8. Taxonomic composition of the bacterial communities for each treatments. Bars show the percentage of the different phyla in term of relative abundance.

- Chapter 4 -

Impact of *Phanerochaete chrysosporium* on the functional diversity of bacterial communities associated with decaying wood

Résumé

Dans le chapitre précédent, nous avons pu mettre en évidence, par une approche non cultivable, le fait que le substrat bois et la présence du champignon de pourriture blanche *Phanerochaete chrysosporium* influençaient la structure et la composition des communautés bactériennes associées au bois en décomposition. La diversité taxonomique de ces communautés bactériennes est donc modifiée. Qu'en est-il de leur diversité fonctionnelle ?

A partir de la même expérience et des mêmes échantillons utilisés dans le chapitre précédent, une approche cultivable a été mise en place pour tenter de répondre à cette question, en travaillant à la fois à l'échelle des communautés et des souches bactériennes. Une collection bactérienne de 311 souches a été réalisée. L'identification taxonomique de ces souches a révélé que les deux OTUs dominants détectés par pyroséquençage (chapitre 3) et représentant 50 % de l'abondance relative dans les microcosmes étaient également les deux OTUs majoritaires de cette collection bactérienne. Ces résultats impliquent que les membres dominants des communautés bactériennes associées au bois en décomposition sont facilement isolables et cultivables. Ainsi une étude sur la diversité fonctionnelle de ces communautés basée sur une approche cultivable est tout à fait pertinente.

Les effets de l'enrichissement dans le substrat bois et de la présence de *P. chrysosporium* sur le potentiel fonctionnel des communautés bactériennes ont été évalués dans un premier temps en quantifiant les densités des communautés cultivables sur des milieux sélectifs dont la composition est en lien avec le processus de dégradation du bois. Au cours des différentes étapes d'enrichissement, ces densités bactériennes ont augmenté, indépendamment de la présence du champignon de pourriture blanche. Après douze semaines d'incubation (première étape d'enrichissement), un effet significatif de la présence du champignon a été détecté, se traduisant par une densité bactérienne plus élevée en présence du champignon qu'en son absence, indépendamment du milieu de culture utilisé. De plus, en absence de *P. chrysosporium*, aucun effet des milieux sélectifs sur les densités de communautés bactériennes cultivables n'a pu être observé alors qu'en présence du champignon lignivore, les densités bactériennes sur les milieux contenant de la cellulose ou du méthanol comme seule source de carbone se sont révélées inférieures à celles obtenues sur le milieu minimal de référence. L'ensemble de ces résultats met en lumière un effet mycosphère sur la diversité fonctionnelle des communautés bactériennes associées au bois en décomposition. Il suggère une compétition pour les ressources carbonées entre le champignon

et les communautés bactériennes.

Différentes analyses ont également été effectuées sur 125 des 311 souches bactériennes isolées. Des tests de confrontations entre le champignon et les souches bactériennes, sur un milieu pauvre en nutriments, nous ont montré que dans nos conditions expérimentales, les souches bactériennes inhibaient la croissance du champignon mais que cette inhibition était beaucoup plus faible avec les souches isolées dans les microcosmes contenant *P. chrysosporium* par rapport aux souches isolées de l'inoculum microbien initial extrait d'un sol forestier. Ces résultats révèlent une contre-sélection par le champignon de communautés bactériennes faiblement antagonistes dans la mycosphère de ce dernier. L'étude de la croissance des souches bactériennes sur des milieux sélectifs a révélé un effet fort de l'enrichissement avec une augmentation de la proportion de bactéries cellulolytiques, xylanolytiques et productrices de sidérophores au cours des différentes étapes d'enrichissement, indépendamment de la présence de *P. chrysosporium*. L'analyse des profils métaboliques BIOLOG de ces souches a également permis de révéler un effet important du substrat bois et des étapes d'enrichissement sur le potentiel fonctionnel de ces souches bactériennes.

La mise en évidence d'un effet mycosphère de *P. chrysosporium* à la fois sur la diversité taxonomique et sur la diversité fonctionnelle des communautés bactériennes associées au bois soulève des questions sur le processus global de décomposition du bois : quel est l'impact de ces communautés bactériennes sur ce processus ? De même, quelle est la contribution respective des bactéries et des champignons décomposeurs lors de la décomposition du bois ? Nous reviendrons sur ces questions dans la discussion générale de ce mémoire (Chapitre 6).

L'ensemble des travaux présentés dans ce chapitre correspond à un tapuscrit en préparation que nous allons prochainement soumettre au journal *Applied and Environmental Microbiology*.

4 Impact of *Phanerochaete chrysosporium* on the functional diversity of bacterial communities associated with decaying wood

The present chapter corresponds to an article in preparation entitled “Impact of *Phanerochaete chrysosporium* on the functional diversity of bacterial communities associated with decaying wood” and which will be submitted in the near future to *Applied and Environmental Microbiology* journal.

Vincent Hervé[1,2], Elodie Ketter[1,2], Jean-Claude Pierrat[3,4], Eric Gelhaye[1,2], Pascale Frey-Klett[1,2]

[1] INRA, Interactions Arbres – Microorganismes, UMR1136, F-54280 Champenoux, France.

[2] Université de Lorraine, Interactions Arbres – Microorganismes, UMR1136, F-54500 Vandoeuvre-lès-Nancy, France.

[3] INRA, UMR 1092 LERFOB, F-54280 Champenoux, France

[4] AgroParisTech, UMR 1092 LERFOB, F-54000 Nancy, France

4.1 Abstract

In a previous study exploring the diversity of the bacterial communities associated with the white-rot fungus *Phanerochaete chrysosporium* during wood decay, it has been reported that both the presence of this fungus and the wood substrate were able to modify the structure of the wood-associated bacterial communities. From the same microcosm experiment combined with an enrichment procedure, we tested using a culturable approach the hypothesis that these mycosphere and wood effects could also impact the functional diversity of these bacterial communities. Taxonomic identification of a 311 bacterial strain collection revealed that the two dominant OTUs associated with decaying wood detected by pyrosequencing and representing more than 50% of the relative abundance were also found to be the dominant OTUs with a culturable approach. After twelve weeks of incubation in sawdust, a significant mycosphere effect on the density of culturable bacterial communities was detected, with an overall increase of the bacterial densities, but a negative effect on the density of the culturable bacterial communities able to grow on cellulose and methanol-based media, suggesting a competition for the carbon resources. At the bacterial strain level, the functional potential of the isolates was more affected by the enrichment steps in a woody environment than by the presence of the fungus. Finally, bacterial strains isolated from *P. chrysosporium* mycosphere showed less antagonism against this fungus compared to the strains isolated from the initial forest soil inoculum, suggesting a selection by the fungus of less inhibitory bacterial communities.

4.2 Introduction

Microorganisms have been described as the main wood decomposers in forest ecosystems (Cornwell *et al.* 2009). By using a plethora of extracellular lignocellulolytic enzymes (Baldrian 2008), white-rot fungi are among the major actors of this wood decay. While they are less studied, bacteria are also part of the decaying-wood microbial biodiversity (Clausen 1996). Indeed, numerous bacteria present the capability of decomposing wood carbohydrates such as cellulose (Berlemont & Martiny 2013; Watts *et al.* 2013) and hemicelluloses (Lee *et al.* 2010; Woo *et al.* 2014). Moreover, a few bacteria have also been described as being involved in lignin degradation (Bugg *et al.* 2011; Větrovský, Steffen & Baldrian 2014; Brown & Chang 2014).

In numerous environments, bacteria and fungi coexist and are known to interact physically and functionally (Frey-Klett *et al.* 2011), such as on decaying-wood in forests (de

Boer *et al.* 2005; Valásková *et al.* 2009). Regardless of the environments, these interactions drive the establishment of specific bacterial communities in the surrounding areas of the fungal hyphae, called mycosphere (Warmink *et al.* 2009). In the case of white-rot fungi, this mycosphere effect on soil and wood-associated bacterial communities composition has been described. The presence of *Resinicium bicolor* or *Hypholoma fasciculare* or *Phanerochaete chrysosporium* on both polluted and unpolluted soils has been shown to change the soil bacterial community composition (Tornberg, Baath & Olsson 2003). The presence of *R. bicolor* and *H. fasciculare* has also been shown to reduce the number of bacteria colonising wood blocks from forest soil and to modify the composition of these bacterial communities (Folman *et al.* 2008). In a previous study, the community composition of wood-associated bacteria has also been shown to be significantly modified by the presence of the white-rot fungus *P. chrysosporium* (Hervé *et al.* 2014b). Wood, as a substrate, also shapes the taxonomic composition of wood-inhabiting bacterial communities (Hervé *et al.* 2014b). Altogether these results raise the question of the functional diversity of the bacterial communities selected by the wood substrate and / or the white-rot fungus and more specifically if these communities are directly or indirectly involved in the wood decay process. Indeed, it has been demonstrated that the mycospheric bacterial communities presented a functional potential significantly different from those of the non-mycospheric bacterial communities. For example, in the mycosphere of ectomycorrhizal fungi, bacteria have been shown to present distinct functional diversity compared to the surrounding bulk soil (Frey-Klett *et al.* 2005; Antony-Babu *et al.* 2013). The mycosphere of lichen also harbors bacterial communities with particular functional diversity, notably involved in nutrient cycling (Grube *et al.* 2009). In the case of the white-rot mycosphere, whether a specific functional diversity of the bacterial communities is selected by the white-rot fungus during the wood decay process still remains an open question.

To address this question, we explored the functional diversity of the bacterial communities associated with the white-rot fungus *P. chrysosporium* and / or with decaying-wood, using a microcosm experiment with sawdust as growth matrix. A bacterial community was extracted from a forest soil and then inoculated in these microcosms, in presence or in absence of *P. chrysosporium*. Three enrichment steps were subsequently performed to create a favorable environment for the coevolution of the bacterial communities with *P. chrysosporium* and / or with decaying-wood. We demonstrated that specific bacterial communities were selected by decaying wood and the white-rot fungus *P. chrysosporium*

(Hervé *et al.* 2014b) and thus investigated the functional diversity of these communities by a cultivation approach, at both community and strain levels on different selective media. These media were chosen in relation to the wood decay process. We hypothesised that, because white-rot fungi create an oxidative environment during the wood-decay process (Hammel *et al.* 2002), bacteria of the white-rot mycosphere would be more tolerant to oxidative stress than wood-associated bacteria. Therefore, we compared the density of the culturable bacterial communities isolated in presence or in absence of *P. chrysosporium*, on two minimal media containing either menadione or hydrogen peroxide as oxidising agent (Jamieson 1992). Because methanol was proved to be produced during lignin degradation by *P. chrysosporium* (Ander & Eriksson 1985), we also hypothesised that bacteria able to grow on methanol as a sole source of carbon would be more numerous in the white-rot mycosphere than in the wood. The last hypothesis posits that bacteria able to grow on cellulose as a sole source of carbon as well as cellulolytic bacteria would be more numerous in the white-rot mycosphere than in the wood, the white-rot fungus giving access to cellulose reachable by bacteria after wood delignification (de Boer *et al.* 2005). Secondly, we isolated and identified 311 bacterial strains from the different treatments, *i.e.* presence or absence of *P. chrysosporium* at the different enrichment steps. A randomly selected subset of 125 strains was then used for phylogenetic analysis and their functional potential was evaluated on selective media for siderophore production, lignolytic, cellulolytic and xylanolytic activities. Their metabolic profile and their impact on the *in vitro* growth of *P. chrysosporium* were also characterised. All these assays were performed in order to progress in the understanding of the potential role of the bacterial communities from the white-rot mycosphere during the wood decay process.

4.3 Materials and methods

4.3.1 Experimental design

Experimental design has been described in a previous study (Hervé *et al.* 2014b) (Figure 4.8). Briefly, a microbial suspension was extracted from soil samples (cambisol) collected in a forest dominated by beech (Lequy *et al.* 2014) using sterilised core borer (20 cm depth), after removing the overlying litter. Microorganisms were extracted using Nycodenz (Axis Shield, Oslo, Norway) density gradient (1.3 $g.ml^{-1}$) centrifugation, according to Lindahl & Bakken (Lindahl & Bakken 1995). The microbial suspension highly enriched in bacteria obtained during this step, called E0, was used as an initial microbial inoculum for the

microcosm assay. Bacterial concentration was estimated at 8.10^3 CFU.ml^{-1} by plate counting on 10% tryptic soy (3 g.l^{-1}, Becton, Dickinson and Company) agar (15 g.l^{-1}) (TSA) medium containing 100 mg.l^{-1} cycloheximide (Sigma Aldrich). The microcosm assay consisted of three successive enrichment steps in microcosms (140 mm Petri dishes sealed with adhesive tape) filled with 75 cm^3 of beech (*Fagus sylvatica* L.) sawdust sieved (2 mm mesh) and autoclaved (20 min, 120 °C) twice, with 2 days in between. Fungal inocula were prepared on beech wood blocks (50×30×10 mm). First, wood blocks were sterilised (autoclaved twice, 20 min, 120 °C, with 2 days in between). The initial sterility of the sawdust and of the wood blocks was checked by plating woodblock suspensions at different dilutions on 10% TSA medium and by incubating them for 7 days at 25°C. No microbial growth was detected. The wood blocks were then incubated with *Phanerochaete chrysosporium* RP78 in Petri dishes, containing malt (30 g.l^{-1}) agar (20 g.l^{-1}) medium for 19 weeks, at 25°C, in dark conditions.

The microcosms were inoculated with two different microbial inocula, corresponding to two different treatments. In one treatment – called BF (for bacteria + fungus *ie. P. chrysosporium*) – the microbial suspension E0 (16 ml) was spread carefully over all of the sterile sawdust after having placed a beech block inoculated with the white-rot fungus *P. chrysosporium* in the center of the microcosm. In a second treatment – called B (for bacteria, *ie* without *P. chrysosporium*) – the microbial suspension E0 (16 ml) was spread carefully over all of the sterile sawdust and a sterile beech wood block was placed over the mixture in the center of the microcosm. For the first step (E1), microcosms were incubated during 12 weeks to allow the establishment of fungal colony and / or bacterial communities. At the end of this period (E1), we used a 2 cm diameter round punch to sample 1.54 cm^3 of the sawdust with associated bacteria and/or fungal hyphae. We conducted sampling at four equally distant sites within each microcosm and pooled and homogenised together these 4×1.54 cm^3 of sawdust. Half of it was used to inoculate sterile sawdust of a new microcosm and the other half was used to extract microbial suspensions by shaking vigorously for 1 min, 0.2 g of sawdust in 3 ml of sterile distilled water. All the microbial suspensions were plated on 10% TSA for bacteria enumeration after 48h at 25°C. All these microbial suspensions were also cryopreserved at -80°C in 25% glycerol prior to further analysis. Two further enrichment steps were performed every three weeks (E2 and E3 samples), using the same procedure for the three treatments. For B and BF treatments, ten replicates were made at each steps. All manipulations were done under sterile conditions, using a biosafety cabinet. All microcosms were incubated at 25°C in the dark.

To monitor the functional diversity of both bacterial communities and strains over time, a subset of 21 microcosms was selected (the same ones that have been used in Hervé et al. 2014b): three for the B treatment for each step (E1, E2 and E3) and four for the BF treatment for each step. The bacterial diversity from the E0 inoculum was also analysed. The presence of *P. chrysosporium* was checked for each BF microcosm using nested PCR (Hervé *et al.* 2014b).

4.3.2 Collection of bacterial strains

Bacterial strains (311) were isolated from the 21 selected microcosms and the E0 inoculum as follow. One microbial suspension was prepared for each sample (enrichment steps x fungal presence) by shaking vigorously for 1 min, 0.2 g of sawdust in 3 ml of sterile distilled water. Different dilutions of the suspensions were plated in duplicate on water yeast agar (WYA) (Folman *et al.* 2008) containing 50 $mg.l^{-1}$ thiabendazole (Sigma) and 100 $mg.l^{-1}$ cycloheximide (Sigma). WYA contained 1 $g.l^{-1}$ NaCl, 0.1 $g.l^{-1}$ yeast extract (Difco), 1.95 $g.l^{-1}$ MES (Sigma), 20 $g.l^{-1}$ agar and its pH was adjusted at pH 5. All plates were incubated at 25°C for 7 days in dark condition. To collect bacterial isolates showing a similar level of dominance within each sample, bacterial isolation from each sample was always performed with samples diluted to the same level as recommended by Frey et al (Frey *et al.* 1997). Bacterial colonies were randomly selected to obtain about fourteen isolates per sample, transferred on WYA for isolation and then subcultured twice on 1/10-strength tryptic soy agar (TSA) medium (3 $g.l^{-1}$ Tryptic Soy Broth from Difco and 15 $g.l^{-1}$ agar). All the bacterial isolates were cryopreserved at -80°C in 25% glycerol. For each condition (*i.e.*, enrichment steps x fungal presence), 40 to 49 bacteria were isolated.

Concerning all the functional assays on the bacterial strains described below, each strain was grown on 10% TSA medium for 24h at 25°C. Subsequently, the bacteria were collected in sterile distilled water and washed once before adjusting the absorbance at 595 nm of the suspension to 0.4, in order to obtain the bacterial inoculum.

4.3.3 Identification of bacterial strains and phylogenetic analysis

An amplified fragment of the 16S rRNA gene with the universal set of primers pA (5′-AGAGTTTGATCCTGGCTCAG-3′) and 907r (5′-CCGTCAATTCMTTTGAGTTT-3′) was used to identify bacterial isolates. Boiled bacterial cells (10 min at 98°C) were directly used as a template in PCR reactions. PCR reactions were performed in a 50 µl final volume containing 20 µl Master Mix (5 PRIME, Germany), 24 µl water Mol Bio grade (5 PRIME,

Germany), 2.5 µl of each primer (10 µM) and 1 µl DNA. The PCR conditions used were 94°C for 4 min, 30 cycles of 30 s at 94°C (denaturation), 53°C for 90 s (annealing) and 72°C for 90 s (extension), followed by 10 min at 72°C. PCR products were purified using MultiScreen HTS filter plates (Millipore, Ireland) and then sequenced using Sanger method at Eurofins MWG (Ebersberg, Germany). All sequences were identified using the EzTaxon-e server (Kim *et al.* 2012) on the basis of 16S rRNA gene sequence data.

All sequences were aligned using ClustalW version 2.1 (Larkin *et al.* 2007) and then manually curated. Maximum likelihood phylogenetic trees were constructed using RAxML version 7.7.2 (Stamatakis 2006) with the GTRGAMMA model of DNA evolution. To obtain the statistical confidence of internal branches, 10000 bootstrapped trees were generated using RAxML. From these trees, unweighted UniFrac distances were computed (Lozupone, Hamady & Knight 2006).

4.3.4 Comparison of different 16S rRNA gene data sets

In order to compare results from cultivation and pyrosequencing methods, an operational taxonomic unit (OTU) based approach was performed using the Mothur software version 1.29.1 (Schloss *et al.* 2009). 16S rRNA gene pyrosequencing reads were processed by largely following the Schloss standard operating procedure (Schloss *et al.* 2011). Briefly, sequencing errors were reduced by implementation of the AmpliconNoise algorithm and low-quality sequences were removed (minimum length 200 bp, allowing 1 mismatch to the barcode, 2 mismatches to the primer, and homopolymers no longer than 8 bp). Sequences were then trimmed to keep only high quality reads ($Q \geq 35$). Subsequently, pyrosequencing sequences were merged with sequences of cultivated bacteria. These sequences were aligned in Mothur and classified against the SILVA bacterial SSU reference database v 102 (Pruesse *et al.* 2007). Chimera were removed using the chimera.uchime mothur command. Singletons were included in the analysis. Finally, sequences were assigned to family-level phylotypes using the naïve Bayesian classifier implemented in Mothur and clustered into OTUs using the average neighbor method. An OTU was defined at the 97% sequence similarity level.

In order to compare our 16S rRNA gene sequences from the cultivated bacteria with other sequences from studies related to bacterial communities associated with decaying wood (Folman *et al.* 2008; Zhang *et al.* 2008a; Valásková *et al.* 2009), the RDP Library Compare tool version 2.6 with 95% confidence threshold was used (Wang *et al.* 2007). The E0 sample, corresponding to the bacteria extracted from a forest soil, was excluded from this analysis.

4.3.5 Selective media and metabolic assays

Functional diversity of the bacterial communities associated with decaying wood was evaluated at both community and strain levels. Selective media were used to test the ability of bacterial communities or bacterial strains to grow on specific substrates linked to wood decay process. WYA is a minimal medium, used as reference.

Bacterial concentrations of all the microcosm samples plus the E0 sample were estimated in $CFU.g^{-1}$ by plate counting on 10% TSA medium containing 100 $mg.l^{-1}$ cycloheximide (Sigma Aldrich) after incubating the plates for 2 days at 25°C in the dark.

To characterise the functional diversity of the bacterial communities, five different media containing two fungicides, 50 $mg.l^{-1}$ thiabendazole (Sigma) and 100 $mg.l^{-1}$ cycloheximide (Sigma) were used: the WYA medium, a medium containing methanol as sole source of carbon (KH_2PO_4 100 $mg.l^{-1}$; $(NH_4)_2SO_4$ 200 $mg.l^{-1}$; $MgSO_4$ 50 $mg.l^{-1}$; $CaCl_2$,$2H_2O$, 20 $mg.l^{-1}$; methanol (Merck) 0.1% (v/v); agar 20 $g.l^{-1}$; pH 5) (Vorob'ev *et al.* 2009), a WYA medium containing 0.2 mM menadione (Sigma), a WYA medium containing 0.01% hydrogen peroxide (BDH Prolabo) and a medium containing carboxymethyl-cellulose (CMC) as sole source of carbon (K_2HPO_4 1.0 $g.l^{-1}$; $(NH_4)_2SO_4$ 1.0 $g.l^{-1}$; $MgSO_4$,$7H_2O$ 0.5 $g.l^{-1}$; NaCl 0.5 $g.l^{-1}$; carboxymethyl-cellulose sodium salt (Sigma) 5 $g.l^{-1}$; agar 20 $g.l^{-1}$; pH 5) (Ulrich, Klimke & Wirth 2008). 50 µl of the diluted microbial suspension of each sample kept at -80°C was plated on each medium in triplicate. The cellulolytic activity of the bacterial colonies growing on the CMC medium was detected using 0.1% Congo red (Sigma) for staining during 40 min followed by a washing with 1M NaCl according to Teather method (Teather & Wood 1982). The colonies surrounded by a yellow halo against a red background were identified as cellulase-positive.

To characterize the functional potential of bacterial strains, 125 strains from the 311 strain collection were randomly selected from five different treatments: E0, E1B, E1BF, E3B and E3BF (n=25). Five media without fungicides were used: the WYA medium, a WYA medium containing 0.05% Remazol Brilliant Blue R (Sigma), a CMC medium (see above), a medium containing xylan as sole source of carbon (K_2HPO_4 1.0 $g.l^{-1}$; $(NH_4)_2SO_4$ 1.0 $g.l^{-1}$; $MgSO_4$,$7H_2O$ 0.5 $g.l^{-1}$; NaCl 0.5 $g.l^{-1}$; beechwood xylan (Sigma) 10 $g.l^{-1}$; agar 20 $g.l^{-1}$; pH 5) and a chrome azurol S (CAS) agar medium prepared following the method of Alexander (Alexander & Zuberer 1991). For each bacterial strain, 10-µl droplets of a bacterial suspension with $A_{595nm} \approx 0.4$ were spotted in triplicate in one Petri dish of each medium. Petri dishes were incubated 7 days at 25°C in dark condition. Lignolysis was indicated by the

Remazol Brilliant Blue R (RBBR) medium turning from blue to pale pink (Murray & Woodward 2007). The cellulolytic activity on CMC medium and xylanolytic activity on xylan medium were detected using 0.1% Congo red (Sigma) for staining during 40 min followed by a washing with 1M NaCl according to Teather method (Teather & Wood 1982). For the siderophore production assay on CAS medium, the discoloration of the medium (blue to orange) indicated siderophore-producing bacterial strains.

Metabolic fingerprint of the same 125 bacterial strains was performed using Biolog GN2 microplate according to the manufacturer's instructions. Microplates were inoculated with 150 µl of a bacterial suspension with A_{595nm}≈0.4 and incubated 24h at 25°C in dark condition. Then, color density of each well was measured at 595 nm using a iMark Microplate Absorbance Reader (Bio-Rad, Hercules, CA, USA). Data were normalised by dividing the raw difference value for each well by the average well color development (AWCD) of the plate, as suggested by Garland & Mills (1991). Negative values were considered as 0 in subsequent data analyses. Shannon index was used to compute the diversity of carbon substrate utilisation for each strain (Zak *et al.* 1994).

4.3.6 Bacterial-fungal confrontations

A confrontation assay was performed in 90-mm diameter Petri dishes to evaluate bacterial-fungal interactions. The fungus *P. chrysosporium* RP78 was grown on malt (30 $g.l^{-1}$) agar (20 $g.l^{-1}$) medium at 25°C. A 6-mm diameter fungal plug of *P. chrysosporium* was taken from the margin of 1-week-old fungal colony and placed in the center of a WYA plate. Two 10-µl droplets of the bacterial inoculum were spotted at 3 cm from the fungal plug, diametrically opposed. Petri dishes were sealed with adhesive tape and incubated at 25°C, in dark condition. The diameters of the fungal colony in the direction of the bacterial colonies (D1) and the one orthogonal to D1 (called D2) were measured twice per day (18, 28, 42, 52 and 66 hours after the inoculation), until the fungal colonies reached the periphery of the plates. Then the ratio R=D1/D2 was used to estimate the influence of each bacterial strain on *P. chrysosporium* growth. For each confrontation, n=5 replicates were made.

4.3.7 Statistical analyses

For each treatment (presence of *P. chrysosporium* x enrichment step), the numbers of bacteria colony-forming units (CFUs) were estimated per gram dry weight of soil or wood, and log-transformed. Concerning the analysis of the functional diversity of the bacterial communities, we used linear mixed-effects models in the *nlme* package (Pinheiro *et al.* 2011)

of R (R Development Core Team 2013) with microcosms and triplicate plating as random factors, to estimate the effects of the selective media, of the enrichment and of the white-rot fungus *P. chrysosporium* on the number of culturable bacterial communities from the microbial suspensions. Differences among treatments (selective media x enrichment steps x presence of the fungus) were determined using multiple comparisons of the least-square means (*lsmeans* in R) with *glhargs* argument. The ability of the 125 bacterial strains to grow on selective media and to use it, was analysed using generalised linear models (glm) under a binomial distribution. Differences in the utilisation of the 95 carbon substrates of the Biolog GN2 microplate among treatments (enrichment steps x presence of the fungus) were evaluated by a multivariate ANOVA (MANOVA) and Wilk's lambda statistic while the utilisation of each substrate was estimated by a one-way ANOVA followed by the Tukey HSD *post hoc* test. All statistical analyses and graphics were computed using R software version 3.0.3 (R Development Core Team 2013).

4.4 Results and discussion

4.4.1 Taxonomy of the wood-associated bacteria

In a previous study, the taxonomic diversity of the same samples used for the present study was explored using 16S rRNA gene-based pyrosequencing (Hervé *et al.* 2014b). Rarefaction curves revealed that all the diversity of wood-associated bacteria was covered in the microcosm samples, but not in the initial forest soil inoculum (E0). To explore the functional diversity of these bacterial communities, we isolated 311 bacterial strains. We compared their identity based on a fragment of the 16S rRNA gene to the results of the pyrosequencing approach, considering three groups of samples: the initial inoculum E0 and the woody microcosms in absence (B) or in presence of the white-rot fungus *P. chrysosporium*, without taking into account the enrichment steps (Figure 4.1). 16S rRNA gene sequence clustering into operational taxonomic units (OTUs) led to 8 OTUs (97% sequence similarity level) included in the 3553 OTUs obtained by 454 pyrosequencing. For the initial inoculum E0, cultivation and pyrosequencing approaches led to very different taxonomic patterns. This can be explained by the relatively low number of isolated bacterial strains (42 strains), but also by the fact that, even using pyrosequencing, we were unable to describe the whole diversity in E0. On the contrary, from the woody environment in the microcosms (B and BF groups of samples) it was possible to isolate the two most abundant

OTUs detected by pyrosequencing. These OTUs belonged to the *Xanthomonadaceae* and *Burkholderiaceae* families and represented together more than 54% and 64% of the relative abundance for B and BF treatments, respectively. Interestingly, these two OTUs were also the most abundant among the bacterial strain collection, representing more than 91% and 97% of the isolated strains for B and BF treatments, respectively. OTU belonging to *Burkholderiaceae* were found to be more abundant in BF samples than in B samples with both cultivation and pyrosequencing approaches. These results confirm that bacteria associated with decaying-wood are mainly culturable (de Boer *et al.* 2005) and more interestingly that it is possible to isolate the dominant members of these bacterial communities. Recently, Vaninsberghe et al. (2013) showed similar results in a study on forest soil bacterial communities where they isolated 22% of the OTUs detected by a pyrosequencing approach. Isolation of major bacteria from a particular ecological niche is very important since it allows to study the physiology and the functional role of the niche members and thus, to better understand the functioning of this niche.

We compared the taxonomic diversity of our bacterial collection with the one revealed in three other publications dedicated to bacterial communities associated to decaying wood (Folman *et al.* 2008; Zhang *et al.* 2008a; Valásková *et al.* 2009) (culture-dependent (Folman *et al.* 2008; Valásková *et al.* 2009), culture-independent (Zhang *et al.* 2008a; Valásková *et al.* 2009)) (Table 4.1). We revealed that regardless of the studies and of the approaches, *Proteobacteria* was the major phylum of the wood-associated bacteria and members of *Xanthomonadaceae* family were always present, indicating that *Xanthomonadaceae* are strongly associated with decaying-wood habitat. Interestingly, these studies embrace both field (Zhang *et al.* 2008a; Valásková *et al.* 2009) and microcosm experiments (Folman *et al.* 2008), as well as decaying wood of both conifers (Zhang *et al.* 2008a; Valásková *et al.* 2009) and broadleaved trees (Folman *et al.* 2008; Valásková *et al.* 2009), suggesting no host-tree specificity for *Xanthomonadaceae.*

4.4.2 Quantification of the culturable bacterial communities

Enumeration of the culturable bacteria by plate count on 10% TSA medium revealed an increase in bacterial concentration over time, from the initial inoculum E0 to the last step of the enrichment E3 (Figure 4.2). The bacterial concentration in the inoculum extracted from forest soil was significantly lower than the bacterial concentration associated to wood inside the microcosms ($p<0.001$). For the first (E1) and the third (E3) steps of the enrichment, there were significantly more bacteria in presence of *P. chrysosporium* (BF) than without the

fungus (B) (p<0.05). This difference was more pronounced for E1 (p<0.001) than more E3 (p<0.05), suggesting a stronger mycosphere effect after twelve weeks of incubation. Interestingly, in a previous study of the same experiment (Hervé *et al.* 2014b), a significant mycosphere effect of the white-rot fungus was observed on the bacterial community composition after twelve of incubation. Altogether, these results highlight an effect of *P. chrysosporium* on both the composition of the bacterial community and on the number of culturable bacteria associated with wood decay. Such an increase of bacterial density in the mycosphere has already been reported with other fungi, symbiotic (Deveau *et al.* 2010) as well as pathogenic (Barret *et al.* 2009), but it is the first time it could be observed in the case of a white-rot fungus. In a previous microcosm experiment where Folman and colleagues (2008) showed that the presence of a white-rot fungus modified the bacterial community composition, a reduced number of culturable wood-associated bacteria was observed in contrast. Such difference with our results might be explained by the fact that here we used sawdust as growth matrix, and not a forest soil. Wood and soil are clearly two different substrates, notably in term of types of carbon sources and nitrogen content, and these two factors have been reported to influence bacterial growth (Meidute, Demoling & Bååth 2008). However, regardless of the growth matrix, both studies highlight the effect of white-rot fungi on the number of culturable bacteria.

4.4.3 Functional diversity of the bacterial communities

Using selective media linked to wood decay process, concentrations of culturable bacterial communities associated with wood in presence or in absence of *P. chrysosporium* were estimated in order to explore the functional diversity of these bacterial communities. Because of the experimental design, the data set was analysed with linear mixed-effects models. Considering the three enrichment steps (E1 to E3), concentrations of culturable bacterial communities were significantly affected by the enrichment steps ($F_{2, 35}$=41.46, p<0.001) and by the selective media ($F_{4, 213}$=26.15, p<0.001), but not by *P. chrysosporium* ($F_{1, 35}$=0.13, p>0.7), meaning that no mycosphere effect could be detected on the densities of the culturable bacterial communities when considering the three enrichment steps. All of the interactions were also statistically significant (p<0.005), indicating dependence of the variables. However, because we observed that bacterial community composition was shaped by the white-rot fungus only at the first enrichment step E1 (Hervé *et al.* 2014b), we conducted the same analysis considering only bacterial communities sampled at the first step of the enrichment procedure. This new analysis revealed that the densities of the culturable

bacterial communities were significantly affected by the selective media used ($F_{4, 71}$=14.41, p<0.001) and by the presence of *P. chrysosporium* in the microcosms ($F_{1, 18}$=120.82, p<0.001). The interaction of these two factors was also statistically significant ($F_{4, 71}$=18.18, p<0.001), indicating dependence of the variables. Regardless of the growth media, concentrations of culturable bacterial communities were significantly lower in absence of *P. chrysosporium* (p<0.001) (Figure 4.3), confirming the results obtained on TSA medium (Figure 4.2). Moreover, there was no effect of the selective media on the concentrations of culturable bacterial communities sampled in the microcosms without *P. chrysosporium* (p>0.5), suggesting functional redundancy among the microbial community (Allison & Martiny 2008). On the contrary, the concentrations of culturable bacterial communities were significantly lower (p<0.001) on cellulose (CMC) and methanol-based media compared to the minimal medium WYA, used here as reference, when the bacteria were sampled in the microcosms inoculated with *P. chrysosporium*. This demonstrates a mycosphere effect of *P. chrysosporium* on the functional diversity of its associated bacterial communities. Since less bacterial colonies are able to grow on CMC and methanol-based media compared to the WYA medium, some antagonistic interactions between fungus and bacteria with competition for carbon resources are suggested. This competition between bacteria and fungi for carbon resources has already been described in leaf litter (Møller, Miller & Kjøller 1999) and in aquatic environment (Mille-Lindblom, Fischer & Tranvik 2006). Moreover, although concentrations of culturable bacteria growing on CMC were significantly higher in presence of *P. chrysosporium*, no significant difference was observed in the number of cellulolytic bacterial colonies with or without the fungus (p>0.25, data not shown), showing that bacterial community of *P. chrysosporium* mycosphere has a lower cellulolytic potential compared to the wood-associated bacterial community. No significant difference was observed between WYA medium and the oxidative media containing either menadione or hydrogen peroxide, suggesting that wood-associated bacteria might be tolerant to oxidative stress, regardless of the presence of a white-rot fungus. This needs to be confirmed using other oxidising agents and using different concentrations of these agents.

4.4.4 Identification of the strains from the bacterial collection and phylogenetic distances

Among the 311 bacterial strains we isolated, we randomly selected 125 strains sampled in five different treatments (n=25). Because we wanted to focus on both wood and mycosphere effects, we chose to work with strains from E0, E1B, E1BF, E3B and E3BF

treatments only (Table 4.2). Based on a fragment of the 16S rRNA gene, we built a maximum likelihood phylogenetic tree, to then compare the phylogenetic distances between the five different treatments. Clustering based on unweighted UniFrac distance revealed a clear distinction between the initial inoculum E0 and the samples from wood-based microcosms, a separation between the enrichment steps (E1 and E3) and finally a separation between the samples inoculated with or without *P. chrysosporium* (BF and B respectively) (Figure 4.4). A similar clustering was observed with a 16S gene-based pyrosequencing approach performed on the same samples (Hervé *et al.* 2014b). This highlights that in the case of wood-associated bacteria, culture-dependent and culture-independent approaches can result in a similar phylogenetic pattern for the bacterial communities. Interestingly, such results were also observed for forest soil bacterial communities (Vaninsberghe *et al.* 2013). This allows to study the functional diversity of bacterial strains which reflect the phylogenetic structure of the related bacterial communities.

4.4.5 Functional potential of the bacterial strains

Confrontation assays between bacterial strains and *P. chrysosporium* were performed to evaluate the effect of these strains on the fungal growth. The fungal growth, here estimated by the R ratio (ratio of the diameter of the fungal colony growing in the direction of the bacterial colonies over the diameter of the colony growing in the orthogonal direction, see Materials and Methods), was significantly affected by the treatments (enrichment steps x fungal presence) (one-way ANOVA, $F_{5, 649}$=10.37, p<0.001) and by the genus of the bacterial strains (one-way ANOVA, $F_{3\,616}$=119.20, p<0.001) (Figure 4.5). Compared to *P. chrysosporium* growth in axenic condition, *P. chrysosporium* growth in presence of bacterial strains from the different treatments (enrichment steps x fungal presence) was significantly lower (p<0.002), indicating antagonism between the two organisms in the *in vitro* assay (Figure 4.5.A). However, fungal growth inhibition was significantly less pronounced (p<0.05) with the bacterial strains isolated in *P. chrysosporium* mycosphere, *i.e.* E1BF and E3BF samples, compared to the bacterial strains isolated from the forest soil inoculum E0, suggesting a selection by the fungus of less inhibitory bacterial communities. On the contrary, in the case of the ectomycorrhizal symbiosis, *Pseudomonas fluorescens* strains from the mycosphere have been reported to inhibit more the growth of *Laccaria bicolor* compared to the *P. fluorescens* strains isolated from the bulk soil of a forest nursery (Frey-Klett *et al.* 2005). Interestingly, no antagonism was detected between the white-rot fungus *Hypholoma fasciculare* and bacterial strains isolated from its mycosphere, as revealed

by *in vitro* confrontation assays (Valásková *et al.* 2009). These assays were however performed on 1/10 TSA whereas our assays were performed on the minimal medium WYA. The differences in the results obtained can be attributed to the growth medium composition which is known to affect fungal growth during confrontations with bacteria (Radtke *et al.* 1994). Our results also revealed a correlation between the fungal growth and the genus of the bacterial strains (Figure 4.5.B). Strains belonging to the *Collimonas* genus reduced the most the fungal growth and were only found in the forest soil inoculum E0 (Table 4.2). This inhibition of fungal growth or fungistasis has already been described as a characteristic of this genus (Leveau, Uroz & de Boer 2010). Interestingly, no member of this genus was isolated or detected by 16S based pyrosequencing in the wood microcosms, suggesting that *Collimonas* might not be adapted to wood environment. This result is in accordance with the oligotrophic lifestyle of this bacterial genus usually found in lower carbon content environments compared to decaying-wood such as dune, forest or tundra soils (Leveau, Uroz & de Boer 2010). On the contrary, strains belonging to the *Burkholderia* genus had the lowest impact on *P. chrysosporium* growth and were isolated in all samples, suggesting tolerance of this bacterial genus to the fungus. This tolerance to the presence of fungi was also mentioned in a study about the biogeography of *Burkholderia* populations (Stopnisek *et al.* 2013).

In order to understand the functional role of the bacterial strains in the process of wood degradation, notably regarding the degradation of three main wood components, namely cellulose, hemicellulose and lignin, the bacterial strains were inoculated on selective media. Since iron plays a role in the oxidative process of wood degradation and that wood-decaying *Basidiomycetes* are known to produce siderophores (Fekete, Chandhoke & Jellison 1989), the production of siderophores was also evaluated for the bacterial strains. All screened strains were able to grow on WYA (control), Remazol Brilliant Blue R (RBBR), carboxymethyl-cellulose (CMC) and xylan media, regardless of the treatment in which they were sampled. Concerning the lignolytic activity, none of the bacterial strains were able to degrade RBBR, but *P. chrysosporium* was (positive control). Similar results were found for bacteria isolated on spruce stumps in a previous study (Murray & Woodward 2007), suggesting an absence of lignolytic activity for the bacterial isolates alone. It can also suggest that RBBR is not an appropriate dye to detect bacterial lignolytic enzymes, as discussed in the same study (Murray & Woodward 2007) and that the use of RBBR is only appropriate to detect fungal lignolytic enzymes (Machado, Matheus & Bononi 2005). Concerning the cellulolytic bacterial strains, there was no effect of *P. chrysosporium* on the proportion of bacterial strains able to degrade

CMC, but there was an enrichment effect leading to a significant increase (p<0.05) in cellulolytic bacteria proportion from the first (E1) to the third (E3) step of the enrichment (Figure 4.6.A). Interestingly, the mycosphere effect on cellulolytic activity described at the community level (Figure 4.3) was not observed at the bacterial strain level, suggesting that a higher number of strains should have been selected for a more representative screening. Regarding the number of xylanolytic bacterial strains, the effect of *P. chrysosporium* was only noticeable at the first step of the enrichment with a higher proportion of xylanolytic bacteria (p<0.02) in presence of the fungus (E1BF) (Figure 4.6.B). There was also a significant increase (p<0.05) in xylanolytic bacteria proportion from the first (E1) to the third (E3) step of the enrichment. This shows that an enrichment procedure in a woody environment allows to isolate efficient cellulose and hemicellulose-degrading bacterial strains. More precisely, compared to the initial inoculum E0, the number of cellulolytic and xylanolytic bacterial strains isolated from E3BF samples was significantly higher (p<0.05), showing that the combined effects of the enrichment procedure in wood and the presence of a white-rot fungus resulted in a selection of cellulose and hemicellulose-degrading bacterial strains. Concerning the siderophore production assay on CAS medium, not all the bacteria were able to grow on the medium (22/25; 10/25; 18/25; 19/25 and 22/25 strains for E0, E1B, E1BF, E3B and E3BF, respectively). There was no effect of *P. chrysosporium* on the proportion of bacterial strains able to produce siderophores, but there was an enrichment effect with a significant increase (p<0.05) in siderophore-producing bacteria proportion from the first (E1) to the third (E3) step of the enrichment, leading to the fact that all strains from E3 able to grow on CAS medium were able to produce siderophores (Figure 4.6.C). This suggests that bacteria might play an important role in iron mobilisation in woody environment, regardless the presence of the presence of *P. chrysosporium*. Moreover, the production of siderophores by bacterial isolates from decaying *Picea sitchensis* has been reported (Murray & Woodward 2007).

Finally, to better characterise the functional potential of these 125 bacterial strains and thus to understand their roles, metabolic profiles were performed using Biolog GN2 microplate. Each microplate contains 95 different carbon substrates, including some carbon compounds produced by the microbial degradation of wood and compounds synthetised by some fungi. Globally, the utilisation of these 95 carbon substrates was significantly affected by the treatment (enrichment steps x presence of the fungus) (one-way MANOVA, $F_{4, 120}$=2.78, p<0.001), indicating differences between the functional potential of the bacterial strains isolated from the five different ecological niches, *i.e.* E0, E1B, E1BF, E3B or E3BF.

Diversity of carbon substrate utilisation, based on Shannon index, increased significantly from E1 to E3 (p<0.01), regardless of the presence of the fungus (Figure 4.9), showing the enrichment effect in a woody environment on the functional diversity of these bacterial strains. Indeed, this functional diversity at the end of the enrichment (E3) was comparable with the functional diversity of the strains isolated from the forest soil (E0), revealing a physiological adaptation of the bacterial communities to a nutrient-poor environment, *i.e.* the wet sawdust. On the 95 carbon substrates, 51 were differentially used (one-way ANOVA, p<0.05) according to the ecological niche where the strains were isolated (E0, E1B, E1BF, E3B or E3BF). The utilisation of these 51 substrates mainly varied between the enrichment steps (Figure 4.7). Strains from E0, E3B and E3BF showed similar metabolic profiles. E1B and E1BF strains differed from them in the utilisation of carbohydrates and carboxylic acids. Indeed, at the first step of the enrichment E1, carbohydrate utilisation was higher, particularly for the D-fructose, D-galactose, alpha D-glucose, D-mannitol and D-mannose, while carboxylic acid utilisation was lower, especially for the *cis* aconitic acid and citric acid, compared to E0 and E3 treatments. Such an increase in the carbohydrate utilisation in E1 might be explained by the fact that incubation time was longer (12 weeks) in E1 than in E3 (3 weeks), leading to a more advanced stage of wood decomposition and thus resulting in more monosaccharides available in the environment, since D-glucose is a product of cellulose degradation (Lynd *et al.* 2002) and hemicellulose contains glucose, galactose and mannose.

4.5 Conclusion

Altogether, these results highlight an effect of *P. chrysosporium* and of the wood substrate on the functional diversity of the bacterial communities during the wood decay process. At the strain level, wood had a strong influence on the bacterial functional diversity, regardless of the presence of the white-rot fungus.

4.6 Acknowledgments

This work was supported by a grant from Lorraine Region, an ANR project (ANR-09-BLAN-0012) and IFR110 / EFABA. The UMR IaM is supported by a grant overseen by the French National Research Agency (ANR) as part of the "Investissements d'Avenir" program (ANR-11-LABX-0002-01, Lab of Excellence ARBRE). We thank S. Antony-Babu, L.C. Kelly and M. Buée for very helpful discussions.

4.7 Figures and tables

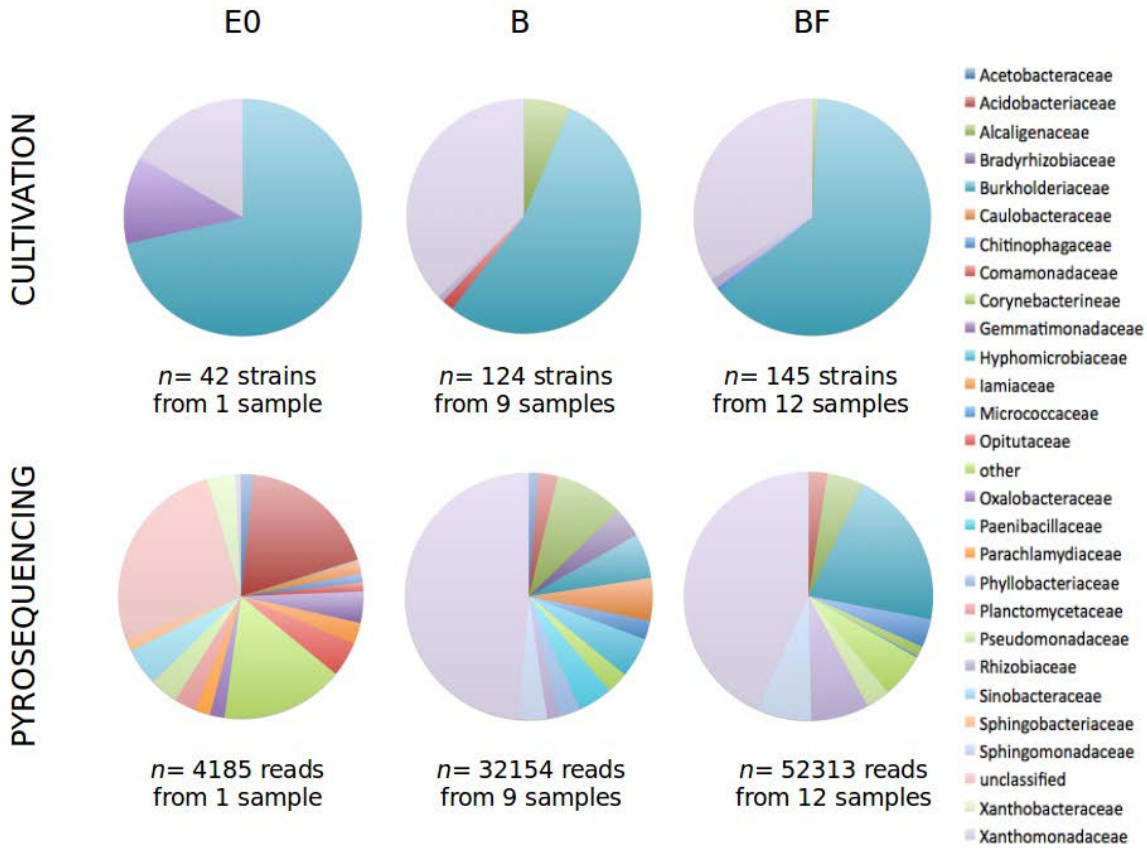

Figure 4.1. Pie charts comparing the bacterial taxonomic diversity from E0, B and BF samples at the family level, using culture-dependent and culture-independent (pyrosequencing) approaches (Hervé *et al.* 2014b). Families that accounted for less than 1% in a sample are summarised in a category termed "other".

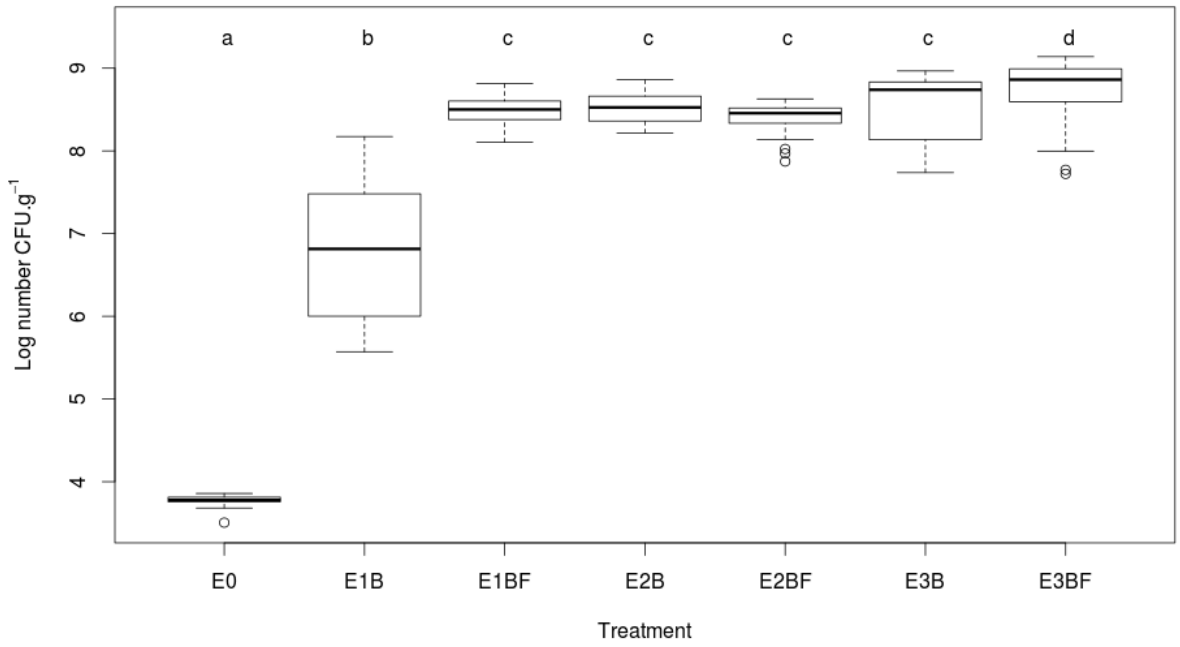

Figure 4.2. Boxplots of the bacterial enumeration on 10% TSA medium for the different treatments (B, without *P. chrysosporium*; BF, with *P. chrysosporium*; E, the different enrichment steps). n=10 except for E0, n=3. All samples were plated in triplicate. Different letters above boxplots indicate significant difference based on non-parametric Kruskal-Wallis test (p<0.05).

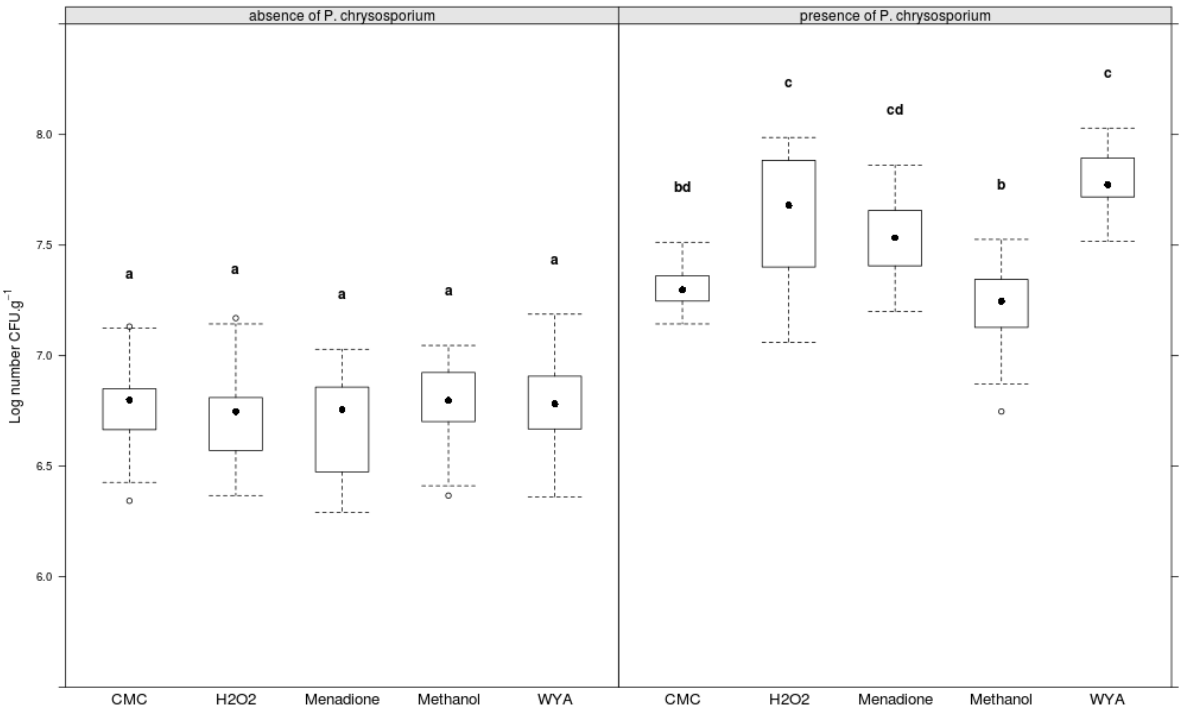

Figure 4.3. Effect of *P. chrysosporium* on the functional potential of culturable wood-associated bacteria after 12 weeks of incubation, revealed by using different selective media and analyzed with a linear mixed-effect model. Different letters above boxplots indicate significant difference based on least-square means (p<0.05).

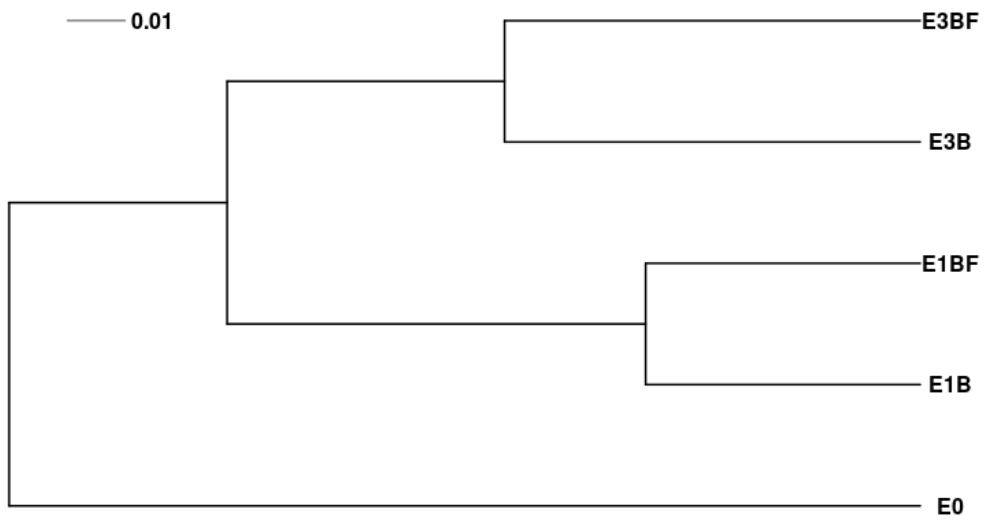

Figure 4.4. UPGMA clustering based on unweighted UniFrac distance. Branches are proportional to this distance.

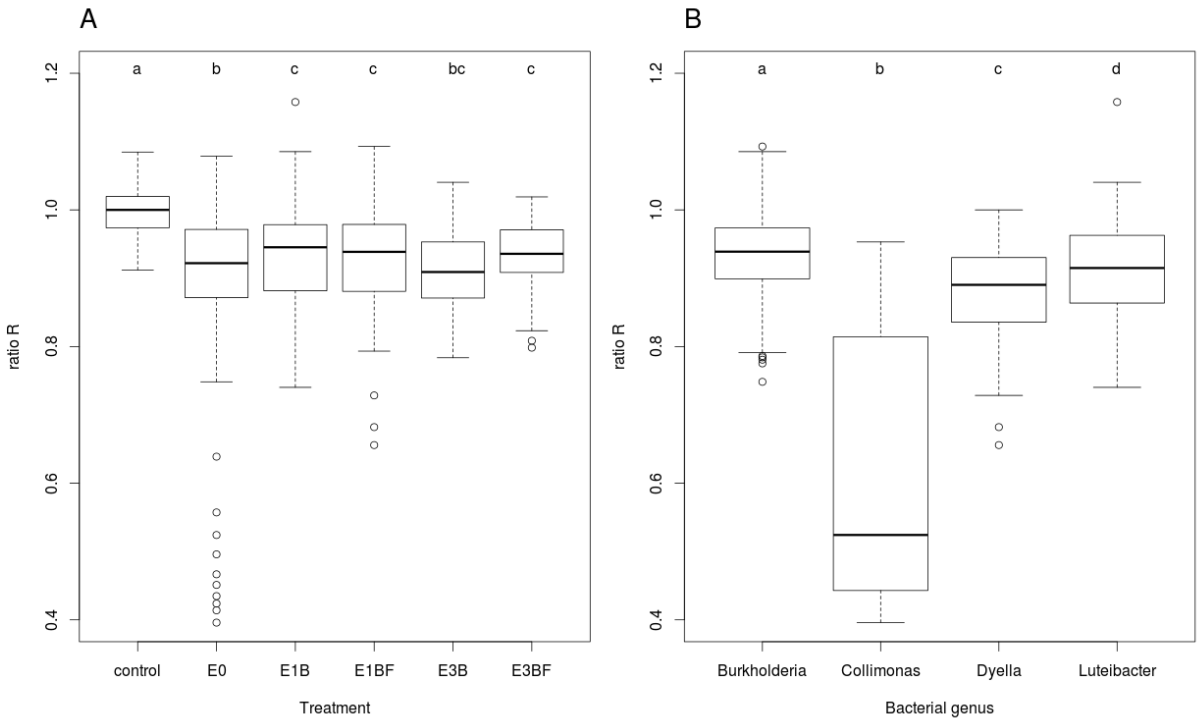

Figure 4.5. Bacterial-fungal confrontations after 66 hours of incubation. Different letters above boxplots indicate significant difference based on ANOVA followed by Tukey's HSD test ($p<0.05$). **A.** Ratio R (ratio of the diameter of the fungal colony growing in the direction of the bacterial colonies over the diameter of the colony growing in the orthogonal direction, see Materials and Methods) of the fungal growth with one bacterial strain, as a function of the treatment. $n=25$ bacterial strains per treatment with 5 replicates per strain. Control corresponded to *P. chrysosporium* growing alone. **B.** Relationships between the genus of the bacterial strains and the effect on the fungal growth based on the R ratio. For *Burkholderia*, $n=90$ strains; for *Collimonas*, $n=3$; for *Dyella*, $n=8$; for *Luteibacter*, $n=23$. *Cupriavidus* was excluded from the analysis because $n=1$.

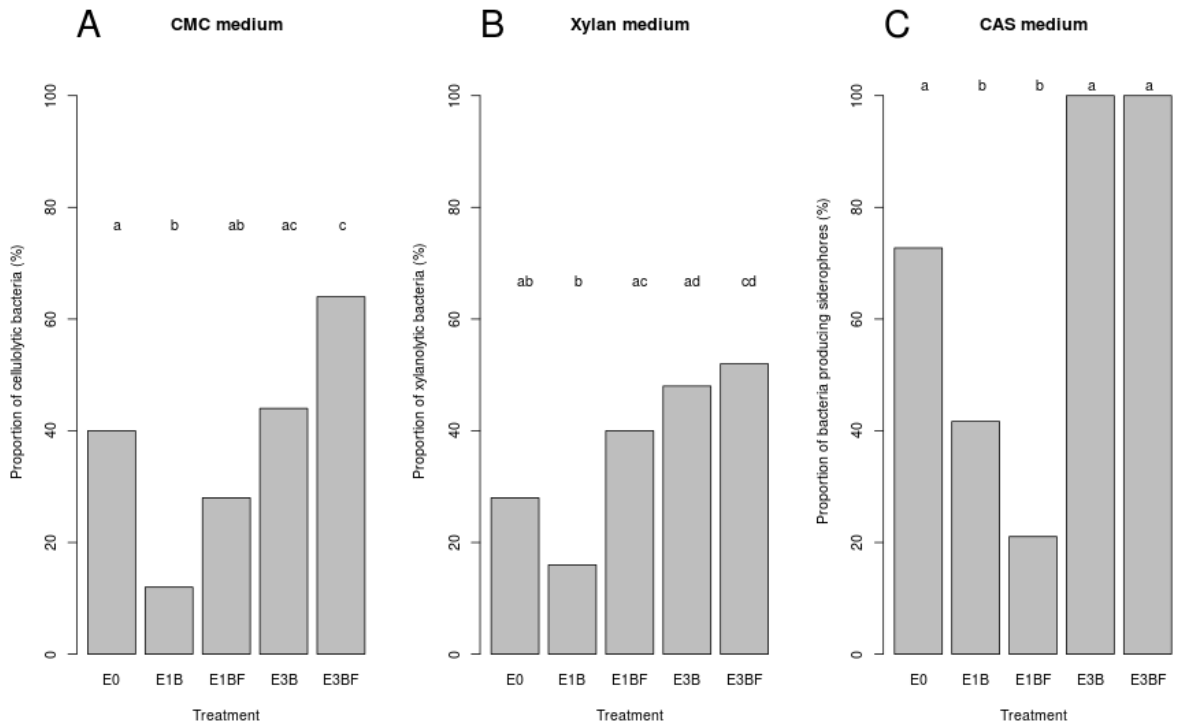

Figure 4.6. Capabilities of the strains able to grow on the selective media to use different substrates. Different letters above barplots indicate significant difference based on glm under a binomial distribution (p<0.05). **A.** Cellulolytic activity on carboxymethyl-cellulose medium. n=25 bacterial strains per treatment with 3 replicates per strain. **B.** Xylanolytic activity on xylan medium. n=25 bacterial strains per treatment with 3 replicates per strain. **C.** Siderophore production assay on CAS medium. n=22 bacterial strains for E0, n=10 for E1B, n=18 for E1BF, n=19 for E3B, n=22 for E3BF; with 3 replicates for each strain. Variation in the number of strains is due to the fact that not all strains could grow on CAS medium.

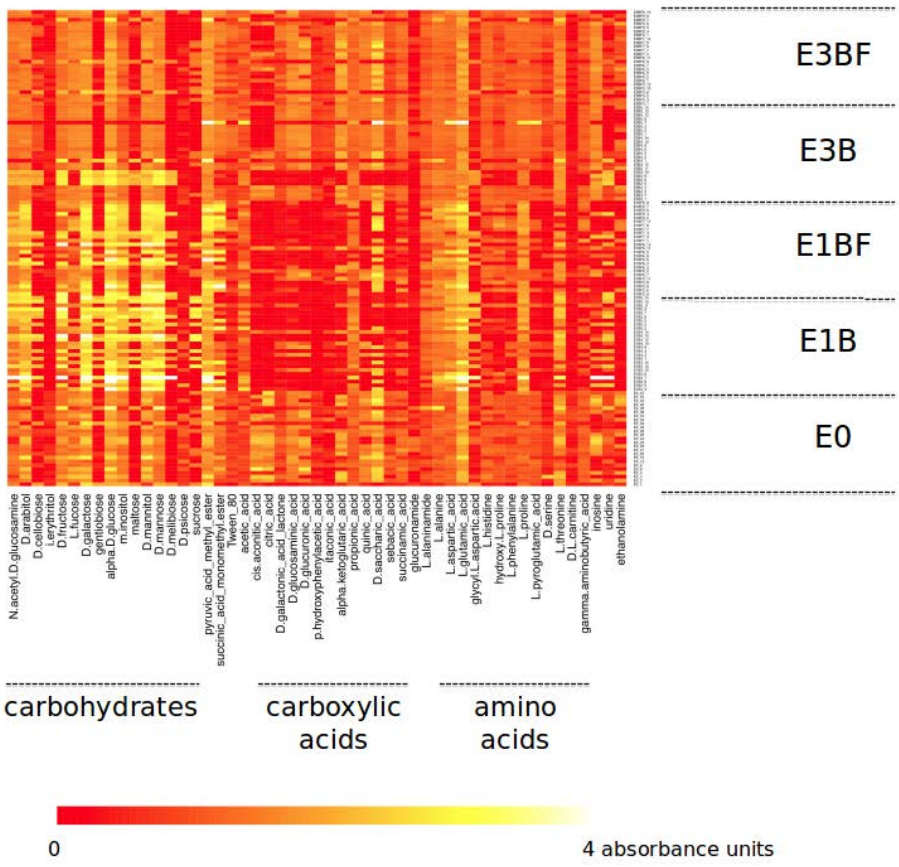

Figure 4.7. Metabolic profiles of 125 bacterial strains randomly selected in the 5 treatments (E0, E1B, E1BF, E3B, E3BF) (*n*=25). The heatmap shows the 51 substrates with statistically significant difference between treatments (enrichment steps E x presence (BF) or absence (B) of *P. chrysosporium*) (ANOVA, $p<0.05$).

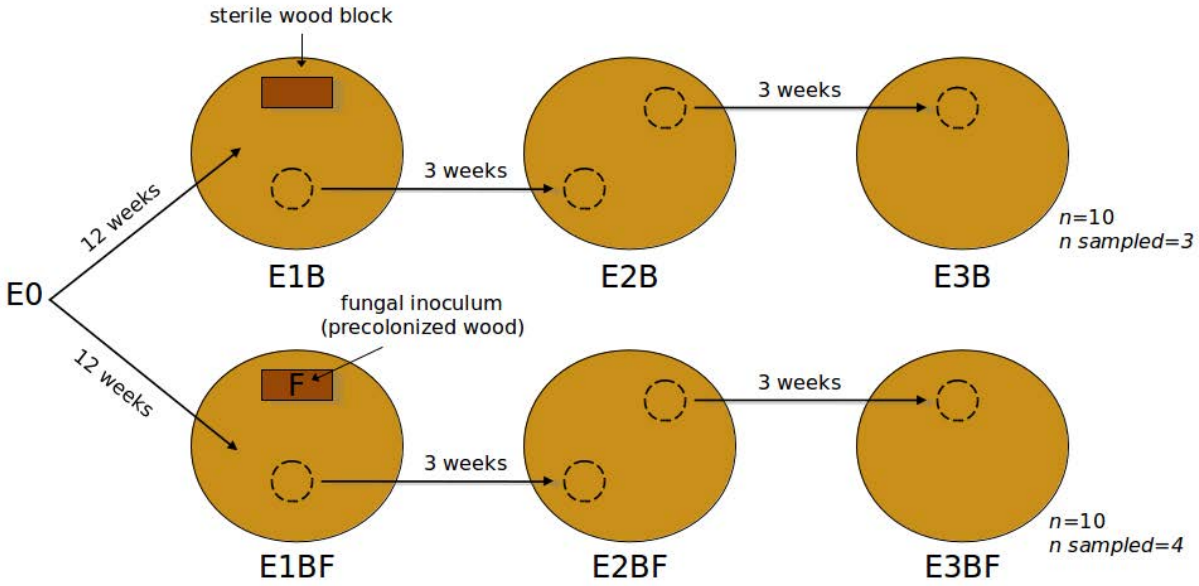

Figure 4.8. Diagram illustrating the experimental design within the microcosms. E0, a microbial suspension extracted from forest soil, was used as the initial inoculum. E0 was mixed with sterile sawdust as growth matrix, in two conditions: including (BF) or excluding (B) white-rot fungus *P. chrysosporium* previously inoculated on a beech wood block (F). After twelve weeks of incubation (E1), an enrichment was performed every three weeks (from E1 to E3) using a fraction taken from on microcosm to inoculate a new sterile microcosm.

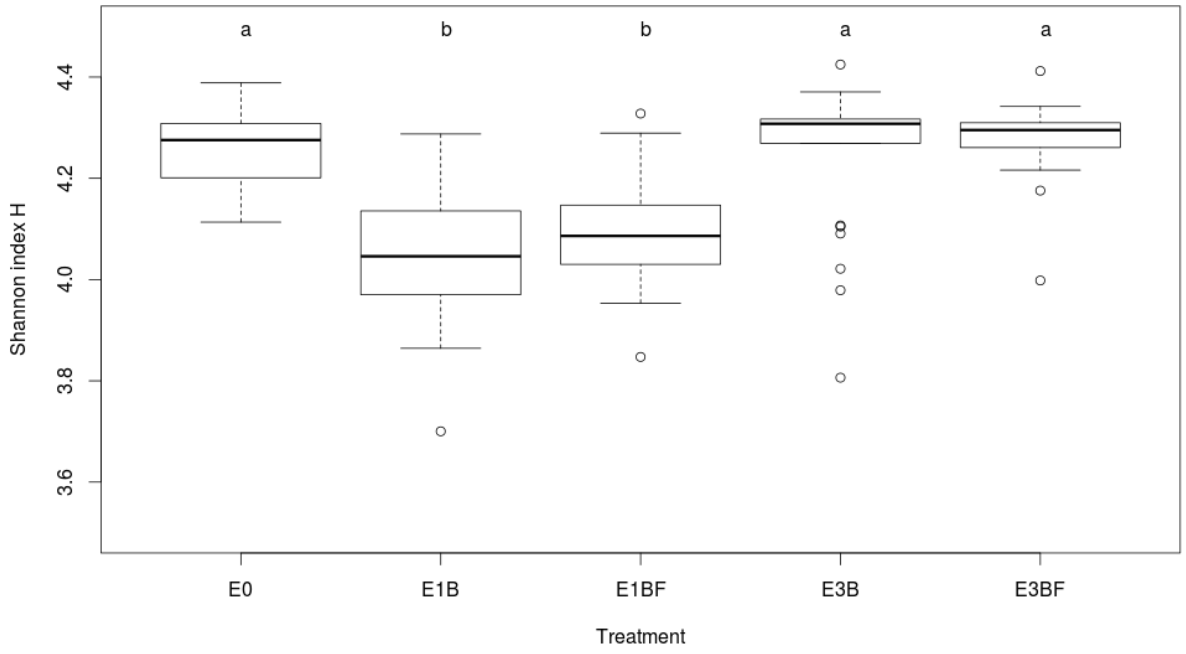

Figure 4.9. Diversity of carbon substrate utilisation for each treatment (n=25) based on Shannon index. Different letters above boxplots indicate significant difference based on non-parametric Kruskal-Wallis test (p<0.05).

	present study	Folman et al. 2008	Zhang et al. 2008	Valaskova et al. 2009	Valaskova et al. 2009
	Culture-dependent	**Culture-dependent**	**Culture-independent**	**Culture-dependent**	**Culture-independent**
Proteobacteria phylum	99.63	82.61	51.85	75.00	55.22
Burkholderiaceae family	59.11	34.78	0.00	27.08	13.43
Xanthomonadaceae family	35.32	4.35	1.23	22.92	3.73
Alcaligenaceae family	3.35	0.87	0.00	0.00	0.00
Comamonadaceae family	0.74	0.87	1.23	0.00	0.00
Rhizobiaceae family	1.12	0.00	0.00	0.00	0.00
Micrococcaceae family	0.37	0.00	0.00	0.00	0.00

Table 4.1. Comparison of the taxonomic composition of bacterial communities associated with decaying wood from different studies, based on 16S rRNA gene sequences and using the RDP Library Compare tool version 2.6 with 95% confidence threshold (Wang *et al.* 2007).

Treatment	Strain	Taxonomic assignment	Accession number	Similarity score (%)
E0	E0_1	*Dyella koreensis* BB4	AY884571	98.95
E0	E0_2	*Burkholderia sediminicola* HU2-65W	EU035613	99.65
E0	E0_3	*Collimonas pratensis* Ter91	AY281137	98.66
E0	E0_4	*Burkholderia sediminicola* HU2-65W	EU035613	99.65
E0	E0_6	*Burkholderia sordidicola* S5-B	AF512826	98.11
E0	E0_8	*Burkholderia caledonica* LMG 19076	AF215704	98.59
E0	E0_13	*Burkholderia bryophila* LMG 23644	AM489501	97.90
E0	E0_15	*Burkholderia sordidicola* S5-B	AF512826	98.95
E0	E0_20	*Burkholderia bryophila* LMG 23644	AM489501	99.30
E0	E0_21	*Burkholderia phenazinium* LMG 2247	U96936	99.41
E0	E0_22	*Burkholderia sediminicola* HU2-65W	EU035613	99.65
E0	E0_23	*Collimonas pratensis* Ter91	AY281137	99.77
E0	E0_24	*Collimonas pratensis* Ter91	AY281137	99.53
E0	E0_25	*Burkholderia sediminicola* HU2-65W	EU035613	99.65
E0	E0_28	*Burkholderia phenazinium* LMG 2247	U96936	99.29
E0	E0_29	*Burkholderia sordidicola* S5-B	AF512826	97.21
E0	E0_33	*Dyella koreensis* BB4	AY884571	98.50
E0	E0_34	*Burkholderia phenazinium* LMG 2247	U96936	99.41
E0	E0_37	*Burkholderia sordidicola* S5-B	AF512826	97.79
E0	E0_38	*Burkholderia bryophila* LMG 23644	AM489501	98.84
E0	E0_39	*Dyella kyungheensis* THG-B117	JX566987	98.37
E0	E0_40	*Burkholderia sediminicola* HU2-65W	EU035613	99.65
E0	E0_44	*Burkholderia sediminicola* HU2-65W	EU035613	99.65
E0	E0_45	*Burkholderia sediminicola* HU2-65W	EU035613	99.65
E0	E0_47	*Burkholderia phenazinium* LMG 2247	U96936	99.41
E1B	E1B3_3	*Burkholderia diazotrophica* JPY461	HM366717	97.67
E1B	E1B3_5	*Luteibacter rhizovicinus* LJ96	AJ580498	99.30
E1B	E1B3_6	*Burkholderia diazotrophica* JPY461	HM366717	97.44
E1B	E1B3_7	*Luteibacter rhizovicinus* LJ96	AJ580498	99.88
E1B	E1B3_8	*Burkholderia diazotrophica* JPY461	HM366717	97.21
E1B	E1B3_10	*Burkholderia sordidicola* S5-B	AF512826	98.73
E1B	E1B3_12	*Luteibacter rhizovicinus* LJ96	AJ580498	99.42
E1B	E1B3_14	*Burkholderia diazotrophica* JPY461	HM366717	97.56
E1B	E1B4_1	*Luteibacter rhizovicinus* LJ96	AJ580498	99.42
E1B	E1B4_3	*Burkholderia sordidicola* S5-B	AF512826	98.37
E1B	E1B4_4	*Luteibacter rhizovicinus* LJ96	AJ580498	99.77

E1B	E1B4_9	*Burkholderia sordidicola* S5-B	AF512826	98.59
E1B	E1B4_10	*Burkholderia sordidicola* S5-B	AF512826	98.72
E1B	E1B4_12	*Luteibacter rhizovicinus* LJ96	AJ580498	99.77
E1B	E1B4_13	*Luteibacter rhizovicinus* LJ96	AJ580498	99.77
E1B	E1B4_14	*Burkholderia sordidicola* S5-B	AF512826	98.71
E1B	E1B5_2	*Burkholderia diazotrophica* JPY461	HM366717	97.44
E1B	E1B5_3	*Luteibacter rhizovicinus* LJ96	AJ580498	100.00
E1B	E1B5_5	*Burkholderia diazotrophica* JPY461	HM366717	97.45
E1B	E1B5_6	*Luteibacter rhizovicinus* LJ96	AJ580498	99.54
E1B	E1B5_7	*Luteibacter rhizovicinus* LJ96	AJ580498	99.65
E1B	E1B5_9	*Luteibacter rhizovicinus* LJ96	AJ580498	99.77
E1B	E1B5_11	*Burkholderia terrae* KMY02	AB201285	95.47
E1B	E1B5_12	*Luteibacter rhizovicinus* LJ96	AJ580498	99.77
E1B	E1B5_14	*Luteibacter rhizovicinus* LJ96	AJ580498	99.31
E1BF	E1BF3_5	*Luteibacter rhizovicinus* LJ96	AJ580498	99.42
E1BF	E1BF3_6	*Burkholderia diazotrophica* JPY461	HM366717	95.77
E1BF	E1BF3_8	*Burkholderia diazotrophica* JPY461	HM366717	97.69
E1BF	E1BF3_9	*Burkholderia diazotrophica* JPY461	HM366717	97.43
E1BF	E1BF3_11	*Burkholderia bryophila* LMG 23644	AM489501	98.83
E1BF	E1BF6_1	*Burkholderia bryophila* LMG 23644	AM489501	99.06
E1BF	E1BF6_2	*Burkholderia bryophila* LMG 23644	AM489501	99.06
E1BF	E1BF6_3	*Burkholderia diazotrophica* JPY461	HM366717	97.80
E1BF	E1BF6_4	*Luteibacter rhizovicinus* LJ96	AJ580498	99.30
E1BF	E1BF6_6	*Burkholderia diazotrophica* JPY461	HM366717	97.43
E1BF	E1BF6_8	*Dyella koreensis* BB4	AY884571	98.60
E1BF	E1BF6_9	*Burkholderia diazotrophica* JPY461	HM366717	97.43
E1BF	E1BF6_11	*Burkholderia bryophila* LMG 23644	AM489501	99.53
E1BF	E1BF6_12	*Luteibacter rhizovicinus* LJ96	AJ580498	99.42
E1BF	E1BF7_1	*Burkholderia diazotrophica* JPY461	HM366717	95.72
E1BF	E1BF7_3	*Luteibacter rhizovicinus* LJ96	AJ580498	99.54
E1BF	E1BF7_4	*Luteibacter rhizovicinus* LJ96	AJ580498	99.42
E1BF	E1BF7_7	*Burkholderia diazotrophica* JPY461	HM366717	95.84
E1BF	E1BF7_8	*Burkholderia diazotrophica* JPY461	HM366717	95.98
E1BF	E1BF7_11	*Burkholderia diazotrophica* JPY461	HM366717	95.72
E1BF	E1BF9_2	*Burkholderia diazotrophica* JPY461	HM366717	97.43
E1BF	E1BF9_4	*Luteibacter rhizovicinus* LJ96	AJ580498	99.08
E1BF	E1BF9_6	*Burkholderia diazotrophica* JPY461	HM366717	97.44
E1BF	E1BF9_7	*Burkholderia diazotrophica* JPY461	HM366717	97.56

E1BF	E1BF9_8	*Burkholderia diazotrophica* JPY461	HM366717	97.56
E3B	E3B3_1	*Burkholderia sediminicola* HU2-65W	EU035613	99.53
E3B	E3B3_2	*Burkholderia bryophila* LMG 23644	AM489501	99.29
E3B	E3B3_3	*Burkholderia sediminicola* HU2-65W	EU035613	99.77
E3B	E3B3_4	*Burkholderia sediminicola* HU2-65W	EU035613	99.65
E3B	E3B3_5	*Luteibacter rhizovicinus* LJ96	AJ580498	99.77
E3B	E3B3_6	*Luteibacter rhizovicinus* LJ96	AJ580498	99.42
E3B	E3B3_8	*Luteibacter rhizovicinus* LJ96	AJ580498	99.77
E3B	E3B3_10	*Luteibacter rhizovicinus* LJ96	AJ580498	99.88
E3B	E3B3_11	*Burkholderia sediminicola* HU2-65W	EU035613	99.65
E3B	E3B3_12	*Burkholderia bryophila* LMG 23644	AM489501	99.53
E3B	E3B4_1	*Dyella japonica* XD53	AB110498	99.77
E3B	E3B4_2	*Burkholderia bryophila* LMG 23644	AM489501	99.53
E3B	E3B4_3	*Burkholderia bryophila* LMG 23644	AM489501	99.42
E3B	E3B4_6	*Burkholderia caledonica* LMG 19076	AF215704	96.98
E3B	E3B4_9	*Burkholderia caledonica* LMG 19076	AF215704	97.09
E3B	E3B4_13	*Burkholderia caledonica* LMG 19076	AF215704	97.10
E3B	E3B4_14	*Burkholderia caledonica* LMG 19076	AF215704	96.86
E3B	E3B5_1	*Burkholderia caledonica* LMG 19076	AF215704	97.07
E3B	E3B5_2	*Burkholderia caledonica* LMG 19076	AF215704	97.19
E3B	E3B5_3	*Burkholderia sartisoli* RP007	AF061872	97.19
E3B	E3B5_7	*Cupriavidus gilardii* CIP 105966	EU024163	97.32
E3B	E3B5_8	*Burkholderia sartisoli* RP007	AF061872	97.19
E3B	E3B5_12	*Burkholderia sartisoli* RP007	AF061872	98.04
E3B	E3B5_13	*Burkholderia caledonica* LMG 19076	AF215704	97.18
E3B	E3B5_14	*Burkholderia caledonica* LMG 19076	AF215704	97.19
E3BF	E3BF3_1	*Burkholderia fungorum* LMG 16225	AF215705	98.25
E3BF	E3BF3_3	*Burkholderia bryophila* LMG 23644	AM489501	98.71
E3BF	E3BF3_5	*Burkholderia caledonica* LMG 19076	AF215704	96.95
E3BF	E3BF3_8	*Dyella koreensis* BB4	AY884571	98.85
E3BF	E3BF3_10	*Burkholderia bryophila* LMG 23644	AM489501	98.94
E3BF	E3BF3_12	*Burkholderia sartisoli* RP007	AF061872	97.19
E3BF	E3BF6_1	*Burkholderia bryophila* LMG 23644	AM489501	98.59
E3BF	E3BF6_2	*Burkholderia caledonica* LMG 19076	AF215704	96.95
E3BF	E3BF6_3	*Burkholderia bryophila* LMG 23644	AM489501	98.94
E3BF	E3BF6_5	*Burkholderia sediminicola* HU2-65W	EU035613	99.53
E3BF	E3BF6_7	*Burkholderia bryophila* LMG 23644	AM489501	98.82
E3BF	E3BF6_9	*Dyella koreensis* BB4	AY884571	98.60

E3BF	E3BF6_11	*Burkholderia bryophila* LMG 23644	AM489501	98.82
E3BF	E3BF7_3	*Burkholderia bryophila* LMG 23644	AM489501	99.53
E3BF	E3BF7_7	*Burkholderia ginsengisoli* KMY03	AB201286	99.30
E3BF	E3BF7_8	*Burkholderia bryophila* LMG 23644	AM489501	98.37
E3BF	E3BF7_9	*Burkholderia bryophila* LMG 23644	AM489501	98.25
E3BF	E3BF7_12	*Burkholderia ginsengisoli* KMY03	AB201286	99.18
E3BF	E3BF9_1	*Burkholderia caledonica* LMG 19076	AF215704	97.29
E3BF	E3BF9_4	*Burkholderia caledonica* LMG 19076	AF215704	97.18
E3BF	E3BF9_5	*Burkholderia sartisoli* RP007	AF061872	97.19
E3BF	E3BF9_6	*Burkholderia sediminicola* HU2-65W	EU035613	99.53
E3BF	E3BF9_7	*Dyella japonica* XD53	AB110498	99.65
E3BF	E3BF9_8	*Burkholderia caledonica* LMG 19076	AF215704	97.06
E3BF	E3BF9_10	*Burkholderia sordidicola* S5-B	AF512826	98.12

Table 4.2. Taxonomic assignment of the 125 strains selected for functional characterisation, using the EzTaxon-e server (Kim *et al.* 2012) and on the basis of 16S rRNA gene sequences (>800 nucleotides).

- Chapter 5 -

Effect of a bacterial community on the process of wood degradation by *Phanerochaete chrysosporium*: a polyphasic approach

Résumé

Les deux précédents chapitres ont permis de mettre en évidence un effet mycosphère du champignon de pourriture blanche *Phanerochaete chrysosporium* sur la diversité taxonomique et fonctionnelle des communautés bactériennes associées au processus de décomposition du bois de hêtre. Dans ce chapitre, une dernière expérience en microcosme a été réalisée afin d'évaluer la contribution respective de *P. chrysosporium* et d'une communauté bactérienne issue de la mycosphère de ce champignon dans le processus de dégradation du bois, ainsi que d'évaluer la nature des interactions bactéries-champignon dans ce même processus. Des microcosmes contenant de la sciure humide stérile ainsi qu'une bûchette stérile de hêtre ont été inoculés avec trois inocula microbiens différents : le champignon *P. chrysosporium* (traitement F), une communauté bactérienne composée de vingt-cinq souches bactériennes isolées dans la mycosphère de *P. chrysosporium* (traitement B) et enfin un consortium microbien constitué de *P. chrysosporium* et de cette même communauté bactérienne (traitement BF). Des microcosmes contrôles inoculés avec de l'eau stérile ont également été réalisés. Ces microcosmes ont été échantillonnés à huit reprises lors d'une cinétique qui a durée six mois. Au total, trois cent dix-huit microcosmes ont été utilisés.

Afin d'analyser simultanément le potentiel fonctionnel des microorganismes associés à la décomposition du bois et le processus de décomposition lui-même, une approche polyphasique a été mise en place. Dix activités enzymatiques, dont sept directement impliquées dans la dégradation de la lignocellulose, ont été mesurées dans la sciure de cent quatre-vingt microcosmes. Le pH et la teneur en carbone (C) et azote (N) de ces échantillons ont également été mesurés. Bien que le mycélium fongique apparaisse moins dense en présence de la communauté bactérienne (traitement BF), aucune différence significative n'a été détectée dans les profils d'activités enzymatiques (bêta-glucosidase, glucuronidase, cellobiohydrolase, bêta-xylosidase, N-acétylglucosaminidase et phosphatase acide) entre les traitements F et BF. Dans les microcosmes du traitement B, aucune de ces activités enzymatiques n'a pu être détectée, le signal étant probablement trop faible. Au cours des six mois d'incubation, le pH de la sciure a diminué de manière significative pour le traitement F mais pas pour les traitements BF et B, indiquant un effet des bactéries sur l'acidification de l'environnement bois par le champignon. Le ratio C/N, connu pour diminuer lors du processus de décomposition du bois, n'a significativement diminué en six mois que pour le traitement BF, suggérant une dégradation notable de la sciure uniquement en présence de

P. chrysosporium et d'une communauté bactérienne qui lui est associée.

Les propriétés physico-chimiques des bûchettes présentes dans les différents microcosmes ont également été analysées. Après six mois d'incubation, l'analyse des variations de masse et de densité de ces éprouvettes de hêtre nous a révélé une perte de masse plus élevée et des densités significativement plus faibles par rapport aux échantillons contrôles, uniquement pour les échantillons BF. Ceci indique que les échantillons BF sont les plus dégradés et que dans nos conditions, l'association bactéries-champignon s'est révélée la plus efficace pour décomposer le bois. Les pertes de masse des échantillons étant extrêmement faibles, l'analyse globale de la composition élémentaire des bûchettes n'a pas révélé de variations significatives en fonction du temps ou des traitements microbiens, sauf pour la concentration en phosphore (P) et le ratio N/P qui apparaissent donc comme des marqueurs de la décomposition du bois.

Les pertes de masse des bûchettes étant relativement faibles dans nos conditions, des analyses de surface des éprouvettes ont également été réalisées en combinant des observations au microscope électronique à balayage (SEM) avec des microanalyses en spectrométrie à rayons X (analyse dispersive en énergie ou EDS et analyse dispersive en longueur d'onde ou WDS), après cinq mois d'incubation. Dans un premier temps, les bûchettes ont été analysées directement après l'échantillonnage, alors qu'elles étaient encore colonisées par les microorganismes. Des variations significatives des concentrations en Mg, S, P, K et Ca ont été observées. La présence de cristaux d'oxalate de calcium a été détectée sur les hyphes de *P. chrysosporium* et la quantité de ces cristaux s'est révélée significativement plus abondante dans le traitement BF que dans le traitement F, indiquant des différences dans le métabolisme fongique en présence de la communauté bactérienne. Après avoir gratté, rincé à l'eau distillée puis brossé la surface des bûchettes pour retirer les microorganismes, ces microanalyses ont été réitérées. Le ratio C/N ainsi que la teneur en oxygène à la surface du bois sont apparus significativement plus faibles pour le traitement BF par rapport aux autres traitements, indiquant une dégradation plus importante à la surface des échantillons dégradés par *P. chrysosporium* et la communauté bactérienne qui lui est associée.

Par une approche polyphasique, nous avons démontré que l'association d'un champignon de pourriture blanche avec une communauté bactérienne issue de la mycosphère de ce dernier résulte en une dégradation accrue de matériau bois par rapport à l'action seule d'un champignon ou d'une communauté bactérienne. Alors que de précédentes études suggéraient des interactions compétitives et antagonistes entre bactéries et champignons dans

le processus de dégradation du bois, nos résultats mettent pour la première fois en exergue une synergie entre bactéries et champignon dans la fonction de décomposition du bois.

5 Effect of a bacterial community on the process of wood degradation by *Phanerochaete chrysosporium*: a polyphasic approach

5.1 Introduction

Bacteria and fungi are known to be involved in biogeochemical cycles (Gadd 2006; Falkowski, Fenchel & Delong 2008; Dürre *et al.* 2011). In forest ecosystems, they interact and participate to wood decomposition, and therefore contribute to carbon cycling and nutrient recycling. During the process of wood decomposition, nutrient contents of wood, especially N, P, K, Ca and Mg, fluctuate (Laiho & Prescott 2004). The flux of these nutrients is a key feature of the biogeochemistry of forest ecosystems (Harmon *et al.* 1986). However, it is not clear what are the respective contributions of bacteria and fungi to the wood degradation process, in term of elemental composition of the substrate.

In the two previous chapters, microcosms were used to monitor the taxonomic and functional diversities of the bacterial communities associated with decaying-wood and with the white-rot fungus *Phanerochaete chrysosporium*. Such approach allows to work under controlled conditions, and to answer specific ecological questions (Benton *et al.* 2007) including the question about the bacterial and fungal contributions to soil decomposition activity (Ushio *et al.* 2013) and to oxalate-carbonate pathway (Martin *et al.* 2012). The aim of the present chapter is to monitor and quantify the respective contribution of fungus-associated bacterial isolates and of a white-rot fungus to the wood degradation process, as well as to evaluate the nature of the bacterial-fungal interactions – neutral, antagonist or synergic – based on the analysis of several functional traits: lignocellulolytic activities, elemental composition and wood density. The temporal dimension was also taken into account since the wood decay process was monitored during six months with eight sampling dates. To achieve the objective, we developed a polyphasic approach in which we analysed both the microbial metabolism and the physicochemical properties of wood along the wood decay process.

A microcosm-scale study was designed with microcosms containing sterile wood and three different types of inoculum: a white-rot fungus, a bacterial community and a complex community constituted by a white-rot fungus and a bacterial community. The fungus we used is the model strain *Phanerochaete chrysosporium* RP78. Concerning the bacterial community,

it corresponded to a mix of 25 strains – 22 *Burkholderia* spp. and 3 *Dyella* spp. – previously isolated from the mycosphere of *P. chrysosporium* in sawdust microcosms after eighteen weeks of incubation. These strains were selected from the culturable bacterial community isolated from the E3BF treatment described in the two previous chapters. These strains were chosen since they were taxonomically identified and corresponded to the dominant OTUs detected by 16S rRNA gene-based pyrosequencing, specifically associated with the E3BF microcosms (see chapters 3 and 4), *i.e.* associated with *P. chrysosporium* in sawdust microcosms. Moreover, these strains were functionally characterised (see chapter 4). They presented higher cellulolytic and xylanolytic activities as well as lower antagonism towards *P. chrysosporium* compared to the bacterial strains isolated from the forest soil used as initial inoculum.

Each microcosm contained two types of beech wood substrate, both types of wood were sterilised. Sawdust was used as growth matrix and wood blocks were put on it. Because of the difference in substrate size, the kinetics of the decomposition process is expected to differ between sawdust and wood blocks. Sawdust was analysed for enzyme activities, pH, C and N concentrations. These environmental variables have been widely studied in various ecosystems to understand biogeochemical processes (Sinsabaugh *et al.* 2008). Indeed, in forest ecosystems, lignocellulolytic activities have been shown to be highly correlated with wood mass loss (Sinsabaugh *et al.* 1992). In the same woody environment, we monitored also the global elemental composition of the wood blocks along time. Because wood degradation can be a slow process, the surface of these wood blocks was simultaneously studied using a microanalysis approach. Scanning electron microscopy (SEM) coupled with energy dispersive X-ray spectroscopy (EDS) and wavelength-dispersive X-ray spectroscopy (WDS) were used to map the wood surface in order to study surface degradation of wood based on variation of the elemental composition, but also to study the metabolism of wood-associated microorganisms on wood surface. Indeed, such techniques have already been used to characterise fungal metabolic processes such as calcium oxalate biomineralisation (Tuason & Arocena 2009; Pylro *et al.* 2013). Moreover, cation concentrations are known to vary in wood degraded by wood-rotting fungi (Ostrofsky *et al.* 1997). Finally, wood blocks were also analysed for mass and density losses. This whole study aimed to understand the impact of a bacterial community on the process of wood decomposition by a white-rot fungus.

5.2 Materials and Methods

5.2.1 Experimental design

The experiment consisted of 318 microcosms (140 mm Petri dishes sealed with adhesive tape) filled with 50 cm^3 of beech (*Fagus sylvatica* L.) sawdust sieved (2 mm mesh) and autoclaved (20 min, 120 °C) twice, with 2 days in between. The sterility of the sawdust was checked by plating sawdust suspensions at different dilutions on 10% tryptic soy agar (TSA) medium and by incubating them for 7 days at 25°C. No microbial growth was detected. In each microcosm, 20 ml of sterile deionised water was spread carefully over all of the sterile sawdust and a sterile beech wood block (50×25×5 mm) was placed over the wet sawdust in the center of the microcosm. This wood block was initially sterilised (autoclaved twice, 20 min, 120 °C, with 2 days in between) and the sterility of the wood block was checked by plating woodblock suspensions at different dilutions on 10% TSA medium and by incubating them for 7 days at 25°C. No microbial growth was detected.

Fungal inocula were prepared using other sterile beech wood blocks (50×25×5 mm), prepared similarly. The wood blocks were incubated with the white-rot fungus *Phanerochaete chrysosporium* RP78 in Petri dishes, containing malt (30 $g.l^{-1}$) agar (20 $g.l^{-1}$) medium for 4 weeks, at 25°C, in dark conditions. The fungal strain was maintained at 25 °C on 3% malt agar slants

The bacterial inoculum was prepared by mixing 25 strains, 22 strains of *Burkholderia* spp. and 3 strains of *Dyella* spp., previously isolated from sawdust microcosms of the E3BF treatment, as described in the chapter 4. These strains were stored at -80°C in 25% glycerol. The bacterial isolates were grown in liquid culture (10% TSB) in an incubator shaker at 25°C for 24h. Each culture was centrifuged and rinsed once with sterile deionised water. Bacterial concentrations were normalised in order to obtain the same optical density (OD) at 600 nm for each culture. The 25 bacterial suspensions were then mixed together and the resulting inoculum was diluted in sterile deionised water in order to obtain a 10^5 $CFU.ml^{-1}$ mixed bacterial inoculum. The bacterial concentration was verified by plating this bacterial inoculum on 10% TSA medium and by incubating the plates for 7 days at 25°C. The concentration of the bacterial inoculum was quantified as 8.6 10^4 $CFU.ml^{-1}$. Because the colonies *Burkholderia* spp. and *Dyella* spp. are morphologically distinct, it was possible to estimate the *Dyella* spp. / *Burkholderia* spp. ratio. We confirmed a ratio close to the expected 3/22 ratio.

The microcosms were inoculated with three different microbial inocula, corresponding

to the three different treatments. In one treatment – called BF (for bacterial inoculum + fungal inoculum *i.e. P. chrysosporium*) – 333 µl of the bacterial inoculum was spread carefully over all of the sterile sawdust and 333 µl of the bacterial inoculum was also spread over the sterile beech block. The fungal inoculum containing *P. chrysosporium* was placed at 4 cm of the sterile wood block. In a second treatment – called B (for bacteria) – 333 µl of the bacterial inoculum was spread carefully over all of the sterile sawdust and 333 µl of the bacterial inoculum was also spread over the sterile beech block. To keep the same conditions, a sterile beech wood block was also placed at 4 cm of the first wood block. In a third treatment – called F (for fungus *i.e. P. chrysosporium*) – the fungal inoculum containing *P. chrysosporium* was placed at 4 cm of the sterile wood block and 333 µl of sterile deionised water was spread over this sterile wood block. A control treatment – called C (for control *i.e.* without any microorganism) – was also performed where a sterile beech wood block humidified with 333 µl of sterile deionised water was also placed at 4 cm of the first sterile wood block. A kinetic study was performed during six months, at eight sampling dates, *i.e.* t=0, 0.5, 1, 2, 3, 4, 5 and 6 months for the three treatments, *i.e.* BF, B and F, and *n*=12 replicates per conditions. It corresponded to 8×3×12=288 inoculated microcosms. Concerning the control treatment C, *n*=15 microcosms were sampled at the beginning, *i.e.* t=0, and at the end of the kinetic study, *i.e.* t=6 months. In total, 288+15×2=318 microcosms were used. It should be mentioned that t=0 was sampled 24 hours after the bacterial inoculation to allow the establishment of the bacterial community. All manipulations were done under sterile conditions, using a biosafety cabinet. All microcosms were incubated at 25°C in the dark.

5.2.2 Sampling procedure

At each sampling date, 36 microcosms were sampled. The presence of bacteria on each colonised wood blocks was checked by putting in contact the inoculated wood block surface with 10% TSA medium containing 100 $mg.l^{-1}$ cycloheximide (Sigma Aldrich) and by incubating the Petri dishes for 7 days at 25°C. Subsequently, wood blocks were cleaned off microorganisms using paper towel and then rinsed with deionised water. Wood samples were dried at 40°C and then brushed with a toothbrush to clean wood surface off mycelial residues.

The totality of the sawdust of each microcosm was sampled and homogenised. In order to extract enzymes, 2 g of sawdust were mixed with 40 ml distilled water. The homogenised substrates were extracted at 4 °C for 2 h on a shaker. Extracts were filtered through Whatman filter paper (17-30 µm pore size) and the filtrates were kept frozen at −20 °C until analysis, according to Valášková et al., 2007. Solid residues of wood were dried

at 65 °C until constant mass and weighed. One microbial suspension was extracted for each sample by shaking vigorously for 1 min, 0.2 g of sawdust in 3 ml of sterile distilled water. Each microbial suspension was stored at -80°C in 25% glycerol. The remainder of the sawdust was stored at −20 °C until analysis.

5.2.3 Enzyme assays

Ten enzyme activities were measured for 180 randomly selected samples among the 318 samples. Seven enzymatic assays were based on fluorogenic substrate release and three were photometric. The fluorogenic assays were based on 4-methylumbelliferone (MU) or 7-amino-4-methylcoumarin (AMC) release upon cleavage by enzymes: MU-β-D-glucopyranoside (MU-BG) for β-glucosidase (BG) (EC 3.2.1.3), MU-β-D-glucuronide hydrate (MU-GC) for β-glucuronidase (GC) (EC 3.2.1.31), MU-β-D-xylopyranoside (MU-XL) for β-xylosidase (XL) (EC 3.2.1.37), MU-β-D-cellobioside (MU-CBH) for 1,4-β-cellobiohydrolase (CBH) (EC 3.2.1.91), MU-N-acetyl-β-D-glucosaminide (MU-NAG) for 1,4-β-poly-N-acetylglucosaminidase (NAG) (EC 3.2.1.14), MU-phosphate (MU-AP) for acid phosphatase (AP) (EC 3.1.3.2) and L-leucine-AMC for leucyl aminopeptidase (LAP) (EC 3.4.11.1). All chemicals were purchased from Sigma Aldrich Chemicals (Lyon, France). Stock (5 mM) and calibration (25 mM) solutions were prepared in 2-methoxyethanol and substrates were diluted with sterile ultra-pure water to a final substrate concentration of 500 µM for MU-BG, MU-GC, MU-XL, MU-NAG, 400 µM for MU-CBH and L-leucine-AMC and 800 µM for MU-AP.

The experimental procedure mainly followed the protocol described by Mathieu et al., 2013. Briefly, the fluorogenic assays were performed in 96-well microplates containing 50 µl of enzymatic extract, 50 µl of Na acetate buffer (100 mM, pH 4.5), and 50 µl of substrate solution for a total volume of 150 µl per well. Depending on enzyme activity, incubation times were 15 min (MU-AP), 30 min (MU-BG, MU-NAG) or 60 min (MU-GC, MU-XL, MU-CBH and L-leucine-AMC). After these incubation times, 100 µl of the reaction mix was added to 100 µl of stopping buffer in a black 96-well microplate before reading. The stopping buffer (Tris 2.5 M, pH 10–11) enabled MU and AMC readings and stopped enzyme reactions. Measurements were carried out with a Victor^3 Wallac 1420 Multilabel counter microplate reader (Wallac Perkin-Elmer Life Sciences, Villebon-Sur-Yvette, France) with excitation wavelength set to 360 nm and emission wavelength to 450 nm. Each series of experiment included calibration wells to correlate fluorescence signal to concentration of released MU

and AMC, which was calculated from the resulting regression lines. Controls related to medium auto fluorescence and quenching were subtracted for all measures. These controls were obtained by boiling 10 min at 95°C an aliquot of each enzymatic extract.

Concerning the photometric assays, three other substrates were used: 2, 2′-azino-di-(3-ethylbenzthiazoline sulfonic acid) (ABTS) (Fluka) for laccase and more generally oxidase, 3-dimethylaminobenzoic acid (DMAB) (Fluka) and 3-methyl-2-benzothiazolinone hydrazone hydrochloride (MBTH) (Fluka) for manganese peroxidase (MnP) and Azure B (Sigma Aldrich Chemicals, Lyon, France) for lignin peroxidase (LiP). The experimental procedure also mainly followed the protocol described by Mathieu et al., 2013. Stock solution of ABTS (2 mM) for laccase assay was diluted in Na acetate buffer pH 4.5. For the enzymatic assay, 50 µl of enzymatic extract, 50 µl of incubation buffer (100 mM Na acetate, pH 4.5), and 50 µl of ABTS stock solution were incubated 60 min at 25 °C in a clear flat bottom 96-well microplate. Then, absorbance was measured at 415 nm with a iMark Microplate Absorbance Reader (Bio-Rad, Hercules, CA, USA). Absorptions values were converted into enzyme activities via the extinction coefficient of the ABTS cation radical formed by laccase activity (36 000 M^{-1} cm^{-1}). Manganese peroxidase (MnP) assay was based on the oxidative coupling of MBTH and DMAB in the presence of H_2O_2 and Mn^{2+}. Two working solutions (A and B) were made. Solution A contained (final volume 7 ml), 5 ml of sodium lactate and sodium succinate buffer (100 mM each, pH 4.5), 0.5 ml of DMAB solution (50 mM in ultra pure water), 0.5 ml of MBTH solution (1 mM in ultra pure water) and 1 ml $MnSO_4$–$4H_2O$ (1 mM in ultra pure water). The solution B contained the same elements except $MnSO_4$, which was replaced by EDTA (2 mM in ultra pure water). For the manganese peroxydase (MnP) assay, 140 µl of working solution A or B was added to 50 µl of enzymatic extract and 10 µl of H_2O_2 (1 mM in ultra pure water) in a clear 96-well flat bottom microplate. After 60 min incubation at 25 °C, measurements were made on a iMark Microplate Absorbance Reader (Bio-Rad, Hercules, CA, USA) at 595 nm. Subtracting values obtained by working solution B from A revealed the MnP activity since only working solution A contained $MnSO_4$ which is required for manganese dependent peroxidases. Absorption was then converted into enzyme activities via the extinction coefficient (32,000 M^{-1} cm^{-1}). Lignin peroxidase (LiP) assay is based on decrease in absorption of Azure B, which is oxidised under lignin peroxidase action (Archibald 1992). In a clear 96-well flat bottom microplate, 100 µl of buffer (100 mM sodium tartrate pH 4.5) was added to 50 µl of enzymatic extract and 30 µl of ultra pure water, then

10 µl of Azure B (640 µM in ultra pure water) was added with 10 µl of H_2O_2 (1 mM in ultra pure water) to start the assay. Decrease in absorbance was followed at 655 nm on a iMark Microplate Absorbance Reader (Bio-Rad, Hercules, CA, USA) during 60 min.

Seven measurements were made for each sample and each enzymatic assay. The mean value was used in the subsequent analyses. Enzyme activities were expressed in $nmol.h^{-1}.g^{-1}$ of dry sawdust. These activities were log(x+1) transformed prior to analysis to normalise variance.

5.2.4 Elemental analyses

Cleaned wood blocks were cut into chips, dried at 50°C and then ground in a 10 ml zirconium oxide mill (Retsch, Haan, Germany). Carbon and nitrogen concentrations of each sample were measured using a CHN analyser NC2500 (ThermoQuest, CE Instruments). Al, Ca, Fe, K, Mg, Mn, Na, P, S concentrations were measured using inductively coupled plasma atomic emission spectroscopy (ICP-AES) (Jobin-Yvon 180 Ultrace). Wood powder was dried 48h at 50°C and then 0.2g was digested overnight with 6ml of 65% HNO_3 (Merck). Samples were mineralised using microwave irradiation (Multiwave 3000, Anton Paar), diluted in 100 ml deionised water and filtered before ICP-AES analysis.

In parallel, a fraction of the sawdust belonging to the 180 microcosms analysed for enzyme activities was also dried at 50°C and then ground in a 10 ml zirconium oxide mill (Retsch, Haan, Germany). Carbon (C) and nitrogen (N) concentrations for each sample were measured using a CHN analyser NC2500 (ThermoQuest, CE Instruments).

5.2.5 pH measurement

For pH measurement, 1.25 g of the homogenised wood sawdust was suspended in 25 ml of distilled water (Gindl & Tschegg 2002). The suspension was then shaken at 100 rpm at 25 °C. After 4 h, the pH of the suspension was determined by means of a Seven easy pH meter (Mettler Toledo) equipped with a InLab Expert Pro electrode (Mettler Toledo). The pH was measured for the 180 microcosms analysed for enzyme activities.

5.2.6 Scanning electron microscopy and X-ray microanalysis

Wood blocks from different treatments were observed and analysed directly after sampling and then after removing the microorganisms from the wood surface, as described in

the “Sampling procedure” section. 12 samples from the 4 treatments, *i.e.,* control (C), bacteria (B), fungus (F), bacteria and fungus (BF) (*n*=3) collected at t=5 months, were observed and analysed by Scanning Electron Microscopy (SEM) (1450 VP, LEO Zeiss) equipped with Energy Dispersive Spectrometer (EDS) (SDD 80 mm^2 X-Max, Oxford Instruments) and Wavelength Dispersive Spectrometer (WDS) (INCA Wave, Oxford Instruments). For each analysis of the 50×25 mm^2 surface, 15×7 = 105 measurements per sample were made, using a defined grid pattern.

First, fresh samples were directly observed in variable pressure mode at 50 Pa and analysed for P, Ca, K, Mg and S contents with EDS operating conditions of 20 kV and scanning time of 60s per spectrum. These EDS analyses were performed directly after sampling and then after removing the microorganisms from the wood surface. Subsequently, dry samples were platinum (Pt) coated under high vacuum conditions, prior to WDS analyses. For WDS, the operating conditions were 10 kV, 50 nA (sample current), and scanning time of 30 s per spectrum. In WDS, semi-quantitative analyses of C, O and N elements were performed in high vacuum conditions and with a specific crystal for N. Calcium oxalate (CaOx) crystals were identified by EDS after platinum coating (see spectrum, Figure 5.22). Carbon coated samples were also observed using Field Emission Guns Scanning Electron Microscopy (FEG-SEM) (ZEISS Supra 55VP access). The resulting images were acquired by Bertrand Van de Moortèle at the ENS of Lyon.

5.2.7 Mass and density measurements

The mass and density of the wood blocks from all microcosms were measured before being placed inside the microcosms, *i.e.* before the autoclaving, and after being incubated with their different treatments, *i.e.* time x inoculum. Only the samples analysed by SEM were not used for mass and density analyses. Mass and density measurements were performed as described in Chapter 2 (Hervé *et al.* 2014a). Briefly, samples were first dried 24h at 103°C. Masses were measured using an AG204 analytical balance (Mettler Toldeo) (nearest 0.1 mg). Wood density data were acquired with a Brightspeed Exel 4 (General Electric Healthcare) computed tomography (CT) scanner using 80 kV voltage and 50 mA intensity (Freyburger *et al.* 2009). The 3D reconstruction process was performed using the “DETAIL” filter, providing 512×512 slices with a transverse resolution of 0.1875 mm/pixel and a distance between slices of 0.625 mm. Then, images were analysed using ImageJ v1.46 (Schneider *et al.* 2012) and an in-house plugin written in Java. The 50×25 mm^2 surface of each CT slice was analysed using 40x20 subdivisions, with one subdivision representing 44 pixels. For each 5-mm-thick side of

each wood block, 7 slices were used. This procedure led to the 3D mapping of 40×20×7 = 5600 elements per scanned wood sample. Pixels with densities less than 0.2 $g.cm^{-3}$ were removed. It was assumed that these pixels corresponded to entirely biodegraded areas. Pixels with a density greater than 0.2 $g.cm^{-3}$ were counted and averaged to compute the area and mean density of each element.

5.2.8 Data analysis

All statistical analyses, ordinations and graphics were computed using R software version 3.0.2 (R Development Core Team 2013). Concerning the enzyme activities, values were log(x+1) transformed prior to analysis to normalise variance. Differences in enzyme activities between the different inoculum type were evaluated by one-way ANOVA followed by the Tukey HSD *post hoc* test. For data that did not fit a normal distribution or whose variances were not homogeneous after transformation, non-parametric Kruskal-Wallis test was used. The effects of incubation time and microbial treatment on the pH and C:N ratio of the sawdusts were estimated by two-way ANOVA followed by the Tukey HSD *post hoc* test. The effects of pH, C:N ratio, incubation time and microbial treatment on the enzyme activities were estimated by a distance-based permutational multivariate ANOVA (PERMANOVA) (Anderson 2001) using “adonis” function of the *vegan* package (Oksanen *et al.* 2012) with Euclidean distance matrix and 100000 random permutations. Non-metric multidimensional scaling (NMDS) based on an Euclidean distance matrix was used to visually assess differences between enzyme activity profiles of the different samples. This analysis was performed with the “metaMDS” function of the *vegan* package (Oksanen *et al.* 2012). Environmental variables were fitted to the ordination plot using the “envfit” function of the same package. The squared correlation coefficients and their significances were computed using 100000 random permutations. To examine relationships among enzyme activities and environmental variables, Pearson's product-moment correlation coefficients (rho, r) were computed. Correlogram were produced with the *corrgram* package.

Concerning the wood blocks, differences in elemental composition between different treatments (microbial treatment x incubation time) were evaluated by two-way ANOVA followed by the Tukey HSD *post hoc* test. For data that did not fit a normal distribution or whose variances were not homogeneous, non-parametric Kruskal-Wallis test was used.

5.3 Results

5.3.1 Sawdust decomposition

The process of wood decomposition inside the microcosms was monitored over six months by measuring ten enzyme activities potentially related to the wood decay process, for four microbial treatments: a white-rot fungus (F), a bacterial community (B), the white-rot fungus with the bacterial community (BF) and a control (C) containing only sterile deionised water. For four of these ten enzyme activities, laccase, lignin peroxidase (LiP), manganese peroxidase (MnP) and leucyl aminopeptidase (LAP), no significant differences were found between the four microbial treatments (one-way ANOVA, $p > 0.05$), meaning that in presence of microorganisms (B, F or BF) these activities did not differ from the control treatment (C) (data not shown). Therefore, these four variables were removed from the subsequent analyses. Concerning the acid phosphatase (AP), beta-glucosidase (BG), cellobiohydrolase (CBH), glucuronidase (GC), N-acetylglucosaminidase (NAG) and beta-xylosidase (XL), the measured enzyme activities were significantly affected by the microbial treatment (two-way ANOVA, $p < 0.001$ for each activity) and the time of incubation (two-way ANOVA, $p < 0.001$ for each activity) as well as by the interaction of these two factors (two-way ANOVA, $p < 0.05$ for each activity). For the microcosms inoculated with only the bacteria (B), none of these six enzyme activities differed from the activities detected in the control microcosms (C) ($p > 0.5$, data not shown), indicating that no enzyme activity signal was recorded in sawdust inoculated only with bacteria. Concerning the F and BF microcosms, patterns of enzyme activities showed similar trend over the incubation time (Figures 5.1 to 5.6) and no significant difference was found between the F and BF treatments, for any of the enzyme activity ($p > 0.5$). Similarly, integrated enzyme activities, corresponding to the area under a plot of activity as a function of time for each sampling interval, and cumulative activities, corresponding to the integrated activities summed over all prior sampling intervals, did not present significant differences ($p > 0.5$) between F and BF treatments. Altogether these results indicated that the presence of bacteria with the white-rot fungus *P. chrysosporium* (BF) did not affect the cellulolytic (BG, CBH, GC, XL), chitinolytic (NAG) and phosphatase (AP) activities in sawdust microcosms, compared to microcosms with the fungus alone (F).

The characteristics of the sawdust originating from the different microcosms were also analysed. The C:N ratio of the sawdust was affected by the microbial treatment ($F_{2, 149}=68.30$, $p < 0.001$), the time of incubation ($F_{7, 149}=21.84$, $p < 0.001$) and the interaction of these two factors ($F_{14, 149}=7.37$, $p < 0.001$). Overall, the C:N ratio for both BF and F treatments differed from B treatment ($p < 0.001$), but not significant difference was found between F and BF

treatments ($p > 0.2$) (Figure 5.7). Comparing initial (t=0) and final values (t=6 months), the C:N ratio significantly decreased in BF microcosms ($p < 0.001$), but not in B or F microcosms ($p > 0.1$), suggesting a more efficient wood degradation by the bacterial-fungal consortium compared to bacteria or fungus alone. Concerning the pH (Figure 5.8), it was also affected by the microbial treatment ($F_{2, 149}=12.57$, $p < 0.001$), the time of incubation ($F_{7, 149}=10.36$, $p < 0.001$) and the interaction of these two factors ($F_{14, 149}=2.03$, $p < 0.05$). The pH of BF and B microcosms did not significantly differ ($p > 0.15$), but the pH of F microcosms was found to be different from the one of BF ($p < 0.05$) and B ($p < 0.001$) microcosms. Comparing initial (t=0) and final values (t=6 months), the pH significantly decreased in F microcosms ($p < 0.05$), but not in B or BF microcosms ($p > 0.2$), indicating that the presence of bacteria reduced the acidification of the sawdust by the fungus. Regardless of the incubation time or the microbial treatment, the C:N ratio and the pH of the sawdust were linearly correlated ($R^2=0.11$, $p < 0.001$). This correlation was higher when considering only the F microcosms ($R^2=0.17$, $p < 0.001$).

The effects of pH, C:N ratio, incubation time and microbial treatment on the enzyme activities were estimated using a PERMANOVA (Table 5.1). These four factors had a significant impact ($p < 0.001$) on the enzyme activity patterns. Interactions between C:N ratio and the microbial treatment, between pH and the microbial treatment and between the C:N ratio and the time of incubation were also found to be significant ($p < 0.05$). These results indicated that cellulolytic (BG, CBH, GC, XL), chitinolytic (NAG) and phosphatase (AP) activities in sawdust microcosms were correlated with pH and C:N ratio. They also confirmed the effects of incubation time and microbial treatment on the enzyme activities. Ordination of enzyme activities using NMDS did not reveal a clear separation between the three types of inoculum (Figure 5.10). Only the samples from the B treatment showed a clear cluster.

Independently of the incubation time or the microbial treatment, the six enzyme activities were significantly positively correlated to each other (Table 5.2). It suggested a synergy of cellulolytic, chitinolytic and phosphatase activities in sawdust microcosms. All these activities were also positively correlated with the N content and negatively correlated with both the pH and the C:N ratio. However, when considering the BF and F treatment datasets separately, the correlations among enzyme activities and with N content differed (Figure 5.11). Indeed, for the F samples, acid phosphatase (AP) activity was not correlated with any other enzyme activity whereas in the case of BF samples, AP activity was positively correlated with both beta-glucosidase (BG) and cellobiohydrolase (CBH) activities. This

suggested differences between F and BF microcosms in the general process of wood degradation at the enzymatic level. Similarly, for the F samples, N-acetylglucosaminidase (NAG) activity was not correlated with N content or C:N ratio whereas in the case of BF samples, NAG activity was positively correlated with N content and negatively correlated with the C:N ratio of sawdust. It revealed that NAG activity was related N recycling only when both bacteria and fungus were present (BF).

5.3.2 Wood block decomposition

Concerning the wood block decomposition inside the microcosms, both global and surface analyses were performed. First, the presence of bacteria at the surface of each wood block was verified directly after sampling. No bacterium was detected in F and C microcosms after six months of incubation, confirming that the controlled conditions were kept. Similarly, no culturable bacteria were detected in B microcosms, at any time of the kinetics, suggesting that a culturable bacterial community was not able to colonise alone the surface of the wood block in the microcosm conditions. In the BF microcosms, bacterial colonies were detected on each wood block over the kinetic study, except for the initial sampling point t= 0 month, *i.e.* 24 hours after the inoculation of the microcosms. Moreover, from 0.5 to 6 months of incubation, it was possible to distinguish both *Dyella spp.* and *Burkholderia* spp. colonies on the plates. It indicates that in presence of *P. chrysosporium*, the mixed bacterial community was able to proliferate on the woodblock surface over months.

Wood blocks from the different microbial treatments were analysed for total elemental composition after 0, 2, 4 and 6 months of incubation. No significant difference between incubation time and microbial treatment were detected for C, N, Al, Ca, Fe, Mg, Na and S contents in wood blocks (two-way ANOVA, $p > 0.05$). K and Mn concentrations varied significantly with time ($p < 0.01$), but there was no difference between the control (C) and the samples inoculated with B, F and BF ($p > 0.05$). However, P concentration of the beech wood blocks was significantly affected by both the time of incubation ($F_{3, 56}$=37.45, $p < 0.0001$) and the microbial treatment ($F_{3, 56}$=11.15, $p < 0.0001$), but not by the interaction of these two factors ($F_{7, 56}$= 1.73, $p > 0.1$). P concentration significantly decreased over time for B, BF and F treatments ($p < 0.05$) (Figure 5.12). No difference in P concentration was found between the B, BF and F treatments ($p > 0.1$), but P concentration for both the BF and F treatments differed from the C treatment ($p < 0.05$). Similarly, the N:P ratio of the beech wood blocks

was significantly affected by both the time of incubation ($F_{3, 56}$=35.22, $p < 0.0001$) and the microbial treatment ($F_{3, 56}$=27.65, $p < 0.0001$) as well as by the interaction of these two factors ($F_{7, 56}$= 4.31, $p < 0.001$). N:P significantly increased over time for B, BF and F treatments ($p < 0.05$) (Figure 5.13). No difference in N:P ratio was found between the BF and F treatments ($p > 0.1$), but N:P ratio for both the BF and F treatments differed from the B and C treatments ($p < 0.05$). Regardless of the incubation time or the microbial treatment, N and P concentrations in wood blocks were linearly correlated (R^2= 0.24, $p < 0.001$) (Figure 5.14). This correlation was higher when considering only the BF (R^2=0.33, $p < 0.005$) or B (R^2=0.57, $p < 0.001$) microcosms, but the case of F microcosms only, N and P concentrations were not correlated (R^2=0.10, $p > 0.05$). This suggests differences in wood nutrient utilisation by the microorganisms depending on the microbial treatment.

Elemental composition of the surface of the wood blocks was also analysed using X-ray microanalyses, namely energy dispersive spectroscopy (EDS) and wavelength dispersive spectroscopy (WDS). Samples were analysed after five months of incubation, before and after cleaning the surface to remove the microorganisms. Observations were also made using scanning electron microscopy (SEM) and FEG-SEM. The colonisation of the surface of the wood blocks by the different inocula revealed differences in Mg, S, P, K and Ca concentrations. Mg concentration significantly increased in presence of inoculated microorganisms (B, F, BF) compared to the non-inoculated control treatment ($p < 0.001$) and this concentration was higher for the BF treatment compared to the F ($p < 0.005$) and B ($p < 0.001$) treatments (Figure 5.15). Similar variations were observed for S (Figure 5.16) and K (Figure 5.17) concentrations except that there was no difference between F and BF treatments ($p > 0.5$). Concerning P concentrations, no difference was observed between B and C treatments ($p > 0.2$). P concentration significantly increased in presence of the white-rot fungus, *i.e.* both F and BF treatments ($p < 0.001$), and this concentration was higher for BF treatment compare to F treatment ($p < 0.03$) (Figure 5.18). Concerning the Ca concentration, it significantly increased in presence of inoculated microorganisms (B, F, BF) compared to the control treatment ($p < 0.03$). No difference between B and F treatments was observed ($p > 0.5$) and both showed lower concentration in Ca compared to BF treatment ($p < 0.001$) (Figure 5.19). SEM and FEG-SEM observations revealed crystal structures on the hyphae of *P. chrysosporium* (Figures 5.20 and 5.21). Qualitatively, these crystals were more abundant on BF samples compared to F samples while the mycelial network seemed to be less dense on BF samples compared to F samples (data not shown). Morphological and chemical

characterisations of these crystals indicated that they were calcium oxalate (CaOx) crystals, containing carbon, oxygen and calcium elements (Figure 5.22).

Similarly, the wood surface of the same samples was analysed after removing the microorganisms by washing and brushing the wood blocks. Mg (Figure 5.23) and Ca (Figure 5.24) concentrations showed similar variations based on the microbial treatment. The presence of microorganisms increased the concentration of both Mg and Ca at the surface compared to the control treatment ($p < 0.01$) and these concentrations were significantly higher for the BF treatment compared to B and F treatments ($p < 0.001$). S concentration was increased by the presence of the fungus (both F and BF treatments) compared to B and C treatments ($p < 0.001$), with a higher concentration for the BF treatment compared to F treatment ($p < 0.001$) (Figure 5.25). P concentration was also higher both F and BF treatments compared to B and C treatments ($p < 0.001$) (Figure 5.26). K concentration for both B and F treatments was lower than the control ($p < 0.001$) while this concentration for BF treatment was higher than for the control ($p < 0.001$) (Figure 5.27). Additionally, samples were platinum-coated to estimate C, N and O contents using WDS analyses. Carbon content was significantly lower at the surface of the B, BF and C wood blocks compared to the F wood blocks ($p < 0.001$) (Figure 5.28). N content was significantly higher at the surface of the B, BF and C wood blocks compared to the F wood blocks ($p < 0.001$) (Figure 5.29). C:N ratio was significantly lower at the surface of the B, BF and F wood blocks compared to the control wood blocks ($p < 0.01$), with the lowest C:N ratio for the surface of the BF samples (compared to the control, $p < 0.001$) (Figure 5.30). Concerning the oxygen content at the wood surface, B and F wood blocks did not significantly differ from the control treatment C ($p > 0.1$), but oxygen content at the surface of BF samples was significantly lower than for B, F and C treatments ($p < 0.001$) (Figure 5.31).

Physical characteristics of the wood blocks, namely mass and density, were also investigated. While mass losses after six months were extremely low, they were significantly affected by the microbial treatment (Kruskal-Wallis test, $p < 0.005$). Only the presence of the BF inoculum led to mass losses significantly superior the control treatment ($p < 0.01$) (Figure 5.32). In term of global wood block density (*i.e.* mean wood density of each wood block) no difference was detected between the different microbial treatments after six months of incubation ($p > 0.2$). However, density mapping of these blocks (*i.e.* use of 5600 density values per samples) revealed that wood density was affected by the microbial treatment ($F_{3, 27196}=21.54$, $p < 0.0001$) (Figure 5.33). Indeed, density of wood blocks inoculated with the

BF treatment was significantly lower than the density of wood blocks inoculated with F, B or C treatments ($p < 0.005$). No difference was found between the density of wood blocks inoculated with F and C treatments ($p > 0.05$). This reveals that wood density was reduced after six months of incubation only when both bacteria and fungus were present.

5.4 Discussion

The contribution of a bacterial community and of the white-rot fungus *P. chrysosporium* to the process of wood degradation was studied over six months, using a polyphasic approach. Two kind of beech wood substrates were analysed, namely sawdust and wood blocks. In presence of *P. chrysosporium* (F and BF treatments), cellulolytic activities (BG, CBH, GC, XL) were detected in the sawdust of the microcosms, indicating that wood carbohydrates were degraded. Chitinolytic (NAG) and phosphatase (AP) activities were also detected in the sawdust. However, no lignolytic (MnP, LiP and laccase) or aminopeptidase (LAP) activity was detected in any microcosm. The absence of the activities in a woody environment colonised by a white-rot fungus has already been reported. For example, no LAP, LiP or MnP was detected in the initial stage of *Fagus sylvatica* colonisation by another white-rot fungus, *Trametes versicolor* (Lekounougou *et al.* 2008). Similarly, Mathieu and colleagues (Mathieu *et al.* 2013b) indicated that when *P. chrysosporium* was grown in a liquid medium supplemented with ground sawdust, no laccase activity was detected. Concerning the microcosms inoculated with the B treatment, no enzyme activity was detected. Although, the majority of the strains composing the bacterial community used to inoculate the B treatment, has been shown to be able to degrade carboxymethyl-cellulose and xylan (see Chapter 4). Such absence of detected enzyme activity might be explained by a too low sensibility of the enzyme assay or by a too low concentration of bacterial enzymes extracted from the sawdust.

The main objective of this study was to understand the impact of a bacterial community isolated from the environment of a white-rot fungus on the process of wood decomposition by this fungus. For the six enzyme activities measured in F and BF microcosms over six months, no significant difference was detected between these two treatments indicating that the presence of the bacterial community did not alter the global microbial enzyme production in the sawdust microcosms. Such result differs from previous studies on organic matter decomposition in which enzyme activities, involved in litter decomposition in freshwater ecosystem (Romaní *et al.* 2006) or in soil decomposition in

microcosms (Ushio *et al.* 2013), significantly differed according to the microbial treatment, *i.e.* a bacterial community, a fungal community or a coexisting bacterial-fungal community. However, while no difference in enzyme activity profiles between F and BF treatments could be detected, differences in correlation coefficients among enzyme activities and with N content of sawdust were observed between F and BF treatments. Indeed, for the F samples, acid phosphatase (AP) activity was not correlated with any other enzyme activity and N-acetylglucosaminidase (NAG) activity was not correlated with N content or C:N ratio whereas in the case of BF samples, AP activity was positively correlated with both beta-glucosidase (BG) and cellobiohydrolase (CBH) activities, and NAG activity was positively correlated with N content and negatively correlated with the C:N ratio of sawdust. A potential explanation for these differences could be the fungal biomass. In our microcosms, it has been observed that the fungal mycelium was more dense in the F treatments compared to the BF treatments (data not shown). Such variations in fungal biomass could result in variations of the fungal metabolism, since no difference were found in the enzyme activity profiles between the F and BF treatments, but microbial biomass seemed to be lower in BF microcosms compared to F microcosms. The potential activities of BG, NAG and AP are frequently used as indicator of carbon, organic nitrogen and organic phosphorus acquisition activities, respectively, as well as indicators of microbial nutrient requirement (Sinsabaugh, Hill & Follstad Shah 2009). Moreover, at global scale, AP and BG activities are known to be positively correlated in soils and freshwater sediments (Sinsabaugh & Follstad Shah 2012). Therefore, our results suggest that only in presence of both bacteria and *P. chrysosporium* in a woody environment, carbon and phosphorus metabolisms were related and NAG activity was linked to N content. Future research should focus on the regulation of these metabolisms during the process of wood decomposition, using for example transcriptome analyses of *P. chrysosporium* (Vanden Wymelenberg *et al.* 2009) or ideally transcriptome analyses of the whole microbial consortium. Indeed, the expression of several genes is involved in the production of BG and CBH activities by *P. chrysosporium* (Larrondo *et al.* 2005; Vanden Wymelenberg *et al.* 2009), and variations in the pattern of expression of these genes could be detected according to the presence or the absence of a bacterial community.

Concerning the pH of the sawdust, a significant acidification for the F microcosms was observed after six months of incubation while no significant variation was detected for B and BF treatments. Mixed fungal-bacterial communities have already been shown to impact the pH of other colonised substrates, including for example soil amended with calcium

oxalate, in which the presence of both bacteria and fungi increased the soil pH while fungi or bacteria alone did not induce any shift in soil pH (Martin *et al.* 2012). Interestingly, while significant difference between the pH of F and BF microcosm was observed, it did not affect the enzyme activities of theses microcosms. However, it has been shown that some soil enzyme activities, including NAG and AP, are strongly related to soil pH (Sinsabaugh *et al.* 2008).

We also measured the C and N concentrations in sawdust over time for the different microbial treatments. The C:N ratio in decaying wood logs (Palviainen *et al.* 2008) and decaying sawdust (see Chapter 3) is known to decrease with time and along the decaying process. In our microcosms, the C:N ratio did not significantly differ between F and BF treatments, and both were significantly lower than the C:N ratio of the control treatment at t=6 months ($p < 0.1$), indicating that sawdust was degraded in both F and BF treatments. Interestingly, from zero to six months the C:N ratio significantly decreased in BF microcosms, but not in C, B or F microcosms. This result suggests that sawdust from BF microcosms was more degraded than the sawdust from C, B and F microcosms. Thus, while bacterial-fungal interactions during wood colonisation have been described as antagonistic (De Boer *et al.* 2010), our results suggest that the wood degradation is enhanced by the presence of both a white-rot fungus and its associated bacterial community.

In parallel to the analysis of the sawdust, the wood blocks of the microcosms were also analysed. No bacterium was detected at the surface of the B samples, even 24 hours after the inoculation with the bacterial suspension. It suggests that either bacteria colonised the inner part of the wood blocks, since wood is a porous material, or that bacteria were not able to survive alone on the wood blocks. Since the detection of the bacteria was based on a culture-dependent method, a last possible explanation is that the bacterial community at the surface of the wood blocks was not in a physiologically appropriate state for cultivation. Interestingly, bacterial colonies were detected on the surface of the wood blocks from the BF treatment all along the kinetics, except at the initial sampling date (24 hours after the inoculation). It suggests that the presence of the fungus might have favoured the survival of the bacterial community. Indeed, such effect of a fungus on the bacterial survival has already been described, for example in the case of *Pseudomonas-Saccharomyces* interactions (Romano & Kolter 2005). These results also raise the question of the origin of the bacterial colonies found at the surface of the BF wood blocks since the bacterial inoculum was spread both on the wood blocks and the sawdust. Indeed, some fungi are known to be able to serve as vector for

the dispersion of bacteria in the environment, a phenomenon also known as fungal highway (Kohlmeier *et al.* 2005; Furuno *et al.* 2010), and wood blocks were already colonised at the second sampling date (t=0.5 month). Therefore, it indicates that bacteria from the sawdust may have colonised the wood blocks thanks to *P. chrysosporium*.

The analysis of the wood blocks was based on both physical and chemical measurements. After six months of incubation, the mass losses were extremely low. This fact can be explained by the composition of the microcosms which contained only wood, a relatively nutrient-poor substrate. What is more, two types of wood substate were present, sawdust and wood blocks, and wood decay is known to be influenced by substrate size (van der Wal *et al.* 2007). Since substrate accessibility is much higher for sawdust than for wood blocks, sawdust is expected to be more degraded. We hypothesise that microorganisms have favored the degradation of sawdust compared to a less accessible substrate, leading to a very low mass loss of the wood blocks. Because of these low mass losses, the analysis of the elemental composition of the wood blocks revealed no significant variations between incubation time and microbial treatment for carbon concentration and most of the nutrient concentration measured (N, Al, Ca, Fe, Mg, Na and S). Even if the mass losses were low, significant variations in mass loss according to the microbial treatment were detected. Indeed, only the wood blocks incubated with the BF treatment showed a mass loss significantly higher than the control samples, after six months of incubation. These results were confirmed by the density measurements. While the global density of the samples was not affected by the microbial treatment after six months of incubation, density mapping of the wood blocks revealed that the BF treatment induced a higher wood degradation compared to the other treatments. Indeed, wood blocks incubated with BF treatment had densities significantly lower than density of wood blocks incubated with B, F or C treatments.

Concerning the global elemental composition of the wood blocks, no variation was detected for C and N concentrations. However, N concentration is known to increase during decay (Laiho & Prescott 2004). Therefore, using WDS we analysed the surface of the wood blocks after removing the inoculated microorganisms. Surface analyses indicated a significant increase in N content on the wood blocks incubated with microorganisms, especially in presence of *P. chrysosporium* (F and BF treatments). Concerning the C content, it was significantly higher at the surface of the wood blocks inoculated with the F treatment compared to the B, BF and C treatments. A potential explanation of these results is that *P. chrysosporium* produced secondary metabolites (*e.g.* oxalic acid) which were still present

on the wood after removing the fungal mycelium and thus, it resulted in an increase of the C content. In presence of bacteria (BF treatment), these secondary metabolites could have been metabolised by the bacterial community and thus the C content did not differ from the control treatment. Indeed, it has been reported that bacteria can consume fungal exudates (de Boer *et al.* 2005). The C:N ratio, known to decrease during wood decay (Palviainen *et al.* 2008), was also significantly affected by the microbial treatment. The lowest C:N ratio at the surface of the wood blocks was observed for the BF treatment, suggesting a more important degradation in presence of the BF treatment. Oxygen content was also significantly lower for the BF treatment compared to F, B anc C treatments. Since oxygen is the second most abundant element in wood after carbon, a decrease of its concentration indicates an alteration of wood. All these results of the surface analyses indicate a more efficient wood degradation by the association of *P. chrysosporium* with the bacterial community, compared to the other microbial treatments. They also corroborate the results obtained by mass and density measurements of the wood blocks and suggest a synergistic bacterial-fungal interaction in the process of wood degradation. These results differ from a previous study where the presence of a bacterial community did not affect the decomposition of *Pinus sylvestris* by the white-rot fungus *Hypholoma fasciculare* (Weißhaupt *et al.* 2012).

The global chemical analyses of the wood blocks revealed that only the P concentration and the N:P ratio were significantly affected by both the time of incubation and the microbial treatment. While it was not possible to distinguish between F and BF treatments using these two measurements, P concentration and N:P ratio appeared to be two good indicators of wood degradation in our conditions, even with very low mass losses of the wood blocks. The N:P ratio has also been shown to increase with time during wood decomposition in mangrove forest (Romero, Smith & Fourqurean 2005). More generally, N and P are correlated at global scale in terrestrial vegetation, especially plant leaves (Reich & Oleksyn 2004). In our microcosms, the relationship between N and P varies with the microbial treatment, indicating a different balance between these two nutrients according to the microorganisms involved in the process of wood degradation. In this context, it has also been shown that the N:P ratios influence microbial cellulose degradation and that bacteria and fungi respond differently to varying N:P supply ratios (Güsewell & Gessner 2009).

The surface of the wood blocks colonised by the different microbial treatments was analysed by EDS, after five months of incubation. The presence of *P. chrysosporium* (F and BF treatments) significantly increased the concentration of Mg, S, P, K and Ca at the surface

of the wood blocks. Concerning Mg, P and Ca concentrations, they were higher for the BF treatment than for the F treatment, indicating differences in microbial metabolism during wood colonisation when bacteria were present. Calcium oxalate (CaOx) crystals were identified on the hyphae of *P. chrysosporium*, but were much more abundant in the BF treatment compared to the F treatment. *P. chrysosporium* has been described as an oxalate producer (Dutton *et al.* 1993) and oxalic acid has been shown to be involved in wood degradation by fungi (Shimada *et al.* 1994). Furthermore, numerous white-rot fungi are known to be able to produce calcium oxalate crystals (Guggiari *et al.* 2011). Some bacteria, called oxalotrophic, have the ability to use oxalate as sole source of carbon and energy (Sahin 2003). Oxalotrophic bacteria have been isolated from decaying wood (Zaitsev *et al.* 1998) as well as from fungal mycelium (Bravo *et al.* 2013). Moreover, some *Dyella* spp. (Jung *et al.* 2009) and *Burkolderia* spp. (Kost *et al.* 2014) have been described as oxalotrophic bacteria. While the bacterial strains used as bacterial inoculum in this experiment were not tested for their oxalotrophic ability, our results suggest that bacteria might benefit from fungal oxalate production during the process of wood degradation.

The analyses of the same surfaces after removing the microorganisms indicated an accumulation of Mg, Ca, P and S for F and BF treatments compared to the control samples, with higher concentrations of Mg, S, and Ca for BF compared to F treatment. Al, Fe, Mg and Ca concentrations have been shown to increase with time in *Picea rubens* wood blocks incubated with *P. chrysosporium* (Ostrofsky *et al.* 1997). Except for P, in our study no variation was detected for the global elemental composition of the wood blocks. Some variations were only detected at the surface, suggesting that SEM coupled with X-ray microanalyses were more appropriate tools to detect fine variations on decaying wood. Additionally, such method allows to acquire a high number of measurements per sample, and so to take into account the heterogeneity of biological materials. Moreover, these results showed a significant effect of the microbial treatment on the elemental composition of the degraded wood surface, especially between the F and BF treatments.

5.5 Conclusion

Altogether, the results of these different analyses revealed that the association of *P. chrysosporium* with a bacterial community (BF treatment) is more efficient to decompose wood than the fungus or the bacterial community alone. While previous studies have mostly described antagonistic interactions in organic matter decomposition and more specifically in decaying wood, our results suggest a synergistic bacterial-fungal interaction between *P. chrysosporium* and a coexisting bacterial community. Depending on the presence or the absence of this coexisting bacterial community with *P. chrysosporium*, our results also suggest differences in microbial metabolism, especially for the calcium and the oxalic acid metabolisms. Future studies should focus on the mechanisms involved in this bacterial-fungal interaction.

5.6 Figures and tables

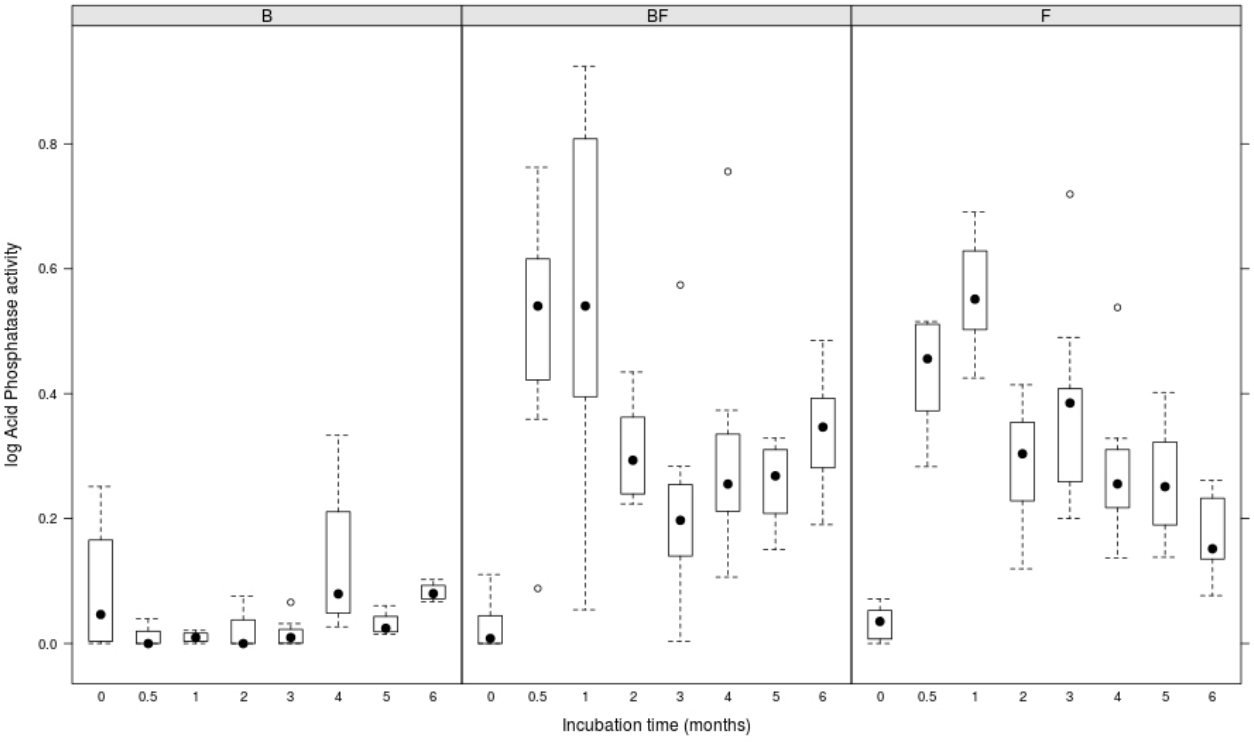

Figure 5.1. Logarithm of acid phosphatase activity (nmol h^{-1} g^{-1} of dry wood) as a function of incubation time and type of microbial inoculum. For B, *n*=4 ; for BF and F, *n*=8.

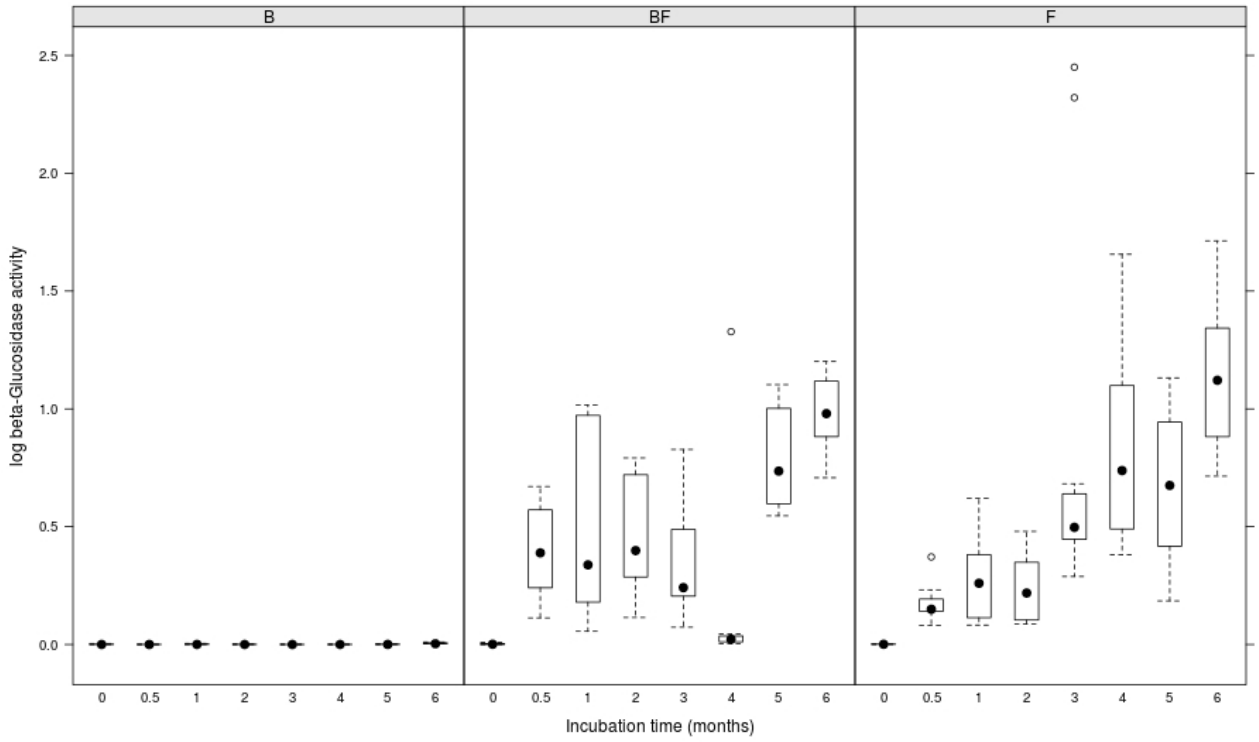

Figure 5.2. Logarithm of beta-glucosidase activity (nmol h^{-1} g^{-1} of dry wood) as a function of incubation time and type of microbial inoculum. For B, *n*=4 ; for BF and F, *n*=8.

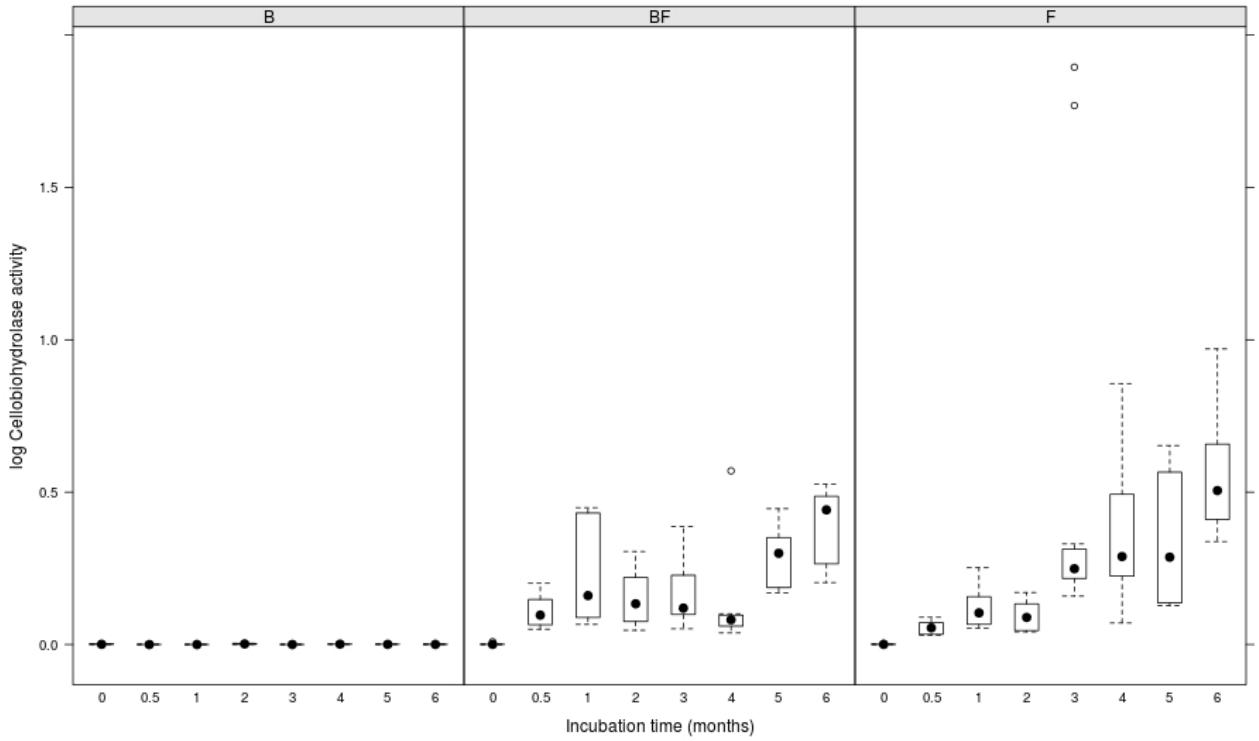

Figure 5.3. Logarithm of cellobiohydrolase activity (nmol h^{-1} g^{-1} of dry wood) as a function of incubation time and type of microbial inoculum. For B, *n*=4 ; for BF and F, *n*=8.

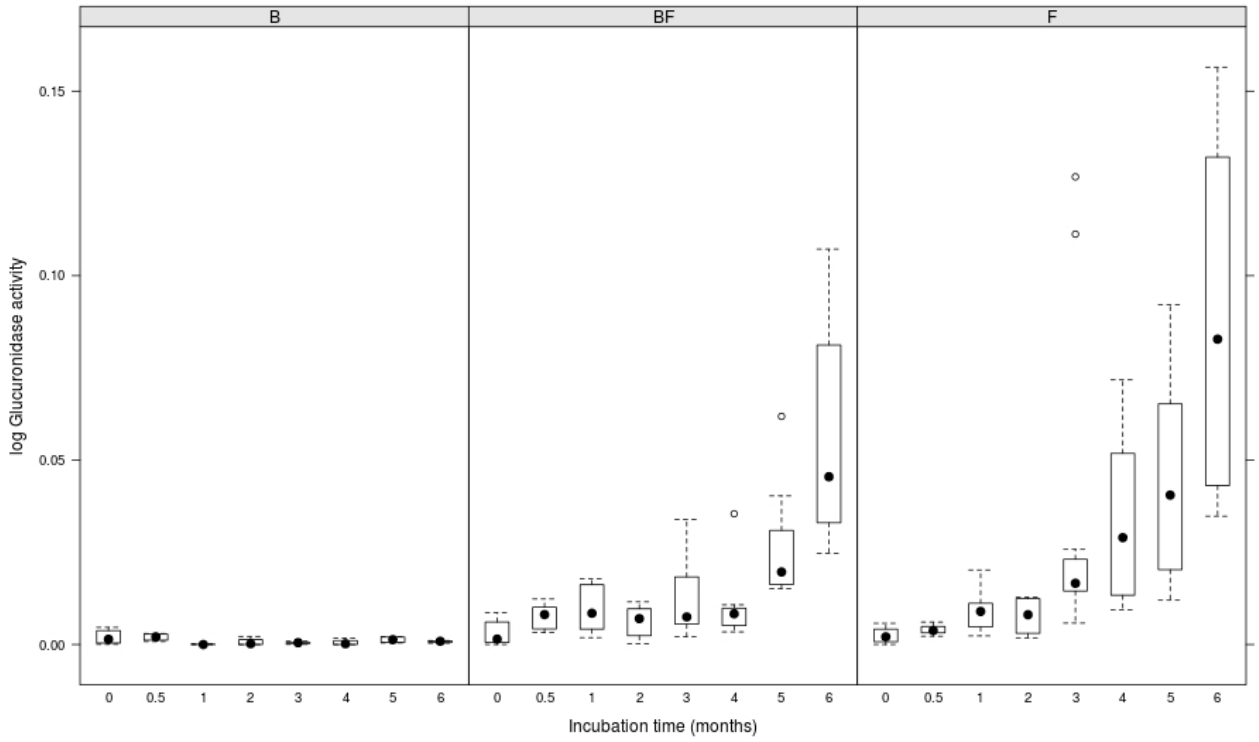

Figure 5.4. Logarithm of glucuronidase activity (nmol h^{-1} g^{-1} of dry wood) as a function of incubation time and type of microbial inoculum. For B, *n*=4 ; for BF and F, *n*=8.

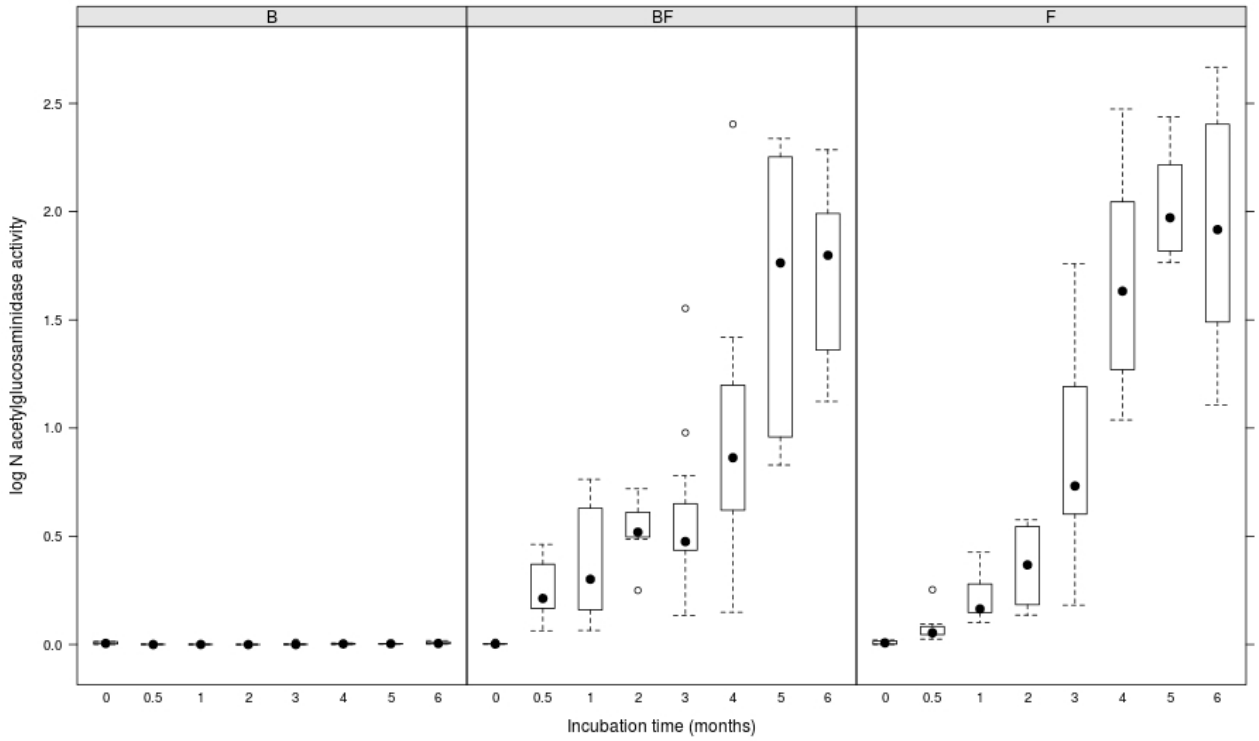

Figure 5.5. Logarithm of N-acetylglucosaminidase activity (nmol h^{-1} g^{-1} of dry wood) as a function of incubation time and type of microbial inoculum. For B, *n*=4 ; for BF and F, *n*=8.

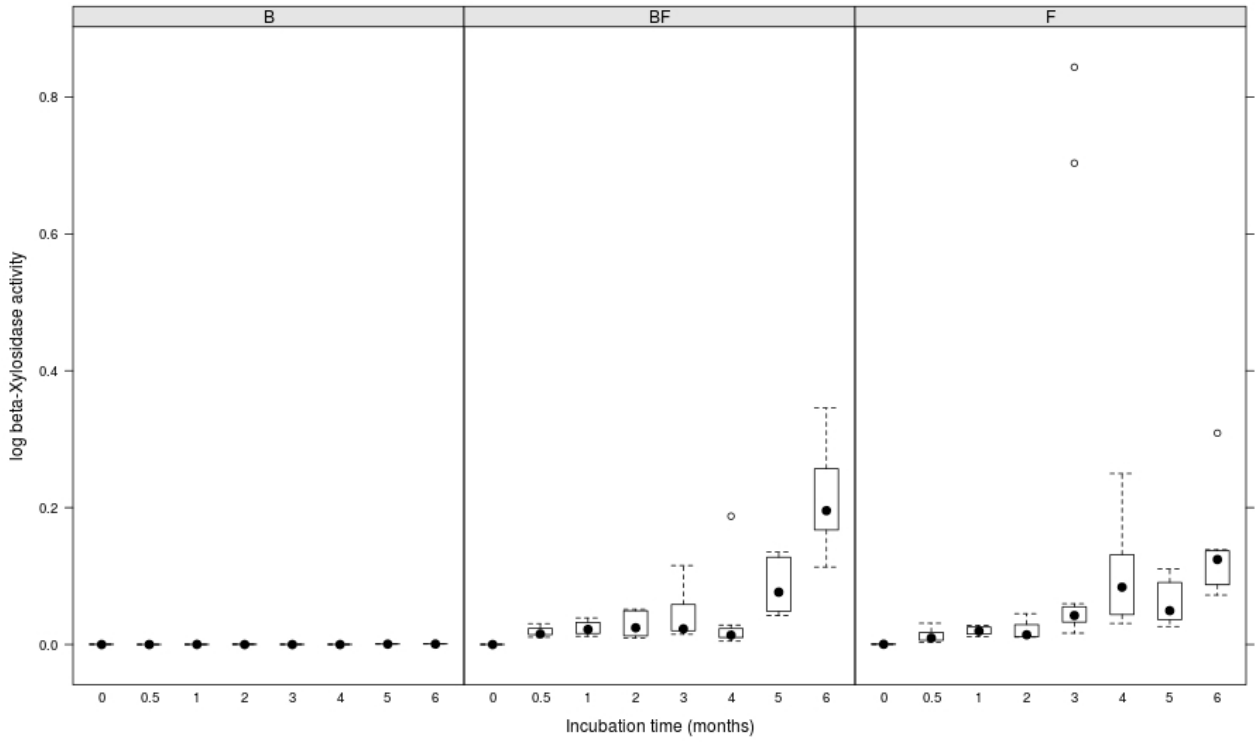

Figure 5.6. Logarithm of beta-xylosidase activity (nmol h^{-1} g^{-1} of dry wood) as a function of incubation time and type of microbial inoculum. For B, *n*=4 ; for BF and F, *n*=8.

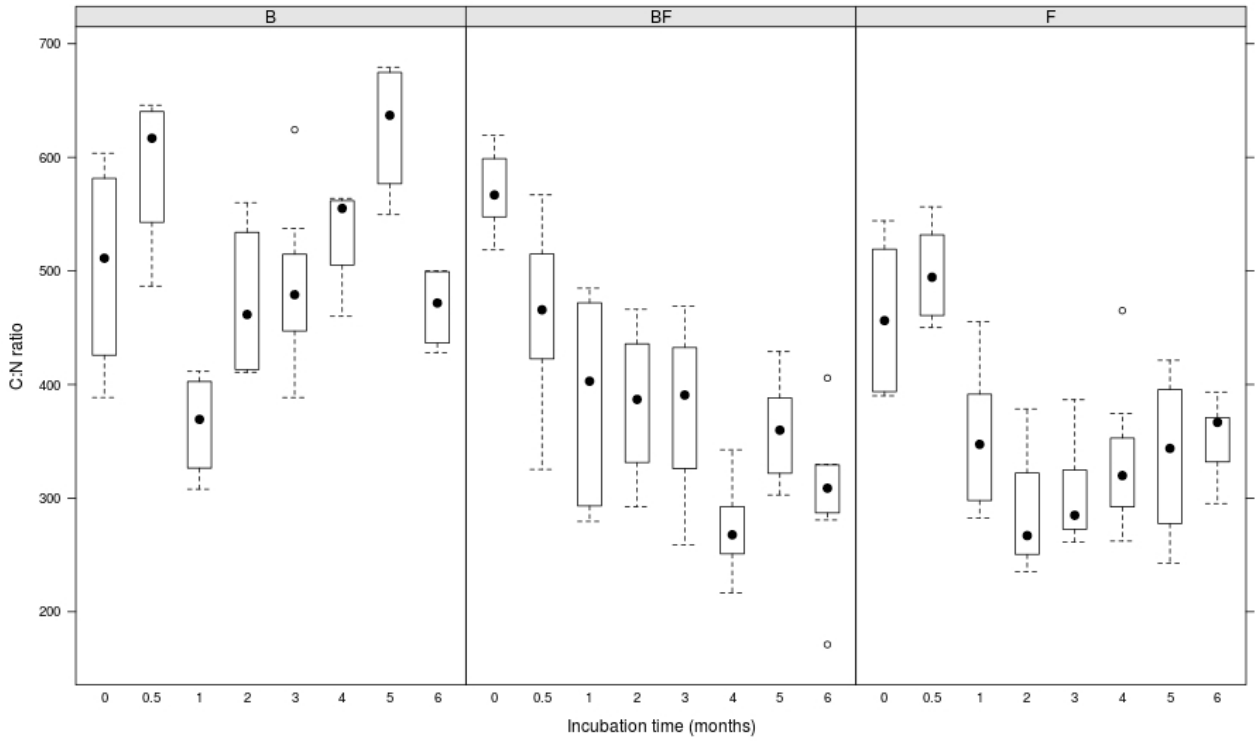

Figure 5.7. C:N ratio of the sawdust as a function of incubation time and type of microbial inoculum. For B, *n*=4 ; for BF and F, *n*=8.

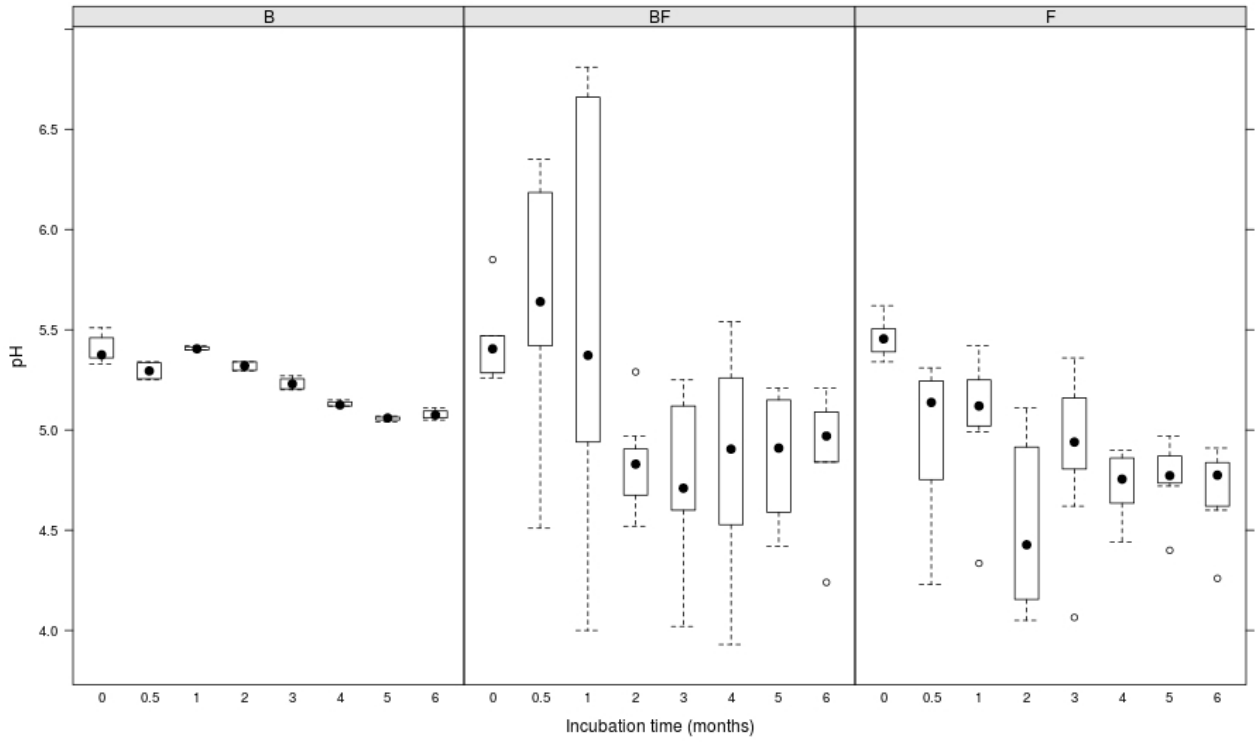

Figure 5.8. pH of the sawdust as a function of incubation time and type of microbial inoculum. For B, *n*=4 ; for BF and F, *n*=8.

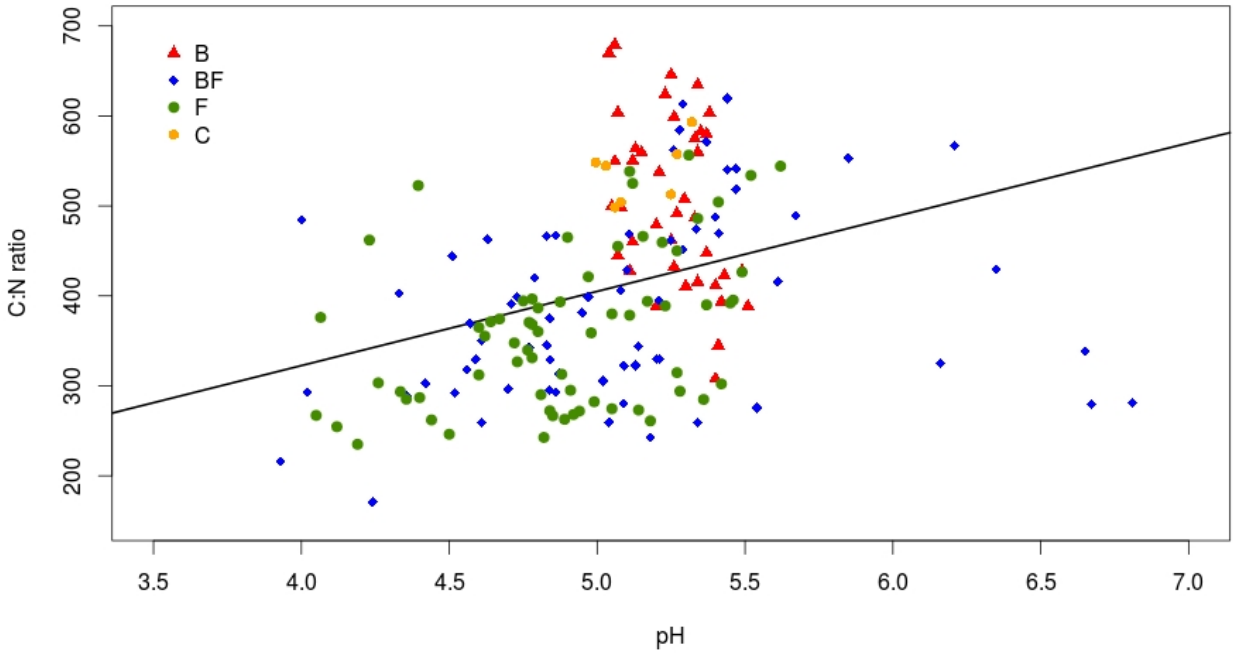

Figure 5.9. Linear relationship between C:N ratio and pH of the sawdust during the process of wood degradation (R^2= 0.11, $p < 0.001$).

	degrees of freedom	sums of squares	*F* statistics	R^2	*p* value
C:N ratio	1	37.18	143.34	0.228	0.0001
pH	1	2.77	10.68	0.017	0.0007
treatment	3	10.85	13.94	0.067	0.0001
incubation	7	45.23	24.92	0.278	0.0001
C:N ratio:pH	1	0.18	0.70	0.001	0.428
C:N ratio:treatment	3	2.93	3.77	0.018	0.0088
pH:treatment	3	18.51	23.79	0.114	0.0001
C:N ratio:incubation	7	3.99	2.20	0.025	0.030
pH:incubation	7	3.52	1.94	0.022	0.058
treatments:incubation	15	8.69	2.23	0.053	0.006
C:N ratio:pH:treatment	3	0.35	0.44	0.002	0.770
C:N ratio:pH:incubation	7	2.07	1.14	0.013	0.338
C:N ratio:treatment:incubation	15	3.50	0.90	0.022	0.581
pH:treatment:incubation	15	2.02	0.52	0.012	0.947
C:N ratio:pH:treatment:incubation	14	1.48	0.41	0.009	0.982
Residuals	75	19.45		0.120	

Table 5.1. Effects of pH, C:N ratio, incubation time and microbial treatment (treatment) on the enzyme activities, estimated using a permutational multivariate analysis of variance (PERMANOVA).

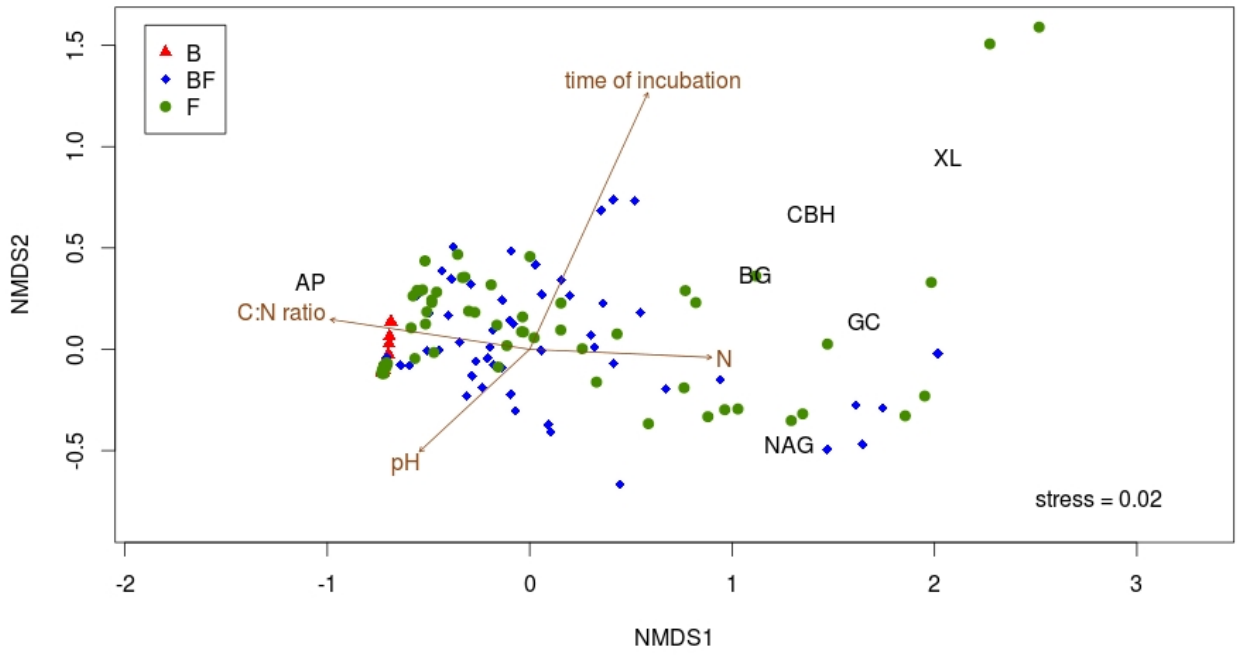

Figure 5.10. Non-metric multidimensional scaling (NMDS) ordination of the different types of sample based on the enzyme activity patterns. Brown vectors represent variables that showed a significant goodness of fit to the ordination plot ($p < 0.001$).

	log(AP)	log(NAG)	log(BG)	log(CBH)	log(GC)	log(XL)	C	N	C:N	pH
log(AP)	-	**0.26**	**0.39**	**0.28**	**0.15**	**0.15**	-0.12	**0.30**	**-0.35**	**-0.15**
log(NAG)		-	**0.81**	**0.69**	**0.75**	**0.59**	-0.03	**0.46**	**-0.51**	**-0.32**
log(BG)			-	**0.93**	**0.82**	**0.83**	-0.04	**0.37**	**-0.43**	**-0.19**
log(CBH)				-	**0.82**	**0.92**	-0.02	**0.36**	**-0.40**	**-0.15**
log(GC)					-	**0.74**	0.01	**0.32**	**-0.35**	**-0.19**
log(XL)						-	-0.01	**0.33**	**-0.35**	-0.08
C							-	0.08	-0.06	0.13
N								-	**-0.95**	**-0.35**
C:N									-	**0.34**
pH										-

Table 5.2. Pearson's product-moment correlation coefficients relating enzyme activities and environmental variables. Significant rho (r) values are in bold ($p < 0.05$).

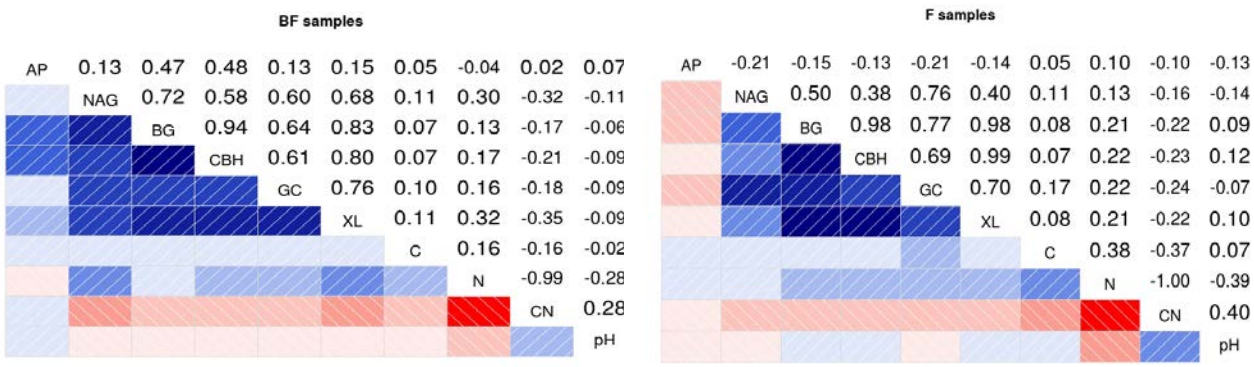

Figure 5.11. Correlograms showing the Pearson's product-moment correlation coefficients relating enzyme activities and environmental variables, for the BF samples (left) and the F samples (righ) (*n*=64). The upper panels indicate the rho (r) values. In the lower panels, blue boxes indicate positive correlations and red boxes negative correlations. The intensity of the colour increases with the degree of correlation.

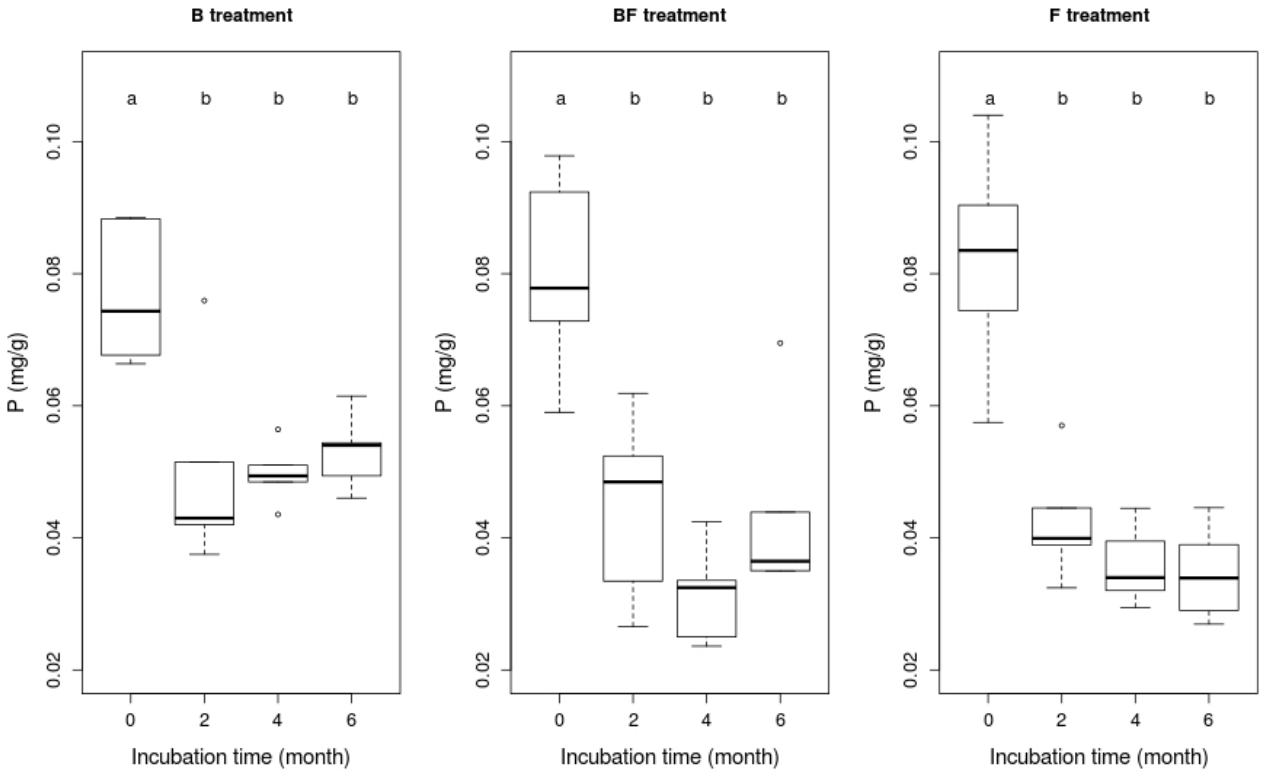

Figure 5.12. Temporal variations of the P concentration of the wood blocks (*n*=5) incubated with different inocula (B, BF or F). Different letters above boxplots indicate significant difference based on one-way ANOVA followed by Tukey's HSD test ($p<0.05$).

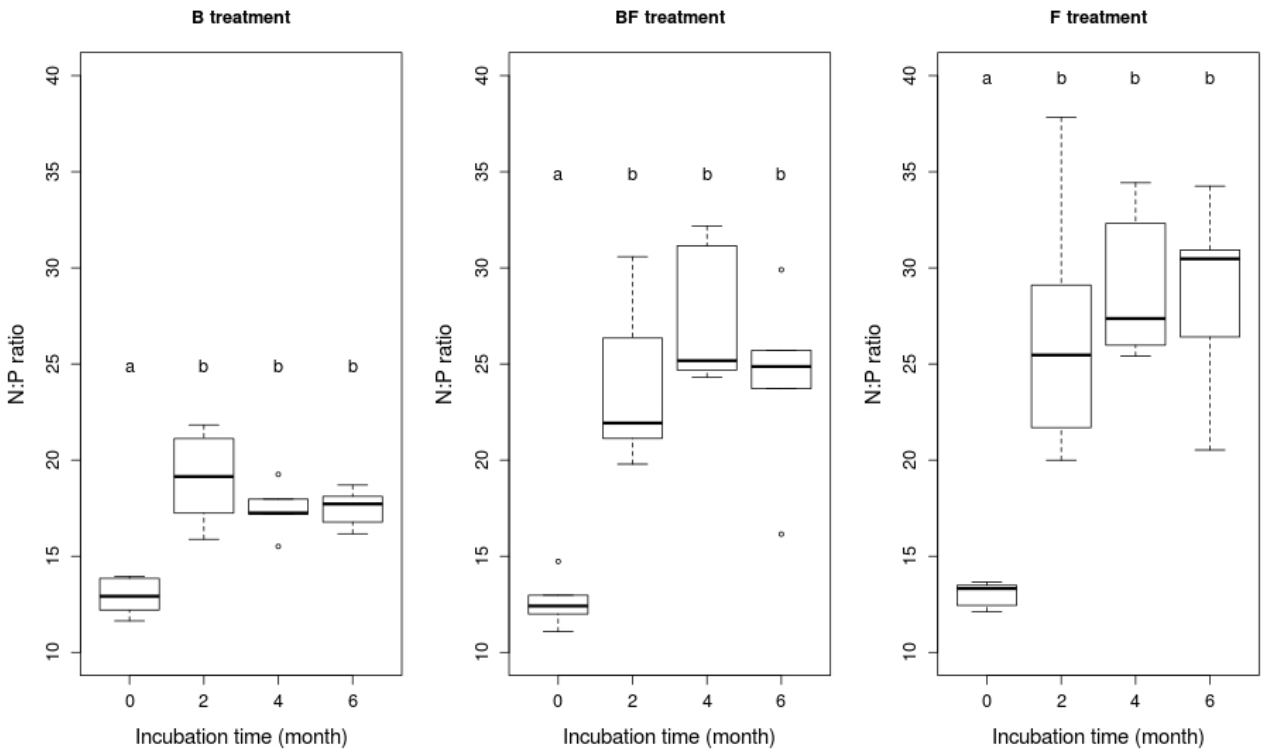

Figure 5.13. Temporal variations of the N:P ratio of the wood blocks (*n*=5) incubated with different inocula (B, BF or F). Different letters above boxplots indicate significant difference based on one-way ANOVA followed by Tukey's HSD test (p<0.05).

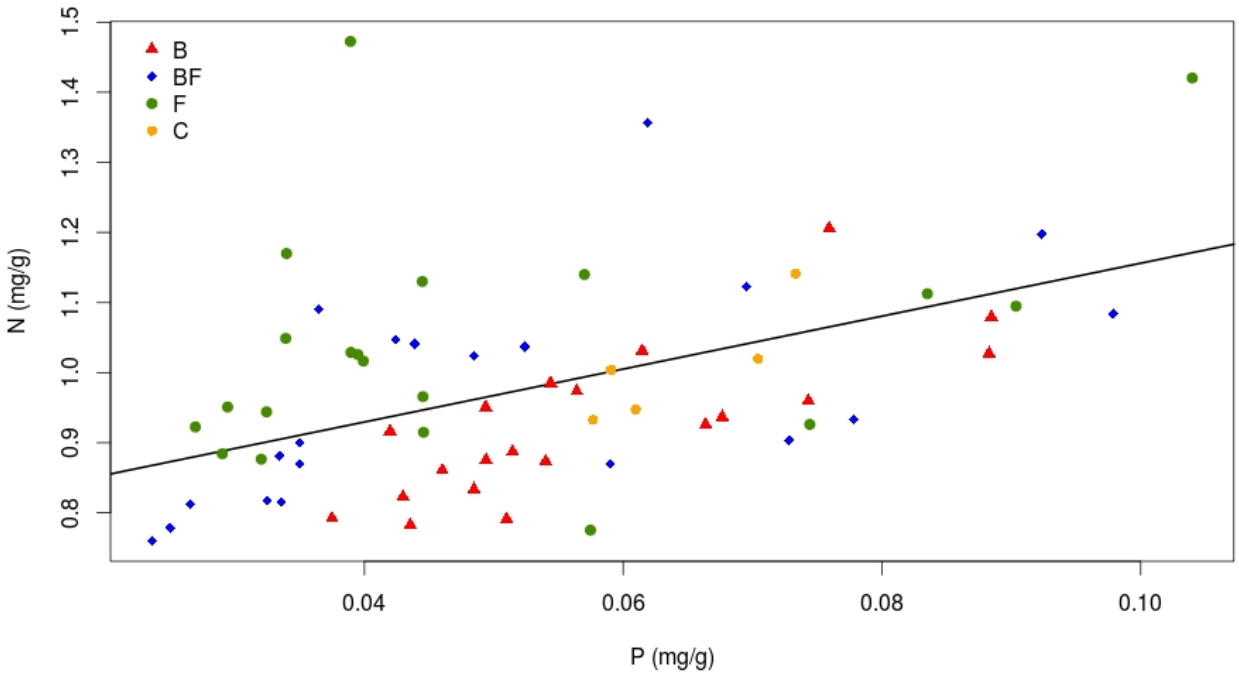

Figure 5.14. Linear relationship between N and P concentrations in wood blocks during the process of wood degradation (R^2= 0.24, p < 0.001).

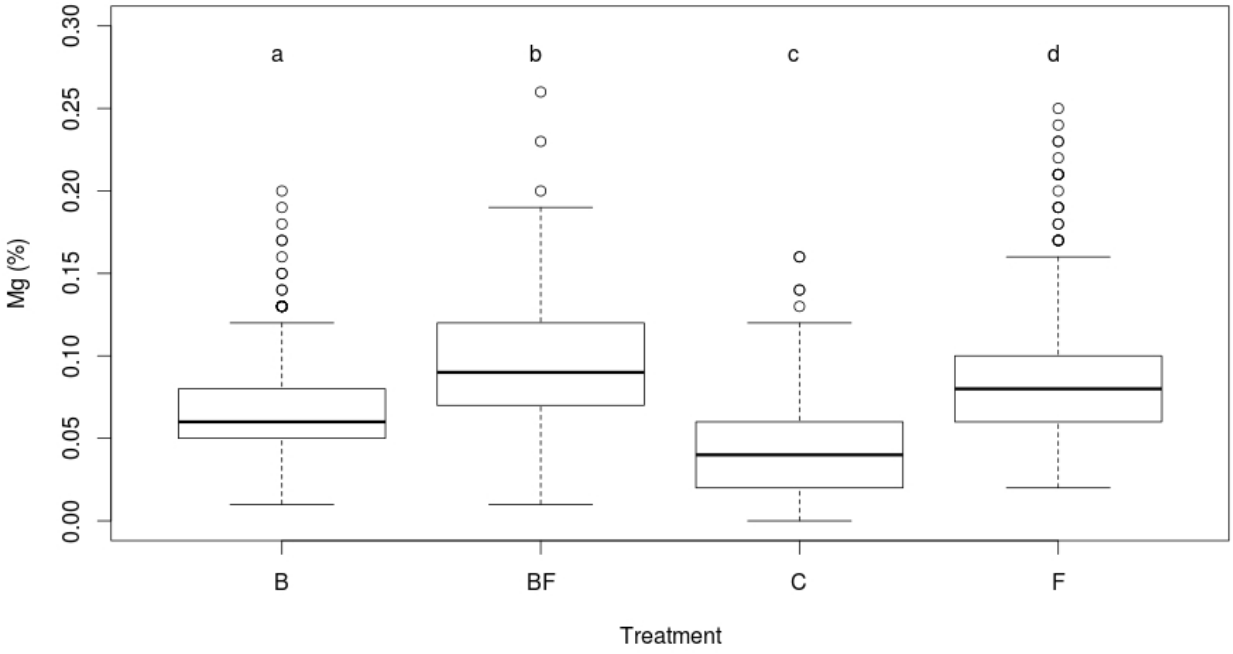

Figure 5.15. Variations of Mg concentration at the surface of the wood blocks (*n*=3) colonised by different inocula (B, BF or F) during five months. For each sample, 105 measurements were made. Different letters above boxplots indicate significant difference based on one-way ANOVA followed by Tukey's HSD test ($p<0.05$).

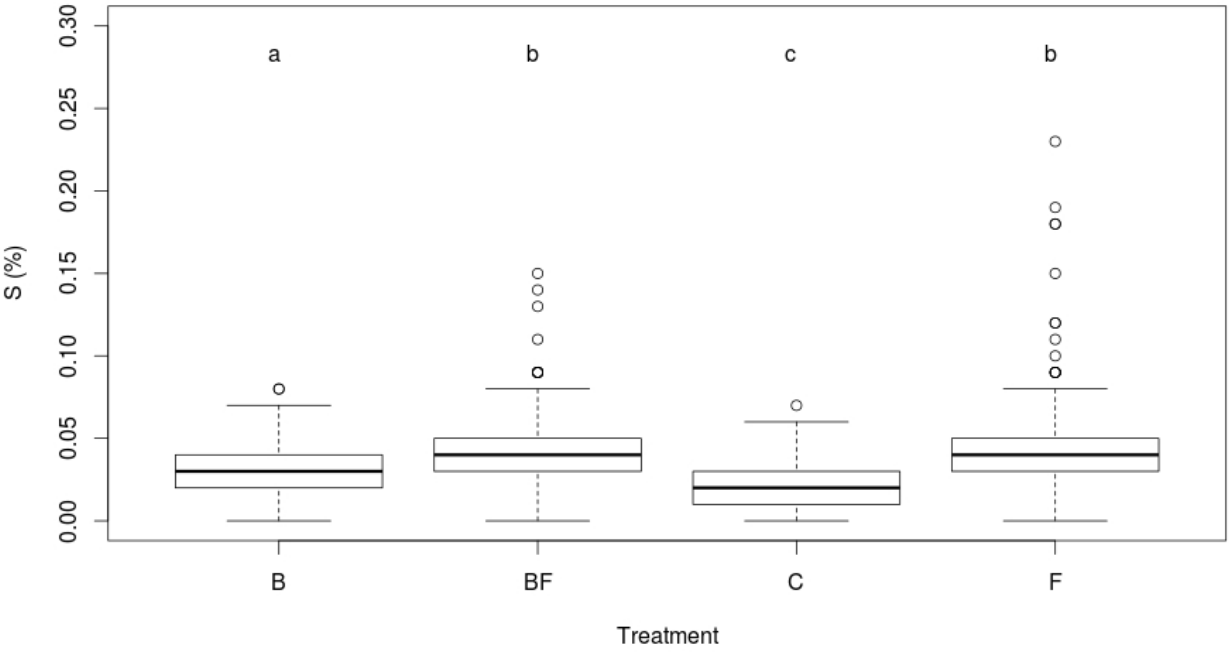

Figure 5.16. Variations of S concentration at the surface of the wood blocks (*n*=3) colonised by different inocula (B, BF or F) during five months. For each sample, 105 measurements were made. Different letters above boxplots indicate significant difference based on one-way ANOVA followed by Tukey's HSD test ($p<0.05$).

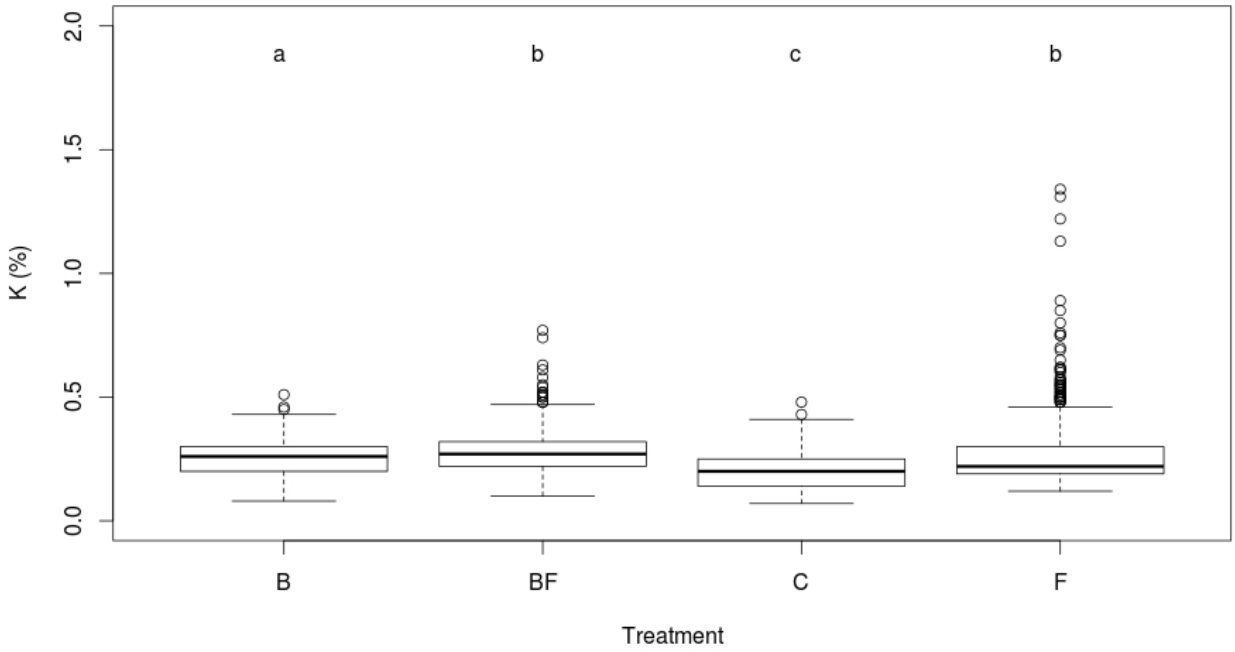

Figure 5.17. Variations of K concentration at the surface of the wood blocks (*n*=3) colonised by different inocula (B, BF or F) during five months. For each sample, 105 measurements were made. Different letters above boxplots indicate significant difference based on one-way ANOVA followed by Tukey's HSD test (p<0.05).

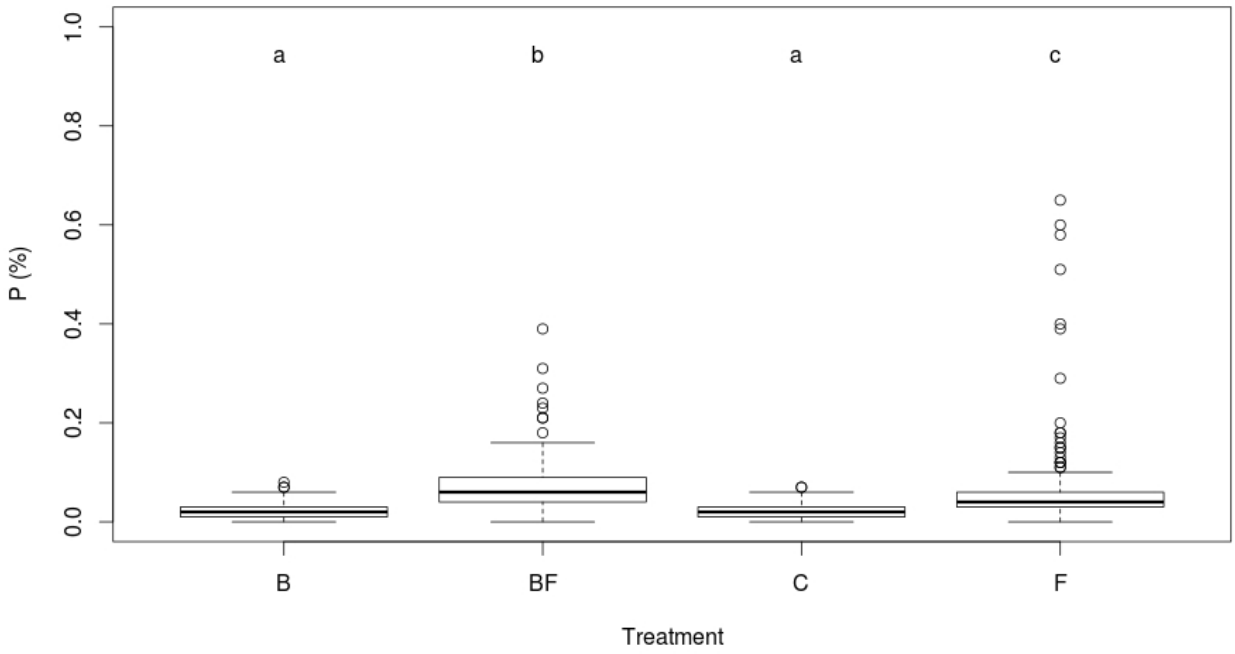

Figure 5.18. Variations of P concentration at the surface of the wood blocks (*n*=3) colonised by different inocula (B, BF or F) during five months. For each sample, 105 measurements were made. Different letters above boxplots indicate significant difference based on one-way ANOVA followed by Tukey's HSD test (p<0.05).

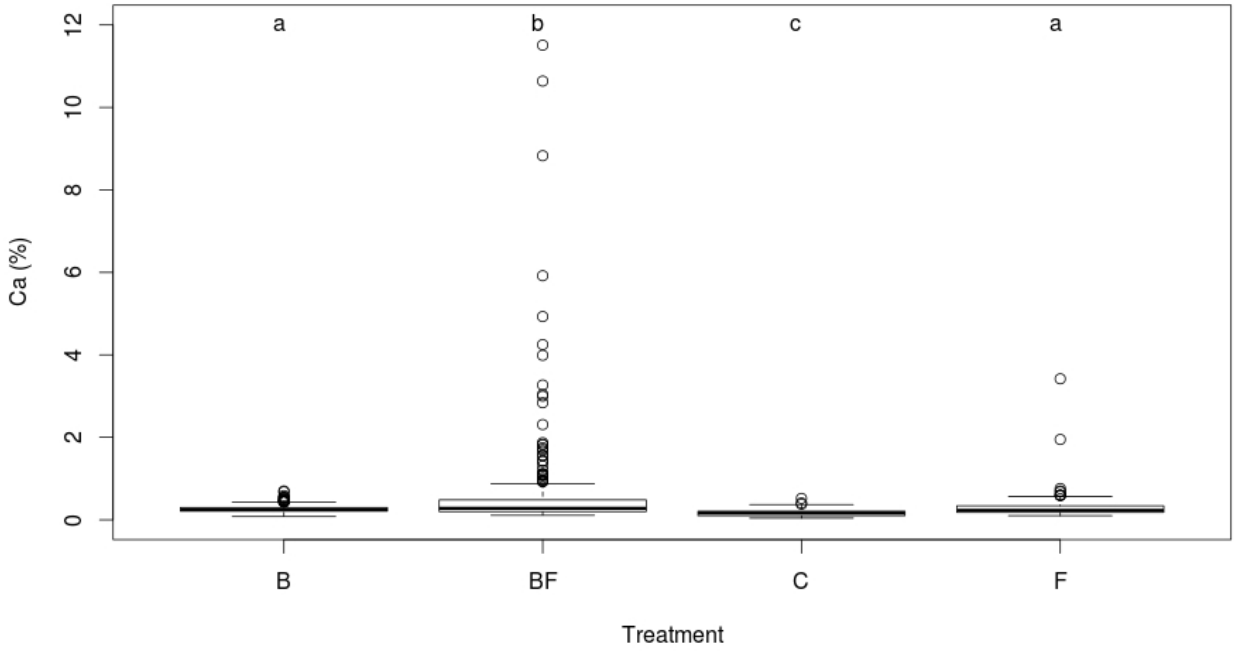

Figure 5.19. Variations of Ca concentration at the surface of the wood blocks (*n*=3) colonised by different inocula (B, BF or F) during five months. For each sample, 105 measurements were made. Different letters above boxplots indicate significant difference based on one-way ANOVA followed by Tukey's HSD test ($p<0.05$).

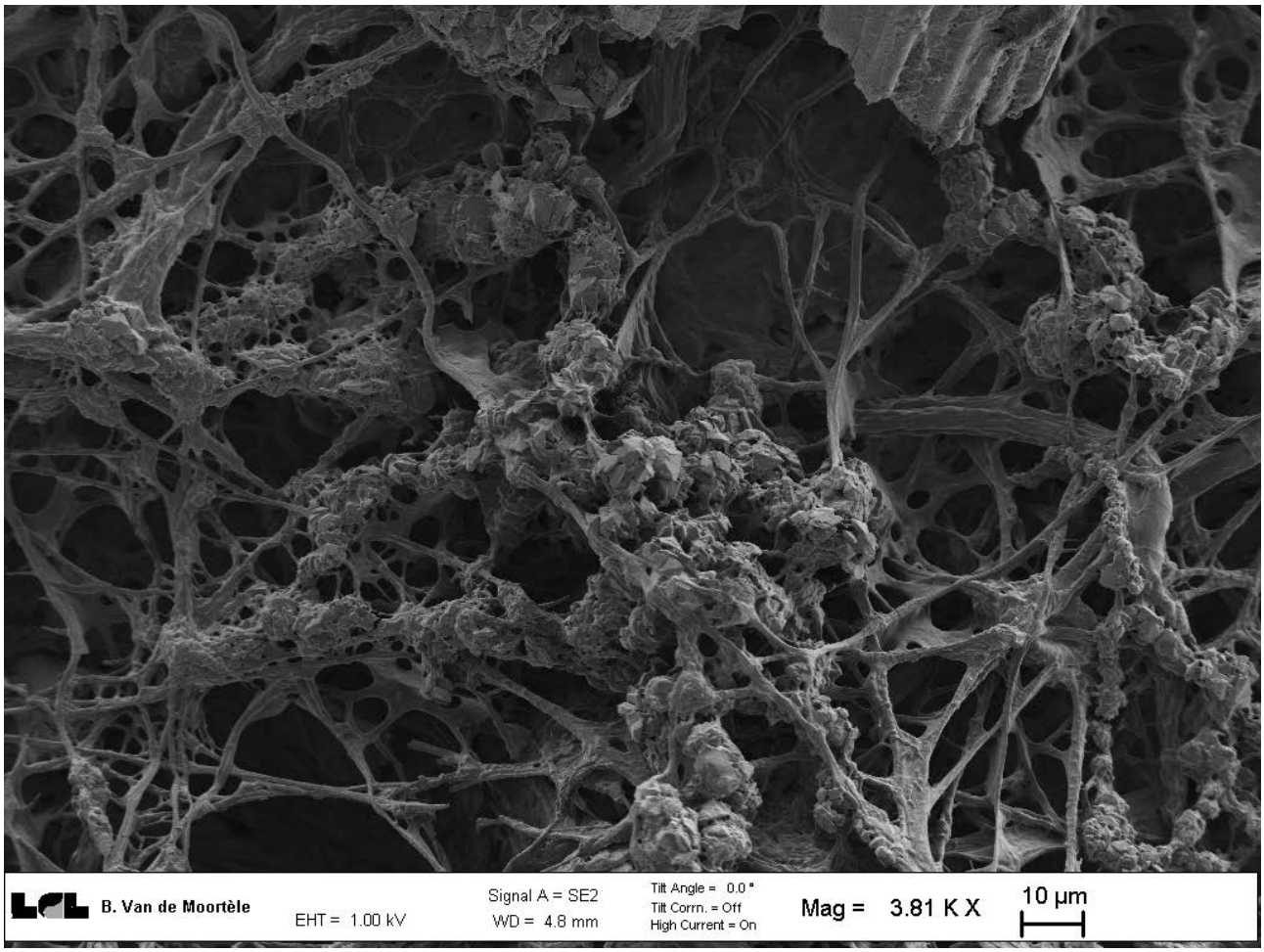

Figure 5.20. FEG-SEM image of a carbon-coated sample inoculated with *P. chrysosporium* and a bacterial community (BF) during 4 months (Courtesy of Bertrand Van de Moortèle, ENS Lyon).

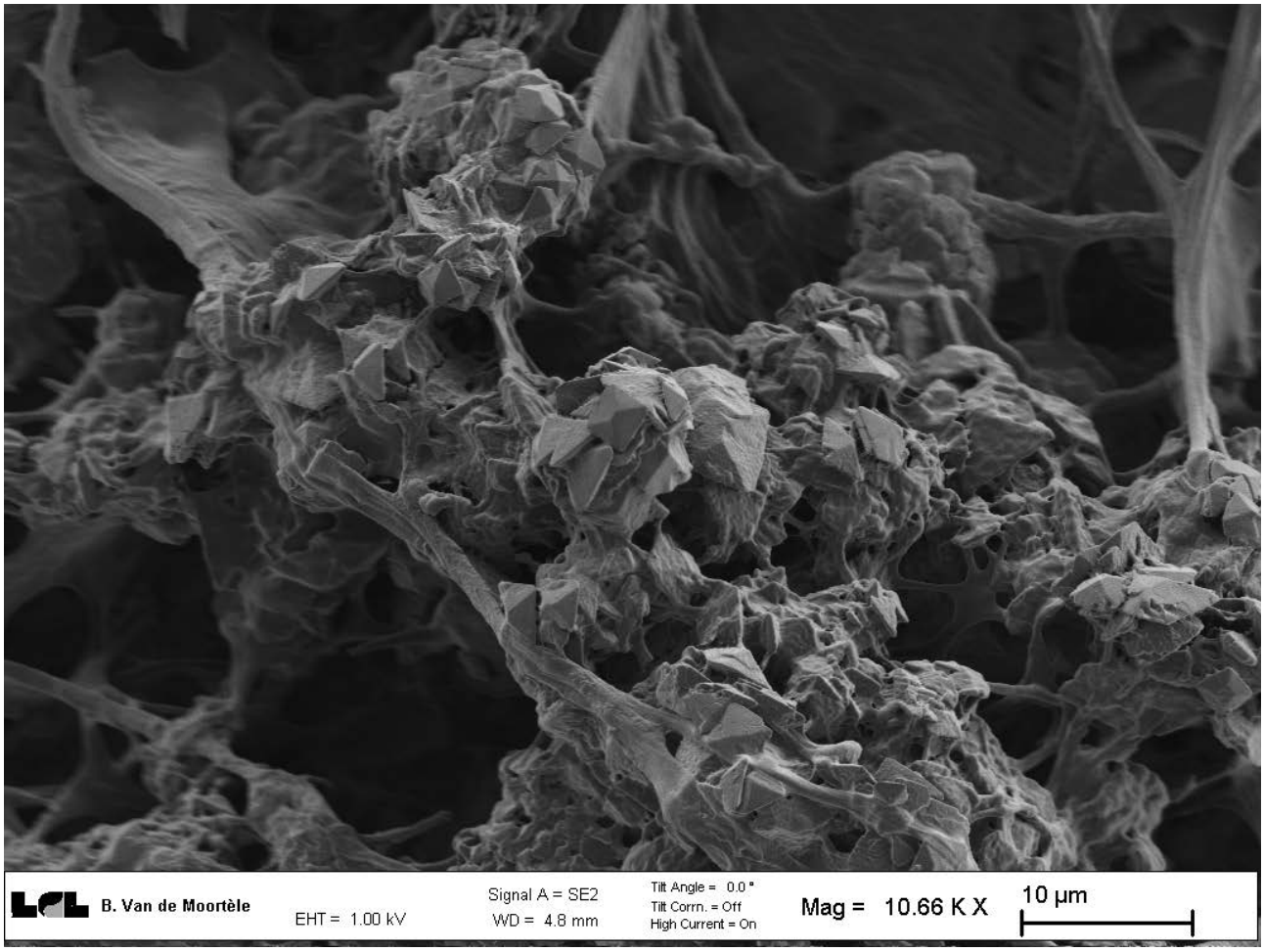

Figure 5.21. FEG-SEM image of a carbon-coated sample inoculated with *P. chrysosporium* and a bacterial community (BF) during 4 months (Courtesy of Bertrand Van de Moortèle, ENS Lyon).

A

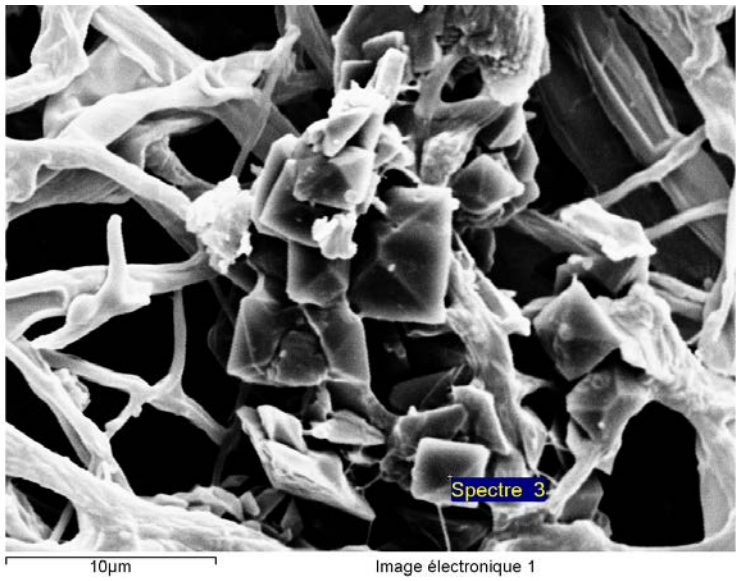

B

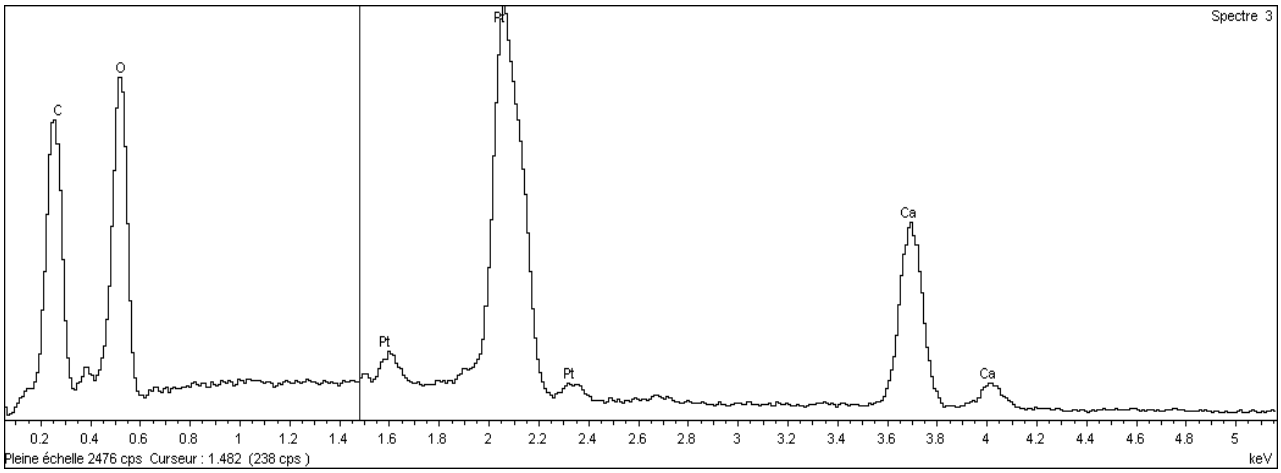

Figure 5.22. A. SEM image of a platinum-coated sample inoculated with *P. chrysosporium* and a bacterial community (BF) during 4 months and presenting crystal structures. **B.** EDS analysis of a crystal showing the presence of carbon, oxygen and calcium. Platinum (Pt) is due to sample coating. Image and spectrum were both acquired by Christophe Rose, INRA Nancy.

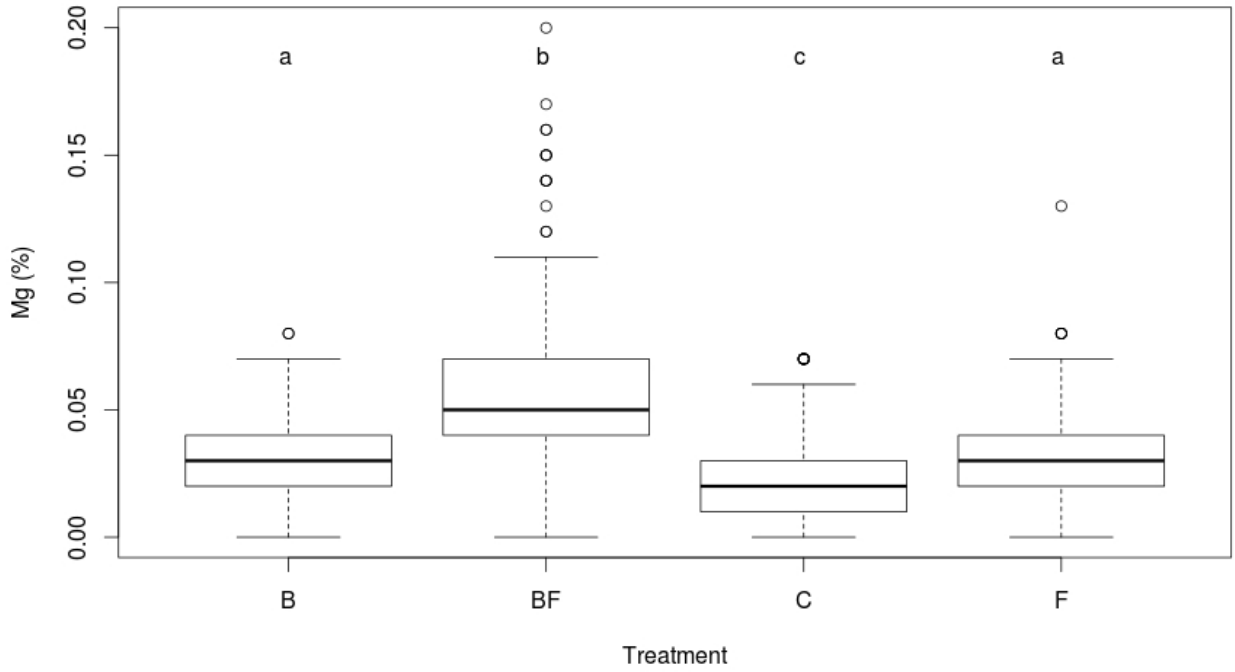

Figure 5.23. Variations of Mg concentration at the surface of the wood blocks (*n*=3) after removing the inoculated microorganisms (B, BF or F) from this surface. For each sample, 105 measurements were made using EDS analysis. Different letters above boxplots indicate significant difference based on one-way ANOVA followed by Tukey's HSD test ($p<0.05$).

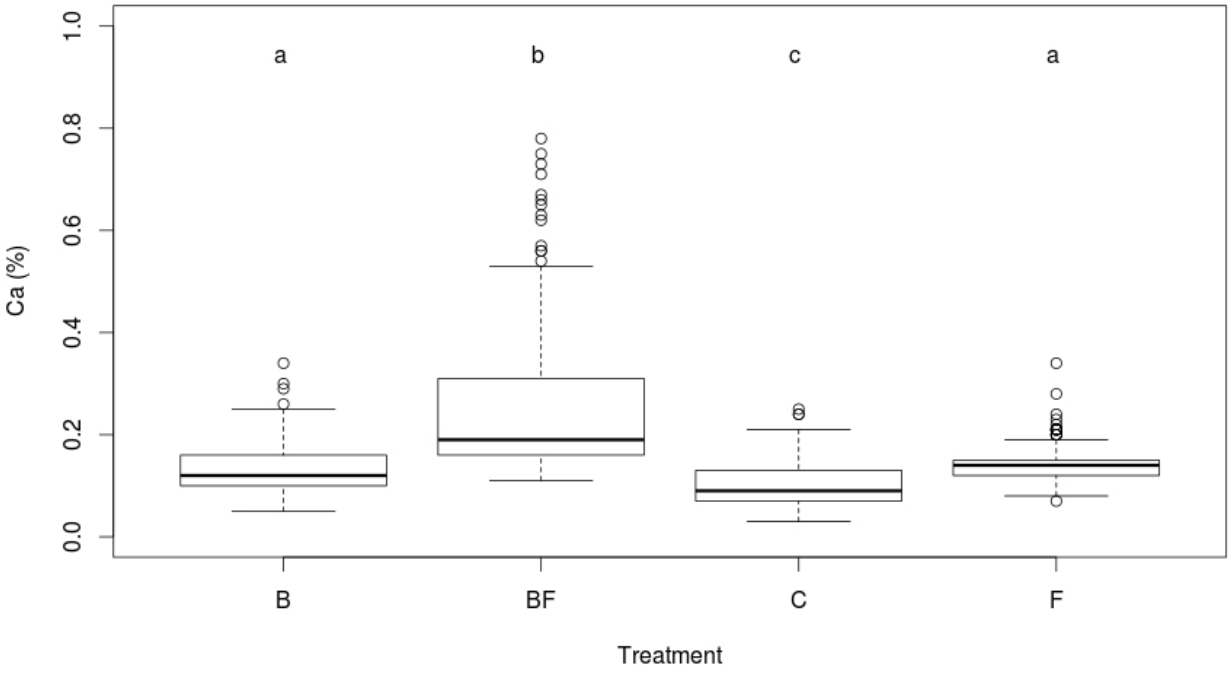

Figure 5.24. Variations of Ca concentration at the surface of the wood blocks (*n*=3) after removing the inoculated microorganisms (B, BF or F) from this surface. For each sample, 105 measurements were made using EDS analysis. Different letters above boxplots indicate significant difference based on one-way ANOVA followed by Tukey's HSD test ($p<0.05$).

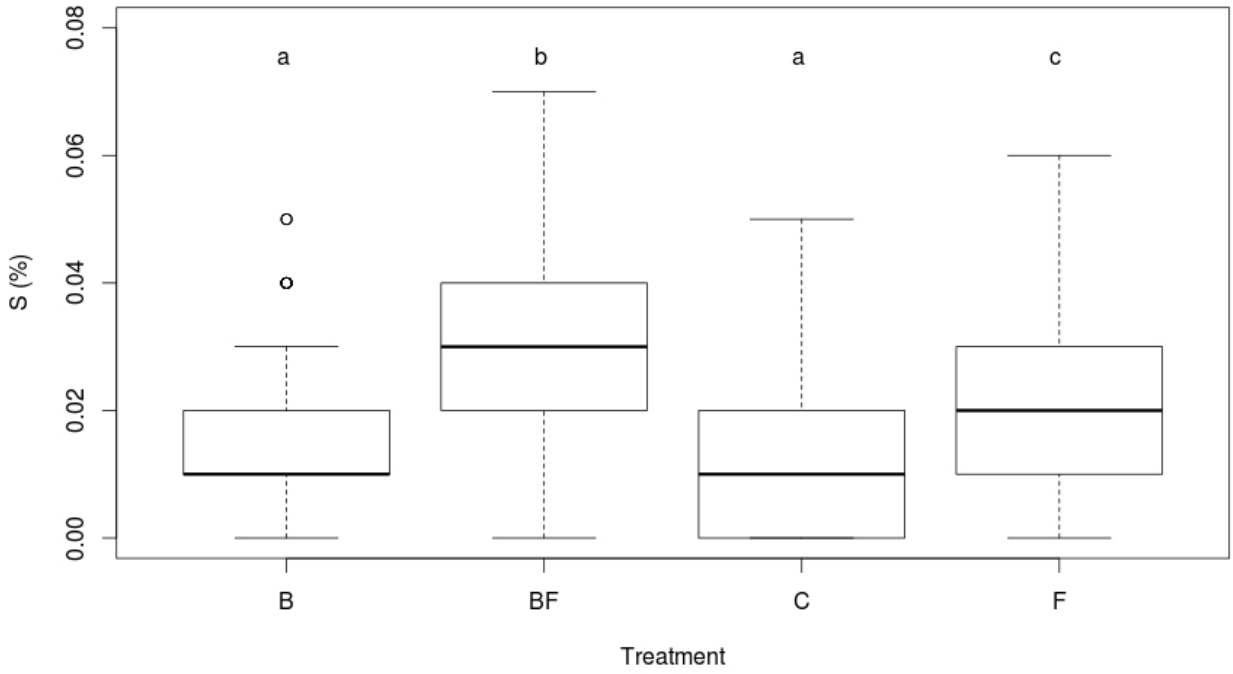

Figure 5.25. Variations of S concentration at the surface of the wood blocks (n=3) after removing the inoculated microorganisms (B, BF or F) from this surface. For each sample, 105 measurements were made using EDS analysis. Different letters above boxplots indicate significant difference based on one-way ANOVA followed by Tukey's HSD test (p<0.05).

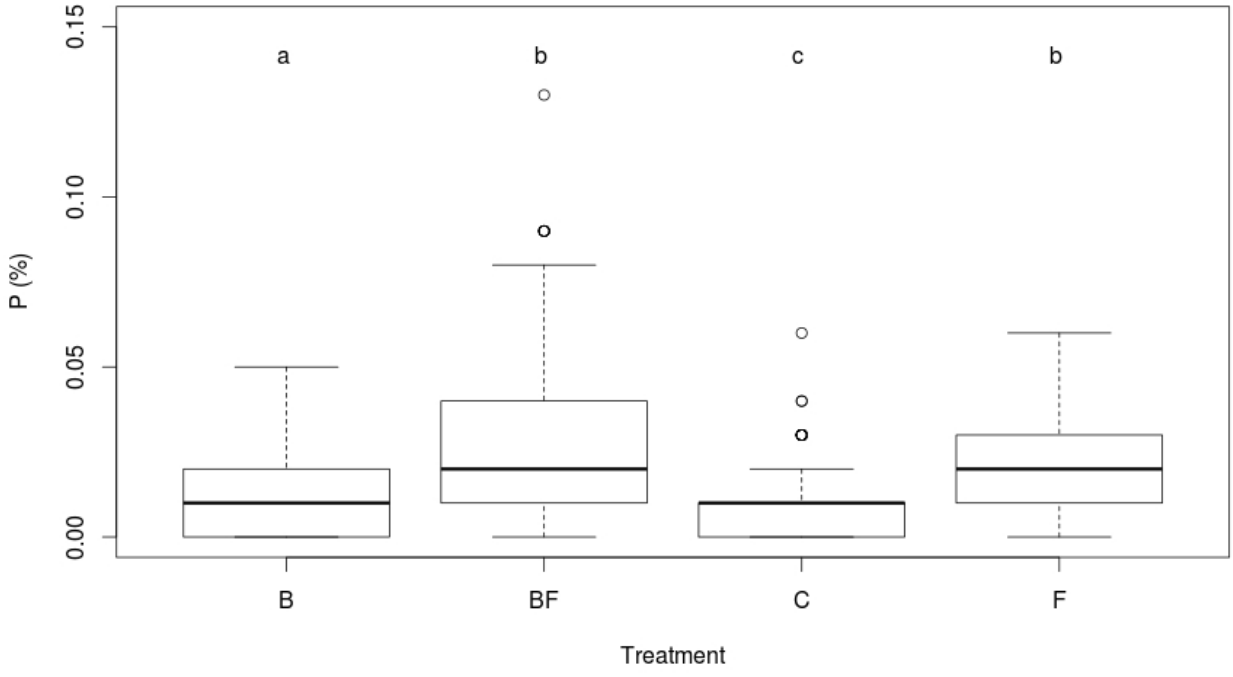

Figure 5.26. Variations of P concentration at the surface of the wood blocks (n=3) after removing the inoculated microorganisms (B, BF or F) from this surface. For each sample, 105 measurements were made using EDS analysis. Different letters above boxplots indicate significant difference based on one-way ANOVA followed by Tukey's HSD test (p<0.05).

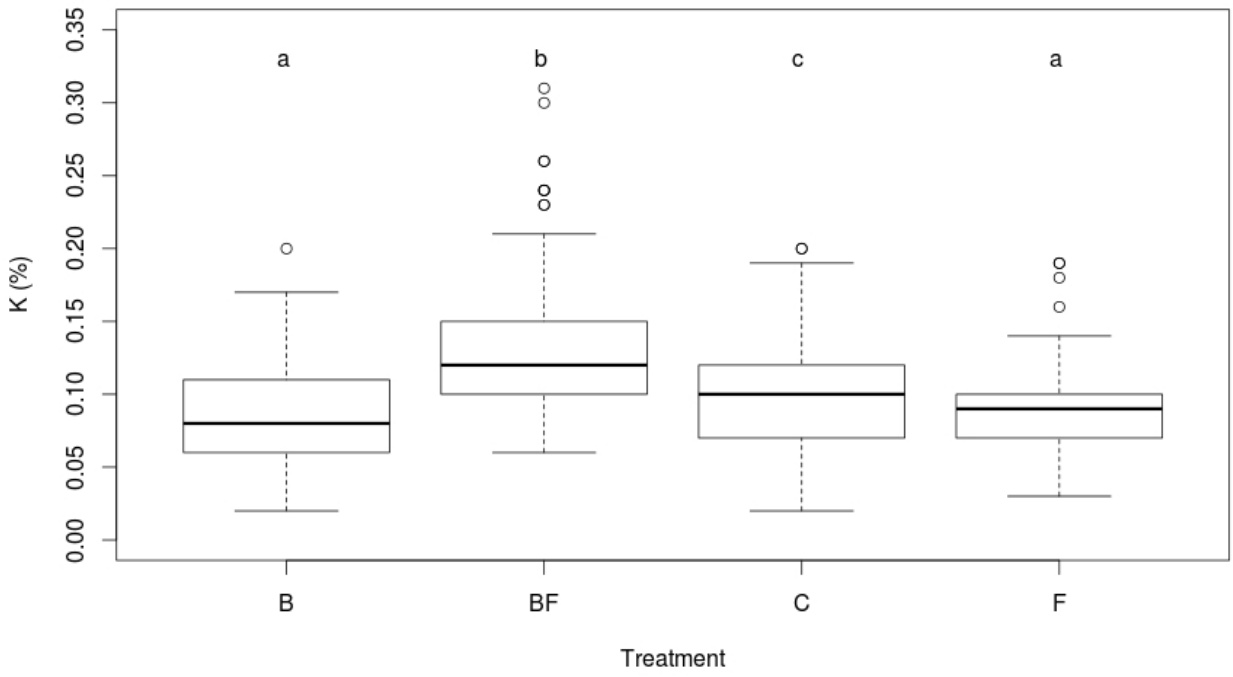

Figure 5.27. Variations of K concentration at the surface of the wood blocks (n=3) after removing the inoculated microorganisms (B, BF or F) from this surface. For each sample, 105 measurements were made using EDS analysis. Different letters above boxplots indicate significant difference based on one-way ANOVA followed by Tukey's HSD test (p<0.05).

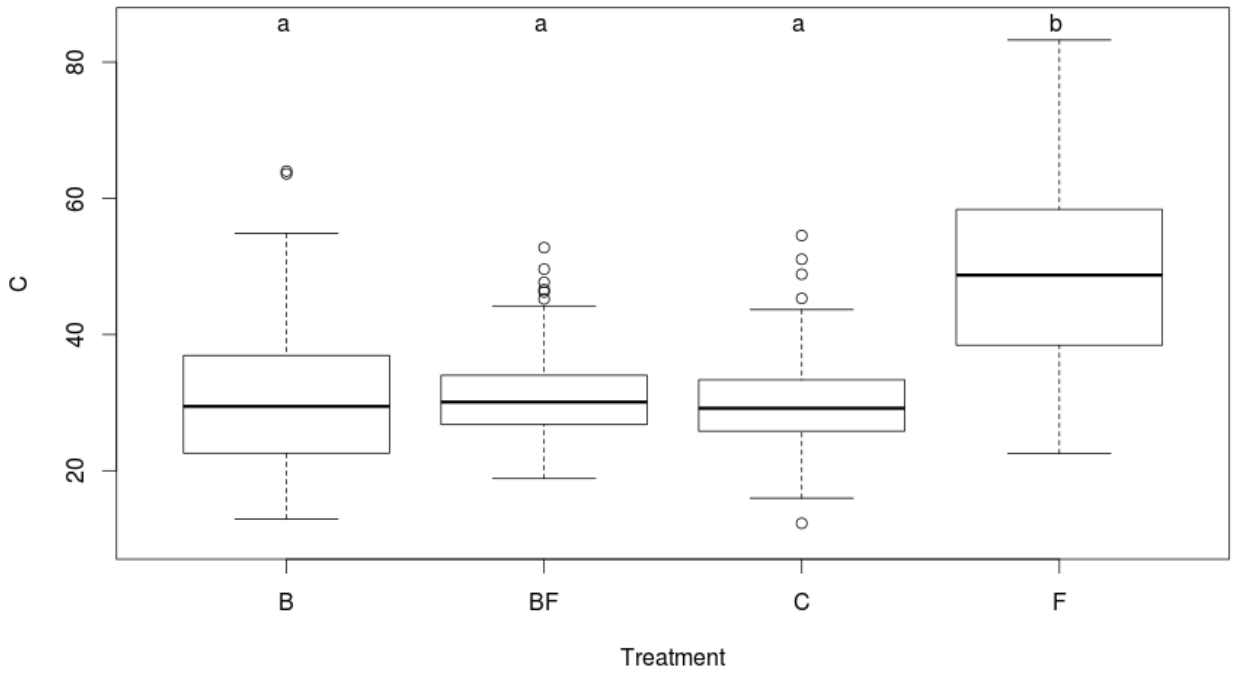

Figure 5.28. Variations of C concentration at the surface of the wood blocks (n=3) after removing the inoculated microorganisms (B, BF or F) from this surface. For each sample, 105 measurements were made using WDS analysis. Different letters above boxplots indicate significant difference based on one-way ANOVA followed by Tukey's HSD test (p<0.05).

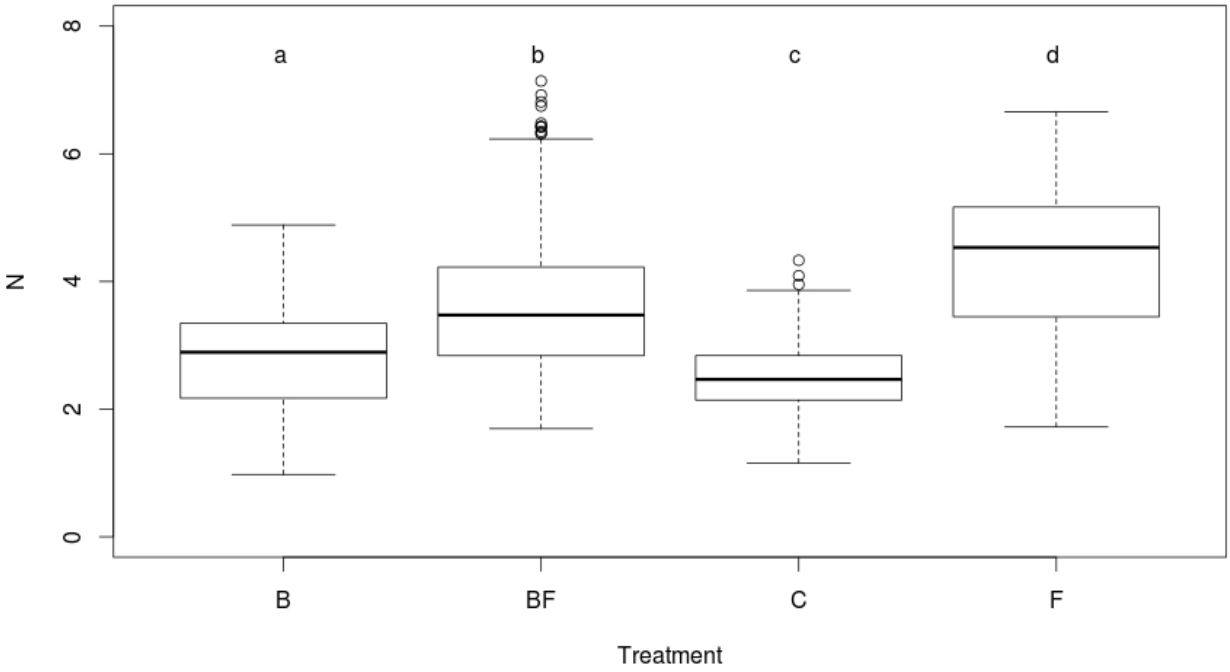

Figure 5.29. Variations of N concentration at the surface of the wood blocks (n=3) after removing the inoculated microorganisms (B, BF or F) from this surface. For each sample, 105 measurements were made using WDS analysis. Different letters above boxplots indicate significant difference based on one-way ANOVA followed by Tukey's HSD test (p<0.05).

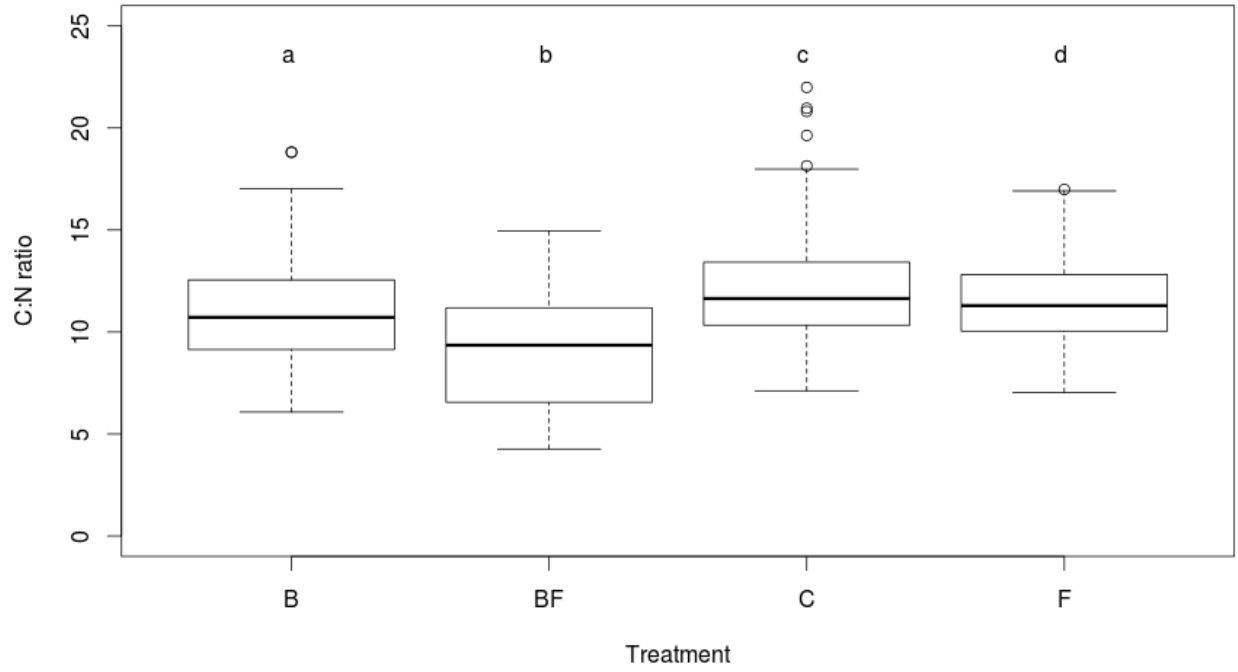

Figure 5.30. C:N ratio at the surface of the wood blocks (n=3) after removing the inoculated microorganisms (B, BF or F) from this surface. For each sample, 105 measurements were made using WDS analysis. Different letters above boxplots indicate significant difference based on one-way ANOVA followed by Tukey's HSD test (p<0.05).

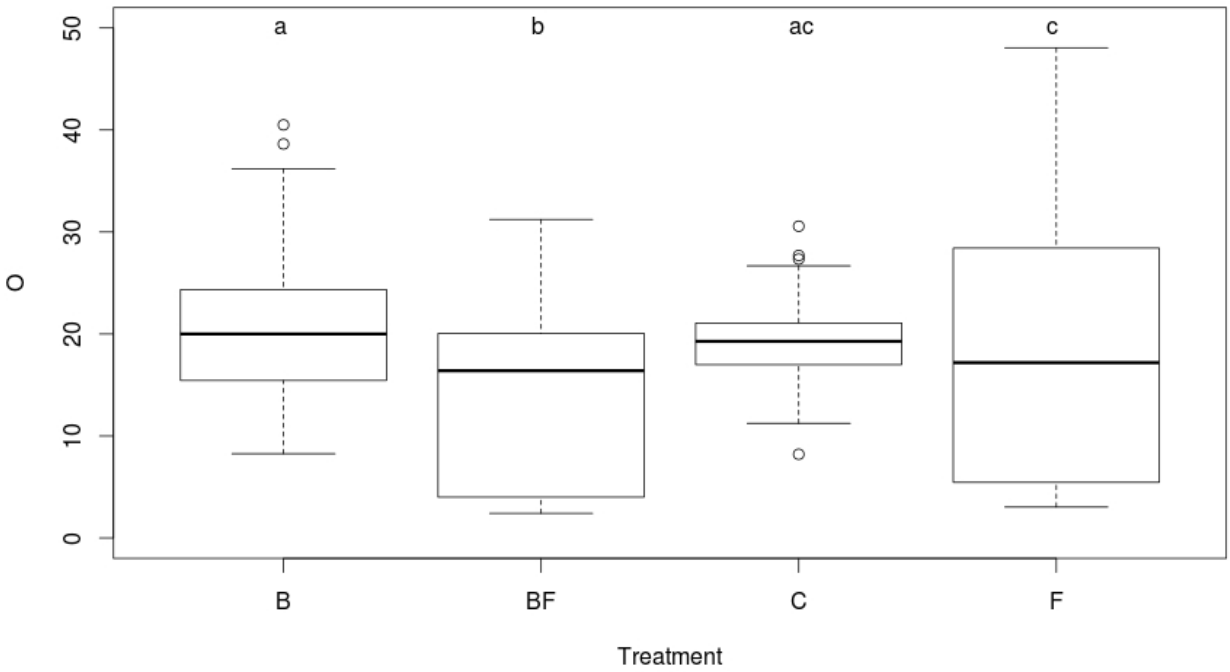

Figure 5.31. Variations of O concentration at the surface of the wood blocks (n=3) after removing the inoculated microorganisms (B, BF or F) from this surface. For each sample, 105 measurements were made using WDS analysis. Different letters above boxplots indicate significant difference based on one-way ANOVA followed by Tukey's HSD test (p<0.05).

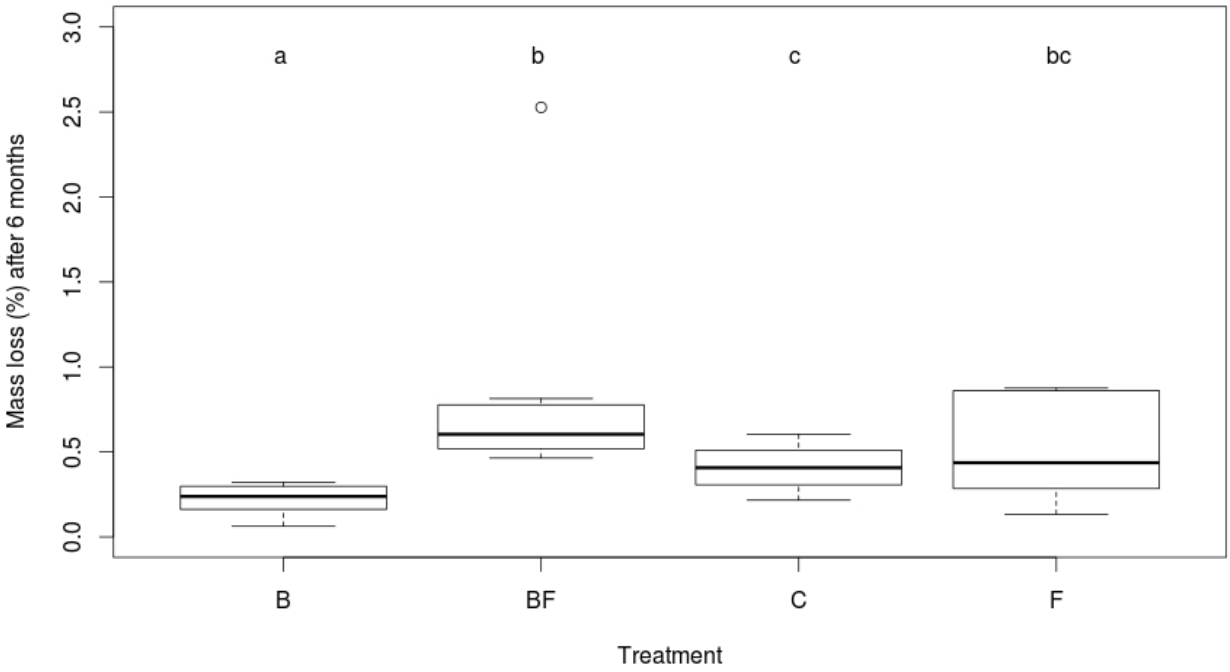

Figure 5.32. Mass loss of the wood blocks (n=8) after 6 months of incubation with the different inocula. Different letters above boxplots indicate significant difference based on non-parametric Kruskal-Wallis test (p<0.05).

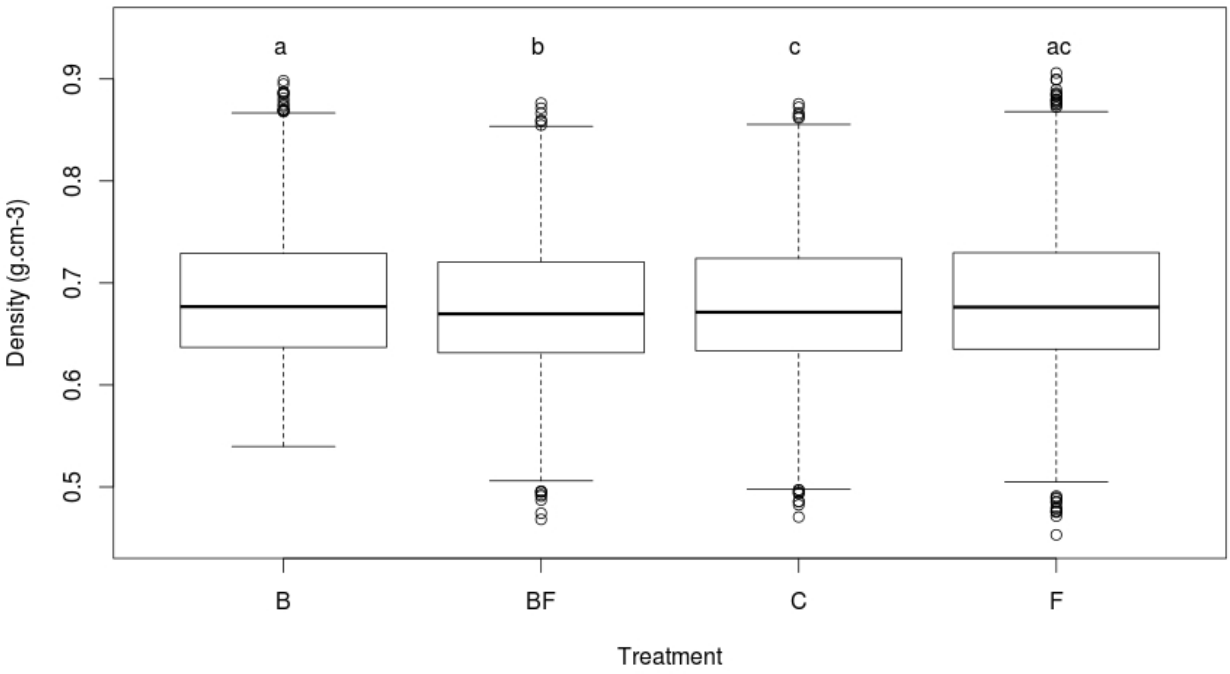

Figure 5.33. Density of the wood blocks (*n*=8) after 6 months of incubation with the different inocula. For each sample, 800 values were computed using density mapping. Different letters above boxplots indicate significant difference based on one-way ANOVA followed by Tukey's HSD test ($p<0.05$).

- Chapter 6 -

Discussion

Résumé

Dans ce dernier chapitre, une discussion générale des travaux de cette thèse est présentée et les perspectives de recherches futures sont abordées, en tenant compte des résultats nouveaux apportés par cette thèse concernant l'écologie microbienne du bois en décomposition.

D'un point de vue méthodologique, l'utilisation nouvelle quant au suivi du processus de dégradation du bois, du scanner tomographique à rayons X et de la microscopie électronique à balayage couplée à des microanalyses en spectrométrie à rayons X, a permis de générer des données quantitatives sur les propriétés physico-chimiques du bois ainsi que sur la composition élémentaire des microorganismes saproxyliques étudiés. Grâce à ces deux méthodes, il a été possible de distinguer le processus de décomposition du hêtre par *Phanerochaete chrysosporium* associé avec une communauté bactérienne de celui réalisé par *P. chrysosporium* seul. La comparaison des différents résultats obtenus dans le cadre de cette thèse avec les résultats de la littérature existante a également permis de souligner la pertinence de l'utilisation de microcosmes pour des études sur la décomposition microbienne du bois. L'analyse, par deux approches différentes, cultivable et non cultivable, de la diversité taxonomique des communautés bactériennes du bois en décomposition a révélé l'intérêt et la complémentarité de ces deux approches pour l'étude de cet habitat particulier. Enfin, l'approche pluridisciplinaire mise en œuvre dans l'ensemble de ce travail souligne l'importance de combiner l'utilisation d'analyses physico-chimiques et moléculaires ainsi que d'étudier à la fois les microorganismes impliqués dans le processus de dégradation du bois et le matériau bois lui même, afin de pouvoir appréhender la complexité de ce processus dans son intégralité.

Concernant l'écologie des communautés bactériennes associées au bois en décomposition, ces travaux de thèse ont permis de décrire la diversité taxonomique et fonctionnelle de ces communautés en présence ou en absence de *P. chrysosporium* et ainsi de démontrer l'effet mycosphère d'un champignon de pourriture blanche dans le bois en décomposition. L'étude des communautés saproxyliques, majoritairement centrée sur les champignons et les arthropodes au cours des dernières décennies, a généré une littérature abondante. De nombreux paramètres structurant ces communautés ont été décrits, tels que la spécificité de certaines espèces saproxyliques pour certaines espèces d'arbres, l'impact des variables climatiques, le phénomène de succession des communautés au cours du temps et

plus généralement l'influence du substrat bois sur ces communautés. Cependant, très peu de travaux ont appréhendé l'impact de ces facteurs sur la diversité taxonomique et fonctionnelle des communautés bactériennes associées au bois en décomposition. Des perspectives de recherche visant à mieux comprendre l'écologie fonctionnelle de ces communautés bactériennes sont donc proposées.

Enfin, une discussion sur les mécanismes de la dégradation du bois par les microorganismes est abordée. Nos résultats ont révélé l'importance de trois genres bactériens dans la décomposition de la lignocellulose : *Luteibacter, Dyella* et *Burkholderia*. Les connaissances actuelles, peu nombreuses, sur les genres *Luteibacter* et *Dyella* sont discutées. Concernant le genre *Burkholderia*, une brève analyse de la diversité taxonomique et fonctionnelle de différentes populations de *Burkholderia* issues d'un écosystème forestier est présentée. Cette analyse est basée sur la comparaison de séquences d'un fragment de l'ARN ribosomal 16S et de données métaboliques Biolog, en utilisant des données du Chapitre 4 et celles d'une précédente étude (Uroz *et al.* 2007). Nos résultats indiquent que pour des populations de *Burkholderia* issues d'un écosystème forestier, les diversités génétique et métabolique des souches bactériennes analysées sont significativement influencées par le substrat d'origine (sol ou bois) ainsi que par la présence d'un champignon (effet mycosphère). De plus, diversités génétique et métabolique apparaissent fortement corrélées. Ces premiers résultats suggèrent une spécificité de niche dans les écosystèmes forestiers pour les différentes populations de *Burkholderia*. Suite aux résultats obtenus dans le Chapitre 5, la question du rôle de l'acide oxalique et du calcium lors de la décomposition du bois par des communautés microbiennes mixtes est également abordée. Finalement, une discussion sur la complémentation fonctionnelle dans les interactions bactéries-champignons lors de la décomposition du bois est proposée.

6 Discussion

The four previous chapters provided new insights into the microbial process of wood degradation, in terms of methodology and microbial ecology. These results raised new hypotheses and perspectives about the ecology of wood degradation, and to some extent potential applications regarding wood protection, wood preservation, biodiversity and conservation.

6.1 Methodological considerations

6.1.1 Detecting the early stages of wood degradation

As discussed in the second chapter, numerous methods exist to study wood decay, with different advantages and drawbacks. An important question for wood protection and wood preservation is how to detect early signs of wood degradation. Which tools are the most appropriate? During this thesis, several methods were employed to monitor wood degradation, including mass loss measurements, light microscope and scanning electron microscope observations, microanalyses, chemical analyses and density measurements. Light microscopy has been used to study wood decay for more than a century (for references, see Schwarze, 2007), to assess both the cell structure and the wood chemical composition. For example on wood sections, safranine can be used to stained lignin regardless of whether cellulose is present whereas astra blue can be used to strain cellulose only in absence of lignin (Srebotnik & Messner 1994). Thus, used together these two stains are appropriated to study wood delignification. We used these two stains in the present study to characterise wood blocks of *Fagus sylvatica* L. degraded by *Phanerochaete chrysosporium* (Figure 6.1, left). Chemical properties of wood components can also be used to monitor wood decomposition. For instance lignin autofluorescence can be observed under UV light, as shown on Figure 6.1, center. Concerning the cellulose, polarised light can be used to observed its degradation, which results in a loss of its birefringence (Figure 6.1, right). These three types of observations were initially used during this thesis to characterise beech wood degradation. However, due to the time required for wood section preparation, we abandoned the idea of using optical microscopy for any quantitative or semi-quantitative study, based on for example morphometric analyses of degraded wood.

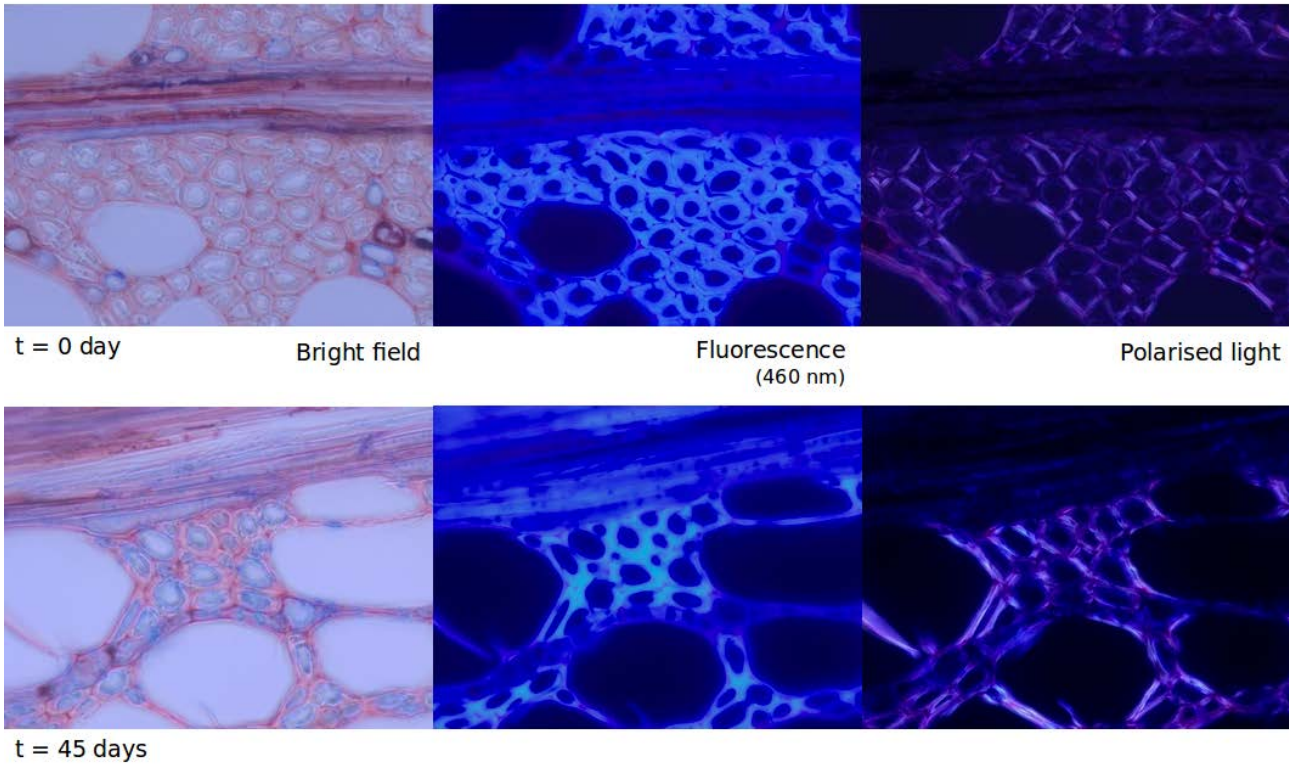

Figure 6.1. *Transverse sections of Fagus sylvatica before (upper panel) and after (lower panel) being colonised by Phanerochaete chrysosporium during 45 days. On the left, safranine / astra-blue staining revealed the delignification of the secondary wall, indicated by the presence of free cellulose (in blue) after 45 days of incubation. On the center, using DAPI filter (460 nm), lignin can be observed in bright blue. On the right, cellulose is observed under polarised light and appears bright.*

Based on both mass and density losses, beech wood degradation was detected after two weeks of incubation with *P. chrysosporium*, in our conditions (Chapter 2). As already mentioned, mass loss is not very informative with regard to the biodegradation process. This is the reason why we used X-ray computed tomography (CT) to monitor the early stages of this process. We were able to generate quantitative data, very useful to describe the wood decay process, especially in terms of spatial heterogeneity. Chemical analyses of wood blocks performed with inductively coupled plasma atomic emission spectroscopy did not reveal significant variation regarding the elemental composition between degraded and non-degraded samples, except for the phosphorus concentration (Chapter 5). However, surface analyses of these wood blocks using scanning electron microscopy (SEM) combined with

energy dispersive spectrometer (EDS) and wavelength dispersive spectrometer (WDS) revealed significant variations not only in terms of elemental composition between degraded and non-degraded samples, but also according to the microbial treatment used to colonise the wood blocks. Thus, a combination of such microanalyses appears to be a very promising way to study the early stages on wood decomposition. Additionally, these methods are non-destructive. EDS analyses should be preferentially considered, since they are cheaper and quicker than WDS analyses. Interestingly EDS microanalyses were used very recently to reveal differences in elemental composition between undamaged parchments and damaged parchments colonised by microorganisms (Piñar, Sterflinger & Pinzari 2014).

In the past 40 years, many methods have been developed to describe the patterns of wood degradation and thus to learn more about the biology of the microorganisms involved in this process. Among these methods, spectroscopy and microspectroscopy have been widely used (Fackler & Schwanninger 2012). In the light of the results we obtained by X-ray CT and microanalyses, future research and analyses should focus on the relationship between wood density and wood elemental composition during wood decay in order to better understand the dynamic of the nutrients used by the saproxylic microorganisms. Indeed, both density and elemental composition of the wood blocks were affected by the microbial treatment. Since for each wood block and with each method, a high number of measurements can be acquired according to a grid pattern at the surface of the wood block or at least on the upper slice in the case of wood density analysis, such relationship could be easily computed. Differences in the degradation of the earlywood and the latewood of *Fagus sylvatica* by *P. chrysosporium* were observed using X-ray CT (Chapter 2). It would be interesting now to evaluate if variations in nutrient concentrations (N, Ca, Mg, P, K) differ in earlywood compared to latewood during the wood degradation and if these variations are correlated with density variations. Such data would provide fine-scale information about the colonisation strategy of the microorganisms involved in the wood degradation.

6.1.2 Microcosm experiments, a pertinent scale to study wood degradation

All the experiments described in this thesis were performed at a microcosm scale. This experimental scale present various advantages such as replicability, statistical power and the possibility to work under controled conditions. However, the use of microcosm experiments for community ecology has been criticised, in particular for their limited relevance compared

to field studies (Carpenter 1996). In the case of wood degradation, our results presented in chapters 3 and 4 revealed that in term of bacterial taxonomic composition, microcosm experiments were comparable with field experiments (see Table 4.1). Comparing our data with few other studies, we showed that *Proteobacteria* was always the major phylum of the wood-associated bacterial communities and that members of *Xanthomonadaceae* family were always present in decaying wood. Compared to a inoculum extracted from a forest soil, we found that both the richness and the diversity of wood-associated bacterial communities were lower (Chapter 3). Same conclusions were reported in a recent study comparing forest soils bacterial communities and bacterial communities colonising wood cubes in these forest soils (Sun *et al.* 2014). Altogether, these results validate the utilisation of microcosm to study the microbial ecology of the communities associated with decaying wood.

In order to characterise the taxonomic and functional diversity of the wood-associated bacterial communities, we used sawdust as a growth matrix while in other studies about wood-associated bacterial communities, wood blocks (Folman *et al.* 2008) or logs, stumps or trunks (Zhang *et al.* 2008a; Valásková *et al.* 2009) were directly sampled. We obtained similar results to those of these studies in term of bacterial taxonomy. This indicates that sawdust can be a pertinent substrate for controlled experiments on wood decomposition. Indeed, the use of sawdust allows to work with a more homogeneous substrate compared to logs or wood blocks which possess their own heterogeneity due to the presence of earlywood / latewood and sapwood / heartwood. Thus, working with a mix of sawdust originating from a single tree is a solution to integrate the wood heterogeneity in a single substrate. Additionally, sawdust appeared to decompose faster than wood blocks (Chapter 5), which is a real advantage for short-term experiments on wood degradation.

6.1.3 The complementarity of culturable and non-culturable approaches

In Chapter 4, we showed that we were able to isolate from decaying wood the two most abundant OTUs detected by pyrosequencing. These two OTUs represented more than fifty percent of the bacterial relative abundance in our microcosms. These results suggest that an important fraction of the bacterial diversity associated with decaying wood is culturable. They also confirm previous remarks from de Boer, Folman, Summerbell, & Boddy, 2005, and show that decaying wood is a particular habitat. Indeed, in most of the environments such as soil, seawater or human gut, only a very small fraction of the bacterial diversity is known to

be culturable (Rappé, Giovannoni & Rappe 2003; Stewart 2012). However, complementarity between culturable and non-culturable approaches for the study of bacterial communities has been found in other habitats such as cheese (Delbès, Ali-Mandjee & Montel 2007). Such results have many consequences. First it suggests that the use of high-throughput sequencing approaches is not mandatory to identify the dominant taxa of the wood-associated bacterial communities in microcosm. More interestingly, working with culturable organisms allows to study the functions of any bacterial strain of interest. Since a bacterial collection of 311 identified strains was generated during this thesis (Chapter 4), many perspectives of research are worth considering to learn more about the functioning of the bacterial communities associated with decaying wood. For instance, one could look for the presence of genes involved in the mechanisms of nitrogen fixation (Hoppe *et al.* 2014) or oxalotrophy (Khammar *et al.* 2009) in the bacterial strains of the collection to better understand the contribution of the bacterial communities to the process of wood decomposition and the related mechanisms.

6.1.4 Toward an integrative view of wood decomposition

Regarding the methodology employed to study wood decomposition, our result highlight the benefits to combine different approaches in order to study both the wood physicochemical properties and the microbial communities involved in this decomposition process. A multidisciplinary approach appears to be required to comprehend the complexity of this process with a global view, or using a “macroscope” as a reference to Joël de Rosnay concept (de Rosnay 1975). In our work, we first described extensively and exhaustively the bacterial communities from the white-rot mycosphere using 16S rRNA amplicon-based pyrosequencing. This taxonomic study was completed by a culturable approach to study both the taxonomic and functional diversity of the wood-associated bacterial communities. Once the mycosphere effect was demonstrated at both taxonomic and functional levels, we investigated the impact of the association between *P. chrysosporium* and a bacterial community isolated from its mycosphere, on the wood decomposition process, using different chemical analyses. Thanks to the measurements of different parameters at different scales such as wood density, carbon and nutrient concentrations, we were able to reveal a synergistic bacterial-fungal interaction in the process of wood degradation. It is also important to underline that we used microscale analyses (wood surface microanalysis, microcosms) to

reveal a synergistic interaction between microorganisms. While microorganisms are involved in biogeochemical cycles at global scale (Sinsabaugh *et al.* 2009), microscopic scale is relevant to study microbial cooperation.

Multiparametric analyses and polyphasic approaches have already been described as being appropriate to study microbial metabolisms since they provide different and complementary measurements of a same process (Hervé *et al.* 2012). In the case of wood degradation, it is noteworthy that some recent studies have taken advantage of the combination of molecular analyses of bacterial diversity and spectroscopic analyses of wood (Preston *et al.* 2014), or molecular analysis of microbial diversity, measurements of microbial respiration and mechanical properties of decaying wood (Prewitt *et al.* 2014), to study both microbial taxonomy and niche functioning. To elucidate this functioning, future projects on wood decomposition should take advantage of the many accessible methods available now to investigate simultaneously the diversity of saproxylic organisms, wood functional traits such as density and C/N ratio, and environmental variables such as moisture and temperature. Such data sets will undoubtedly provide a framework to unravel the complexity of the process of wood decomposition.

6.2 Ecology of the wood-associated bacteria

6.2.1 Diversity of the bacterial communities

Over the last decades, most of the studies about the community ecology of coarse woody debris have focused on fungal and arthropod species (Stockland *et al.* 2012). As a result, various factors shaping the assemblage of these communities have been described. Community succession in decaying wood was described for fungi (Rajala *et al.* 2011) and insects (Vanderwel *et al.* 2006). Does this patten also exist for bacterial communities? Does the decay stage influence the taxonomic, phylogenetic or functional diversity of wood-associated bacterial communities? While we did not directly address these questions on community succession, the results of our enrichment experiment in microcosm (Chapters 3 and 4) suggest temporal changes in the overall structure of the wood-associated bacterial communities. At each new step of the enrichment procedure, sterile sawdust was used as growth matrix. Thus, wood composition should not have change much along the experiment. However, variations in community composition were observed within and between treatments. These variations originated from a high number of low abundant OTUs, whereas

core microbiomes were described and included notably the most abundant OTUs. Our results thus highlight the presence of a stable wood-associated core microbiome composed of few dominant bacterial OTUs, after eighteen weeks of incubation. A recent study showed that in boreal forests, the taxonomic composition of the primary wood-inhabiting bacterial communities remained stable over the first four months of wood colonisation (Sun *et al.* 2014). However, four months of incubation or eighteen weeks in our case, is a too short period to be able to monitor significant modifications in wood chemical composition using classical approaches. Thus, long-term studies such as the LOGLIFE experiment (Cornelissen *et al.* 2012) or studies comparing the bacterial communities according to the wood decay stage are required to fully answer these questions.

In terms of bacterial taxonomy, the comparison between the 16S rRNA gene sequences from different studies we presented in Chapter 4 (Table 4.1) revealed similarities among the wood-associated bacterial communities, regardless of the biogeography, the stage of wood decay, the environmental variables or the tree species. Indeed, *Proteobacteria* was found to be the major phylum in all the studies. This result was confirmed by two recent studies on wood-associated bacterial communities (Prewitt *et al.* 2014; Sun *et al.* 2014). Our analysis has also revealed that among the *Proteobacteria* phylum, members of the *Xanthomonadaceae* family were found in the five data sets we compared (Table 4.1). Thus, this family appears strongly associated with decaying wood and could be a potential bioindicator of this environment. Is there a core microbiome across the globe in decaying wood? Are the members of the *Xanthomonadaceae* family part of this core microbiome? A global-scale biogeographical study or a meta-analysis of the different published studies about wood decomposition in forest ecosystems would be required to answer this question. In addition, such study would provide useful information about the potential effects of environmental variables, such as temperature and moisture, on the bacterial community composition, since these variables are known to influence the wood decay rate (Boddy 1983).

6.2.2 Bacterial genera specifically associated with wood

From both the non-culturable (Chapter 3) and culturable (Chapter 4) approaches, three bacterial genera were identified as dominant in our wood microcosms: *Burkholderia, Dyella* and *Luteibacter*. As discussed in Chapter 3, *Dyella* sp. and *Luteibacter* sp. have been previously described in lignocellulosic environments. However, only few information are

available about the *Luteibacter* genus. Currently only four species have been fully described: *Luteibacter rhizovicinus*, isolated from the rhizosphere of spring barley (Johansen *et al.* 2005), *Luteibacter anthropi*, *Luteibacter yeojuensis* (Kämpfer, Lodders & Falsen 2009) and *Luteibacter jiangsuensis* (Wang *et al.* 2011). Several strains of *Luteibacter rhizovicinus* were isolated from our wood microcosms and functionally characterised for their ability to degrade wood components (Chapter 4). None of these strains was able to degrade the carboxymethyl-cellulose or the xylan, in our experimental conditions. However, in a very recently published article, bacteria from the *Luteibacter rhizovicinus* species were the most frequently isolated from spruce and birch sawdust kept under storage during 3 months at 20°C (Blomqvist *et al.* 2014). Thus, it would be relevant to investigate which are the metabolic properties and the mechanisms that allow *Luteibacter rhizovicinus* to grow and to become a major bacterial species in lignocellulosic environments. The Biolog profiles we obtained for the strains of our collection suggest that all of our *L. rhizovicinus* strains should be able to use simple carbohydrates produced during cellulose and hemicellulose degradation such as cellobiose, glucose, galactose and mannose. *L. rhizovicinus* strains from our microcosms could thus be able to survive in wood using the products of lignocellulose degradation generated by other microorganisms.

Bacteria belonging to the *Dyella* genus were also important in our microcosms. Like the *Luteibacter* genus, *Dyella* belongs to the class of Gammaproteobacteria. Currently nine species have described in the literature. In our microcosms, we isolated strains belonging to three of them: *Dyella japonica* (Xie & Yokota 2005), *Dyella koreensis* (An *et al.* 2005) and *Dyella kyungheensis* (Son *et al.* 2013). These three species were originally isolated from soil, but members of the *Dyella* genus have also been found in lignocellulosic environments (Folman *et al.* 2008; Reid *et al.* 2011). To date, two genomes of *Dyella* sp. have been sequenced and assembled (Chen & Chan 2012; Kong *et al.* 2013). To explore the functional potential for wood degradation of these two strains, I looked at the number of predicted cellulases, hemicellulases and pectinases using the Carbohydrate-Active Enzyme (CAZy) database (Cantarel *et al.* 2009; Levasseur *et al.* 2013). For this analysis I used the same criteria as in Mba Medie, Davies, Drancourt, & Henrissat, 2012. Using the dbCAN pipeline (Yin *et al.* 2012), I observed that the genome of *Dyella japonica* A8 contains four sequences predicted to code for cellulases (Glycoside Hydrolase 8, GH9 and two GH74) and six sequences predicted to code for hemicellulases or pectinases. Concerning the genome of *Dyella ginsengisoli* LA-4, it contains six sequences predicted to code for cellulases (six

GH74) and four sequences predicted to code for hemicellulases or pectinases. In a wide-scale analysis of bacterial genomes in which these two genomes where not included (Mba Medie *et al.* 2012), it has been reported that only 7% of the Gammaproteobacteria possessed more than three genes coding for a cellulase and that 41% of them did not possess any gene coding for a cellulase. This suggests that compared to other members of the Gammaproteobacteria class, the *Dyella* genus would be more adapted to lignocellulosic environments. Thus, future research should focus on this genus which could provide good biological models for studies on bacterial wood degradation, especially to understand the molecular mechanisms involved in this degradation. The bacterial community we built to be used as an inoculum in the B and BF treatments of our last microcosm experiment (Chapter 5) was composed of 22 *Burkholderia* strains and 3 *Dyella* strains. Among the *Dyella*, two were identified as *Dyella koreensis* and one as *Dyella japonica*. Since we demonstrated that the association of this bacterial community with *P. chrysosporium* resulted in an increase of the wood degradation, these three strains appear as relevant candidates for mechanistic studies on this bacterial genus.

The *Burkholderia* genus has been much more studied than the two previous genera and members of this genus have been isolated from both natural and clinical environments (Coenye & Vandamme 2003; Compant *et al.* 2008). To date, 82 species have been described according the to EzTaxon-e database (Kim *et al.* 2012). In soil, this genus has been reported to show tolerance to acid pH (Stopnisek *et al.* 2013), which could also explain the presence of *Burkholderia* strains in decaying wood, another low pH environment. Another characteristic trait of this genus is that it has been found to be associated with fungi in different environments such as the mycosphere of ectomycorrhizal fungi (Uroz *et al.* 2012) and of lichens (Grube *et al.* 2009). In our microcosm experiment (Chapters 3 and 4), OTUs belonging to the genus *Burkholderia* were detected in all the microcosm samples, regardless of the presence of *P. chrysosporium*. They were also present in the initial inoculum extracted from a forest soil. However, we showed that these OTUs were more abundant in the woody microcosms where *P. chrysosporium* was present and that some of these OTUs were specifically associated with this white-rot fungus (BF cores in Chapter 3). Thus the specificity of these OTUs suggests a specific diversity among the members of the *Burkholderia* genus colonising different niches in forest ecosystems.

6.2.3 Is there a niche specificity for *Burkholderia* populations in forest ecosystems ?

The fact that this genus can be found in different environments (forest soils and wood), closely associated or not with a fungus raises the question of the genetic and metabolic diversity inside the *Burkholderia* genus as well as the question of niche specificity for this genus in forest ecosystems. To answer these questions, I compared the genetic diversity, based on partial 16S rRNA gene sequences, and the metabolic diversity, based on the metabolic profiles obtained from Biolog GN2 microplates, of two *Burkholderia* data sets. The first data set corresponded to the data presented in Chapter 4 (n= 90 strains from five distinct niches related to wood) and the second one corresponded to a published study (Uroz *et al.* 2007) comparing bacterial strains from the mycorrhizosphere *Scleroderma citrinum* (two niches) with strains from the surrounding forest soil (one niche) (n= 52 strains). The resulted set of data thus encompassed 8 niches (n= 12 to 22 strains), including two substrates as growth matrix (forest soil, n= 71 strains and beech wood, n= 71 strains), both in presence (n= 73 strains) or in absence (n= 69 strains) of a fungus (*P. chrysosporium* or *S. citrinum*). To explore the genetic diversity, the 16S rRNA gene sequences were aligned using ClustalW version 2.1 (Larkin *et al.* 2007) and then manually curated. The alignment resulted in 540 nucleotides. A matrix of pairwise distances of the DNA sequences was generated and analyses of molecular variance (AMOVA) based on 100000 iterations were computed using Mothur version 1.33 (Schloss *et al.* 2009). I showed that the *Burkholderia* populations were phylogenetically more similar within a niche than among niches (AMOVA, Fs=16.54, p<0.0001). This difference was explained mainly by the substrate (soil vs wood), but also by the mycosphere effect. Indeed, the *Burkholderia* populations isolated from soil showed a genetic diversity significantly different compared to those isolated from sawdust (AMOVA, Fs=40.75, p<0.0001). The genetic diversity of the strains isolated in presence of a fungus (*P. chrysosporium* or *S. citrinum*) was also significantly different from the genetic diversity of the strains isolated in absence these fungi (AMOVA, Fs=3.52, p<0.02). Concerning the metabolic diversity, all the data from the Biolog GN2 microplates were normalised by dividing the raw difference value for each well by the average well color development (AWCD) of the plate, as suggested by Garland et al. (Garland & Mills 1991). The effects of the ecological niche, the substrate and the presence of a fungus on the metabolic profiles of the *Burkholderia* strains were estimated by a distance-based permutational multivariate ANOVA (PERMANOVA) (Anderson 2001) using “adonis” function of the *vegan* package (Oksanen *et al.* 2012) in R version 3.0.2 (R Development Core Team 2013) with a Euclidean

distance matrix and 100000 random permutations. A significant effect of the niche on the utilisation of the 95 carbon substrates was observed (PERMANOVA, $F_{7, 141}$=12.57, R^2=0.40, p<0.0001). More precisely, the utilisation of these carbon substrates was significantly affected by the type of substrate (PERMANOVA, $F_{1, 141}$=27.09, R^2=0.16, p<0.0001) and by the presence of a fungus (PERMANOVA, $F_{1, 141}$=3.21, R^2=0.02, p<0.005). This analysis demonstrates that the substrates (soil vs wood) and the presence of a fungus influenced both the genetic and metabolic diversity of *Burkholderia* populations from forest ecosystems. To evaluate the relationship between genetic and metabolic diversity, a Mantel test with 100000 permutations was performed. The result indicated a strong correlation between genetic and metabolic diversity (r_M=0.55, p<0.0001). Altogether these results suggest a niche specificity for the *Burkholderia* genus in forest ecosystems. Indeed, both substrate (soil or wood) and mycosphere effects influence the structure of the *Burkholderia* populations. Since these strains are part of a bacterial collection, future research should focus on a better characterisation of these strains, in order to identify the functional traits of the *Burkholderia* specifically associated with the white-rot mycosphere.

6.2.4 Perspectives

Regarding the ecology of the wood-associated bacterial communities, many questions remain open and need to be answered. In addition to those that were proposed above, it remains the question of tree specificity. Indeed, host-tree specificity is well-known for fungi (Junninen & Komonen 2011) and invertebrates (Wu, Yu & Zhou 2008). Moreover, it has been shown that fungal diversity was significantly higher on softwood compared to hardwood (Mathieu 2012; Mathieu *et al.* 2013a). Concerning bacterial communities, most of the studies have however focused only on one tree species. The question of the existence of host generalist bacterial communities specifically colonising hardwood or softwood is also an open question. Because of the difference in wood chemistry between hardwood and softwood, differences in bacterial community composition are expected. In the same wood species, difference in microbial richness between heartwood and sapwood has been reported. Both fungal (Zhang *et al.* 2008b) and bacterial (Zhang *et al.* 2008a) richness were found to be higher in the heartwood of *Keteleeria evelyniana* compared to the sapwood. The functional diversity of these two different microbial communities should be explored in order to understand the specificity of these communities, since differences in decay rate between heartwood and sapwood have been observed (Schowalter 1992).

At global scale, much more questions remain open. Beyond the question of the taxonomic diversity of the wood-associated bacterial communities across the globe, the question of the contribution of bacteria to wood decomposition has never been clearly investigated. Compare to fungi or arthropods (Ulyshen & Wagner 2013), how important are bacteria for lignocellulose decomposition? Indeed, bacterial contribution to the terrestrial carbon budget has been shown to be important and underestimated (Braissant, Verrecchia & Aragno 2002). The estimation of this bacterial contribution could be also important for global carbon cycle modelling, notably in the context of predicting carbon cycle responses to global change (Cornwell *et al.* 2009). A potential approach to evaluate this contribution will be to study the global functional diversity of wood-associated bacterial communities, using for example GeoChip microarrays (He *et al.* 2010).

6.3 Ecology of the white-rot mycosphere

6.3.1 Bacterial-fungal interactions in decaying wood

In Chapters 3 and 4, we demonstrated a mycosphere effect of *P. chrysosporium* on both the taxonomic and functional diversity of the wood-associated bacterial communities. The presence of the white-rot fungus in our microcosms increased the concentration of culturable bacterial communities in our microcosms. This mycosphere effect was also characterised by a significant decrease in the concentration of bacterial colonies able to grow on cellulose and methanol-based media, indicating potential competitive relationships between *P. chrysosporium* and the wood-associated bacterial communities. Competitive and antagonistic interactions between saprotrophic basidiomycetes and bacteria in decaying wood have already been described (de Boer *et al.* 2005; de Boer & van der Wal 2008). However, in the case of methanol, a product of lignin degradation (Ander & Eriksson 1985), mutualistic interactions between fungi and bacteria have been suggested. More precisely it has been hypothesised that nitrogen-fixing, methylotroph bacteria could use the methanol produced by the fungal lignin degradation as growth substrate. In return, part of the biomass of the methylotrophic bacteria would be lysed by the fungal partner and used as nitrogen source (de Boer & van der Wal 2008). This hypothesis was based on the identification of of methylotrophic bacterial strains in the mycosphere of *Hypholoma fasciculare* (Folman *et al.* 2008; Vorob'ev *et al.* 2009). Our work performed on another white-rot fungus, *P. chrysosporium*, gives results that contradict this hypothesis since *P. chrysosporium* presence reduced the number of culturable bacterial communities able to growth on methanol

(Chapter 4). One should now quantify the number of genes involved in nitrogen fixation, such as *nifH* (Hoppe *et al.* 2014) and in methylotrophy such as *mxaF* (McDonald & Murrell 1997) in the bacterial communities from our microcosms in presence or in absence of *P. chrysosporium* to go further in the analysis of de Boer and van der Wal hypothesis.

Regarding the wood decomposition, after 190 days no significant difference was observed in C/N ratio between the sawdust incubated with *P. chrysosporium* (F) and the sawdust incubated with *P. chrysosporium* and a bacterial community extracted from a forest soil (BF) in our microcosm conditions (Chapter 3), suggesting no difference in the wood decay rate (Figure 3.4). Thus, no synergism or antagonism could be detected, certainly because of the duration of the experiment which was too short compared to the dynamics of the wood decay process. However, differences in sawdust colour between these two treatments indicate differences in the chemical alteration of the sawdust, notably regarding the cellulose and lignin concentrations. Indeed, the sawdust inoculated only with the white-rot fungus was lighter in colour and appeared bleached (Figure 3.4.E), indicating loss of lignin while for the BF treatment the sawdust appeared brown and darker in colour (Figure 3.4.D), indicating cellulose degradation. These results are qualitative and it would have been useful to confirm them by quantitative measurements of the cellulose and lignin contents. The fact that no significant difference was observed in wood decay rate between the sawdust incubated with either *P. chrysosporium* alone or with *P. chrysosporium* and a bacterial community extracted from a forest soil and which was not selected by *P. chrysosporium*, suggests that in a natural bacterial community from a forest soil, most of the bacteria have a neutral or deleterious effect on the process of wood decomposition by a white-rot fungus.

When using a bacterial community composed of 25 bacterial strains isolated from *P. chrysosporium* mycosphere, *i.e.* which have been selected from a forest soil microbial inoculum by the presence of *P. chrysosporium*, we revealed for the first time synergistic bacterial-fungal interactions in the process of wood decomposition (Chapter 5). Indeed, the association of *P. chrysosporium* with this selected bacterial community resulted in a higher rate of decomposition of *Fagus sylvatica* wood blocks, compared to the decomposition by the white-rot fungus alone. This result contrasts with the literature in which bacterial-fungal interactions have been described as antagonistic and competitive in wood decay process (Folman *et al.* 2008; De Boer *et al.* 2010), and more generally in the degradation of organic matter (Møller *et al.* 1999; Mille-Lindblom & Tranvik 2003; Mille-Lindblom *et al.* 2006). From an ecological perspective, these results are very interesting. We selected a specific

bacterial community from *P. chrysosporium* mycosphere and then we used twenty-five bacterial strains representative of this bacterial community in an experiment of interaction with *P. chrysosporium*. This approach allowed to reveal a synergistic interaction between this selected bacterial community and *P. chrysosporium* in the process of wood decomposition. Thus, this shows that in a natural bacterial community from a forest soil, there are bacteria able to promote the process of wood degradation when they interact with a white-rot fungus. This result raises the question of the mechanism of this increased biodegradation efficiency. Indeed, bacterial communities could be directly involved in this process, by degrading the lignocellulose complex. On the other hand, bacterial communities could just be indirectly involved in wood degradation, by inducing the lignocellulolytic activities of the fungus. In terms of potential applications, such artificial mixed microbial communities with higher biodegradation efficiency could be used to improve the performance of biodegradation of synthetic dyes, polycyclic aromatic hydrocarbons and other organic pollutants (Mikesková *et al.* 2012). Concerning the production of second-generation biofuels from lignocellulosic biomass, these synergistic bacterial-fungal interactions could also be used to improve this production (Pu *et al.* 2011).

Biodiversity is known to influence ecosystem functioning and productivity has been shown to increase with species richness (Loreau *et al.* 2001; Hooper *et al.* 2005). These ecological rules have also been demonstrated for fungal (van der Heijden *et al.* 1998) and bacterial (Bell *et al.* 2005) communities. However, for the particular function of wood decomposition it has reported that decomposition rate was negatively correlated with fungal species richness (Fukami *et al.* 2010). To date, this relationship between species richness and wood decomposition has not been studied in the case of bacterial communities or mixed microbial communities. Our results from chapter 5 suggest that increasing the microbial species richness tends to increase the decomposition rate since beech wood blocks decomposition was more efficient in presence of one white-rot fungus associated with twenty-five bacterial strains compared to one fungus alone. On the contrary, our results from chapter 3 suggest that microbial species richness does not influence wood decay rate since there was not significant difference in C/N ratio between sawdust degraded by *P. chrysosporium* compared to sawdust degraded by *P. chrysosporium* associated with a richer bacterial community originating from forest soil (Figure 3.4). Nonetheless, a dedicated study with multiple combination of mixed microbial communities colonising wood would be required to evaluate the species richness – decomposition rate relationship.

6.3.2 Oxalate in decaying wood

Trophic interactions between bacteria and fungi have been well documented (Frey-Klett *et al.* 2011). For example, *Pseudomonas fluorescens* from the mycorrhizosphere of *Laccaria bicolor* have been shown to use the trehalose produced by the fungus (Frey *et al.* 1997). It has also been reported that *Burkholderia terrae* was able to induce the production of glycerol by the fungus *Lyphyllum* sp. in order to metabolise it (Nazir *et al.* 2013). In chapter 5, we identified calcium oxalate (CaOx) crystals on the hyphae of *P. chrysosporium* colonising wood blocks. When a bacterial community from *P. chrysosporium* mycosphere was associated with the fungus on beech wood, significantly more CaOx were observed. *P. chrysosporium* is known to be an oxalate producer (Dutton *et al.* 1993) and acid oxalic has been reported to be involved in wood degradation by fungi (Shimada *et al.* 1994). While we did not test for oxalotrophy the twenty-five bacterial strains used in Chapter 5, we know that some members of the *Dyella* (Jung *et al.* 2009) and *Burkolderia* genera (Kost *et al.* 2014) have been described as oxalotrophic bacteria. Moreover, oxalotrophic bacteria have been isolated from decaying wood (Zaitsev *et al.* 1998) as well as from fungal mycelium (Bravo *et al.* 2013). Recently, *Burkholderia* spp. and O*xalicibacterium faecigallinarum*, an oxalotrophic bacteria were found to be the predominant bacteria on decaying wood (Prewitt *et al.* 2014). Altogether these result suggest that the bacteria selected in the mycosphere of *P. chrysosporium* benefit from fungal oxalate production during the process of wood degradation. This hypothesis should be checked by characterising the oxalotrophic ability of the 145 isolates from *P. chrysosporium* mycosphere we have in our collection.

Is oxalate a key molecule between wood-rotting basidiomycetes and bacteria during the process of wood decomposition? Numerous white-rot fungi are known to be able to produce calcium oxalate crystals (Guggiari *et al.* 2011) and as mentioned above oxalotrophic bacteria have been found on decaying wood. To test this hypothesis, we could investigate the presence of oxalotrophic bacteria on dead wood in forest, using the amplification of the *frc* gene, a molecular marker of oxalate-oxidising bacteria (Khammar *et al.* 2009). Then the diversity of *frc* gene sequences could be compared to the fungal diversity present in the same wood samples, using internal transcribed spacer (ITS) sequencing (Schoch *et al.* 2012), in order to look for species co-occurrence patterns between oxalotrophic bacteria and wood-rotting fungi (Gotelli 2000). Such network analysis would allow to reveal the coexistence of the two microorganisms. Additionally, oxalate concentration in wood should be quantified (Clausen, Kenealy & Lebow 2008) and compared to the *frc* gene copy number. Such study

should be performed on different tree species at different stage of decay to take into account the heterogeneity of the process of wood decomposition.

6.4 Conclusion

In the editorial of a special issue of *Fungal Ecology* journal dedicated to decomposition in forest ecosystems, Baldrian & Lindahl (2011) indicated that after decades of research on this topic there were still new findings. The numerous studies on microbial wood decomposition published in the last three years confirm this idea. However, most studies on the organisms involved in wood decomposition have focused on one particular kingdom, namely Bacteria, Fungi or Animalia, or have described separately their findings about bacterial and fungal communities (see for example Zhang, Yang, & Tu, 2008 and Zhang, Yang, Tu, Gao, & Zhao, 2008). Since dead wood is a habitat for a high number of species (Harmon *et al.* 1986; Stockland *et al.* 2012), it is necessary to take into account not only this diversity, but also the interactions that occur inside the community to understand the complexity of the process of decomposition. Our work clearly highlights that the interactions between bacterial and fungal communities and more generally, the interactions between saproxylic organisms influence the dynamics of decomposition. Thus, these interactions should be considered as driving forces of the process of wood decomposition.

- References -

7 References

Aanen, D.K., Eggleton, P., Rouland-Lefevre, C., Guldberg-Froslev, T., Rosendahl, S. & Boomsma, J.J. (2002) The evolution of fungus-growing termites and their mutualistic fungal symbionts. *Proceedings of the National Academy of Sciences of the United States of America*, **99**, 14887–92.

A'Bear, A.D., Jones, T.H., Kandeler, E. & Boddy, L. (2014) Interactive effects of temperature and soil moisture on fungal-mediated wood decomposition and extracellular enzyme activity. *Soil Biology and Biochemistry*.

Adams, A.S., Currie, C.R., Cardoza, Y., Klepzig, K.D. & Raffa, K.F. (2009) Effects of symbiotic bacteria and tree chemistry on the growth and reproduction of bark beetle fungal symbionts. *Canadian Journal of Forest Research*, **39**, 1133–1147.

Addis, E., Fleet, G.., Cox, J.., Kolak, D. & Leung, T. (2001) The growth, properties and interactions of yeasts and bacteria associated with the maturation of Camembert and blue-veined cheeses. *International Journal of Food Microbiology*, **69**, 25–36.

Ahmad, M., Roberts, J.N., Hardiman, E.M., Singh, R., Eltis, L.D. & Bugg, T.D.H. (2011) Identification of DypB from *Rhodococcus jostii* RHA1 as a lignin peroxidase. *Biochemistry*, **50**, 5096–107.

Ahmad, M., Taylor, C.R., Pink, D., Burton, K., Eastwood, D., Bending, G.D. & Bugg, T.D.H. (2010) Development of novel assays for lignin degradation: comparative analysis of bacterial and fungal lignin degraders. *Molecular BioSystems*, **6**, 815.

Alexander, D.B. & Zuberer, D.A. (1991) Use of chrome azurol S reagents to evaluate siderophore production by rhizosphere bacteria. *Biology and Fertility of Soils*, **12**, 39–45.

Alexandre, H., Costello, P.J., Remize, F., Guzzo, J. & Guilloux-Benatier, M. (2004) *Saccharomyces cerevisiae-Oenococcus oeni* interactions in wine: current knowledge and perspectives. *International journal of food microbiology*, **93**, 141–54.

Allison, S.D. & Martiny, J.B.H. (2008) Resistance, resilience, and redundancy in microbial communities. *Proceedings of the National Academy of Sciences of the United States of America*, **105**, 11512–9.

Ander, P. & Eriksson, K.K.-E. (1985) Methanol formation during lignin degradation by *Phanerochaete chrysosporium*. *Appl Microbiol Biotechnol*, **21-21**, 96–102.

Anderson, M.J. (2001) A new method for non-parametric multivariate analysis of variance. *Austral Ecology*, **26**, 32–46.

Andersson, B.., Welinder, L., Olsson, P.., Olsson, S. & Henrysson, T. (2000) Growth of inoculated white-rot fungi and their interactions with the bacterial community in soil contaminated with polycyclic aromatic hydrocarbons, as measured by phospholipid fatty acids. *Bioresource Technology*, **73**, 29–36.

An, D.-S., Im, W.-T., Yang, H.-C., Yang, D.-C. & Lee, S.-T. (2005) *Dyella koreensis* sp. nov., a beta-glucosidase-producing bacterium. *International Journal of Systematic and Evolutionary Microbiology*, **55**, 1625–1628.

Antony-Babu, S., Deveau, A., Van Nostrand, J.D., Zhou, J., Le Tacon, F., Robin, C., Frey-Klett, P. & Uroz, S. (2013) Black truffle-associated bacterial communities during the development and maturation of *Tuber melanosporum* ascocarps and putative functional roles. *Environmental Microbiology*.

Archibald, F.S. (1992) A new assay for lignin-type peroxidases employing the dye azure B. *Appl. Envir. Microbiol.*, **58**, 3110–3116.

Ausec, L., Zakrzewski, M., Goesmann, A., Schlüter, A. & Mandic-Mulec, I. (2011) Bioinformatic analysis reveals high diversity of bacterial genes for laccase-like enzymes. (ed O Lespinet). *PloS one*, **6**, e25724.

Ausmus, B.S. (1977) Regulation of wood decomposition rates by arthropod and annelid populations. *Ecological Bulletins (Stockholm)*, **25**, 180–192.

Austin, A.T. & Ballaré, C.L. (2010) Dual role of lignin in plant litter decomposition in terrestrial ecosystems. *Proceedings of the National Academy of Sciences of the United States of America*, **107**, 4618–22.

Austin, A.T. & Vivanco, L. (2006) Plant litter decomposition in a semi-arid ecosystem controlled by photodegradation. *Nature*, **442**, 555–8.

Ayres, M.P., Wilkens, R.T., Ruel, J.J., Lombardero, M.J. & Vallery, E. (2000) Nitrogen budgets of phloem-feeding bark beetles with and without symbiotic fungi. *Ecology*, **81**, 2198–2210.

Baldrian, P. (2006) Fungal laccases - occurrence and properties. *FEMS microbiology reviews*, **30**, 215–42.

Baldrian, P. (2008) Enzymes of Saprotrophic Basidiomycetes. *Ecology of Saprotrophic*

Basidiomycetes, Academic P (eds L. Boddy, J.C. Frankland & P. van West), pp. 19–41. Oxford, UK.

Baldrian, P. & Lindahl, B. (2011) Decomposition in forest ecosystems: after decades of research still novel findings. *Fungal Ecology*, **4**, 359–361.

Baldrian, P. & Valášková, V. (2008) Degradation of cellulose by basidiomycetous fungi. *FEMS microbiology reviews*, **32**, 501–521.

Barford, C.C., Wofsy, S.C., Goulden, M.L., Munger, J.W., Pyle, E.H., Urbanski, S.P., Hutyra, L., Saleska, S.R., Fitzjarrald, D. & Moore, K. (2001) Factors controlling long- and short-term sequestration of atmospheric CO2 in a mid-latitude forest. *Science*, **294**, 1688–91.

Barret, M., Frey-Klett, P., Boutin, M., Guillerm-Erckelboudt, A. -Y, Martin, F., Guillot, L. & Sarniguet, A. (2009) The plant pathogenic fungus *Gaeumannomyces graminis* var. *tritici* improves bacterial growth and triggers early gene regulations in the biocontrol strain *Pseudomonas fluorescens* Pf29Arp. *New Phytologist*, **181**, 435–447.

Bell, T., Newman, J.A., Silverman, B.W., Turner, S.L. & Lilley, A.K. (2005) The contribution of species richness and composition to bacterial services. *Nature*, **436**, 1157–1160.

Benton, T.G., Solan, M., Travis, J.M.J. & Sait, S.M. (2007) Microcosm experiments can inform global ecological problems. *Trends in Ecology & Evolution*, **22**, 516–521.

Berlemont, R. & Martiny, A.C. (2013) Phylogenetic distribution of potential cellulases in bacteria. *Applied and environmental microbiology*, **79**, 1545–54.

Bianciotto, V. & Bonfante, P. (2002) Arbuscular mycorrhizal fungi: a specialised niche for rhizospheric and endocellular bacteria. *Antonie van Leeuwenhoek*, **81**, 365–371.

Bieker, D., Kehr, R., Weber, G. & Rust, S. (2010) Non-destructive monitoring of early stages of white rot by *Trametes versicolor* in *Fraxinus excelsior*. *Annals of Forest Science*, **67**, 210–210.

Björdal, C.G., Nilsson, T. & Daniel, G. (1999) Microbial decay of waterlogged archaeological wood found in Sweden Applicable to archaeology and conservation. *International Biodeterioration & Biodegredation*, **43**, 63–73.

Blanchette, R.A. (1984) Screening wood decayed by white rot fungi for preferential lignin degradation. *Applied and Environmental Microbiology*, **48**, 647.

Blanchette, R.A. (2000) A review of microbial deterioration found in archaeological wood

from different environments. *International Biodeterioration & Biodegradation*, **46**, 189–204.

Blanchette, R.A., Burnes, T.A., Leatham, G.F. & Effland, M.J. (1988) Selection of white-rot fungi for biopulping. *Biomass*, **15**, 93–101.

Blanchette, R.A., Held, B.W., Jurgens, J.A., McNew, D.L., Harrington, T.C., Duncan, S.M. & Farrell, R.L. (2004) Wood-Destroying Soft Rot Fungi in the Historic Expedition Huts of Antarctica. *Appl. Environ. Microbiol.*, **70**, 1328–1335.

Blomqvist, J., Leong, S.-L.L., Sandgren, M., Lestander, T. & Passoth, V. (2014) Temperature-dependent changes in the microbial storage flora of birch and spruce sawdust. *Biotechnology and applied biochemistry*, **61**, 58–64.

Boddy, L. (1983) Carbon dioxide release from decomposing wood: Effect of water content and temperature. *Soil Biology and Biochemistry*, **15**, 501–510.

Boddy, L. (2000) Interspecific combative interactions between wood-decaying basidiomycetes. *FEMS microbiology ecology*, **31**, 185–194.

Boddy, L. & Watkinson, S.C. (1995) Wood decomposition, higher fungi, and their role in nutrient redistribution. *Canadian Journal of Botany*, **73**, 1377–1383.

De Boer, W., Folman, L., Klein Gunnewiek, P., Svensson, T., Bastviken, D., Öberg, G., Del Rio, J. & Boddy, L. (2010) Mechanism of antibacterial activity of the white-rot fungus *Hypholoma fasciculare* colonizing wood. *Canadian Journal of Microbiology*, **56**, 380–388.

De Boer, W., Folman, L.B., Summerbell, R.C. & Boddy, L. (2005) Living in a fungal world: impact of fungi on soil bacterial niche development. *FEMS Microbiology Reviews*, **29**, 795–811.

De Boer, W. & van der Wal, A. (2008) Interactions between saprotrophic basidiomycetes and bacteria. *Ecology of Saprotrophic Basidiomycetes*, British My (eds L. Boddy, J.C. Frankland & P. van West), pp. 143–153. Academic Press.

Boerjan, W., Ralph, J. & Baucher, M. (2003) Lignin Biosynthesis. *Annual Review of Plant Biology*, **54**, 519–546.

Boersma, F.G.H., Warmink, J. a, Andreote, F. a & van Elsas, J.D. (2009) Selection of *Sphingomonadaceae* at the base of *Laccaria proxima* and *Russula exalbicans* fruiting bodies. *Applied and Environmental Microbiology*, **75**, 1979–1989.

Bonnarme, P. & Jeffries, T.W. (1990) Mn(II) Regulation of Lignin Peroxidases and Manganese-Dependent Peroxidases from Lignin-Degrading White Rot Fungi. *Appl. Envir. Microbiol.*, **56**, 210–217.

Bontemps, C., Toussaint, M., Revol, P.-V., Hotel, L., Jeanbille, M., Uroz, S., Turpault, M.-P., Blaudez, D. & Leblond, P. (2013) Taxonomic and functional diversity of *Streptomyces* in a forest soil. *FEMS Microbiology Letters*, **342**, 157–167.

Botha, A. (2011) The importance and ecology of yeasts in soil. *Soil Biology and Biochemistry*, **43**, 1–8.

Botting, R.S. & DeLong, C. (2009) Macrolichen and bryophyte responses to coarse woody debris characteristics in sub-boreal spruce forest. *Forest Ecology and Management*, **258**, S85–S94.

Bourdais, A., Bidard, F., Zickler, D., Berteaux-Lecellier, V., Silar, P. & Espagne, E. (2012) Wood utilization is dependent on catalase activities in the filamentous fungus *Podospora anserina*. *PloS one*, **7**, e29820.

Bouriaud, O., Bréda, N., Le Moguédec, G. & Nepveu, G. (2004) Modelling variability of wood density in beech as affected by ring age, radial growth and climate. *Trees*, **18**, 264–276.

Bradford, M.A., Watts, B.W. & Davies, C.A. (2010) Thermal adaptation of heterotrophic soil respiration in laboratory microcosms. *Global Change Biology*, **16**, 1576–1588.

Braissant, O., Verrecchia, E.P. & Aragno, M. (2002) Is the contribution of bacteria to terrestrial carbon budget greatly underestimated? *Naturwissenschaften*, **89**, 366–70.

Bravo, D., Cailleau, G., Bindschedler, S., Simon, A., Job, D., Verrecchia, E. & Junier, P. (2013) Isolation of oxalotrophic bacteria able to disperse on fungal mycelium. *FEMS microbiology letters*, **348**, 157–66.

Breznak, J.A. (1982) Intestinal microbiota of termites and other xylophagous insects. *Annual review of microbiology*, **36**, 323–43.

Brown, M.E. & Chang, M.C. (2014) Exploring bacterial lignin degradation. *Current opinion in chemical biology*, **19C**, 1–7.

Bucur, V., Garros, S., Navarrete, A., Troya, M.T. & Guyonnet, R. (1997) Kinetics of wood degradation by fungi with x-ray microdensitometric technique. *Wood Science and Technology*, **31**, 383–389.

Bugg, T.D.H., Ahmad, M., Hardiman, E.M. & Singh, R. (2011) The emerging role for bacteria in lignin degradation and bio-product formation. *Current Opinion in Biotechnology*, **22**, 394–400.

Burdsall, H.. & Eslyn, W.. (1974) A new *Phanerochaete* with a chrysosporium imperfect state. *Mycotaxon*, **1**, 123–133.

Cantarel, B.L., Coutinho, P.M., Rancurel, C., Bernard, T., Lombard, V. & Henrissat, B. (2009) The Carbohydrate-Active EnZymes database (CAZy): an expert resource for Glycogenomics. *Nucleic acids research*, **37**, D233–8.

Carpenter, S.R. (1996) Microcosm Experiments have Limited Relevance for Community and Ecosystem Ecology. *Ecology*, **77**, 677.

Caruso, T., Chan, Y., Lacap, D.C., Lau, M.C.Y., McKay, C.P. & Pointing, S.B. (2011) Stochastic and deterministic processes interact in the assembly of desert microbial communities on a global scale. *The ISME Journal*, **5**, 1406–1413.

Chaucheyras-Durand, F., Masséglia, S., Fonty, G. & Forano, E. (2010) Influence of the composition of the cellulolytic flora on the development of hydrogenotrophic microorganisms, hydrogen utilization, and methane production in the rumens of gnotobiotically reared lambs. *Applied and environmental microbiology*, **76**, 7931–7.

Chave, J. (2004) Neutral theory and community ecology. *Ecology Letters*, **7**, 241–253.

Chave, J., Coomes, D., Jansen, S., Lewis, S.L., Swenson, N.G. & Zanne, A.E. (2009) Towards a worldwide wood economics spectrum. *Ecology Letters*, **12**, 351–66.

Chen, J.-W. & Chan, K.-G. (2012) Genome Sequence of *Dyella japonica* Strain A8, a Quorum-Quenching Bacterium That Degrades N-Acylhomoserine Lactones, Isolated from Malaysian Tropical Soil. *Journal of Bacteriology*, **194**, 6331.

Clarke, K.R. (1993) Non-parametric multivariate analyses of changes in community structure. *Australian Journal of Ecology*, **18**, 117–143.

Clausen, C.A. (1996) Bacterial associations with decaying wood: a review. *International Biodeterioration & Biodegradation*, **37**, 101–107.

Clausen, C.A., Kenealy, W. & Lebow, P.K. (2008) Oxalate analysis methodology for decayed wood. *International Biodeterioration & Biodegradation*, **62**, 372–375.

Coenye, T. & Vandamme, P. (2003) Diversity and significance of *Burkholderia* species

occupying diverse ecological niches. *Environmental Microbiology*, **5**, 719–729.

Compant, S., Nowak, J., Coenye, T., Clément, C. & Ait Barka, E. (2008) Diversity and occurrence of *Burkholderia* spp. in the natural environment. *FEMS microbiology reviews*, **32**, 607–26.

Cornelissen, J.H.C., Sass-Klaassen, U., Poorter, L., van Geffen, K., van Logtestijn, R.S.P., van Hal, J., Goudzwaard, L., Sterck, F.J., Klaassen, R.K.W.M., Freschet, G.T., van der Wal, A., Eshuis, H., Zuo, J., de Boer, W., Lamers, T., Weemstra, M., Cretin, V., Martin, R., Ouden, J. den, Berg, M.P., Aerts, R., Mohren, G.M.J. & Hefting, M.M. (2012) Controls on coarse wood decay in temperate tree species: birth of the LOGLIFE experiment. *Ambio*, **41 Suppl 3**, 231–45.

Cornwell, W.K., Cornelissen, J.H.C., Allison, S.D., Bauhus, J., Eggleton, P., Preston, C.M., Scarff, F., Weedon, J.T., Wirth, C. & Zanne, A.E. (2009) Plant traits and wood fates across the globe: rotted, burned, or consumed? *Global Change Biology*, **15**, 2431–2449.

Crawford, R.L., Kirk, T.K., Harkin, J.M. & McCoy, E. (1973) Bacterial cleavage of an arylglycerol-beta-aryl ether bond. *Applied Microbiology*, **25**, 322.

Crowther, T.W., Boddy, L. & Hefin Jones, T. (2012) Functional and ecological consequences of saprotrophic fungus-grazer interactions. *The ISME journal*, **6**, 1992–2001.

Currie, C.R. (2001) A community of ants, fungi, and bacteria: a multilateral approach to studying symbiosis. *Annual review of microbiology*, **55**, 357–80.

Day, T.A., Zhang, E.T. & Ruhland, C.T. (2007) Exposure to solar UV-B radiation accelerates mass and lignin loss of Larrea tridentata litter in the Sonoran Desert. *Plant Ecology*, **193**, 185–194.

DeAngelis, K.M., D'Haeseleer, P., Chivian, D., Fortney, J.L., Khudyakov, J., Simmons, B., Woo, H., Arkin, A.P., Davenport, K.W., Goodwin, L., Chen, A., Ivanova, N., Kyrpides, N.C., Mavromatis, K., Woyke, T. & Hazen, T.C. (2011) Complete genome sequence of *Enterobacter lignolyticus* SCF1. *Standards in Genomic Sciences*, **5**, 69–85.

Delalibera, I., Handelsman, J. & Raffa, K.F. (2005) Contrasts in Cellulolytic Activities of Gut Microorganisms Between the Wood Borer, *Saperda vestita* (Coleoptera: Cerambycidae), and the Bark Beetles, *Ips pini* and *Dendroctonus frontalis* (Coleoptera: Curculionidae). *Environmental Entomology*, **34**, 541–547.

Delbès, C., Ali-Mandjee, L. & Montel, M.-C. (2007) Monitoring bacterial communities in raw

milk and cheese by culture-dependent and -independent 16S rRNA gene-based analyses. *Applied and Environmental Microbiology*, **73**, 1882–91.

DeSantis, T.Z., Hugenholtz, P., Keller, K., Brodie, E.L., Larsen, N., Piceno, Y.M., Phan, R. & Andersen, G.L. (2006a) NAST: a multiple sequence alignment server for comparative analysis of 16S rRNA genes. *Nucleic Acids Research*, **34**, 394–399.

DeSantis, T.Z., Hugenholtz, P., Larsen, N., Rojas, M., Brodie, E.L., Keller, K., Huber, T., Dalevi, D., Hu, P. & Andersen, G.L. (2006b) Greengenes, a chimera-checked 16S rRNA gene database and workbench compatible with ARB. *Applied and Environmental Microbiology*, **72**, 5069–5072.

Deveau, A., Brulé, C., Palin, B., Champmartin, D., Rubini, P., Garbaye, J., Sarniguet, A. & Frey-Klett, P. (2010) Role of fungal trehalose and bacterial thiamine in the improved survival and growth of the ectomycorrhizal fungus *Laccaria bicolor* S238N and the helper bacterium *Pseudomonas fluorescens* BBc6R8. *Environmental microbiology reports*, **2**, 560–8.

Dewar, R.C. & Cannell, M.G.R. (1992) Carbon sequestration in the trees, products and soils of forest plantations: an analysis using UK examples. *Tree Physiology*, **11**, 49–71.

Dewey, F., Wong, Y. & Seery, R. (1999) Bacteria associated with *Stagonospora* (*Septoria*) *nodorum* increase pathogenicity of the fungus. *New Phytologist*, **144**, 489–497.

Dlauchy, D., Lee, C.-F. & Péter, G. (2012) *Spencermartinsiella ligniputridi* sp. nov., a yeast species isolated from rotten wood. *International journal of systematic and evolutionary microbiology*, **62**, 2799–804.

Donnelly, P.K., Entry, J.A., Crawford, D.L. & Cromack, K. (1990) Cellulose and lignin degradation in forest soils: response to moisture, temperature, and acidity. *Microbial Ecology*, **20**, 289–295.

Dresler-Nurmi, A., Kaijalainen, S., Lindström, K. & Hatakka, A. (1999) Grouping of lignin degrading corticioid fungi based on RFLP analysis of 18S rDNA and ITS regions. *Mycological Research*, **103**, 990–996.

Dreyfus, B.L., Elmerich, C. & Dommergues, Y.R. (1983) Free-Living Rhizobium Strain Able To Grow on N2 as the Sole Nitrogen Source. *Appl. Envir. Microbiol.*, **45**, 711–713.

Dürre, P., Richard, T., Eltis, L., Kushmaro, A. & Madsen, E.L. (2011) Microorganisms and their roles in fundamental biogeochemical cycles. *Current Opinion in Biotechnology*, **22**,

456–464.

Dutton, M. V., Evans, C.S., Atkey, P.T. & Wood, D.A. (1993) Oxalate production by Basidiomycetes, including the white-rot species *Coriolus versicolor* and *Phanerochaete chrysosporium*. *Applied Microbiology and Biotechnology*, **39**, 5–10.

EN113. Wood Preservatives. Test Method for Determining the Protective Effectiveness against Wood Destroying Basidiomycetes. Determination of the Toxic Values. CEN. European Committee for Standardization. (1996) Brussels.

Espagne, E., Lespinet, O., Malagnac, F., Da Silva, C., Jaillon, O., Porcel, B.M., Couloux, A., Aury, J.-M., Ségurens, B., Poulain, J., Anthouard, V., Grossetete, S., Khalili, H., Coppin, E., Déquard-Chablat, M., Picard, M., Contamine, V., Arnaise, S., Bourdais, A., Berteaux-Lecellier, V., Gautheret, D., de Vries, R.P., Battaglia, E., Coutinho, P.M., Danchin, E.G., Henrissat, B., Khoury, R. El, Sainsard-Chanet, A., Boivin, A., Pinan-Lucarré, B., Sellem, C.H., Debuchy, R., Wincker, P., Weissenbach, J. & Silar, P. (2008) The genome sequence of the model ascomycete fungus *Podospora anserina*. *Genome biology*, **9**, R77.

Fackler, K., Schmutzer, M., Manoch, L., Schwanninger, M., Hinterstoisser, B., Ters, T., Messner, K. & Gradinger, C. (2007) Evaluation of the selectivity of white rot isolates using near infrared spectroscopic techniques. *Enzyme and Microbial Technology*, **41**, 881–887.

Fackler, K. & Schwanninger, M. (2012) How spectroscopy and microspectroscopy of degraded wood contribute to understand fungal wood decay. *Applied microbiology and biotechnology*, **96**, 587–99.

Fackler, K., Stevanic, J.S., Ters, T., Hinterstoisser, B., Schwanninger, M. & Salmén, L. (2010) Localisation and characterisation of incipient brown-rot decay within spruce wood cell walls using FT-IR imaging microscopy. *Enzyme and microbial technology*, **47**, 257–267.

Falkowski, P.G., Fenchel, T. & Delong, E.F. (2008) The microbial engines that drive Earth's biogeochemical cycles. *Science*, **320**, 1034–9.

Fekete, F.A., Chandhoke, V. & Jellison, J. (1989) Iron-Binding Compounds Produced by Wood-Decaying Basidiomycetes. *Appl. Envir. Microbiol.*, **55**, 2720–2722.

Filley, T.R., Blanchette, R.A., Simpson, E. & Fogel, M.L. (2001) Nitrogen cycling by wood decomposing soft-rot fungi in the "King Midas tomb," Gordion, Turkey. *Proceedings of the National Academy of Sciences of the United States of America*, **98**, 13346–50.

Floudas, D., Binder, M., Riley, R., Barry, K., Blanchette, R.A., Henrissat, B., Martínez, A.T., Otillar, R., Spatafora, J.W., Yadav, J.S., Aerts, A., Benoit, I., Boyd, A., Carlson, A., Copeland, A., Coutinho, P.M., Vries, R.P. de, Ferreira, P., Findley, K., Foster, B., Gaskell, J., Glotzer, D., Górecki, P., Heitman, J., Hesse, C., Hori, C., Igarashi, K., Jurgens, J.A., Kallen, N., Kersten, P., Kohler, A., Kües, U., Kumar, T.K.A., Kuo, A., LaButti, K., Larrondo, L.F., Lindquist, E., Ling, A., Lombard, V., Lucas, S., Lundell, T., Martin, R., McLaughlin, D.J., Morgenstern, I., Morin, E., Murat, C., Nagy, L.G., Nolan, M., Ohm, R.A., Patyshakuliyeva, A., Rokas, A., Ruiz-Dueñas, F.J., Sabat, G., Salamov, A., Samejima, M., Schmutz, J., Slot, J.C., John, F.S., Stenlid, J., Sun, H., Sun, S., Syed, K., Tsang, A., Wiebenga, A., Young, D., Pisabarro, A., Eastwood, D.C., Martin, F., Cullen, D., Grigoriev, I. V. & Hibbett, D.S. (2012) The Paleozoic Origin of Enzymatic Lignin Decomposition Reconstructed from 31 Fungal Genomes. *Science*, **336**, 1715–1719.

Folman, L.B., Klein Gunnewiek, P.J., Boddy, L. & De Boer, W. (2008) Impact of white-rot fungi on numbers and community composition of bacteria colonizing beech wood from forest soil. *FEMS Micriobiology Ecology*, **63**, 181–191.

Franceschi, V.R., Krokene, P., Christiansen, E. & Krekling, T. (2005) Anatomical and chemical defenses of conifer bark against bark beetles and other pests. *The New phytologist*, **167**, 353–75.

Frankland, J.C. (1998) Fungal succession — unravelling the unpredictable. *Mycological Research*, **102**, 1–15.

Freschet, G.T., Weedon, J.T., Aerts, R., van Hal, J.R. & Cornelissen, J.H.C. (2012) Interspecific differences in wood decay rates: insights from a new short-term method to study long-term wood decomposition. *Journal of Ecology*, **100**, 161–170.

Freyburger, C., Longuetaud, F., Mothe, F., Constant, T. & Leban, J.-M. (2009) Measuring wood density by means of X-ray computer tomography. *Annals of Forest Science*, **66**, 804–804.

Frey, P., Frey-Klett, P., Garbaye, J., Berge, O. & Heulin, T. (1997) Metabolic and Genotypic Fingerprinting of Fluorescent Pseudomonads Associated with the Douglas Fir-*Laccaria bicolor* Mycorrhizosphere. *Applied and environmental microbiology*, **63**, 1852–60.

Frey-Klett, P., Burlinson, P., Deveau, A., Barret, M., Tarkka, M. & Sarniguet, A. (2011) Bacterial-fungal interactions: hyphens between agricultural, clinical, environmental, and food microbiologists. *Microbiology and Molecular Biology Reviews*, **75**, 583–609.

Frey-Klett, P., Chavatte, M., Clausse, M.-L., Courrier, S., Le Roux, C., Raaijmakers, J., Martinotti, M.G., Pierrat, J.-C. & Garbaye, J. (2005) Ectomycorrhizal symbiosis affects functional diversity of rhizosphere fluorescent pseudomonads. *The New Phytologist*, **165**, 317–28.

Frey-Klett, P., Garbaye, J. & Tarkka, M. (2007) The mycorrhiza helper bacteria revisited. *New Phytologist*, **176**, 22–36.

Fukami, T., Dickie, I. a, Paula Wilkie, J., Paulus, B.C., Park, D., Roberts, A., Buchanan, P.K. & Allen, R.B. (2010) Assembly history dictates ecosystem functioning: evidence from wood decomposer communities. *Ecology letters*, **13**, 675–84.

Fukasawa, Y., Osono, T. & Takeda, H. (2009) Microfungus communities of Japanese beech logs at different stages of decay in a cool temperate deciduous forest. *Canadian Journal of Forest Research*, **39**, 1606–1614.

Fukasawa, Y., Osono, T. & Takeda, H. (2011) Wood decomposing abilities of diverse lignicolous fungi on nondecayed and decayed beech wood. *Mycologia*, **103**, 474–82.

Furuno, S., Päzolt, K., Rabe, C., Neu, T.R., Harms, H. & Wick, L.Y. (2010) Fungal mycelia allow chemotactic dispersal of polycyclic aromatic hydrocarbon-degrading bacteria in water-unsaturated systems. *Environmental microbiology*, **12**, 1391–1398.

Gadd, G.M. (2006) *Fungi in Biogeochemical Cycles*, Cambridge . Cambridge.

Gallo, M.E., Porras-Alfaro, A., Odenbach, K.J. & Sinsabaugh, R.L. (2009) Photoacceleration of plant litter decomposition in an arid environment. *Soil Biology and Biochemistry*, **41**, 1433–1441.

Gao, D., Zeng, Y., Wen, X. & Qian, Y. (2008) Competition strategies for the incubation of white rot fungi under non-sterile conditions. *Process Biochemistry*, **43**, 937–944.

Garland, J.L. & Mills, A.L. (1991) Classification and Characterization of Heterotrophic Microbial Communities on the Basis of Patterns of Community-Level Sole-Carbon-Source. *Applied and Environmental Microbiology*, **57**, 2351–2359.

Giesecke, T., Hickler, T., Kunkel, T., Sykes, M.T. & Bradshaw, R.H.W. (2006) Towards an understanding of the Holocene distribution of Fagus sylvatica L. *Journal of Biogeography*, **34**, 118–131.

Gilbertson, R.L. (1981) North American wood-rotting fungi that cause brown rots. *Mycotaxon*, **12**, 372–416.

Gindl, M. & Tschegg, S. (2002) Significance of the Acidity of Wood to the Surface Free Energy Components of Different Wood Species. *Langmuir*, **18**, 3209–3212.

Gírio, F.M., Fonseca, C., Carvalheiro, F., Duarte, L.C., Marques, S. & Bogel-Łukasik, R. (2010) Hemicelluloses for fuel ethanol: A review. *Bioresource Technology*, **101**, 4775–4800.

Good, I.J. (1953) The population frequencies of species and the estimation of population parameters. *Biometrika*, **40**, 237–264.

Gotelli, N.J. (2000) Null model analysis of species co-occurrence patterns. *Ecology*, **81**, 2606–2621.

Greaves, H. (1969) Micromorphology of the bacterial attack of wood. *Wood Science and Technology*, **3**, 150–166.

Greaves, H. (1971) The bacterial factor in wood decay. *Wood Science and Technology*, **5**, 6–16.

Green, F. & Highley, T.L. (1997) Mechanism of brown-rot decay: Paradigm or paradox. *International Biodeterioration & Biodegradation*, **39**, 113–124.

Grove, S.J. (2002) Saproxylic insect ecology and the sustainable management of forests. *Annual Review of Ecology and Systematics*, **33**, 1–23.

Grube, M., Cardinale, M., de Castro, J.V., Müller, H. & Berg, G. (2009) Species-specific structural and functional diversity of bacterial communities in lichen symbioses. *The ISME Journal*, **3**, 1105–1115.

Guggiari, M., Bloque, R., Aragno, M., Verrecchia, E., Job, D. & Junier, P. (2011) Experimental calcium-oxalate crystal production and dissolution by selected wood-rot fungi. *International Biodeterioration & Biodegradation*, **65**, 803–809.

Guillén, F., Martínez, M.J., Muñoz, C. & Martínez, A.T. (1997) Quinone Redox Cycling in the Ligninolytic Fungus *Pleurotus eryngii* Leading to Extracellular Production of Superoxide Anion Radical. *Archives of Biochemistry and Biophysics*, **339**, 190–199.

Guo, X., Zhu, H. & Bai, F.-Y. (2012) *Candida cellulosicola* sp. nov., a xylose-utilizing anamorphic yeast from rotten wood. *International journal of systematic and evolutionary microbiology*, **62**, 242–5.

Güsewell, S. & Gessner, M.O. (2009) N : P ratios influence litter decomposition and

colonization by fungi and bacteria in microcosms. *Functional Ecology*, **23**, 211–219.

Gutierrez, A., Caramelo, L., Prieto, A., Martinez, M.J. & Martinez, A.T. (1994) Anisaldehyde production and aryl-alcohol oxidase and dehydrogenase activities in ligninolytic fungi of the genus *Pleurotus*. *Appl. Envir. Microbiol.*, **60**, 1783–1788.

Hammel, K.E., Kapich, A.N., Jensen Jr, K.A. & Ryan, Z.C. (2002) Reactive oxygen species as agents of wood decay by fungi. *Enzyme and Microbial Technology*, **30**, 445–453.

Harmon, M.E., Franklin, J.F., Swanson, F.J., Sollins, P., Gregory, S.V., Lattin, J.D., Anderson, N.H., Cline, S.P., Aumen, N.G., Sedell, J.R., Lienkaemper, G.W., Cromack, K. & Cummins, K.W. (1986) Ecology of coarse woody debris in temperate ecosystems. *Advances in Ecological Research*, **15**, 133–302.

Hartmann, M., Howes, C.G., Vaninsberghe, D., Yu, H., Bachar, D., Christen, R., Henrik Nilsson, R., Hallam, S.J. & Mohn, W.W. (2012) Significant and persistent impact of timber harvesting on soil microbial communities in Northern coniferous forests. *The ISME Journal*, **6**, 2199–2218.

Ten Have, R. & Teunissen, P.J.M. (2001) Oxidative mechanisms involved in lignin degradation by white-rot fungi. *Chemical Reviews*, **101**, 3397–3414.

Heckman, D.S., Geiser, D.M., Eidell, B.R., Stauffer, R.L., Kardos, N.L. & Hedges, S.B. (2001) Molecular evidence for the early colonization of land by fungi and plants. *Science*, **293**, 1129–33.

He, Z., Deng, Y., Van Nostrand, J.D., Tu, Q., Xu, M., Hemme, C.L., Li, X., Wu, L., Gentry, T.J., Yin, Y., Liebich, J., Hazen, T.C. & Zhou, J. (2010) GeoChip 3.0 as a high-throughput tool for analyzing microbial community composition, structure and functional activity. *The ISME journal*, **4**, 1167–79.

Van der Heijden, M.G.A., Klironomos, J.N., Ursic, M., Moutoglis, P., Streitwolf-Engel, R., Boller, T., Wiemken, A. & Sanders, I.R. (1998) Mycorrhizal fungal diversity determines plant biodiversity, ecosystem variability and productivity. *Nature*, **396**, 69–72.

Hervé, V., Derr, J., Douady, S., Quinet, M., Moisan, L. & Lopez, P.J. (2012) Multiparametric Analyses Reveal the pH-Dependence of Silicon Biomineralization in Diatoms. *PLoS ONE*, **7**, e46722.

Hervé, V., Mothe, F., Freyburger, C., Gelhaye, E. & Frey-Klett, P. (2014a) Density mapping of decaying wood using X-ray computed tomography. *International Biodeterioration &*

Biodegradation, **86**, 358–363.

Hervé, V., Le Roux, X., Uroz, S., Gelhaye, E. & Frey-Klett, P. (2014b) Diversity and structure of bacterial communities associated with *Phanerochaete chrysosporium* during wood decay. *Environmental Microbiology*.

Hillis, W.E. (1984) High temperature and chemical effects on wood stability. *Wood Science and Technology*, **18**, 281–293.

Hodge, S.J. & Peterken, G.F. (1998) Deadwood in British forests: priorities and a strategy. *Forestry*, **71**, 99–112.

Hofrichter, M. (2002) Review: lignin conversion by manganese peroxidase (MnP). *Enzyme and Microbial technology*, **30**, 454–466.

Hon, D.N.-S. (1994) Degradative effects of ultraviolet light and acid rain on wood surface quality. *Wood and Fiber Science*, **26**, 185–191.

Hooper, D.U., Chapin, F.S., Ewel, J.J., Hector, A., Inchausti, P., Lavorel, S., Lawton, J.H., Lodge, D.M., Loreau, M., Naeem, S., Schmid, B., Setälä, H., Symstad, A.J., Vandermeer, J. & Wardle, D.A. (2005) Effects of biodiversity on ecosystem functioning: a consensus of current knowledge. *Ecological Monographs*, **75**, 3–35.

Hoppe, B., Kahl, T., Karasch, P., Wubet, T., Bauhus, J., Buscot, F. & Krüger, D. (2014) Network Analysis Reveals Ecological Links between N-Fixing Bacteria and Wood-Decaying Fungi. *PLoS ONE*, **9**, e88141.

Hubbell, S.P. (2001) *The Unified Neutral Theory of Biodiversity and Biogeography* (ed Princeton University Press). Princeton, NJ.

Hukka, A. & Viitanen, H.A. (1999) A mathematical model of mould growth on wooden material. *Wood Science and Technology*, **33**, 475–485.

Hulcr, J. & Dunn, R.R. (2011) The sudden emergence of pathogenicity in insect-fungus symbioses threatens naive forest ecosystems. *Proceedings. Biological sciences / The Royal Society*, **278**, 2866–73.

Hulcr, J., Rountree, N.R., Diamond, S.E., Stelinski, L.L., Fierer, N. & Dunn, R.R. (2012) Mycangia of ambrosia beetles host communities of bacteria. *Microbial ecology*, **64**, 784–93.

Hyodo, F., Tayasu, I., Inoue, T., Azuma, J.I., Kudo, T. & Abe, T. (2003) Differential role of

symbiotic fungi in lignin degradation and food provision for fungus-growing termites (Macrotermitinae: Isoptera). *Functional Ecology*, **17**, 186–193.

Jamieson, D.J. (1992) Saccharomyces cerevisiae has distinct adaptive responses to both hydrogen peroxide and menadione. *Journal of Bacteriology*, **174**, 6678–6681.

Johansen, J.E., Binnerup, S.J., Kroer, N. & Mølbak, L. (2005) *Luteibacter rhizovicinus* gen. nov., sp. nov., a yellow-pigmented gammaproteobacterium isolated from the rhizosphere of barley (Hordeum vulgare L.). *International journal of systematic and evolutionary microbiology*, **55**, 2285–91.

Johjima, T., Itoh, N., Kabuto, M., Tokimura, F., Nakagawa, T., Wariishi, H. & Tanaka, H. (1999) Direct interaction of lignin and lignin peroxidase from *Phanerochaete chrysosporium*. *Proceedings of the National Academy of Sciences of the United States of America*, **96**, 1989.

Jung, H.-M., Ten, L.N., Kim, K.-H., An, D.S., Im, W.-T. & Lee, S.-T. (2009) *Dyella ginsengisoli* sp. nov., isolated from soil of a ginseng field in South Korea. *International journal of systematic and evolutionary microbiology*, **59**, 460–5.

Junninen, K. & Komonen, A. (2011) Conservation ecology of boreal polypores: A review. *Biological Conservation*, **144**, 11–20.

Kamei, I., Yoshida, T., Enami, D. & Meguro, S. (2012) Coexisting *Curtobacterium* bacterium promotes growth of white-rot fungus *Stereum* sp. *Current Microbiology*, **64**, 173–178.

Kämpfer, P., Lodders, N. & Falsen, E. (2009) *Luteibacter anthropi* sp. nov., isolated from human blood, and reclassification of *Dyella yeojuensis* Kim et al. 2006 as *Luteibacter yeojuensis* comb. nov. *International journal of systematic and evolutionary microbiology*, **59**, 2884–7.

Kauffman, J.B., Cummings, D.L., Ward, D.E. & Babbitt, R. (1995) Fire in the Brazilian Amazon: 1. Biomass, nutrient pools, and losses in slashed primary forests. *Oecologia*, **104**, 397–408.

Kersten, P.J. (1990) Glyoxal oxidase of *Phanerochaete chrysosporium*: its characterization and activation by lignin peroxidase. *Proceedings of the National Academy of Sciences*, **87**, 2936–2940.

Khammar, N., Martin, G., Ferro, K., Job, D., Aragno, M. & Verrecchia, E. (2009) Use of the *frc* gene as a molecular marker to characterize oxalate-oxidizing bacterial abundance and

diversity structure in soil. *Journal of Microbiological Methods*, **76**, 120–127.

Kim, O.-S., Cho, Y.-J.Y.-J., Lee, K., Yoon, S.-H.S.-H., Kim, M., Na, H., Park, S.-C.S.-C., Jeon, Y.S., Lee, J.-H.J.-H., Yi, H., Won, S. & Chun, J. (2012) Introducing EzTaxon-e: a prokaryotic 16S rRNA gene sequence database with phylotypes that represent uncultured species. *International Journal of Systematic and Evolutionary Microbiology*, **62**, 716–721.

Kim, D.-W., Kim, A., Kim, R.N., Nam, S.-H., Kang, A., Chung, W.-T., Choi, S.-H. & Park, H.-S. (2010) Comparative analysis of expressed sequence tags from the white-rot fungi (*Phanerochaete chrysosporium*). *Molecules and Cells*, **29**, 131–144.

Kirby, R. (2005) *Actinomycetes* and Lignin Degradation. *Advances in Applied Microbiology* (ed S.S. (eds) Laskin AI, Bennett JW, Gadd GM), pp. 125–168. Elsevier Academic Press Inc, San Diego, USA.

Kirk, T.K. & Farrell, R.L. (1987) Enzymatic “combustion”: the microbial degradation of lignin. *Annual Reviews in Microbiology*, **41**, 465–505.

Kohlmeier, S., Smits, T.H.M., Ford, R.M., Keel, C., Harms, H. & Wick, L.Y. (2005) Taking the Fungal Highway: Mobilization of Pollutant-Degrading Bacteria by Fungi. *Environmental Science & Technology*, **39**, 4640–4646.

De Koker, T.H., Nakasone, K.K., Haarhof, J., Burdsall, H.H. & Janse, B.J.H. (2003) Phylogenetic relationships of the genus *Phanerochaete* inferred from the internal transcribed spacer region. *Mycological Research*, **107**, 1032–1040.

De Koker, T.H., Zhao, J., Cullen, D. & Janse, B.J.H. (1998) Biochemical and molecular characterization of South African strains of *Phanerochaete chrysosporium*. *Mycological Research*, **102**, 88–92.

Kong, C., Wang, L., Li, P., Qu, Y., Tang, H., Wang, J., Zhou, H., Ma, Q., Zhou, J. & Xu, P. (2013) Genome Sequence of *Dyella ginsengisoli* Strain LA-4, an Efficient Degrader of Aromatic Compounds. *Genome announcements*, **1**, e00961–13.

Ko, T.W.K., Stephenson, S.L., Jeewon, R., Lumyong, S. & Hyde, K.D. (2009) Molecular diversity of myxomycetes associated with decaying wood and forest floor leaf litter. *Mycologia*, **101**, 592–598.

Kost, T., Stopnisek, N., Agnoli, K., Eberl, L. & Weisskopf, L. (2014) Oxalotrophy, a widespread trait of plant-associated Burkholderia species, is involved in successful root

colonization of lupin and maize by *Burkholderia phytofirmans*. *Frontiers in microbiology*, **4**, 421.

Kubartová, A., Ottosson, E., Dahlberg, A. & Stenlid, J. (2012) Patterns of fungal communities among and within decaying logs, revealed by 454 sequencing. *Molecular Ecology*, **21**, 4514–4532.

Laiho, R. & Prescott, C.E. (2004) Decay and nutrient dynamics of coarse woody debris in northern coniferous forests: a synthesis. *Canadian Journal of Forest Research*, **34**, 763–777.

Lamlom, S.H. & Savidge, R.A. (2003) A reassessment of carbon content in wood: variation within and between 41 North American species. *Biomass and Bioenergy*, **25**, 381–388.

Landy, E.T., Mitchell, J.I., Hotchkiss, S. & Eaton, R.A. (2008) Bacterial diversity associated with archaeological waterlogged wood: Ribosomal RNA clone libraries and denaturing gradient gel electrophoresis (DGGE). *International Biodeterioration & Biodegradation*, **61**, 106–116.

Larkin, M.A., Blackshields, G., Brown, N.P., Chenna, R., McGettigan, P.A., McWilliam, H., Valentin, F., Wallace, I.M., Wilm, A., Lopez, R., Thompson, J.D., Gibson, T.J. & Higgins, D.G. (2007) Clustal W and Clustal X version 2.0. *Bioinformatics*, **23**, 2947–2948.

Larrondo, L.F., Vicuna, R. & Cullen, D. (2005) *Phanerochaete chrysosporium* genomics. *Applied Mycology and Biotechnology*, **5**, 315–352.

Larsson, K.-H. (2007) Re-thinking the classification of corticioid fungi. *Mycological Research*, **111**, 1040–1063.

Lecomte, J., St-Arnaud, M. & Hijri, M. (2011) Isolation and identification of soil bacteria growing at the expense of arbuscular mycorrhizal fungi. *FEMS Microbiology Letters*, **317**, 43–51.

Lee, C.S., Jung, Y.-T., Park, S., Oh, T.-K. & Yoon, J.-H. (2010) *Lysinibacillus xylanilyticus* sp. nov., a xylan-degrading bacterium isolated from forest humus. *International journal of systematic and evolutionary microbiology*, **60**, 281–6.

Lekounougou, S., Mounguengui, S., Dumarçay, S., Rose, C., Courty, P.E., Garbaye, J., Gérardin, P., Jacquot, J.P. & Gelhaye, E. (2008) Initial stages of Fagus sylvatica wood colonization by the white-rot basidiomycete *Trametes versicolor*: Enzymatic

characterization. *International Biodeterioration & Biodegradation*, **61**, 287–293.

Leonowicz, A., Cho, N., Luterek, J., Wilkolazka, A., Wojtas-Wasilewska, M., Matuszewska, A., Hofrichter, M., Wesenberg, D. & Rogalski, J. (2001) Fungal laccase: properties and activity on lignin. *Journal of Basic Microbiology*, **41**, 185–227.

Lequy, E., Calvaruso, C., Conil, S. & Turpault, M.-P. (2014) Atmospheric particulate deposition in temperate deciduous forest ecosystems: Interactions with the canopy and nutrient inputs in two beech stands of Northeastern France. *The Science of the total environment*, **487**, 206–15.

Levasseur, A., Drula, E., Lombard, V., Coutinho, P.M. & Henrissat, B. (2013) Expansion of the enzymatic repertoire of the CAZy database to integrate auxiliary redox enzymes. *Biotechnology for biofuels*, **6**, 41.

Leveau, J.H.J. & Preston, G.M. (2008) Bacterial mycophagy: definition and diagnosis of a unique bacterial-fungal interaction. *The New phytologist*, **177**, 859–876.

Leveau, J.H.J., Uroz, S. & De Boer, W. (2010) The bacterial genus *Collimonas*: mycophagy, weathering and other adaptive solutions to life in oligotrophic soil environments. *Environmental Microbiology*, **12**, 281–292.

Levy, A., Chang, B.J., Abbott, L.K., Kuo, J., Harnett, G. & Inglis, T.J.J. (2003) Invasion of Spores of the Arbuscular Mycorrhizal Fungus *Gigaspora decipiens* by *Burkholderia* spp. *Applied and Environmental Microbiology*, **69**, 6250–6256.

Lewis, N.G. & Yamamoto, E. (1990) Lignin: occurrence, biogenesis and biodegradation. *Annual review of plant physiology and plant molecular biology*, **41**, 455–96.

Liers, C., Ullrich, R., Steffen, K.T., Hatakka, A. & Hofrichter, M. (2006) Mineralization of 14C-labelled synthetic lignin and extracellular enzyme activities of the wood-colonizing ascomycetes *Xylaria hypoxylon* and *Xylaria polymorpha*. *Applied Microbiology and Biotechnology*, **69**, 573–579.

Lim, Y.W., Baik, K.S., Chun, J., Lee, K.H., Jung, W.J. & Bae, K.S. (2007) Accurate delimitation of *Phanerochaete chrysosporium* and *Phanerochaete sordida* by specific PCR primers and cultural approach. *Journal of Microbiology and Biotechnology*, **17**, 468–473.

Lim, Y.W., Baik, S.K., Han, S.K., Kim, B.S. & Bae, K.S. (2003) *Burkholderia sordidicola* sp. nov., isolated from the white-rot fungus *Phanerochaete sordida*. *International Journal of*

Systematic and Evolutionary Microbiology, **53**, 1631–1636.

Lindahl, V. & Bakken, L.R. (1995) Evaluation of methods for extraction of bacteria from soil. *FEMS Microbiology Ecology*, **16**, 135–142.

Li, J., Yuan, H. & Yang, J. (2008) Bacteria and lignin degradation. *Frontiers of Biology in China*, **4**, 29–38.

Longuetaud, F., Mothe, F., Kerautret, B., Krähenbühl, A., Hory, L., Leban, J.M. & Debled-Rennesson, I. (2012) Automatic knot detection and measurements from X-ray CT images of wood: A review and validation of an improved algorithm on softwood samples. *Computers and Electronics in Agriculture*, **85**, 77–89.

Longuetaud, F., Mothe, F. & Leban, J.-M. (2007) Automatic detection of the heartwood/sapwood boundary within Norway spruce (*Picea abies* (L.) Karst.) logs by means of CT images. *Computers and Electronics in Agriculture*, **58**, 100–111.

Loreau, M., Naeem, S., Inchausti, P., Bengtsson, J., Grime, J.P., Hector, A., Hooper, D.U., Huston, M.A., Raffaelli, D., Schmid, B., Tilman, D. & Wardle, D.A. (2001) Biodiversity and ecosystem functioning: current knowledge and future challenges. *Science*, **294**, 804–8.

Lozupone, C., Hamady, M. & Knight, R. (2006) UniFrac - an online tool for comparing microbial community diversity in a phylogenetic context. *BMC bioinformatics*, **7**, 371.

Lozupone, C. & Knight, R. (2005) UniFrac: a New Phylogenetic Method for Comparing Microbial Communities. *Applied and Environmental Microbiology*, **71**, 8228–8235.

Lynd, L.R., Weimer, P.J., Van Zyl, W.H. & Pretorius, I.S. (2002) Microbial Cellulose Utilization: Fundamentals and Biotechnology. *Microbiology and Molecular Biology Reviews*, **66**, 506–577.

Macchioni, N., Palanti, S. & Rozenberg, P. (2007) Measurements of fungal wood decay on Scots pine and beech by means of X-ray microdensitometry. *Wood Science and Technology*, **41**, 417–426.

Machado, K.M.G., Matheus, D.R. & Bononi, V.L.R. (2005) Ligninolytic enzymes production and Remazol Brilliant Blue R decolorization by tropical Brazilian basidiomycetes fungi. *Brazilian Journal of Microbiology*, **36**, 246–252.

Mackensen, J., Bauhus, J. & Webber, E. (2003) Decomposition rates of coarse woody debris—A review with particular emphasis on Australian tree species. *Australian Journal of*

Botany, **51**, 27.

Martin, K. & Eadie, J.M. (1999) Nest webs: A community-wide approach to the management and conservation of cavity-nesting forest birds. *Forest Ecology and Management*, **115**, 243–257.

Martinez, D., Larrondo, L.F., Putnam, N., Gelpke, M.D.S., Huang, K., Chapman, J., Helfenbein, K.G., Ramaiya, P., Detter, J.C., Larimer, F., Coutinho, P.M., Henrissat, B., Berka, R., Cullen, D. & Rokhsar, D. (2004) Genome sequence of the lignocellulose degrading fungus *Phanerochaete chrysosporium* strain RP78. *Nature biotechnology*, **22**, 695–700.

Martinez, S. & Nakasone, K.K. (2005) The genus *Phanerochaete* (Corticiaceae, Basidiomycotina) *sensu lato* in Uruguay. *Sydowia*, **57**, 94–101.

Martínez, A.T., Speranza, M., Ruiz-Dueñas, F.J., Ferreira, P., Camarero, S., Guillén, F., Martínez, M.J., Gutiérrez, A. & del Río, J.C. (2005) Biodegradation of lignocellulosics: microbial, chemical, and enzymatic aspects of the fungal attack of lignin. *International Microbiology*, **8**, 195–204.

Martin, G., Guggiari, M., Bravo, D., Zopfi, J., Cailleau, G., Aragno, M., Job, D., Verrecchia, E. & Junier, P. (2012) Fungi, bacteria and soil pH: the oxalate-carbonate pathway as a model for metabolic interaction. *Environmental Microbiology*, **14**, 2960–2970.

Masai, E., Katayama, Y. & Fukuda, M. (2007) Genetic and Biochemical Investigations on Bacterial Catabolic Pathways for Lignin-Derived Aromatic Compounds. *Bioscience, Biotechnology, and Biochemistry*, **71**, 1–15.

Mathieu, Y. (2012) *Diversité Écologique et Fonctionnelle Des Champignons Décomposeurs Du Bois : L'influence Du Substrat de La Communauté À L'enzyme*. Université de Lorraine.

Mathieu, Y., Dassé, A., Lebayon, I., Kutnik, M., Harvengt, L., Gelhaye, E. & Buée, M. (2013a) High-throughput sequencing highlighted contrasted pioneer fungal communities associated to coniferous and deciduous wood preservation assays. *The 44th Annual Meeting of the IRG* Stockholm, Sweden.

Mathieu, Y., Gelhaye, E., Dumarçay, S., Gérardin, P., Harvengt, L. & Buée, M. (2013b) Selection and validation of enzymatic activities as functional markers in wood biotechnology and fungal ecology. *Journal of microbiological methods*, **92**, 157–63.

Mba Medie, F., Davies, G.J., Drancourt, M. & Henrissat, B. (2012) Genome analyses highlight the different biological roles of cellulases. *Nature Reviews Microbiology*, **10**, 227–34.

McCay, T.S. (2000) Use of woody debris by cotton mice (*Peromyscus gossypinus*) in a southeastern pine forest. *Journal of Mammalogy*, **81**, 527–535.

McDonald, I.R. & Murrell, J.C. (1997) The methanol dehydrogenase structural gene *mxaF* and its use as a functional gene probe for methanotrophs and methylotrophs. *Applied and environmental microbiology*, **63**, 3218–3224.

McDonald, R., Schreier, H.J. & Watts, J.E.M. (2012) Phylogenetic analysis of microbial communities in different regions of the gastrointestinal tract in *Panaque nigrolineatus*, a wood-eating fish. *PLoS One*, **7**, e48018.

Meerts, P. (2002) Mineral nutrient concentrations in sapwood and heartwood: a literature review. *Annals of Forest Science*, **59**, 713–722.

Meidute, S., Demoling, F. & Bååth, E. (2008) Antagonistic and synergistic effects of fungal and bacterial growth in soil after adding different carbon and nitrogen sources. *Soil Biology and Biochemistry*, **40**, 2334–2343.

Michaelsen, A., Piñar, G. & Pinzari, F. (2010) Molecular and microscopical investigation of the microflora inhabiting a deteriorated Italian manuscript dated from the thirteenth century. *Microbial ecology*, **60**, 69–80.

Mikesková, H., Novotný, C., Svobodová, K. & Novotný, Č. (2012) Interspecific interactions in mixed microbial cultures in a biodegradation perspective. *Applied Microbiology and Biotechnology*, **95**, 861–70.

Mille-Lindblom, C., Fischer, H. & J. Tranvik, L. (2006) Antagonism between bacteria and fungi: substrate competition and a possible tradeoff between fungal growth and tolerance towards bacteria. *Oikos*, **113**, 233–242.

Mille-Lindblom, C. & Tranvik, L.J. (2003) Antagonism between bacteria and fungi on decomposing aquatic plant litter. *Microbial ecology*, **45**, 173–82.

Møller, J., Miller, M. & Kjøller, A. (1999) Fungal–bacterial interaction on beech leaves: influence on decomposition and dissolved organic carbon quality. *Soil Biology and Biochemistry*, **31**, 367–374.

Morel, M., Meux, E., Mathieu, Y., Thuillier, A., Chibani, K., Harvengt, L., Jacquot, J.-P. &

Gelhaye, E. (2013) Xenomic networks variability and adaptation traits in wood decaying fungi. *Microbial Biotechnology*, **6**, 248–263.

Mowat, E., Rajendran, R., Williams, C., McCulloch, E., Jones, B., Lang, S. & Ramage, G. (2010) *Pseudomonas aeruginosa* and their small diffusible extracellular molecules inhibit *Aspergillus fumigatus* biofilm formation. *FEMS microbiology letters*, **313**, 96–102.

Mueller, U.G. & Gerardo, N. (2002) Fungus-farming insects: multiple origins and diverse evolutionary histories. *Proceedings of the National Academy of Sciences of the United States of America*, **99**, 15247–9.

Murray, A.C. & Woodward, S. (2007) Temporal changes in functional diversity of culturable bacteria populations in Sitka spruce stumps. *Forest Pathology*, **37**, 217–235.

Nazir, R., Warmink, J.A., Voordes, D.C., van de Bovenkamp, H.H. & van Elsas, J.D. (2013) Inhibition of mushroom formation and induction of glycerol release-ecological strategies of *Burkholderia terrae* BS001 to create a hospitable niche at the fungus *Lyophyllum* sp. strain Karsten. *Microbial ecology*, **65**, 245–54.

Noll, M., Naumann, A., Ferrero, F. & Malow, M. (2010) Exothermic processes in industrial-scale piles of chipped pine-wood are linked to shifts in gamma-, alphaproteobacterial and fungal ascomycete communities. *International Biodeterioration & Biodegradation*, **64**, 629–637.

Nuccio, E.E., Hodge, A., Pett-Ridge, J., Herman, D.J., Weber, P.K. & Firestone, M.K. (2013) An arbuscular mycorrhizal fungus significantly modifies the soil bacterial community and nitrogen cycling during litter decomposition. *Environmental Microbiology*, **15**, 1870–1881.

Ohkuma, M. (2003) Termite symbiotic systems: efficient bio-recycling of lignocellulose. *Applied microbiology and biotechnology*, **61**, 1–9.

Oh, D.-C., Scott, J.J., Currie, C.R. & Clardy, J. (2009) Mycangimycin, a polyene peroxide from a mutualist *Streptomyces* sp. *Organic letters*, **11**, 633–6.

Oksanen, J., Blanchet, F.G., Kindt, R., Legendre, P., O'Hara, R.B., Simpson, G.L., Solymos, P., Stevens, M.H.H. & Wagner, H. (2012) vegan: Community Ecology Package. *R package version*, **1**, R package version 2.0–4.

Ostrofsky, A., Jellison, J., Smith, K.T. & Shortle, W.C. (1997) Changes in cation

concentrations in red spruce wood decayed by brown rot and white rot fungi. *Canadian Journal of Forest Research*, **27**, 567–571.

Otjen, L. & Blanchette, R.A. (1986) A discussion of microstructural changes in wood during decomposition by white rot basidiomycetes. *Canadian Journal of Botany*, **64**, 905–911.

Palmer, J.D., Soltis, D.E. & Chase, M.W. (2004) The plant tree of life: an overview and some points of view. *American journal of botany*, **91**, 1437–45.

Palviainen, M.;, Laiho, R.;, Mäkinen, H.; & Finér, L. (2008) Do decomposing Scots pine, Norway spruce, and silver birch stems retain nitrogen? *Canadian Journal of Forest Research*, **38**, 3047–3055.

Parmasto, E., Nilsson, R.H. & Larsson, H. (2004) Cortbase version 2 – extensive updates of a nomenclatural database for corticioid fungi (*Hymenomycetes*). *PhyloInformatics*, **5**, 1–7.

Partida-Martinez, L.P., Groth, I., Schmitt, I., Richter, W., Roth, M. & Hertweck, C. (2007) *Burkholderia rhizoxinica* sp. nov. and *Burkholderia endofungorum* sp. nov., bacterial endosymbionts of the plant-pathogenic fungus Rhizopus microsporus. *International Journal of Systematic and Evolutionary Microbiology*, **57**, 2583–2590.

Pereira, H., Graça, J. & Rodrigues, J.C. (2003) Wood chemistry in relation to quality. *Wood quality and its biological basis*, Oxford pp. 30–52. Blackweel Publishing.

Pérez, J., Muñoz-Dorado, J., de la Rubia, T. & Martínez, J. (2002) Biodegradation and biological treatments of cellulose, hemicellulose and lignin: an overview. *International microbiology : the official journal of the Spanish Society for Microbiology*, **5**, 53–63.

Péter, G., Dlauchy, D., Tornai-Lehoczki, J., Suzuki, M. & Kurtzman, C.P. (2011) *Spencermartinsiella europaea* gen. nov., sp. nov., a new member of the family *Trichomonascaceae*. *International journal of systematic and evolutionary microbiology*, **61**, 993–1000.

Péter, G., Tornai-Lehoczki, J., Fülöp, L. & Dlauchy, D. (2003) Six new methanol assimilating yeast species from wood material. *Antonie van Leeuwenhoek*, **84**, 147–159.

Piñar, G., Sterflinger, K. & Pinzari, F. (2014) Unmasking the measles-like parchment discoloration: molecular and microanalytical approach. *Environmental microbiology*.

Pinheiro, J., Bates, D., DebRoy, S., Sarkar, D. & R Core Team. (2011) nlme: Linear and Nonlinear Mixed Effects Models.

Preston, J., Smith, A.D., Schofield, E.J., Chadwick, A. V, Jones, M.A. & Watts, J.E.M. (2014) The effects of Mary rose conservation treatment on iron oxidation processes and microbial communities contributing to Acid production in marine archaeological timbers. *PloS one*, **9**, e84169.

Prewitt, L., Kang, Y., Kakumanu, M.L. & Williams, M. (2014) Fungal and Bacterial Community Succession Differs for Three Wood Types during Decay in a Forest Soil. *Microbial ecology*.

Prosser, J.I. (2010) Replicate or lie. *Environmental Microbiology*, **12**, 1806–1810.

Pruesse, E., Quast, C., Knittel, K., Fuchs, B.M., Ludwig, W., Peplies, J. & Glöckner, F.O. (2007) SILVA: a comprehensive online resource for quality checked and aligned ribosomal RNA sequence data compatible with ARB. *Nucleic Acids Research*, **35**, 7188–7196.

Pu, Y., Kosa, M., Kalluri, U.C., Tuskan, G.A. & Ragauskas, A.J. (2011) Challenges of the utilization of wood polymers: how can they be overcome? *Applied microbiology and biotechnology*, **91**, 1525–36.

Pylro, V.S., de Freitas, A.L.M., Otoni, W.C., da Silva, I.R., Borges, A.C. & Costa, M.D. (2013) Calcium oxalate crystals in eucalypt ectomycorrhizae: morphochemical characterization. (ed A Guerrero-Hernandez). *PloS one*, **8**, e67685.

Quinto, J., Marcos-García, M.Á., Díaz-Castelazo, C., Rico-Gray, V., Brustel, H., Galante, E. & Micó, E. (2012) Breaking down complex Saproxylic communities: understanding sub-networks structure and implications to network robustness. *PloS one*, **7**, e45062.

Råberg, U., Terziev, N. & Daniel, G. (2013) Degradation of Scots pine and beech wood exposed in four test fields used for testing of wood preservatives. *International Biodeterioration & Biodegradation*, **79**, 20–27.

Radtke, C., Cook, W. & Anderson, A. (1994) Factors affecting antagonism of the growth of *Phanerochaete chrysosporium* by bacteria isolated from soils. *Applied Microbiology and Biotechnology*, **41**, 274–280.

Rajala, T., Peltoniemi, M., Hantula, J., Mäkipää, R. & Pennanen, T. (2011) RNA reveals a succession of active fungi during the decay of Norway spruce logs. *Fungal Ecology*, **4**, 437–448.

Rajala, T., Peltoniemi, M., Pennanen, T. & Mäkipää, R. (2012) Fungal community dynamics

in relation to substrate quality of decaying Norway spruce (Picea abies [L.] Karst.) logs in boreal forests. *FEMS microbiology ecology*, **81**, 494–505.

Ramachandra, M., Crawford, D.L. & Hertel, G. (1988) Characterization of an extracellular lignin peroxidase of the lignocellulolytic actinomycete *Streptomyces viridosporus*. *Applied and environmental microbiology*, **54**, 3057.

Rappé, M., Giovannoni, S.S.J. & Rappe, M.S. (2003) The uncultured microbial majority. *Annual Reviews in Microbiology*, **57**, 369–394.

R Development Core Team. (2013) R: A Language and Environment for Statistical Computing.

Reich, P.B. & Oleksyn, J. (2004) Global patterns of plant leaf N and P in relation to temperature and latitude. *Proceedings of the National Academy of Sciences of the United States of America*, **101**, 11001–11006.

Reid, N.M., Addison, S.L., Macdonald, L.J. & Lloyd-Jones, G. (2011) Biodiversity of active and inactive bacteria in the gut flora of wood-feeding huhu beetle larvae (*Prionoplus reticularis*). *Applied and Environmental Microbiology*, **77**, 7000–7006.

Renvall, P. (1995) Community structure and dynamics of wood-rotting Basidiomycetes on decomposing conifer trunks in northern Finland. *Karstenia*, **35**, 1–51.

Robinson, J.M. (1990) Lignin, land plants, and fungi: Biological evolution affecting Phanerozoic oxygen balance. *Geology*, **18**, 607–610.

Rodríguez Couto, S. & Toca Herrera, J.L. (2006) Industrial and biotechnological applications of laccases: a review. *Biotechnology advances*, **24**, 500–13.

Romaní, A.M., Fischer, H., Mille-Lindblom, C. & Tranvik, L.J. (2006) Interactions of bacteria and fungi on decomposing litter: differential extracellular enzyme activities. *Ecology*, **87**, 2559–2569.

Romano, J. & Kolter, R. (2005) *Pseudomonas-Saccharomyces* interactions: influence of fungal metabolism on bacterial physiology and survival. *Journal of bacteriology*, **187**, 940–948.

Romero, L.M., Smith, T.J. & Fourqurean, J.W. (2005) Changes in mass and nutrient content of wood during decomposition in a south Florida mangrove forest. *Journal of Ecology*, **93**, 618–631.

De Rosnay, J. (1975) *Le Macroscope, Vers Une Vision Globale*.

Ruiz-Dueñas, F.J., Camarero, S., Pérez-Boada, M., Martínez, M.J. & Martínez, A.T. (2001) A new versatile peroxidase from *Pleurotus*. *Biochemical Society Transactions*, **29**, 116.

Sahin, N. (2003) Oxalotrophic bacteria. *Research in Microbiology*, **154**, 399–407.

Savory, J.G. (1954) Breakdown of timber by ascomycetes and fungi imperfecti. *Annals of Applied Biology*, **41**, 336–347.

Schellenberger, S., Kolb, S. & Drake, H.L. (2010) Metabolic responses of novel cellulolytic and saccharolytic agricultural soil bacteria to oxygen. *Environmental Microbiology*, **12**, 845–861.

Schloss, P.D. (2009) A high-throughput DNA sequence aligner for microbial ecology studies. *PloS One*, **4**, e8230.

Schloss, P.D., Gevers, D. & Westcott, S.L. (2011) Reducing the effects of PCR amplification and sequencing artifacts on 16S rRNA-based studies. *PloS One*, **6**, e27310.

Schloss, P.D., Westcott, S.L., Ryabin, T., Hall, J.R., Hartmann, M., Hollister, E.B., Lesniewski, R.A., Oakley, B.B., Parks, D.H., Robinson, C.J., Sahl, J.W., Stres, B., Thallinger, G.G., Van Horn, D.J. & Weber, C.F. (2009) Introducing mothur: open-source, platform-independent, community-supported software for describing and comparing microbial communities. *Applied and Environmental Microbiology*, **75**, 7537–7541.

Schmidt, O. (2007) Indoor wood-decay basidiomycetes: damage, causal fungi, physiology, identification and characterization, prevention and control. *Mycological Progress*, **6**, 281–281.

Schneider, C.A., Rasband, W.S. & Eliceiri, K.W. (2012) NIH Image to ImageJ: 25 years of image analysis. *Nature Methods*, **9**, 671–675.

Schoch, C.L., Seifert, K.A., Huhndorf, S., Robert, V., Spouge, J.L., Levesque, C.A. & Chen, W. (2012) Nuclear ribosomal internal transcribed spacer (ITS) region as a universal DNA barcode marker for Fungi. *Proceedings of the National Academy of Sciences of the United States of America*, **109**, 6241–6.

Schowalter, T.D. (1992) Heterogeneity of decomposition and nutrient dynamics of oak (*Quercus*) logs during the first 2 years of decomposition. *Canadian Journal of Forest Research*, **22**, 161–166.

Schowalter, T.D., Zhang, Y.L. & Sabin, T.E. (1998) Decomposition and nutrient dynamics of oak *Quercus* spp. logs after five years of decomposition. *Ecography*, **21**, 3–10.

Schwanninger, M., Hinterstoisser, B., Gradinger, C., Messner, K. & Fackler, K. (2004) Examination of spruce wood biodegraded by *Ceriporiopsis subvermispora* using near and mid infrared spectroscopy. *Journal of Near Infrared Spectroscopy*, **12**, 397–409.

Schwarze, F.W.M.R. (2007) Wood decay under the microscope. *Fungal Biology Reviews*, **21**, 133–170.

Schwarze, F.W.M.R., Engels, J. & Mattheck, C. (2004) *Fungal Strategies of Wood Decay in Trees*, Second edi (ed Springer). Berlin Heidelberg New York.

Scott, J.J., Oh, D.-C., Yuceer, M.C., Klepzig, K.D., Clardy, J. & Currie, C.R. (2008) Bacterial protection of beetle-fungus mutualism. *Science (New York, N.Y.)*, **322**, 63.

Seigle-Murandi, F., Guiraud, P., Croize, J., Falsen, E. & Eriksson, K.L. (1996) Bacteria Are Omnipresent on *Phanerochaete chrysosporium* Burdsall. *Applied and Environmental Microbiology*, **62**, 2477–2481.

Shade, A. & Handelsman, J. (2012) Beyond the Venn diagram: the hunt for a core microbiome. *Environmental Microbiology*, **14**, 4–12.

Sheneman, L., Evans, J. & Foster, J.A. (2006) Clearcut: a fast implementation of relaxed neighbor joining. *Bioinformatics*, **22**, 2823–2824.

Shi, T., Fredrickson, J.K. & Balkwill, D.L. (2001) Biodegradation of polycyclic aromatic hydrocarbons by *Sphingomonas* strains isolated from the terrestrial subsurface. *Journal of Industrial Microbiology and Biotechnology*, **26**, 283–289.

Shimada, M., Ma, D.-B., Akamatsu, Y. & Hattori, T. (1994) A proposed role of oxalic acid in wood decay systems of wood-rotting basidiomycetes. *FEMS Microbiology Reviews*, **13**, 285–295.

Shim, S.-S. & Kawamoto, K. (2002) Enzyme production activity of *Phanerochaete chrysosporium* and degradation of pentachlorophenol in a bioreactor. *Water research*, **36**, 4445–4454.

Singh, A.P. (2007) Role of electron microscopy in understanding deterioration of wooden objects of cultural heritage. *COST Meeting* Hamburg.

Singh, A.P. & Butcher, J.A. (1991) Bacterial degradation of wood cell walls: a review of

degradation patterns. *Journal of the Institute of Wood Science*, **12**, 143–157.

Singh, P., Sulaiman, O., Hashim, R., Rupani, P.F. & Peng, L.C. (2010) Biopulping of lignocellulosic material using different fungal species: a review. *Reviews in Environmental Science and Biotechnology*, **9**, 141–151.

Sinsabaugh, R.L., Antibus, R.K., Linkins, A.E., McClaugherty, C.A., Rayburn, L., Repert, D. & Weiland, T. (1992) Wood decomposition over a first-order watershed: Mass loss as a function of lignocellulase activity. *Soil Biology and Biochemistry*, **24**, 743–749.

Sinsabaugh, R.L. & Follstad Shah, J.J. (2012) Ecoenzymatic Stoichiometry and Ecological Theory. *Annual Review of Ecology, Evolution, and Systematics*, **43**, 313–343.

Sinsabaugh, R.L., Hill, B.H. & Follstad Shah, J.J. (2009) Ecoenzymatic stoichiometry of microbial organic nutrient acquisition in soil and sediment. *Nature*, **462**, 795–8.

Sinsabaugh, R.L., Lauber, C.L., Weintraub, M.N., Ahmed, B., Allison, S.D., Crenshaw, C., Contosta, A.R., Cusack, D., Frey, S., Gallo, M.E., Gartner, T.B., Hobbie, S.E., Holland, K., Keeler, B.L., Powers, J.S., Stursova, M., Takacs-Vesbach, C., Waldrop, M.P., Wallenstein, M.D., Zak, D.R. & Zeglin, L.H. (2008) Stoichiometry of soil enzyme activity at global scale. *Ecology Letters*, **11**, 1252–64.

Šnajdr, J., Dobiášová, P., Větrovský, T., Valášková, V., Alawi, A., Boddy, L. & Baldrian, P. (2011) Saprotrophic basidiomycete mycelia and their interspecific interactions affect the spatial distribution of extracellular enzymes in soil. *FEMS Microbiology Ecology*, **78**, 80–90.

Son, H.-M., Yang, J.-E., Yi, E.-J., Park, Y., Won, K.-H., Kim, J.-H., Han, C.-K., Kook, M. & Yi, T.-H. (2013) *Dyella kyungheensis* sp. nov., isolated from the soil of a cornus fruit field. *International journal of systematic and evolutionary microbiology*, **63**, 3807–3811.

Spears, J.D.H. & Lajtha, K. (2004) The imprint of coarse woody debris on soil chemistry in the Western Oregon Cascades. *Biogeochemistry*, **71**, 163–175.

Srebotnik, E. & Messner, K. (1994) A Simple Method That Uses Differential Staining and Light Microscopy To Assess the Selectivity of Wood Delignification by White Rot Fungi. *Applied and Environmental Microbiology*, **60**, 1383–1386.

Stamatakis, A. (2006) RAxML-VI-HPC: maximum likelihood-based phylogenetic analyses with thousands of taxa and mixed models. *Bioinformatics*, **22**, 2688–2690.

Stewart, E.J. (2012) Growing unculturable bacteria. *Journal of Bacteriology*, **194**, 4151–60.

Stewart, P., Gaskell, J. & Cullen, D. (2000) A Homokaryotic Derivative of a *Phanerochaete chrysosporium* Strain and Its Use in Genomic Analysis of Repetitive Elements. *Applied and Environmental Microbiology*, **66**, 1629–1633.

Stockland, J.N., Siitonen, J. & Jonsson, B.G. (2012) *Biodiversity in Dead Wood*, Cambridge. Cambridge.

Stopnisek, N., Bodenhausen, N., Frey, B., Fierer, N., Eberl, L. & Weisskopf, L. (2013) Genus-wide acid tolerance accounts for the biogeographical distribution of soil *Burkholderia* populations. *Environmental microbiology*, n/a–n/a.

Stursová, M., Zifčáková, L., Leigh, M.B., Burgess, R. & Baldrian, P. (2012) Cellulose utilization in forest litter and soil: identification of bacterial and fungal decomposers. *FEMS microbiology ecology*, **80**, 735–46.

Sundquist, A., Bigdeli, S., Jalili, R., Druzin, M.L., Waller, S., Pullen, K.M., El-Sayed, Y.Y., Taslimi, M.M., Batzoglou, S. & Ronaghi, M. (2007) Bacterial flora-typing with targeted, chip-based Pyrosequencing. *BMC Microbiology*, **7**, 108.

Sun, H., Terhonen, E., Kasanen, R. & Asiegbu, F.O. (2014) Diversity and Community Structure of Primary Wood-Inhabiting Bacteria in Boreal Forest. *Geomicrobiology Journal*, **31**, 315–324.

Suzuki, H., Macdonald, J., Syed, K., Salamov, A., Hori, C., Aerts, A., Henrissat, B., Wiebenga, A., Vankuyk, P.A., Barry, K., Lindquist, E., Labutti, K., Lapidus, A., Lucas, S., Coutinho, P., Gong, Y., Samejima, M., Mahadevan, R., Abou-Zaid, M., de Vries, R.P., Igarashi, K., Yadav, J.S., Grigoriev, I. V & Master, E.R. (2012) Comparative genomics of the white-rot fungi, *Phanerochaete carnosa* and P. *chrysosporium*, to elucidate the genetic basis of the distinct wood types they colonize. *BMC genomics*, **13**, 444.

Takahashi, K. & Hada, Y. (2009) Distribution of Myxomycetes on coarse woody debris of *Pinus densiflora* at different decay stages in secondary forests of western Japan. *Mycoscience*, **50**, 253–260.

Teather, R.M. & Wood, P.J. (1982) Use of Congo red-polysaccharide interactions in enumeration and characterization of cellulolytic bacteria from the bovine rumen. *Applied and Environmental Microbiology*, **43**, 777–80.

Tian, B.-Y., Huang, Q.-G., Xu, Y., Wang, C.-X., Lv, R.-R. & Huang, J.-Z. (2009) Microbial community structure and diversity in a native forest wood-decomposed hollow-stump

ecosystem. *World Journal of Microbiology and Biotechnology*, **26**, 233–240.

Tien, M. & Kirk, T.K. (1983) Lignin-Degrading Enzyme from the Hymenomycete *Phanerochaete chrysosporium* Burds. *Science*, **221**, 661 –663.

Tokuda, G. & Watanabe, H. (2007) Hidden cellulases in termites: revision of an old hypothesis. *Biology letters*, **3**, 336–9.

Toljander, Y.K., Lindahl, B.D., Holmer, L. & Högberg, N.O.S. (2006) Environmental fluctuations facilitate species co-existence and increase decomposition in communities of wood decay fungi. *Oecologia*, **148**, 625–631.

Tornberg, K., Baath, E. & Olsson, S. (2003) Fungal growth and effects of different wood decomposing fungi on the indigenous bacterial community of polluted and unpolluted soils. *Biology and Fertility of Soils*, **37**, 190–197.

Tuason, M.M.S. & Arocena, J.M. (2009) Calcium oxalate biomineralization by *Piloderma fallax* in response to various levels of calcium and phosphorus. *Applied and environmental microbiology*, **75**, 7079–85.

Tuor, U., Winterhalter, K. & Fiechter, A. (1995) Enzymes of white-rot fungi involved in lignin degradation and ecological determinants for wood decay. *Journal of Biotechnology*, **41**, 1–17.

Ulrich, A., Klimke, G. & Wirth, S. (2008) Diversity and activity of cellulose-decomposing bacteria, isolated from a sandy and a loamy soil after long-term manure application. *Microbial Ecology*, **55**, 512–22.

Ulyshen, M.D. & Wagner, T.L. (2013) Quantifying arthropod contributions to wood decay (ed H Muller-Landau). *Methods in Ecology and Evolution*, **4**, 345–352.

Um, S., Fraimout, A., Sapountzis, P., Oh, D.-C. & Poulsen, M. (2013) The fungus-growing termite *Macrotermes natalensis* harbors bacillaene-producing *Bacillus* sp. that inhibit potentially antagonistic fungi. *Scientific reports*, **3**, 3250.

Uroz, S., Calvaruso, C., Turpault, M.P., Pierrat, J.C., Mustin, C. & Frey-Klett, P. (2007) Effect of the mycorrhizosphere on the genotypic and metabolic diversity of the bacterial communities involved in mineral weathering in a forest soil. *Applied and environmental microbiology*, **73**, 3019–27.

Uroz, S., Oger, P., Morin, E. & Frey-Klett, P. (2012) Distinct ectomycorrhizospheres share similar bacterial communities as revealed by pyrosequencing-based analysis of 16S

rRNA genes. *Applied and Environmental Microbiology*, **78**, 3020–3024.

Ushio, M., Miki, T. & Balser, T.C. (2013) A coexisting fungal-bacterial community stabilizes soil decomposition activity in a microcosm experiment. *PloS One*, **8**, e80320.

Valásková, V., de Boer, W., Gunnewiek, P.J.A.K., Pospísek, M. & Baldrian, P. (2009) Phylogenetic composition and properties of bacteria coexisting with the fungus *Hypholoma fasciculare* in decaying wood. *The ISME journal*, **3**, 1218–21.

Valášková, V., Šnajdr, J., Bittner, B., Cajthaml, T., Merhautová, V., Hofrichter, M. & Baldrian, P. (2007) Production of lignocellulose-degrading enzymes and degradation of leaf litter by saprotrophic basidiomycetes isolated from a *Quercus petraea* forest. *Soil Biology and Biochemistry*, **39**, 2651–2660.

Vanderwel, M.C., Malcolm, J.R., Smith, S.M. & Islam, N. (2006) Insect community composition and trophic guild structure in decaying logs from eastern Canadian pine-dominated forests. *Forest Ecology and Management*, **225**, 190–199.

Vaninsberghe, D., Hartmann, M., Stewart, G.R. & Mohn, W.W. (2013) Isolation of a Substantial Proportion of Forest Soil Bacterial Communities Detected via Pyrotag Sequencing. *Applied and environmental microbiology*, **79**, 2096–8.

Vannette, R.L., Gauthier, M.-P.L. & Fukami, T. (2013) Nectar bacteria, but not yeast, weaken a plant-pollinator mutualism. *Proceedings. Biological sciences / The Royal Society*, **280**, 20122601.

Větrovský, T., Steffen, K.T. & Baldrian, P. (2014) Potential of Cometabolic Transformation of Polysaccharides and Lignin in Lignocellulose by Soil Actinobacteria. *PLoS ONE*, **9**, e89108.

Visser, A.A., Nobre, T., Currie, C.R., Aanen, D.K. & Poulsen, M. (2012) Exploring the potential for actinobacteria as defensive symbionts in fungus-growing termites. *Microbial Ecology*, **63**, 975–85.

Vorob'ev, A. V., de Boer, W., Folman, L.B., Bodelier, P.L.E., Doronina, N. V., Suzina, N.E., Trotsenko, Y.A. & Dedysh, S.N. (2009) *Methylovirgula ligni* gen. nov., sp. nov., an obligately acidophilic, facultatively methylotrophic bacterium with a highly divergent *mxaF* gene. *International Journal of Systematic and Evolutionary Microbiology*, **59**, 2538 –2545.

Van der Wal, A., Boer, W. de, Smant, W. & Veen, J.A. (2007) Initial decay of woody

fragments in soil is influenced by size, vertical position, nitrogen availability and soil origin. *Plant and Soil*, **301**, 189–201.

Wang, Q., Garrity, G.M., Tiedje, J.M. & Cole, J.R. (2007) Naive Bayesian classifier for rapid assignment of rRNA sequences into the new bacterial taxonomy. *Applied and Environmental Microbiology*, **73**, 5261–5267.

Wang, L., Wang, G., Li, S. & Jiang, J. (2011) *Luteibacter jiangsuensis* sp. nov.: a methamidophos-degrading bacterium isolated from a methamidophos-manufacturing factory. *Current microbiology*, **62**, 289–95.

Warmink, J.A. & van Elsas, J.D. (2009) Migratory Response of Soil Bacteria to *Lyophyllum* sp. Strain Karsten in Soil Microcosms. *Applied and Environmental Microbiology*, **75**, 2820–2830.

Warmink, J.A., Nazir, R. & van Elsas, J.D. (2009) Universal and species-specific bacterial “fungiphiles” in the mycospheres of different basidiomycetous fungi. *Environmental Microbiology*, **11**, 300–312.

Watts, J., McDonald, R., Daniel, R. & Schreier, H. (2013) Examination of a Culturable Microbial Population from the Gastrointestinal Tract of the Wood-Eating Loricariid Catfish *Panaque nigrolineatus*. *Diversity*, **5**, 641–656.

Weedon, J.T., Cornwell, W.K., Cornelissen, J.H.. C., Zanne, A.E., Wirth, C. & Coomes, D.A. (2009) Global meta-analysis of wood decomposition rates: a role for trait variation among tree species? *Ecology Letters*, **12**, 45–56.

Wei, Q., Leblon, B. & La Rocque, A. (2011) On the use of X-ray computed tomography for determining wood properties: a review. *Canadian Journal of Forest Research*, **41**, 2120–2140.

Weißhaupt, P., Naumann, A., Pritzkow, W. & Noll, M. (2012) Nitrogen uptake of *Hypholoma fasciculare* and coexisting bacteria. *Mycological Progress*, **12**, 283–290.

Winandy, J.E. & Morrell, J.J. (1993) Relationship between incipient decay, strength, and chemical composition of Douglas-fir heartwood. *Wood and Fiber Science*, **25**, 278–288.

Woo, H.L., Hazen, T.C., Simmons, B.A. & DeAngelis, K.M. (2014) Enzyme activities of aerobic lignocellulolytic bacteria isolated from wet tropical forest soils. *Systematic and applied microbiology*, **37**, 60–7.

Wu, S.-H. (1998) Nine new species of *Phanerochaete* from Taiwan. *Mycological Research*,

102, 1126–1132.

Wu, S.-H., Nilsson, H.R., Chen, C.-T., Yu, S.-Y. & Hallenberg, N. (2010) The white-rotting genus *Phanerochaete* is polyphyletic and distributed throughout the phleboid clade of the *Polyporales* (Basidiomycota). *Fungal Diversity*, **42**, 107–118.

Wu, J., Yu, X.-D. & Zhou, H.-Z. (2008) The saproxylic beetle assemblage associated with different host trees in Southwest China. *Insect Science*, **15**, 251–261.

Vanden Wymelenberg, A., Gaskell, J., Mozuch, M., Kersten, P., Sabat, G., Martinez, D. & Cullen, D. (2009) Transcriptome and secretome analyses of *Phanerochaete chrysosporium* reveal complex patterns of gene expression. *Applied and environmental microbiology*, **75**, 4058–68.

Xie, C.-H. & Yokota, A. (2005) *Dyella japonica* gen. nov., sp. nov., a gamma-proteobacterium isolated from soil. *International journal of systematic and evolutionary microbiology*, **55**, 753–6.

Yelle, D.J., Ralph, J., Lu, F. & Hammel, K.E. (2008) Evidence for cleavage of lignin by a brown rot basidiomycete. *Environmental Microbiology*, **10**, 1844–1849.

Yin, Y., Mao, X., Yang, J., Chen, X., Mao, F. & Xu, Y. (2012) dbCAN: a web resource for automated carbohydrate-active enzyme annotation. *Nucleic acids research*, **40**, W445–51.

Zaitsev, G.M., Tsitko, I. V., Rainey, F.A., Trotsenko, Y.A., Uotila, J.S., Stackebrandt, E. & Salkinoja-Salonen, M.S. (1998) New aerobic ammonium-dependent obligately oxalotrophic bacteria: description of *Ammoniphilus oxalaticus* gen. nov., sp. nov. and *Ammoniphilus oxalivorans* gen. nov., sp. nov. *International Journal of Systematic Bacteriology*, **48**, 151–163.

Zak, J., Willig, M., Moorhead, D. & Wildman, H. (1994) Functional diversity of microbial communities: A quantitative approach. *Soil Biology and Biochemistry*, **26**, 1101–1108.

Zhang, H.B., Yang, M.X. & Tu, R. (2008a) Unexpectedly high bacterial diversity in decaying wood of a conifer as revealed by a molecular method. *International Biodeterioration & Biodegradation*, **62**, 471–474.

Zhang, H.B., Yang, M.X., Tu, R., Gao, L. & Zhao, Z.W. (2008b) Fungal communities in decaying sapwood and heartwood of a conifer *Keteleeria evelyniana*. *Current microbiology*, **56**, 358–62.

Zugmaier, W., Bauer, R. & Oberwinkler, F. (1994) Mycoparasitism of some *Tremella* species. *Mycologia*, **86**, 49–56.

Abstract

Wood decomposition is an important process in forest ecosystems in terms of their carbon and nutrient cycles. In temperate forests, saprotrophic basidiomycetes such as white-rot fungi are the main wood decomposers. While they have been less studied, bacterial communities also colonise decaying wood and coexist with these fungal communities. Although the impact of bacterial-fungal interactions on niche functioning has been highlighted in a wide range of environments, little is known about their role in wood decay. Based on microcosm experiments and using a culture-independent approach, we showed that the presence of the white-rot fungus *Phanerochaete chrysosporium* significantly modified the structure and diversity of the bacterial communities associated with the degradation of beech wood (*Fagus sylvatica*). Using a culture-dependent approach, it was confirmed that in the presence of the fungus the mycosphere effect resulted in increased bacterial abundance and modified the functional diversity of the fungal-associated bacterial communities. Lastly, a polyphasic approach simultaneously analysing wood physicochemical properties and extracellular enzyme activities was developed. This approach revealed that *P. chrysosporium* associated with a bacterial community isolated from its mycosphere was more efficient in degrading wood compared to the fungus on its own, highlighting for the first time synergistic bacterial-fungal interactions in decaying wood.

Keywords: wood decomposition, bacterial-fungal interactions, mycosphere effect, bacterial diversity, white rot, *Phanerochaete chrysosporium*, *Fagus sylvatica*, *Burkholderia*.

Résumé

Dans les écosystèmes forestiers, la décomposition du bois est un processus majeur, notamment impliqué dans le cycle du carbone et des nutriments. Les champignons basidiomycètes saprotrophes, incluant les pourritures blanches, sont les principaux agents de cette décomposition dans les forêts tempérées. Bien que peu étudiées, des communautés bactériennes sont également présentes dans le bois en décomposition et cohabitent avec ces communautés fongiques. L'impact des interactions bactéries-champignons sur le fonctionnement d'une niche écologique a été décrit dans de nombreux environnements. Cependant, leur rôle dans le processus de décomposition du bois n'a été que très peu investigué. A partir d'expériences en microcosme et en utilisant une approche non cultivable, il a été démontré que la présence du champignon *Phanerochaete chrysosporium* influençait significativement la structure et la diversité des communautés bactériennes associées au processus de décomposition du hêtre (*Fagus sylvatica*). Par une approche cultivable, cet effet mycosphère a été confirmé, se traduisant par une augmentation de la densité des communautés bactériennes en présence du champignon ainsi que par une modification de la diversité fonctionnelle de ces communautés. Enfin, une approche polyphasique a été développée, combinant l'analyse des propriétés physico-chimiques du bois et des activités enzymatiques extracellulaires. Les résultats de cette expérience ont révélé que l'association de *P. chrysosporium* avec une communauté bactérienne issue de la mycosphère de ce dernier aboutissait à une dégradation plus importante du matériau bois par rapport à la dégradation par le champignon seul, démontrant pour la première fois des interactions bactéries-champignons synergiques dans le bois en décomposition.

Mots-clefs : décomposition du bois, interactions bactéries-champignons, effet mycosphère, diversité bactérienne, pourriture blanche, *Phanerochaete chrysosporium*, *Fagus sylvatica*, *Burkholderia*.